



City Research Online

City, University of London Institutional Repository

Citation: Leong, S. H. (2021). Modelling and Testing Financial Risk. (Unpublished Doctoral thesis, City, University of London)

This is the accepted version of the paper.

This version of the publication may differ from the final published version.

Permanent repository link: <https://openaccess.city.ac.uk/id/eprint/26864/>

Link to published version:

Copyright: City Research Online aims to make research outputs of City, University of London available to a wider audience. Copyright and Moral Rights remain with the author(s) and/or copyright holders. URLs from City Research Online may be freely distributed and linked to.

Reuse: Copies of full items can be used for personal research or study, educational, or not-for-profit purposes without prior permission or charge. Provided that the authors, title and full bibliographic details are credited, a hyperlink and/or URL is given for the original metadata page and the content is not changed in any way.

Modelling and Testing Financial Risk

Soon Heng Leong

Centre for Econometric Analysis
Faculty of Finance
Bayes Business School
City, University of London

This dissertation is submitted for the degree of
Doctor of Philosophy

September 2021

PREFACE

This dissertation represents the tangible outcome of my doctoral studies at the Centre for Econometric Analysis (CEA), Faculty of Finance, Bayes Business School, City, University of London and was written from September 2017 to September 2021. I am grateful to Bayes Business School, CEA and Timberlake Consultants for providing generous research funding including the “2017/2021 PhD Studentship in Memory of Ana Timberlake” along with expenses on numerous academic conferences and visits.

I wish to express my gratitude to a multitude of people for their supports in many ways throughout this journey: my PhD advisor and mentor Giovanni Urga, for always providing research advice, discussions, supports and opportunities; Lynda Khalaf, for acting as my PhD external examiner, for her feedback on my work and for sharing her life advice during our visit to Oxford in September 2019; Babara Casu, for her suggestions on my summer project in 2018 and for acting as my PhD internal examiner; Thorsten Beck and Fa Wang, for their feedback on my work, for acting as my transfer examiners, for their advice about the academic job market, for acting as my references and for their kind offers to provide further assistance; Ian Marsh, for a series of valuable advice about academic job interviews.

Finally, I thank my mother Lay Sen Ang, for her unconditional love and my fiancée Luqi, for her never-ending support, love and patience.

Soon Heng Leong

London, September 2021

CONTENTS

List of figures	vii
List of tables	ix
Abstract	1
Introductory remarks	3
1 Modelling and testing systemic risk	7
1.1 Introduction	7
1.2 Data, variables and methodology	10
1.2.1 Data preparation	10
1.2.2 Shadow insurance	10
1.2.3 Dependent variables: $\Delta CoVaR$ and <i>SRISK</i>	13
1.2.4 Explanatory variables	16
1.2.5 Descriptive statistics	18
1.3 Empirical results	21
1.4 Conclusions	29
Appendix 1.A	31
1.A.1 Full sample	31
1.A.2 Robustness checks	35
2 Modelling and testing volatility spillover	41
2.1 Introduction	41
2.2 Multivariate Granger causality in variance	43
2.2.1 From univariate to multivariate Granger causality in variance	44
2.2.2 Test statistic and asymptotic properties	45
2.2.3 Bidirectional Granger causality in variance	52
2.3 Estimation	53

2.4	Monte Carlo simulations	57
2.4.1	The bivariate case	58
2.4.2	Higher dimensions	60
2.5	Empirical application	63
2.6	Conclusions	70
	Appendix 2.A	71
	Appendix 2.B	73
	Appendix 2.C	82
	Appendix 2.D	85
	Appendix 2.E	85
	Appendix 2.F	86
	Appendix 2.G	86
	Appendix 2.H	87
	2.H.1 Simulation results of Tables 2.3 and 2.4 for all M	87
	2.H.2 Monte Carlo study of the bidirectional test	90
	2.H.3 GARCH misspecification	97
	2.H.4 Computational efficiency study	99
3	Unifying and testing causality-based risk measures	101
3.1	Introduction	101
3.2	Literature review	104
3.3	Methodology	105
3.4	Data	108
3.5	Results	109
	3.5.1 Model estimates	110
	3.5.2 Causality results	112
	3.5.3 Implications for investors and policymakers	119
3.6	Conclusions	120
	Conclusive remarks	123
	Bibliography	129

LIST OF FIGURES

1.1	Market capitalisation. The figure displays the market capitalisation of our sample of 215 insurers over the period 2004Q1–2017Q4, in billion US dollar. Data source: <i>Datastream</i>	12
1.2	Total reinsurance ceded. The figure displays the growth of the reinsurance industry over the period 2004–2017, in billion US dollar. Data source: <i>Market Intelligence</i> . . .	12
1.3	Shadow insurance. The figure displays the growth of shadow insurance activity over the period 2004–2017, in billion US dollar. Data source: <i>Market Intelligence</i>	13
1.4	Shadow insurance (public) vs shadow insurance (non-public). The figure displays the amount of shadow insurance practised by entity belonging to a public company vs non-public company over the period 2004–2017, in billion US dollar. Data source: <i>Market Intelligence</i>	14
1.5	Time evolution of systemic risk. The figures plot the mean quarterly systemic risk measures $\Delta CoVaR$ and <i>SRISK</i> of all insurers (solid line), shadow insurers (dashed line) and non-shadow insurers (dotted line), over the full sample period 2004Q1–2017Q4. The positive dollar term of <i>SRISK</i> is used.	20
1.6	Systemic risk and shadow indicator series of Manulife. The figures plot the quarterly shadow indicator (dashed line) and systemic risk measures $\Delta CoVaR$ and <i>SRISK</i> (solid lines) of Manulife over the full sample period 2004Q1–2017Q4. The positive dollar term of <i>SRISK</i> is used.	23
3.1	Crude oil imports. This figure plots the crude oil imports in China (solid line) and in the US (dashed line) over the 2005–2019 period, in million barrels per day. Data source: <i>Datastream</i> and <i>EIA</i>	102

LIST OF TABLES

1.1	Sample composition	11
1.2	Shadow insurers	15
1.3	Descriptive statistics	19
1.4	Descriptive statistics: Shadow and non-shadow insurers	22
1.5	Correlation matrix: Full period	24
1.6	Correlation matrix: Distress period	25
1.7	Regression results: LS estimation	28
1.8	Regression results: GMM estimation	30
1.A.1	Main sample	31
1.A.2	Regression results: Robustness 1	37
1.A.3	Regression results: Robustness 2	38
1.A.4	Regression results: Robustness 3	39
1.A.5	Regression results: Robustness 4	40
2.1	Empirical sizes	61
2.2	Empirical powers	62
2.3	Empirical sizes	63
2.4	Empirical powers	64
2.5	Diagnostic tests (UK-NA)	66
2.6	Spillover results (UK-NA)	67
2.7	Diagnostic tests (EU-NA)	68
2.8	Diagnostic tests (EU-NA)	69
2.9	Spillover results (EU-NA)	69
2.H.1	Empirical sizes	88
2.H.2	Empirical powers	89
2.H.3	Empirical sizes	91
2.H.4	Empirical powers	92
2.H.5	Empirical sizes	93

2.H.6	Empirical powers	94
2.H.7	Empirical sizes	95
2.H.8	Empirical powers	96
2.H.9	Diagnostic tests (UK–NA, Control)	97
2.H.10	Spillover results (UK–NA, Control)	98
2.H.11	Diagnostic tests (UK–NA, Misspecified)	98
2.H.12	Spillover results (UK–NA, Misspecified)	98
3.1	Descriptive statistics	110
3.2	Model estimations and diagnostics	113
3.3	Model estimations and diagnostics	114
3.4	Model estimations and diagnostics	115
3.5	Causality results	116

ABSTRACT

This dissertation centres on the modelling and testing of risk with the emphasis on gauging novel issues in finance. The first chapter models the stability of financial system using prominent systemic risk measures, and examines for various risk factors affecting financial stability including the risky practice of shadow insurance. The collected dataset suggests that shadow insurance has been increasingly exploited to reduce risk exposure and that entities exploiting shadow insurance are generally riskier and more interconnected with the financial system. Using panel analysis, I find statistical evidence that the practice of shadow insurance does affect financial stability based on two distinct systemic risk measures. In the second chapter, I propose a new multivariate econometric strategy for examining the spillover of volatility — the most fundamental risk measure. The asymptotic theory of the testing strategy is established under regularity conditions. The chapter includes an extensive simulation study to confirm the finite sample performance of the proposed econometric strategy and an empirical study based on the new test to examine volatility spillover between the North American and European financial markets before and after the Brexit referendum. In the third chapter, I consolidate the comprehensive literature on Granger causality methods, and I apply the unified methodology to examine different components of risk spillover between international crude oil and the Chinese equity markets that are fuel intensive. This unified analysis disentangles the complex oil-equity nexus to find that it has been nontrivially related to various factors such as demand and supply of oil, economic growth rate, government subsidies and the Chinese oil pricing reformation.

INTRODUCTORY REMARKS

This dissertation centres on the modelling and testing of financial risk. I derive from the central topic three pieces of self-contained research papers — composed as the dissertation chapters — covering different aspects of risk in finance with their economic and policy implications.

Chapter 1 focuses on modelling systemic risk and testing for its risk factors, where systemic risk can be regarded as the risk an entity poses to the financial system. To quantify systemic risk, I summarise the existing literature to obtain four widely used methods: the delta conditional value-at-risk ($\Delta CoVaR$), the marginal expected shortfall (MES), the systemic expected shortfall (SES) and the systemic risk measure ($SRISK$). I then exclude the MES because it captures largely the market beta instead of systemic risk (see, e.g., [Benoit et al., 2017](#)). Since SES is closely related to MES , the chapter therefore focuses on modelling the $\Delta CoVaR$ and $SRISK$ systemic risk proxies. Besides, I include in the chapter various factors that could potentially affect systemic risk such as size and interconnectedness. Additionally, I construct a shadow indicator based on the lesser known risky practice of shadow insurance. This shadow activity deserves public attention and scrutiny because it is exploited by leading insurance entities to increase risk exposure (see, e.g., [Kojen and Yogo, 2016](#)). Naturally, I construct a representative dataset covering global insurance entities and their shadow activities. Based on the data universe, I estimate $\Delta CoVaR$ and $SRISK$ to find that both measures are able to capture the well-known financial crises, with $\Delta CoVaR$ being relatively more reactive to the period of US subprime crisis in 2008–2009 while $SRISK$ being more responsive towards the period of UK Brexit in 2016. My findings highlight the distinctive features between the two systemic risk measures. This is expected because the two measures are unique by construction: $\Delta CoVaR$ is a function of value-at-risk whereas $SRISK$ is based on expected shortfall. As a result, they capture different aspects of risk in the financial system. In testing for the factors driving systemic risk, I use both measures for rigour. My panel analysis suggests that the shadow indicator is one of the key determinants that increases systemic risk. This finding is robust across both measures. The conclusion in this chapter implies that the practice of shadow insurance does affect financial stability, and calls for new policies to regulate this risky activity.

The application of the systemic risk measures discussed in Chapter 1 is limited to cases where risk is transmitted or spilled in a single direction. In the absence of prior information, it is appro-

priate to first determine the direction of risk spillover. Therefore, in Chapter 2 I propose a novel (bi)directional test for volatility spillover, where volatility spillover is defined using the notion of Granger causality in variance. By definition, there is evidence of volatility spillover from X to Y if any of the past variances of X is able to predict the current variance of Y . The chapter focuses on volatility since it is the most fundamental risk measures. The new test can handle markets consisting of multiple countries such as the North America and European Union markets. The proposed test can be viewed as the multivariate generalisation of the univariate results in [Hong \(2001\)](#). To compute the test statistic, conditional volatility has to be first estimated. Because modelling volatility can be challenging in the higher dimension, I further provide a new nonparametric specification to facilitate the estimation of volatility and hence the computation of my test statistic. The new model can be viewed as an extension of the Constant Conditional Correlation (CCC) model in [Bollerslev \(1990\)](#), where I propose to use the general infinite order autoregressive conditional heteroskedasticity [ARCH(∞)] process to minimise the risk misspecification. In terms of estimation, the chapter proposes consistent least-squares estimators which are free from the complications of their likelihood-based counterparts such as convergence issue. Moreover, I develop the asymptotic theory of the new approach. An extensive simulation study shows that the proposed method has reasonable finite sample performance in the higher dimension. The chapter completes with an empirical study in which I apply the new method to examine spillover relations between the North American and European equity markets before and after the Brexit referendum. Other practical applications of the new approach include the identification of risk transmitters and recipients in the financial system, which could assist policymakers to shape targeted policies to protect vulnerable risk recipients whenever necessary.

Although volatility is considered the most fundamental risk measure, the causality literature has proposed other methods to capture different components of financial risk spillover where each component has its own interest (see, e.g., [Candelon and Tokpavi, 2016](#); [Du and He, 2015](#); [Hong, 2001](#); [Hong et al., 2009](#)). This calls for a unification. In Chapter 3 I consolidate the extensive literature on causality tests to show that various forms of spillover can be examined. The unified framework allows examining spillovers in the mean, variance, risky quantiles (both positive and negative) and distribution, where each element uncovers a unique relation. The causality-in-mean analysis reveals return spillover, whereas the presence of variance causality can be viewed as volatility spillover. The causality-in-risk analysis detects the existence of extreme risk spillovers and it covers both positive and negative relations. The long-term spillover effects can be evaluated by the causality-in-distribution examination. Because all of the analyses are based on causality methods within the same family, inferential biases due to methodological disparities are minimised. I apply the unified methodology to study spillover relations between international crude oil and the Chinese oil-intensive industries. I use subsample analysis to study changes in spillover nexus after the Chinese domestic oil reformation in 2013. My findings highlight that government intervention may distort the spillover relations between the Chinese sectors and global oil. For instance, my analysis suggests that the Chinese industries are not significantly affected by extreme international

oil price movement before the reformation because domestic oil price in China is capped and strictly regulated by its central government. Consequently, the Chinese sectors are mostly shielded against large fluctuations in global oil price. As the Chinese markets become more exposed to international oil after the reformation, extreme negative returns of global oil benefit most oil-intensive sectors while positive outlook in Brent adversely affect most the industries. The findings in this chapter encourage policymakers to be cautious when implementing similar regulations in the future because they may distort statistical relations on an international level.

THE CONTRIBUTION OF SHADOW INSURANCE TO SYSTEMIC RISK*

1.1 Introduction

The main objective of this paper is to assess the contribution of shadow insurance to systemic risk of the global financial sector. To this aim, we use a sample of 215 public insurance entities across 40 countries over the period 2004–2017. To detect shadow activities, we examine all reinsurance agreements from the Schedule S filings. To measure interconnectedness between the insurance and banking sectors, we analyse an additional sample of 745 traditional banks. On the basis of both delta conditional value-at-risk ($\Delta CoVaR$) and systemic risk measure (*SRISK*), we find statistically significant evidence that the practice of shadow insurance affects the stability of global financial system.

In recent years, the financial stability literature has proposed a large number of systemic risk measures. A comprehensive review is provided by [Benoit et al. \(2017\)](#), who distinguish measures that study sources of systemic risk from global approaches that could support a more efficient regulation. The prominent global measures are the $\Delta CoVaR$ of [Adrian and Brunnermeier \(2016\)](#), the *SRISK* of [Acharya et al. \(2012\)](#) and [Brownlees and Engle \(2017\)](#), the marginal expected shortfall (*MES*) and systemic expected shortfall (*SES*) of [Acharya et al. \(2017\)](#). These measures have been used extensively to identify determinants that drive systemic risk, with more emphasis on the banking sector. For instance, [López-Espinosa et al. \(2012\)](#) use $\Delta CoVaR$ to study a sample of 54 large international banks to find that short-term wholesale funding increases systemic risk. [Adrian and Brunnermeier \(2016\)](#) study the systemic relevance of all publicly listed financial entities in the United States to find that leverage, maturity mismatch and size are the main drivers of systemic

*A research article (joint with C. Bellavite Pellegrini and G. Urga) based on the results in this chapter entitled “The contribution of shadow insurance to systemic risk” has been published in the *Journal of Financial Stability* (2020), vol. 51, p. 100778/1–12. <https://doi.org/10.1016/j.jfs.2020.100778>.

risk. [Brownlees and Engle \(2017\)](#) employ *SRISK* to find that major banks such as Bear Stearns, Fannie Mae, Freddie Mac, Lehman Brothers and Morgan Stanley play a significant role in systemic risk contribution. Using both $\Delta CoVaR$ and *SRISK*, [Laeven et al. \(2016\)](#) study a panel of 412 large banks from 56 countries to find that systemic risk grows with bank size. [Abedifar et al. \(2017\)](#) combine both Islamic and conventional financial entities to find that traditional banks with Islamic windows are highly interconnected during the subprime financial crisis.

The aforementioned literature revolves around the financial sector or the banking industry, with minimal emphasis on the insurance sector. Traditionally, insurance entities are not deemed to be of systemic relevance to destabilise the greater financial system. Unlike banks, insurers are not subject to a bank run and therefore do not face the potential of sudden liquidity risk. However, the bailout of American Insurance Group (AIG) in 2008 suggests otherwise. Using *MES*, *SRISK* and $\Delta CoVaR$, [Bierth et al. \(2015\)](#) analyse the exposure and contribution of 253 international insurance entities to systemic risk between 2000 and 2012. The authors find that interconnectedness with the financial system increases insurers' systemic risk exposure and highly levered entities contribute more to systemic risk. The authors, however, do not address the role played by shadow insurance.

The risk profile of insurance entities becomes increasingly complicated when they practice shadow insurance to move blocks of liability to affiliated reinsurers. [Kojien and Yogo \(2016\)](#) define shadow insurance as “*reinsurance ceded to affiliated and unauthorised reinsurer without A.M. Best rating*”. In this paper, we adopt a more stringent definition by also considering Fitch, Moody's and S&P ratings. In a typical shadow insurance deal, a parent insurance entity first sets up a “captive” subsidiary, which is essentially a shell company that is often located offshore with a looser reserve requirement. The shell entity is usually unauthorised to sell insurance to third parties, and its primary function is to re-insure the parent company. Next, an operating entity belonging to the company group cedes a portion of existing liability to the subsidiary. Consequently, the insurance group can reduce its risk-based capital to underwrite more contracts. By practising shadow insurance, a “shadow insurer” could increase its risk exposure to drive potential return. We define *shadow insurer* as the ultimate parent company of an insurance group practising shadow insurance.

[Lawsky \(2013\)](#) describes shadow insurance as “*a little-known loophole that puts insurance policyholders and taxpayers at greater risk*”, and suggests that the practice of shadow insurance could disrupt the stability of the entire financial system. [Schwarcz \(2015\)](#) conjectures that shadow insurance could increase the interconnectedness between the insurance and banking sectors, thus driving systemic risk. Using A.M. Best rating of insurance entities, [Kojien and Yogo \(2016\)](#) propose a theoretical framework to estimate the term structure of default probabilities of a company practising shadow insurance. Under plausible assumptions, the authors show that an entity using shadow insurance is three and a half times more likely to default over ten years. [Kojien and Yogo \(2017\)](#) document that a large portion of shadow insurance is funded through letters of credit, which is mostly written by banks. These documentations suggest further that there is a remarkable level

of interconnectedness between the shadow insurance business and the entire banking system, which raises systemic concern.

In this paper, we empirically examine the contribution of shadow insurance to systemic risk of the global financial industry. To this aim, we collect all reinsurance agreements from the National Association of Insurance Commissioners (NAIC) Schedule S filings to identify 29 publicly listed shadow insurers. We also document that about 2.8 cents every dollar ceded were shadow in 2004 with the amount growing substantially to 21 cents every dollar in 2017. For a global study, we include all publicly listed insurance entities across the world as our main sample. To measure the interconnectedness between our sample insurers and the banking industry, we employ the principal component measure proposed by [Billio et al. \(2012\)](#). In particular, we compute the interconnectedness between our main sample and the banking system by further considering all publicly listed banks available in *Datastream*.

In terms of systemic risk measures, we employ the prominent global measures $\Delta CoVaR$ of [Adrian and Brunnermeier \(2016\)](#) and *SRISK* of [Acharya et al. \(2012\)](#) and [Brownlees and Engle \(2017\)](#). We do not use the *MES* measure because it is proportional to market beta that captures only systematic risk ([Benoit et al., 2017](#), p. 136–137). Conversely, *SRISK* is less related to beta because it also depends on the debt and market capitalisation of an entity. Although [Benoit et al. \(2017\)](#) show that the dynamics of $\Delta CoVaR$ matches value-at-risk (*VaR*) in the time series dimension, there is only a weak relationship between them in the cross-sectional dimension. An entity might not be risky individually with a low *VaR*, but it could be of significant systemic relevance as indicated by a high $\Delta CoVaR$. On the one hand, $\Delta CoVaR$ measures the *VaR* of the financial system, conditional on an insurer being in distress. On the other hand, *SRISK* evaluates the expected shortfall (*ES*) of an insurance entity, conditional on a distressed financial system.

Both $\Delta CoVaR$ and *SRISK* measures quantify the contribution of an entity to systemic risk of the financial system. However, [Benoit et al. \(2013\)](#) show that $\Delta CoVaR$ and *SRISK* do not provide similar systemic rankings unless under certain strict conditions such as the correlation with the financial system of riskier insurers is always higher than that of less risky entities. Moreover, [Zhang et al. \(2015\)](#) find that $\Delta CoVaR$ is more reactive to the subprime financial crisis than other popular measures including *SRISK*. To accommodate the distinct features of the employed measures, we analyse both the full sample period and a subsample that focuses on the period of financial distress.

From the descriptive statistics, we find that shadow insurers are typically larger, riskier, more interconnected with other market participants and more likely to contribute to financial instability compared with non-shadow entities. Next, we perform panel analyses to examine the hypothesis that the practice of shadow insurance increases systemic risk of the global financial system, after controlling for factors such as the magnitude of shadow insurance, size of the entity and its degree of interconnectedness with the banking system. In line with the theory and regulatory expectations, our findings confirm the pivotal role played by size and interconnectedness in the spreading of systemic risk. We also find that the practice of shadow insurance increases systemic risk, with

$\Delta CoVaR$ showing a stronger effect during distress period and *SRISK* suggesting a more profound long-run impact. Overall, our results suggest that shadow insurance poses non-trivial risks to the financial system, which confirms the main hypothesis of the paper.

The remainder of this paper is organised as follows. In Section 1.2, we describe the data and methodology used in the study. Section 1.3 presents the results of our analysis. Section 1.4 concludes.

1.2 Data, variables and methodology

In this section, we present the procedures outlining the preparation of our dataset and the detection of shadow activities. We describe the formulation of our systemic risk measures, which serve as the main dependent variables, and introduce the explanatory and control variables involved in the study. Finally, we summarise all of the variables.

1.2.1 Data preparation

We select all public and active insurance entities that are available in *Datastream*. Next, we select entities that are continuously listed between the first quarter of 2004 (2004Q1) and the fourth quarter of 2017 (2017Q4), leading to a total of 56 quarters for the analysis. We focus on primary issues and therefore we exclude secondary listings from the selection. Insurers with unavailable share price and total asset data are omitted. Insurance entities with zero share price data are further excluded. We also exclude entities whose daily share price does not fluctuate for more than a quarter. With this filter, we obtain a sample of 215 insurers across 40 countries. Missing data points of a few entities are estimated using the nearest observation. Lastly, we collect the data in US dollar to minimise potential bias due to currency risk. In Table 1.1, we report the number of entities by country in our main sample. Given that United States is the leading country in the global financial industry, it is not surprising that its entities make up about a quarter of our sample. The names and *Datastream Mnemonics* of the full sample are reported in the Appendix. Fig. 1.1 plots the market capitalisation of our sample. We observe that the global insurance industry was growing steadily until the subprime mortgage crisis in 2008 that saw a sharp decline in the market value of the sector. After the financial crisis, the industry remained stagnant for a few years, and it began to grow gradually from 2012.

1.2.2 Shadow insurance

To detect shadow insurance, we collect current and past reinsurance agreements from the Schedule S filings, available to us through *Market Intelligence*, a data provider owned by S&P Global. As of April 2018, we have collected a total of 195,717 reinsurance contracts. In each agreement, we observe the name of the operating entity, the name of the ultimate parent company of the

Table 1.1 Sample composition

Country	# Entities	Country	# Entities
Australia	4	Kenya	1
Austria	2	Korea, Republic of	7
Belgium	1	Malaysia	6
Bermuda	8	Malta	1
Brazil	1	Mexico	2
Canada	10	Morocco	2
Chile	2	Netherlands	2
Cyprus	2	New Zealand	1
Denmark	2	Norway	1
Egypt	1	Pakistan	8
Finland	1	Singapore	4
France	5	South Africa	5
Germany	9	Spain	2
Greece	1	Sri Lanka	3
Hong Kong	2	Switzerland	7
India	3	Taiwan, Province of China	9
Ireland	1	Thailand	8
Israel	8	Turkey	5
Italy	6	United Kingdom	9
Japan	2	United States	61

NOTES: The table reports the number of insurance entities by country in our international sample. Data source: *Datastream*.

operating entity, the name of the reinsurer and the amount of reinsurance ceded to the reinsurer.¹ Moreover, we observe whether the reinsurance is authorised, whether the reinsurer is affiliated with the ceding entity and whether it is rated.²

Fig. 1.2 summarises the growth of the reinsurance industry. We observe that reinsurance has become increasingly popular in the insurance sector as a practice to transfer risks and liabilities to other parties. The amount grew nearly two and a half times from about \$550 billion in 2004 to about \$1300 billion in 2017. Fig. 1.3 reveals the dollar amount of shadow insurance ceded in the industry. We observe an upward trend in the practice of shadow insurance, growing considerably from about \$15 billion in 2004 to over \$250 billion in 2017. In particular, about 2.8 cents every dollar ceded was shadow in 2004 with this figure rising significantly to 21 cents every dollar in 2017. Overall, we observe a substantial increase in the practice that is used to artificially boost risk-based capital buffers reported to the regulators.

Fig. 1.4 disentangles shadow insurance practised by those belonging to a public parent company from the non-public counterpart. The plot reveals that a large portion of shadow insurance business involves entities that belong to publicly listed shadow insurers. This finding conveniently allows us to analyse the balance sheet data of these shadow insurers using prominent global systemic risk measures such as $\Delta CoVaR$ and $SRISK$ to evaluate the impact of shadow insurance on global financial stability. In the following, we refer to publicly listed shadow insurers simply as shadow insurers.

¹Following [Kojen and Yogo \(2016\)](#), we define reinsurance ceded as the sum of reserve credit taken and modified coinsurance reserve ceded.

²An authorised reinsurer is subject to the same capital requirement as the ceding entity.

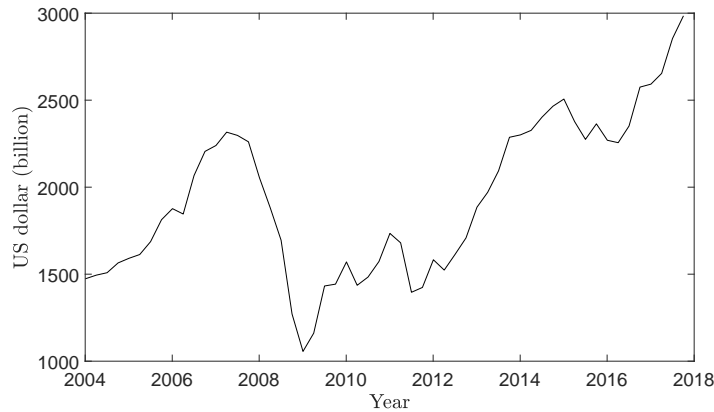


Figure 1.1 Market capitalisation. The figure displays the market capitalisation of our sample of 215 insurers over the period 2004Q1–2017Q4, in billion US dollar. Data source: *Datastream*.

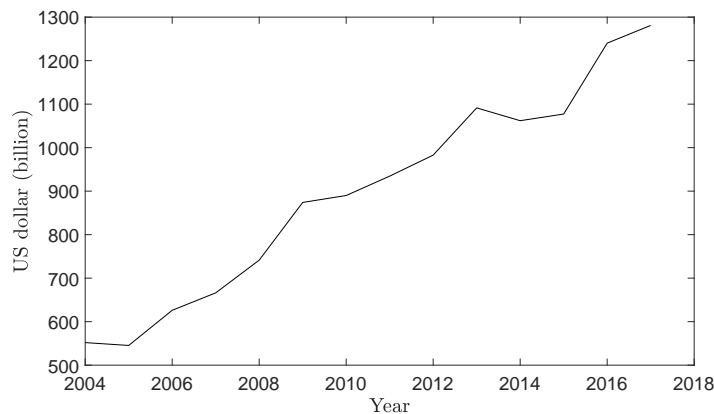


Figure 1.2 Total reinsurance ceded. The figure displays the growth of the reinsurance industry over the period 2004–2017, in billion US dollar. Data source: *Market Intelligence*.

We identify a total of 29 shadow insurers by scrutinising every reinsurance agreement from the Schedule S filings for the period 2004–2017.³ We report the names of these shadow entities, their corresponding locations and the extent to which they are involved in shadow insurance in Table 1.2. Particularly, we compute the shadow index to measure how aggressive an entity participates in shadow activity. The shadow index is computed as the ratio of total shadow insurance to the average reserve held. A high shadow index suggests high aggressiveness as the shadow activities

³In the main analysis, we omit 7 of the 29 shadow insurers due to them being relatively new companies and lack sufficiently long historical data. The omitted entities are Brighthouse Financial, Inc., Dai-ichi Life Holdings, Inc., FGL Holdings, Genworth Financial, Inc., National General Holdings Corporation, Primerica, Inc. and Voya Financial Inc. Although Voya Financial Inc. was recently listed in 2013, the entity was an operating subsidiary under ING Group. Hence, we include ING Group as shadow insurer to obtain 23 shadow insurers in total. The magnitude of shadow insurance practised by the omitted entities is relatively small, and we keep a significant portion of shadow insurance in the analysis. Specifically, the omitted amount represents 6.7% of the total shadow insurance.

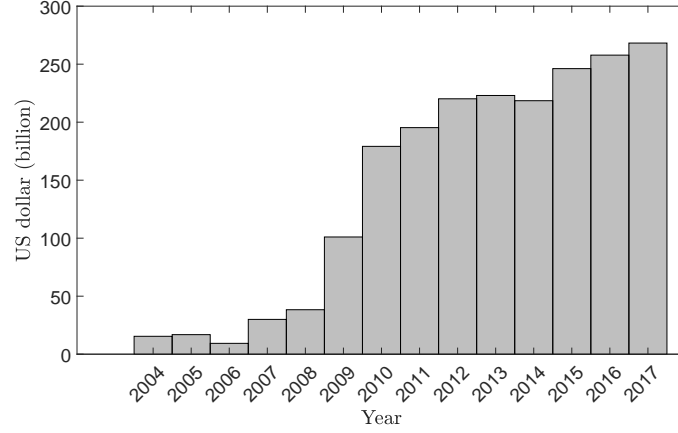


Figure 1.3 Shadow insurance. The figure displays the growth of shadow insurance activity over the period 2004–2017, in billion US dollar. Data source: *Market Intelligence*.

have been carried out with a low insurance reserve on average. For instance, although the dollar amount of shadow insurance practised by MetLife, Inc. (\$238,144 million) is higher than Unum Group (\$181,381 million), the latter, however, has been engaging the shadow business with higher risk exposure. This is revealed by a shadow index of 4154 from Unum Group compared with 700 from MetLife, Inc.

1.2.3 Dependent variables: $\Delta CoVaR$ and $SRISK$

The $\Delta CoVaR$ measure of [Adrian and Brunnermeier \(2016\)](#) makes use of the value-at-risk (VaR). The $q\%$ - VaR is the expected maximum dollar loss within the $q\%$ confidence level. Formally, the $q\%$ - VaR of an entity i , denoted by VaR_i^q is given by:

$$\mathbb{P}(X_i \leq VaR_i^q) = q\%, \quad (1.1)$$

where X_i is the stock return of entity i . We employ historical simulation method to estimate VaR_i^q . In particular, we compute VaR_i^q for a given quarter t using daily stock returns observed in that quarter, scaled using the root- T rule. The computation is repeated for every quarter to obtain a time-varying quarterly VaR_{it}^q series.

Next, $CoVaR$ is defined as the VaR of the financial system conditional on some event $C(X_i)$ on entity i . Formally, $CoVaR_{m|C(X_i)}^q$ is defined by the q -th quantile of the conditional probability distribution:

$$\mathbb{P}\left(X_m | C(X_i) \leq CoVaR_{m|C(X_i)}^q\right) = q\%, \quad (1.2)$$

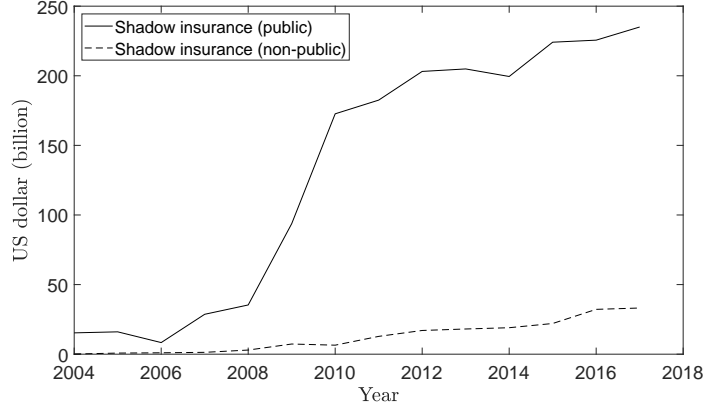


Figure 1.4 Shadow insurance (public) vs shadow insurance (non-public). The figure displays the amount of shadow insurance practised by entity belonging to a public company vs non-public company over the period 2004–2017, in billion US dollar. Data source: *Market Intelligence*.

where X_m is the return of the global financial system, computed using the *MSCI World Financials Index*.⁴ An entity's contribution to systemic risk is measured by $\Delta CoVaR$, namely the difference between $CoVaR$ conditional on the entity being in distress and $CoVaR$ in the median state of the entity. As far as the estimation method is concerned, we follow [Adrian and Brunnermeier \(2016\)](#) to employ quantile regressions to estimate $CoVaR$.

The estimate of the q %-quantile of X_m given the value of X_i is given by:

$$\hat{X}_{mt|X_{it}}^q = \hat{\alpha}_i^q + \hat{\beta}_i^q X_{it}, \quad (1.3)$$

where $\hat{\alpha}_i^q$ and $\hat{\beta}_i^q$ are obtained by performing q %-quantile regression of X_{mt} on X_{it} . From the definition of VaR in (1.1), we have that:

$$VaR_{mt|X_{it}}^q = \hat{X}_{mt|X_{it}}^q. \quad (1.4)$$

Using predicted value of $X_{it} = VaR_{it}^q$ yields the $CoVaR_{it}^q$ measure. More formally, within the quantile regression framework, the $CoVaR_{it}^q$ measure is:

$$CoVaR_{it}^q = VaR_{mt|X_{it}=VaR_{it}^q}^q = \hat{\alpha}_i^q + \hat{\beta}_i^q VaR_{it}^q. \quad (1.5)$$

The $\Delta CoVaR$ of entity i for a given quarter t is given by:

$$\Delta CoVaR_{it} = CoVaR_{it}^q - CoVaR_{it}^{50} = \hat{\beta}_i^q (VaR_{it}^q - VaR_{it}^{50}). \quad (1.6)$$

⁴Our conclusions remain unchanged if we use an alternative *FTSE World Financials Index*. See Appendix 1.A.2.

Table 1.2 Shadow insurers

Shadow insurer	Country	Shadow insurance	Shadow index
AEGON N.V.	Netherlands	68,287.88	499.647
Allianz Group	Germany	1,748.39	3.125
American International Group, Inc.	United States	68,460.47	204.889
AXA	France	100,183.64	184.810
Brighthouse Financial, Inc.	United States	2,109.62	-
Centene Corporation	United States	13.64	10.056
Chubb Limited	Switzerland	6.73	0.133
Cigna Corporation	United States	0.45	0.018
Dai-ichi Life Holdings, Inc.	Japan	8,590.69	-
FGL Holdings	United States	7,720.02	-
Genworth Financial, Inc.	United States	13,994.92	-
Legal & General Group Plc	United Kingdom	15,154.48	60.311
Lincoln National Corporation	United States	63,208.69	766.231
Manulife Financial Corporation	Canada	831,154.11	5262.104
MetLife, Inc.	United States	238,144.41	700.263
National General Holdings Corporation	United States	0.01	-
Primerica, Inc.	United States	26,166.18	-
Prudential Financial, Inc.	United States	13,306.91	48.574
Prudential Plc	United Kingdom	0.49	0.001
Reinsurance Group of America, Incorporated	United States	15,500.06	1076.965
SCOR SE	France	113.08	4.341
Security National Financial Corporation	United States	0.11	0.276
Sun Life Financial Inc.	Canada	30,496.34	368.483
Swiss Re AG	Switzerland	37,335.80	279.541
Tokio Marine Holdings, Inc.	Japan	23.23	0.181
Torchmark Corporation	United States	33,341.90	3276.872
Unum Group	United States	181,380.69	4153.791
Voya Financial, Inc.	United States	64,801.15	-
Zurich Insurance Group AG	Switzerland	23,667.59	126.654

NOTES: The table displays the names of shadow insurers and the corresponding countries they are located. Besides, the table reports the amount of shadow insurance practised (in million US dollar), aggregated over 2004–2017. The shadow index is the ratio of total shadow insurance to the average quarterly reserve held. We do not report the shadow index of some entities as these entities are subsequently dropped in the analysis due to data availability. Data source: *Market Intelligence*.

To simplify the notation, in the following q is always set to be 5%, so that $CoVaR_{it}$ identifies the system losses predicted on the 5%- VaR of entity i , while $\Delta CoVaR_{it}$ identifies the deterioration in the system, when entity i moves from its median state to its 5% worst scenario.

The *SRISK* measure of [Acharya et al. \(2012\)](#) and [Brownlees and Engle \(2017\)](#) is based on the notion of expected shortfall (*ES*). Formally, the conditional *ES* of a system with N financial entity at time t is defined as:

$$ES_{mt} = - \sum_{i=1}^N w_{it} \mathbb{E}_{t-1} [R_{it} | R_{mt} < C], \quad (1.7)$$

where C is a threshold, and it is set to be the worst 5% daily return of the global financial system R_{mt} in each quarter, R_{it} is entity i 's stock return, and w_{it} is the weight of entity i . As in $\Delta CoVaR$, we use the return of *MSCI World Financials Index* as a proxy for R_{mt} . Next, the daily marginal expected shortfall (*MES*) is given by the partial derivative of the system expected shortfall ES_{mt}

with respect to the weight of entity i :

$$MES_{it} = \frac{\partial ES_{mt}}{\partial w_{it}} = -\mathbb{E}_{t-1}[R_{it}|R_{mt} < C]. \quad (1.8)$$

Subsequently, the quarterly systemic risk measure $SRISK$ (in dollar) is given by:

$$SRISK_{it} = kD_{it} - (1 - k)W_{it}(1 - LRMES_{it}), \quad (1.9)$$

where k is the prudential capital fraction, D_{it} is the book value of debt, W_{it} is the market value of equity, and $LRMES_{it}$ stands for long-run MES_{it} . Following [Brownlees and Engle \(2017\)](#), we set k to be 8%. We approximate $LRMES_{it}$ using $LRMES_{it} \approx 1 - \exp(-18MES_{it})$ following the suggestion of [Acharya et al. \(2012\)](#). The contribution of entity i to $SRISK$ is given by:

$$SRISK\%_{it} = \frac{(SRISK_{it})_+}{\sum_{i=1}^N (SRISK_{it})_+}, \quad (1.10)$$

where $(x)_+$ denotes $\max(x, 0)$.

1.2.4 Explanatory variables

In this subsection, we present all explanatory variables used in this study.

Shadow indicator

To measure the impact of shadow insurance, we construct the following indicator:

$$Shadow_{it}(SI_{it}, TR_{it}) = \begin{cases} SI_{it}/TR_{it} & \text{if } SI_{it} > SI_0, \\ 0 & \text{otherwise,} \end{cases} \quad (1.11)$$

where SI_{it} is the amount of shadow insurance practised by entity i at time t ; and TR_{it} is the total insurance reserve entity i has at time t which serves as the scaling variable.⁵ A large value of $Shadow_{it}$ is an indication of high risk because it means that insurer i is heavily engaged in shadow insurance with little reserve, at time t .⁶ Finally, SI_0 is set to be zero as we are interested in all the shadow insurance deals regardless of the dollar amount.

Size and interconnectedness

We include *size* and *interconnectedness* in the analysis as these regulatory metrics are often criticised for being the leading factors driving systemic risk. As a proxy for size, we use the log of total market equity for each entity divided by the log of the cross-sectional average of market equity

⁵Note that we observe shadow insurance and total reserve on the yearly and quarterly basis, respectively. To solve the mixed frequency problem, we create quarterly SI_{it} by taking the simple average of annual shadow insurance.

⁶Replacing total reserve with total assets does not alter our conclusions. See Appendix 1.A.2.

following [Adrian and Brunnermeier \(2016\)](#).⁷ The default of a large financial institution might create a domino effect leading to the failure of other entities in the financial system. Thus, we expect size to be positively related to systemic risk.⁸

To measure the interconnectedness of our sample insurers with the banking system, we use the principal component approach proposed by [Billio et al. \(2012\)](#). For a given quarter, we let σ_i^2 denotes the variance of entity i 's daily return. We then denote Z_i as the standardised daily stock returns of entity i and $V = \text{Cov}(Z_i, Z_j)$ as the covariance matrix of the standardised daily returns across a total of N financial entities.⁹ Next, we decompose matrix V by means of principal component analysis to obtain eigenvalues $\lambda_1, \dots, \lambda_N$, and a matrix $L = (L_{ik})_{ik}$ that contains the eigenvectors of V . The variance of the system is given by:

$$\sigma_s^2 = \sum_{i=1}^N \sum_{j=1}^N \sum_{k=1}^N \sigma_i \sigma_j L_{ik} L_{jk} \lambda_k. \quad (1.12)$$

The univariate measure (in logarithm) of an entity's interconnectedness with the system is given by:

$$PCAS_{i,n} = \log \left(\sum_{k=1}^n \frac{\sigma_i^2}{\sigma_s^2} L_{ik}^2 \lambda_k \Big|_{h_n > H} \right), \quad (1.13)$$

where $h_n = \sum_{k=1}^n \lambda_k / \sum_{k=1}^N \lambda_k$. Following [Billio et al. \(2012\)](#), H is set to be 0.33. In general, the literature agrees that a high degree of interconnectedness with the financial system increases an entity's systemic relevance. We therefore expect this variable to be positively related to systemic risk.¹⁰

Insurer-specific control variables

In addition to the main explanatory variables, we include insurer-specific features as control variables. However, some insurers do not report the control variables needed for our analysis. Specifically, 13 entities do not report *loss ratio*; 11 insurers do not report *total reserves*; 5 entities do not report *total operating expenses*; 2 insurers do not report *return on assets*; and 8 entities do not report *return on equity*. These missing series are estimated using the cross-sectional average.

To control for entity idiosyncratic risk, we use both *VaR* defined in (1.1) and *leverage*.¹¹ Clearly, the former is more related to $\Delta CoVaR$, whereas the latter is more relevant for *SRISK* because *SRISK* is a function of debt and market value of equity. Indeed, our empirical analysis shows that leverage and *VaR* are often redundant in the regression of $\Delta CoVaR$ and *SRISK*, respectively. Therefore, we include according *VaR* in the analysis of $\Delta CoVaR$ and leverage in the regression of

⁷Our conclusions remain unaltered if we replace total market equity with total assets. See Appendix 1.A.2.

⁸See, e.g., [Adrian and Brunnermeier \(2016\)](#), [Bierth et al. \(2015\)](#), [Huang et al. \(2012\)](#) and [Laeven et al. \(2016\)](#).

⁹We consider an additional of 745 banks worldwide available on *Datastream* for the computation of interconnectedness between our main sample and the banking system. This leads to a total of $N = 960$ financial entities.

¹⁰See, e.g., [Billio et al. \(2012\)](#), [Cai et al. \(2018\)](#), [Drehmann and Tarashev \(2013\)](#), [Kojien and Yogo \(2017\)](#) and [Schwarcz \(2015\)](#).

¹¹We thank an anonymous referee for this suggestion.

SRISK for parsimony. To proxy for leverage, we follow Acharya et al. (2017) to use the book value of assets net book value of equity plus the market value of equity, divided by the market value of equity.

We also include other insurer features previously studied by Bierth et al. (2015) as control variables. We use *debt maturity* which is computed using long-term debt divided by total debt to control for the financial health of an entity.¹² To control for insurance portfolio quality, we include the *loss ratio*. Loss ratio is computed by adding claim and loss expenses plus long term insurance reserves, divided by premiums earned. We use *market-to-book ratio* as another control variable to capture market's perception of an entity's value, calculated using the ratio between the market value of equity and book value of equity. To control for manager quality, we include *expense ratio* that is computed as the ratio of operating expenses to total book assets. We use *other income* to control for the degree to which an insurer engages in non-traditional and non-insurance activities. As a proxy for profitability of the insurance entity, we employ the conventional *return on assets* (RoA).¹³

1.2.5 Descriptive statistics

Given the evidence in Zhang et al. (2015) that the extent to which $\Delta CoVaR$ and *SRISK* react to economic downturn vary, we conduct our analysis over two periods: The full sample period and a subsample that focuses on financial distress. In particular, our subsample spans from 2006Q1 to 2011Q2, covering both the United States subprime mortgage crisis and the European great depression. We begin from 2006 because there exists evidence suggesting that is when the accumulation of risk leading to the subprime financial crisis started (see, e.g., Dou et al., 2014; Garriga and Hedlund, 2020). The most notable spillover effect from this crisis is the economic depression in Europe, with Greece being one of the hardest hit countries (Ureche-Rangau and Burietz, 2013). From November 2009 to April 2010, the spread of Greek bonds over German ones increased by an astonishing 451 basis points (Argyrou and Tsoukalas, 2011). Finally, the credit rating of Greece was downgraded by S&P to its lowest rating in 2011Q2, which marks the end of our subsample.

Table 1.3 summarises the quarterly variables for both sample periods. Note that a low (high) $\Delta CoVaR$ (*SRISK*) estimate is the indication of systemic risk relevance. Besides, we summarise the positive dollar term of *SRISK* for ease of comparison with the literature. For the full sample period, the mean estimate of $\Delta CoVaR$ yields -0.14 with a maximum and a minimum of 0.16 and -1.77, respectively. We observe that the average $\Delta CoVaR$ estimate is closer to its maximum than its minimum, suggesting fat tail on the left side of the distribution. This is confirmed by a skewness estimate of -3.29, indicating that the systemic importance of average insurers is less significant economically than certain entities, over a certain period of time. The descriptive

¹²Among all observations for debt maturity, 21 are erroneous (larger than one), and we replace them with the value of one.

¹³Replacing *return on assets* with *return on equity* does not alter our conclusions. See Appendix 1.A.2.

statistics for *SRISK* over the entire sample period yield similar pattern. The mean estimate of *SRISK* is \$2.5 million with a positive skewness of 6.65, highlighting that on average, certain insurance entities significantly contribute more to financial instability, at certain points in time. During the period of financial distress, the mean estimates of $\Delta CoVaR$ (-0.17) and *SRISK* (\$2.7 million) are, respectively, lower and higher than their full sample counterparts. This is expected because systemic risk measures should reflect the financial downturn, though the average *SRISK* is relatively less sensitive to the event. Overall, the descriptive statistics of the distress period show similar pattern to those obtained under the full sample.

Table 1.3 Descriptive statistics

	Mean	Std. dev.	Min	Max	Skew.	Kur.
<i>Full period (2004Q1–2017Q4)</i>						
$\Delta CoVaR$	-0.1400	0.1139	-1.7713	0.1637	-3.2869	24.9535
<i>SRISK</i> (in billions)	0.0025	0.0098	0.0000	0.1619	6.6536	62.2597
<i>Shadow</i>	0.0014	0.0098	0.0000	0.1855	9.9587	116.4354
<i>Size</i>	0.9111	0.1018	0.5558	1.1528	-0.1726	2.2689
<i>Interconnectedness</i>	-10.5645	1.2537	-18.7689	-4.7360	-0.8222	5.9034
<i>VaR</i>	-0.2832	0.2144	-4.0539	0.0000	-3.9369	34.1056
<i>Leverage</i>	8.3289	10.5084	1.0066	298.0079	7.4118	128.9634
<i>Debt maturity</i>	0.7885	0.3400	0.0000	1.0000	-1.5208	3.7719
<i>Loss ratio</i>	159.0058	1869.8982	-1097.2800	79649.2800	34.7699	1313.3755
<i>Market to book</i>	1.6024	1.2586	-5.9023	22.5108	3.4185	25.0726
<i>Operating expenses</i>	2.2513	113.7546	-0.5462	9027.2415	76.4974	5914.9003
<i>Other income</i>	0.0155	1.4927	-0.4524	162.0860	106.6433	11550.5592
<i>RoA</i>	2.5750	16.8849	-919.1300	1056.2500	24.6892	3060.3365
<i>Distress period (2006Q1–2011Q2)</i>						
$\Delta CoVaR$	-0.1725	0.1473	-1.7713	0.1564	-3.0127	18.6358
<i>SRISK</i> (in billions)	0.0027	0.0113	0.0000	0.1619	6.7317	60.2114
<i>Shadow</i>	0.0011	0.0094	0.0000	0.1855	11.5949	158.9202
<i>Size</i>	0.9113	0.1022	0.6587	1.1497	-0.1639	2.2449
<i>Interconnectedness</i>	-10.6507	1.3150	-18.7689	-5.5103	-1.1110	6.2675
<i>VaR</i>	-0.3463	0.2591	-4.0539	0.0000	-3.2934	24.5015
<i>Leverage</i>	8.2505	12.4927	1.0232	298.0079	9.5724	157.1713
<i>Debt maturity</i>	0.7867	0.3440	0.0000	1.0000	-1.5130	3.7186
<i>Loss ratio</i>	89.1225	123.9234	-1097.2800	1928.9600	7.6980	110.5074
<i>Market to book</i>	1.6673	1.2767	-0.7595	13.1590	2.9601	16.5473
<i>Operating expenses</i>	1.1155	15.3583	-0.2476	357.5246	15.9248	268.4476
<i>Other income</i>	0.0340	2.3570	-0.3863	162.0860	68.7305	4725.9244
<i>RoA</i>	2.6214	6.9056	-55.9100	111.7700	6.7756	113.9995

NOTES: The table reports descriptive statistics of the systemic risk measures $\Delta CoVaR$ and *SRISK* estimated at quarterly frequency for a sample of 215 insurance entities worldwide. The positive dollar term of *SRISK* is used. Besides, the tables reports descriptive statistics for the set of quarterly independent variables. We report the mean, standard deviation, minimum, maximum, skewness and kurtosis. Data source: *Datastream* and *Market Intelligence*.

To compare the response of $\Delta CoVaR$ and *SRISK*, in Fig. 1.5 we plot the time evolutions for the cross-sectional means of the two systemic risk measures. Focusing on the average of all entities (solid lines), we observe that $\Delta CoVaR$ is relatively more reactive to the distress period while *SRISK* exhibits much more resilience. For instance, $\Delta CoVaR$ displays the expected spike at the height of the subprime crisis, while the response from *SRISK* is less profound. This is consistent with Zhang et al. (2015), who find $\Delta CoVaR$ to be the most subprime-sensitive among other measures including *SRISK*, based on a diverse group of 240 international financial institutions. We also

notice that *SRISK* is relatively more reactive to other economic events such as the UK's Brexit and China's economic slowdown in 2016. This pattern is in line with Coleman et al. (2018), who focus on a group of Canadian insurance entities. Next, we disentangle the systemic risk of shadow insurers (dashed line) from non-shadow insurers (dotted line). We observe that the dashed line is always lower (higher) than the dotted line for $\Delta CoVaR$ (*SRISK*), implying that an entity practising shadow insurance is, on average, more likely to destabilise the financial system. Interestingly, the *SRISK* of shadow insurers is more responsive to financial distress than that of non-shadow entities, suggesting that the resilience feature of average *SRISK* is primarily driven by those entities not participating in the shadow banking activity.

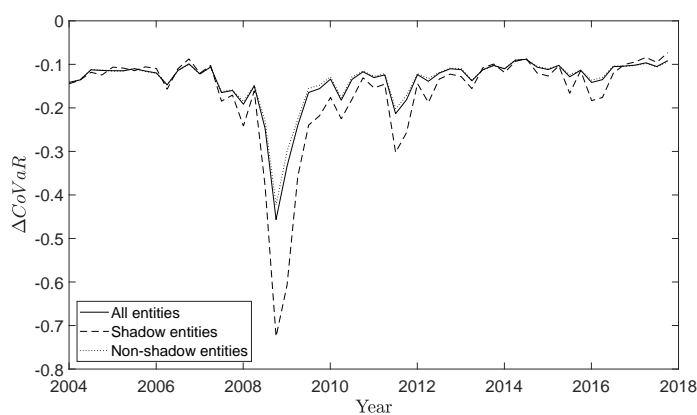
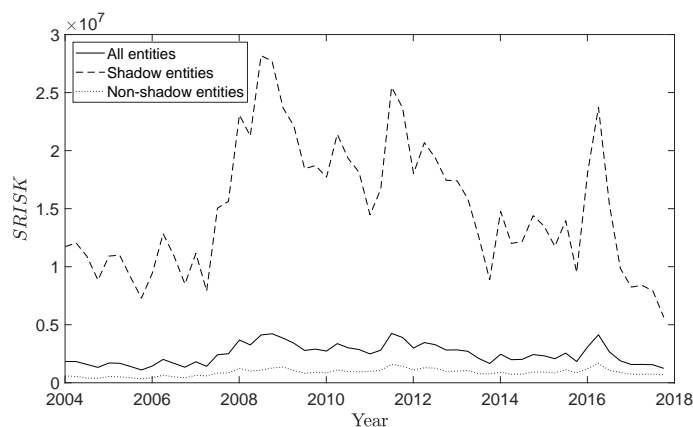
(a) $\Delta CoVaR$ (b) *SRISK*

Figure 1.5 Time evolution of systemic risk. The figures plot the mean quarterly systemic risk measures $\Delta CoVaR$ and *SRISK* of all insurers (solid line), shadow insurers (dashed line) and non-shadow insurers (dotted line), over the full sample period 2004Q1–2017Q4. The positive dollar term of *SRISK* is used.

To understand the driving forces behind an entity's systemic relevance, Table 1.4 summarises several risk-related factors of our sample by periods of study and by whether it uses shadow insurance. For both periods, we observe that entities engaging in shadow insurance are more systemic relevant than their non-shadow counterparts with the shifts in *SRISK* being more profound, as per Fig. 1.5. Besides, we notice that shadow insurers are, on average, larger and more interconnected with the financial system. They also carry higher idiosyncratic risk as shown by a lower *VaR* and a higher leverage. This is consistent with Benoit et al. (2013), who show that if an entity is more interconnected with the financial system and exhibits higher idiosyncratic risk, it should be more systemic relevant irrespective of which of the two systemic risk measures is used. Interestingly, the leverage of shadow insurers experiences some major upshifts during financial distress, while that of non-shadow entities encounters a weak opposite alleviation. Because *SRISK* is closely related to leverage, this explains why, in Fig. 1.5, the *SRISK* of shadow entities is relatively more responsive to financial distress than that of non-shadow insurers.

From the descriptive statistics reported thus far, we learn that an entity using shadow insurance is generally more systemic relevant. Without taking into account the shadow activity's magnitude — as measured by the shadow indicator in (1.11) — we cannot yet imply that the practice of shadow insurance has a direct impact on systemic risk of the financial system. To have an idea about the relation between shadow activity and systemic relevance, in Fig. 1.6 we plot the shadow indicator and systemic risk estimates of Manulife, the most active shadow entity in our sample. We observe that the shadow indicator co-moves with $\Delta CoVaR$ during financial distress. On the other hand, the co-movement with *SRISK* appears to be stronger in the long run. Overall, the plot suggests that shadow insurance seems to drive the risk of financial system at various points in time depending on the employed systemic risk measures. This visual inspection is, of course, unconditional and specific to the case of Manulife.

1.3 Empirical results

In this section, we evaluate and report the factors driving an entity's contribution to systemic risk. First, we report the correlation matrix of the panel variables in Table 1.5. Given the negative (positive) nature of $\Delta CoVaR_{it}$ (*SRISK%*_{*it*}), negative (positive) correlation implies systemic relevance. We observe a weak but statistically significant correlation between the two systemic risk measures, in line with the cross-sectional averages in Fig. 1.5. The shadow indicator shows the expected negative and positive pairwise relations with $\Delta CoVaR_{it}$ and *SRISK%*_{*it*}, respectively. This suggests that, on average, the practice of shadow insurance poses unconditional risks to the financial system. The regulatory metrics size and interconnectedness also display the expected signs of correlation with systemic risk. Most of the control variables show statistically significant pairwise associations with the systemic risk measures. Table 1.6 reports the correlation matrix focusing on the distress period. We observe a strengthened absolute correlation between $\Delta CoVaR_{it}$ and *SRISK%*_{*it*}, suggesting that they exhibit stronger co-movement during the period of financial distress. The key metrics

Table 1.4 Descriptive statistics: Shadow and non-shadow insurers

	Shadow insurers				Non-shadow insurers			
	Mean	Std. dev.	Min	Max	Mean	Std. dev.	Min	Max
<i>Full period (2004Q1-2017Q4)</i>								
<i>ACoVaR</i>	-0.1685	0.1428	-1.3786	-0.0225	-0.1364	0.1092	-1.7713	0.1637
<i>SRSK (in billions)</i>	0.0151	0.0234	0.0000	0.1619	0.0009	0.0041	0.0000	0.0846
<i>Shadow Size</i>	0.0122	0.0269	0.0000	0.1855	0.0000	0.0000	0.0000	0.0000
	1.0237	0.0682	0.7363	1.1470	0.8969	0.0963	0.5558	1.1528
<i>Interconnectedness</i>	-10.0184	0.7847	-13.0931	-7.3624	-10.6331	1.2844	-18.7689	-4.7360
<i>VAR</i>	-0.2861	0.2532	-3.2678	-0.0446	-0.2828	0.2091	-4.0539	0.0000
<i>Leverage</i>	15.0538	19.5413	1.1787	298.0079	7.4838	8.3638	1.0066	128.9460
<i>Distress period (2006Q1-2011Q2)</i>								
<i>ACoVaR</i>	-0.2266	0.1980	-1.3786	-0.0225	-0.1657	0.1382	-1.7713	0.1564
<i>SRSK (in billions)</i>	0.0174	0.0271	0.0000	0.1619	0.0009	0.0045	0.0000	0.0846
<i>Shadow Size</i>	0.0101	0.0265	0.0000	0.1855	0.0000	0.0000	0.0000	0.0000
	1.0219	0.0718	0.7427	1.1332	0.8974	0.0968	0.6587	1.1497
<i>Interconnectedness</i>	-10.0235	0.7950	-13.0931	-7.3624	-10.7295	1.3460	-18.7689	-5.5103
<i>VAR</i>	-0.3889	0.3499	-3.2678	-0.0561	-0.3410	0.2449	-4.0539	0.0000
<i>Leverage</i>	17.5090	28.3108	1.2780	298.0079	7.0871	7.9378	1.0232	108.5136

NOTES: The table reports descriptive statistics of the systemic risk measures *ACoVaR* and *SRSK* estimated at quarterly frequency for shadow and non-shadow insurers. The positive dollar term of *SRSK* is used. Besides, the tables reports descriptive statistics for selected independent variables. We report the mean, standard deviation, minimum and maximum. Data source: *Datastream* and *Market Intelligence*.

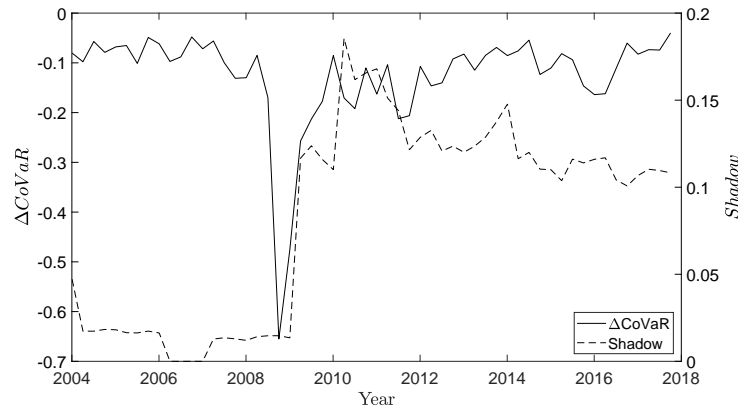
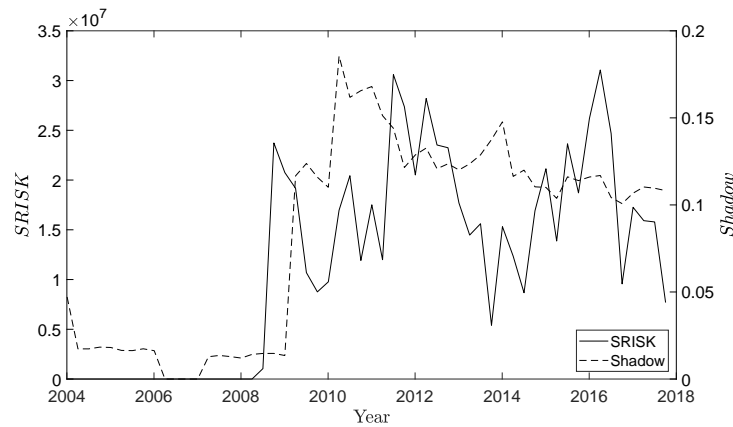
(a) Manulife: $\Delta CoVaR$ and *Shadow*(b) Manulife: *SRISK* and *Shadow*

Figure 1.6 Systemic risk and shadow indicator series of Manulife. The figures plot the quarterly shadow indicator (dashed line) and systemic risk measures $\Delta CoVaR$ and *SRISK* (solid lines) of Manulife over the full sample period 2004Q1–2017Q4. The positive dollar term of *SRISK* is used.

shadow indicator, size and interconnectedness display the expected stronger correlations with $\Delta CoVaR_{it}$, but weaker associations with $SRISK\%_{it}$. In particular, the decrease in correlation is more profound for the shadow indicator. Given the increase in co-movement between $\Delta CoVaR_{it}$ and $SRISK\%_{it}$ during financial distress, the weaker association between the shadow variable and $SRISK\%_{it}$ can be attributed to their stronger long-run correlation, as in the case of Manulife in Fig. 1.6.

In what follows, we specify a panel model that allows testing for the main hypothesis of the paper that shadow insurance increases global systemic risk while properly controlling for other

Table 1.5 Correlation matrix: Full period

	$\Delta CoVaR_{it}$	$SRI SK\%_{it}$	$Shadow_{it}$	$Size_{it}$	$Interconnect-edness_{it}$	Var_{it}	$Leverage_{it}$
$\Delta CoVaR_{it}$	1						
$SRI SK\%_{it}$	-0.0569***	1					
$Shadow_{it}$	-0.0368***	0.0841***	1				
$Size_{it}$	-0.1259***	0.3423***	0.1353***	1			
$Interconnect-edness_{it}$	-0.1187***	0.1928***	0.0531***	0.1355***	1		
Var_{it}	0.6284***	-0.0345***	0.0215**	0.2268***	0.2166***	1	
$Leverage_{it}$	-0.1269***	0.4470***	0.0347***	0.1125***	0.1725***	-0.1602***	1
$Debt\ maturity_{it}$	-0.0708***	-0.0350***	0.0540***	0.3310***	0.0432***	0.0735***	0.1172***
$Lossratio_{it}$	-0.0042	0.0022	-0.0045	0.0216**	0.0193*	0.0144	0.0235**
$Market\ to\ book_{it}$	0.0323***	-0.0864***	-0.0588***	0.0559***	-0.0088	0.0690***	-0.2626***
$Operating\ expenses_{it}$	-0.0220**	-0.0125	-0.007	-0.0721***	0.0530***	-0.0835***	-0.0190*
$Other\ income_{it}$	0.0108	-0.0032	-0.0033	-0.0177*	0.0109	-0.0002	-0.0139
RoA_{it}	0.0584***	-0.1064***	-0.0281***	-0.0196*	-0.1213***	0.1421***	-0.2295***
	$Debt\ maturity_{it}$	$Lossratio_{it}$	$Market\ to\ book_{it}$	$Operating\ expenses_{it}$	$Other\ income_{it}$	RoA_{it}	
$Debt\ maturity_{it}$	1						
$Lossratio_{it}$	0.0233***	1					
$Market\ to\ book_{it}$	-0.1608***	0.0875***	1				
$Operating\ expenses_{it}$	-0.0535***	0.0002	-0.0550***	1			
$Other\ income_{it}$	0.0195*	0.001	0.0260**	0.1086***	1		
RoA_{it}	-0.0758***	-0.0172*	0.2116***	-0.2344***	-0.0348***	1	

NOTES: The table reports the pairwise correlation of all variables for the full period 2004Q1–2017Q4. ***, ** and * represents the significance level at 1%, 5% and 10%, respectively. Data source: *Datastream* and *Market Intelligence*.

Table 1.6 Correlation matrix: Distress period

	$\Delta CoVaR_{it}$	$SRISK_{it}$	$Shadow_{it}$	$Size_{it}$	$Interconnect-edness_{it}$	Var_{it}	$Leverage_{it}$
$\Delta CoVaR_{it}$	1						
$SRISK_{it}$	-0.0784***	1					
$Shadow_{it}$	-0.0702***	0.0333**	1				
$Size_{it}$	-0.2055***	0.3384***	0.1201***	1			
$Interconnectedness_{it}$	-0.1471***	0.1789***	0.0573***	0.2453***	1		
Var_{it}	0.6252***	-0.0619***	-0.0038	0.1373***	-0.2105***	1	
$Leverage_{it}$	-0.1489***	0.4438***	0.0169	0.1706***	0.1844***	-0.1761***	1
$Debt\ maturity_{it}$	-0.0887***	-0.0498***	0.0450***	0.3343***	0.1018***	0.0304*	0.0906***
$Loss\ ratio_{it}$	-0.0141	0.0665***	0.0173	0.1030***	0.0969***	0.0253*	0.1224***
$Market\ to\ book_{it}$	0.0714***	-0.0612***	-0.0443***	0.0979***	0.0363**	0.0650***	-0.2150***
$Operating\ expenses_{it}$	0.0164	-0.017	-0.0084	-0.1138***	0.0135	-0.0523***	-0.0385***
$Other\ income_{it}$	0.0174	-0.0035	-0.0018	-0.0351**	-0.0698***	0.0196	-0.0006
RoA_{it}	0.0436***	-0.0770***	-0.0181	-0.0464***	-0.0984***	0.1376***	-0.1642***
$Debt\ maturity_{it}$		$Loss\ ratio_{it}$	$Market\ to\ book_{it}$	$Operating\ expenses_{it}$	$Other\ income_{it}$	RoA_{it}	
$Debt\ maturity_{it}$	1						
$Loss\ ratio_{it}$	0.0706***	1					
$Market\ to\ book_{it}$	-0.1913***	0.0147	1				
$Operating\ expenses_{it}$	0.0157	0.0002	0.0534***	1			
$Other\ income_{it}$	0.0456***	-0.0018	-0.0148	-0.0005	1		
RoA_{it}	-0.1086***	-0.0700***	0.0936***	-0.1325***	-0.0093	1	

NOTES: The table reports the pairwise correlation of all variables for the distress period 2006Q1–2011Q2. ***, ** and * represents the significance level at 1%, 5% and 10%, respectively. Data source: *Datastream* and *Market Intelligence*.

potential risk factors:

$$\begin{aligned} SystemicRisk_{it} = & \beta_0 + \beta_1 Shadow_{it-1} + \beta_2 Size_{it-1} \\ & + \beta_3 Interconnectedness_{it-1} + \Omega Controls'_{it-1} \\ & + \alpha_i + \eta_t + \epsilon_{it}, \end{aligned} \quad (1.14)$$

where i represents each entity and t represents each quarter; $SystemicRisk_{it}$ is one of the two systemic risk measures ($\Delta CoVaR_{it}$ and $SRISK\%_{it}$) that quantifies entity i 's contribution to systemic risk at time t ; $Shadow_{it-1}$, $Size_{it-1}$, $Interconnectedness_{it-1}$, and $Controls_{it-1}$ denote, respectively, the shadow indicator, size, interconnectedness, and the vector of control variables of entity i at time $t-1$; α_i are entity dummies; η_t are time dummies; and ϵ_{it} is the error term. We analyse both full sample and the distress period to investigate the behaviour of our results. We use both least-squares (LS) and generalised method of moments (GMM) to estimate model (1.14). The former is straightforward to implement, whereas the latter mitigates concern on possible endogeneity of regressors. Specifically, the GMM estimation first-differences each variable so as to eliminate any potential bias that may arise from unobserved entity-specific effects. We perform all of the analyses with clustered standard errors at both country and time levels. Therefore, our setup is such that the clustered standard errors allow for observations of multiple entities in a single country to be dependent for each time period, whereas the inclusion of time dummies correct for any potentially unobservable time-dependent effects that do not vary across entities.

Table 1.7 reports the estimates of model (1.14) using LS for both $\Delta CoVaR_{it}$ and $SRISK\%_{it}$ systemic risk measures. Specification (i) reports the results using $\Delta CoVaR_{it}$ measure for the full sample period. In line with the theory, we find statistically significant evidence showing an entity that is highly interconnected with the financial system contributes more to systemic risk. Besides, size shows the expected negative coefficient and is significant at the 5% level, implying that a larger entity tends to be more systemic relevant because it contributes more to systemic risk. We observe that the shadow indicator is negative and statistically significant at the 5% level. This finding suggests that the practice of shadow insurance increases systemic risk, as we hypothesised. In particular, an increase in the shadow indicator by one standard deviation leads to a decrease of 0.11% in $\Delta CoVaR_{it}$ (0.0098×-0.1108), in the long run. Specification (ii) reports the analysis results using $\Delta CoVaR_{it}$ for the period of financial distress. Size and interconnectedness continue to play a crucial role in driving systemic risk. The shadow indicator shows the expected negative coefficient and is significant at the 1% level. It also displays a higher economic significance: An increase in the shadow indicator by one standard deviation leads to a decrease of 0.22% in $\Delta CoVaR_{it}$ (0.0094×-0.2328). To test whether the impact of shadow insurance is stronger during distress period, in the full sample analysis we add an interaction term given by the shadow indicator and a dummy variable that takes the value of one during financial distress.¹⁴ The results are reported in specification (iii). Indeed, we observe a negative and statistically significant coefficient for the

¹⁴We thank an anonymous referee for this suggestion.

interaction variable, suggesting that the practice of shadow insurance has a more pronounced economic effect during the distress period. Besides, the impact is so significant that the non-distress period effect diminishes, as implied by the insignificant shadow indicator.

Next, we refer to specifications (iv) and (v) in Table 1.7 that report the regressions of $SRISK\%_{it}$ over the full sample and the distress periods, respectively. For both estimation periods, size is positive and statistically significant, suggesting that a larger entity contributes more to systemic risk. Interconnectedness also displays the expected positive sign and is significant at the 5% level. Our shadow indicator shows the expected positive and statistically significant coefficient for the analysis of both the full sample as well as the distress period. Particularly, a unit standard deviation increment of the shadow indicator increases $SRISK\%_{it}$ by 0.20% and 0.12% for the full sample (0.0098×0.1999) and distress period (0.0094×0.1324), respectively. We test whether the shadow variable has a lower impact during the distress period in specification (vi). Interestingly, the shadow-distress interaction term displays a negative and significant coefficient, implying that shadow insurance has relatively weaker effect on systemic risk during financial distress. From the pairwise associations reported in Table 1.5 and Table 1.6, we note that the absolute correlation between $\Delta CoVaR_{it}$ and $SRISK\%_{it}$ increases during financial distress. Specifications (i)–(iii) in Table 1.7 further suggest that shadow insurance has a higher impact on $\Delta CoVaR_{it}$ during the period of distress. Therefore, the relatively weaker impact on $SRISK\%_{it}$ from the shadow variable during financial distress can be attributed to their stronger long-run association that depreciates other subsample effects. Overall, the analysis of $SRISK\%_{it}$ provides further statistical evidence that shadow insurance poses non-trivial risks to the financial system.

Table 1.8 reports the estimates of model (1.14) via GMM for both $\Delta CoVaR_{it}$ and $SRISK\%_{it}$ systemic risk measures. First, we follow the conventional procedure by allowing the use of all possible lagged values of each variable as instruments. Next, we rigorously reduce the number of instruments as Roodman (2009) shows via simulations the potential detrimental effects on the Hansen test given an extensive instrument collection. The author also suggests that the Hansen test should be satisfied with a high p -value to avoid the danger of false positive. In this paper, we carry out both Hansen and difference-in-Hansen tests, and the p -values of the two tests are well above the usual rejection level. The former ensures the joint validity of the selected instruments, whereas the latter assures that instrument exogeneity is satisfied. Finally, we perform the Arellano-Bond test for second-order serial correlation AR(2) to ensure the validity of our GMM results further.

Specifications (i) and (ii) in Table 1.8 report the analysis results using $\Delta CoVaR_{it}$ as the dependent variable for the full sample and the distress periods, respectively. For both estimation windows, we find that the regulatory systemic metrics size and interconnectedness yield the expected negative and significant coefficients; and we observe statistically significant evidence that shadow insurance poses systemic threat to the global financial sector. In particular, an increase in the shadow indicator by one standard deviation decreases $\Delta CoVaR_{it}$ by 0.26% and 0.60% for the full sample (0.0098×-0.2686) and the distress period (0.0094×-0.6361), respectively. In specification (iii), we observe a negative and significant coefficient for the shadow-distress interaction

Table 1.7 Regression results: LS estimation

	$\Delta CoVaR_{it}$ Full (i)	$\Delta CoVaR_{it}$ Distress (ii)	$\Delta CoVaR_{it}$ Full (iii)	$SRISK\%_{it}$ Full (iv)	$SRISK\%_{it}$ Distress (v)	$SRISK\%_{it}$ Full (vi)
$Shadow_{it-1}$	-0.1108** (0.0466)	-0.2328*** (0.0894)	0.1032 (0.0842)	0.1999*** (0.0199)	0.1324*** (0.0206)	0.2288*** (0.0199)
$Size_{it-1}$	-0.0965** (0.0451)	-0.1769** (0.0860)	-0.0916** (0.0450)	0.0868*** (0.0105)	0.1127*** (0.0249)	0.0874*** (0.0105)
$Interconnectedness_{it-1}$	-0.0063*** (0.0017)	-0.0108*** (0.0035)	-0.0063*** (0.0017)	0.0002** (0.0001)	0.0003** (0.0002)	0.0002** (0.0001)
VaR_{it-1}	0.3523*** (0.0106)	0.3731*** (0.0150)	0.3518*** (0.0107)			
$Leverage_{it-1}$				0.0005*** (0.0000)	0.0003*** (0.0001)	0.0005*** (0.0000)
$Debt\ maturity_{it-1}$	0.0047** (0.0021)	0.0133*** (0.0050)	0.0047** (0.0021)	-0.0065*** (0.0010)	-0.0061*** (0.0014)	-0.0065*** (0.0010)
$Loss\ ratio_{it-1}$	0.0000 (0.0000)	0.0000** (0.0000)	0.0000 (0.0000)	0.0000*** (0.0000)	0.0000 (0.0000)	0.0000*** (0.0000)
$Market\ to\ book_{it-1}$	0.0020** (0.0008)	0.0033* (0.0019)	0.0020** (0.0008)	-0.0006*** (0.0001)	-0.0009*** (0.0002)	-0.0006*** (0.0001)
$Operating\ expenses_{it-1}$	0.0003 (0.0003)	-0.0529*** (0.0175)	0.0003 (0.0003)	-0.0000 (0.0000)	-0.0013 (0.0010)	-0.0000 (0.0000)
$Other\ income_{it-1}$	0.0132 (0.0147)	0.0756 (0.0472)	0.0133 (0.0146)	0.0016 (0.0011)	-0.0002 (0.0024)	0.0016 (0.0011)
RoA_{it-1}	-0.0002 (0.0002)	-0.0001 (0.0002)	-0.0002 (0.0002)	-0.0001*** (0.0000)	-0.0001*** (0.0000)	-0.0001*** (0.0000)
$Shadow_{it-1} \times \mathbb{1}(Distress)$			-0.5206*** (0.2003)			-0.0704*** (0.0125)
# Observations	9,319	3,642	9,319	9,319	3,642	9,319
# Entities	215	215	215	215	215	215
Adjusted R^2	0.8262	0.8298	0.8268	0.8032	0.8763	0.8036

NOTES: The table reports the estimates of panel model regressions of quarterly $\Delta CoVaR$ and $SRISK\%$ systemic risk measures for a sample of international insurance entities on shadow indicator and various control variables using LS. The model is given by:

$$SystemicRisk_{it} = \beta_0 + \beta_1 Shadow_{it-1} + \beta_2 Size_{it-1} + \beta_3 Interconnectedness_{it-1} + \Omega Controls'_{it-1} + \alpha_i + \eta_t + \epsilon_{it},$$

where i represents each entity and t represents each time period; $SystemicRisk_{it}$ is one of the two systemic risk measures ($\Delta CoVaR_{it}$ and $SRISK\%_{it}$) that quantify the contribution of entity i to systemic risk at time t ; $Shadow_{it-1}$, $Size_{it-1}$, $Interconnectedness_{it-1}$, and $Controls_{it-1}$ are, respectively, shadow indicator, size, interconnectedness, and the vector of control variables for entity i at time $t-1$; α_i are entity dummies; η_t are time dummies; and ϵ_{it} is the error term. The full sample period runs from 2004Q1 to 2017Q4, whereas the distress period runs from 2006Q1 to 2011Q2. $\mathbb{1}(Distress)$ is a dummy variable that takes the value of one during the distress period. Standard errors (reported in parentheses) are clustered by country and time. ***, ** and * represents the significance level at 1%, 5% and 10%, respectively. Data source: *Datastream* and *Market Intelligence*.

variable, suggesting that the impact shadow insurance has on the financial system is economically more pronounced during the period of distress.

Next, specifications (iv) and (v) report the regressions of $SRISK\%_{it}$ measure for the full sample and the distress periods, respectively. For both estimation windows, size and interconnectedness display the positive and significant coefficients as per our expectation. The coefficient of shadow is positive and statistically significant for both the analysis of the full period and the financial distress. In particular, a unit standard deviation increment of the shadow indicator increases $SRISK\%_{it}$ by 0.13% and 0.08% for the full sample (0.0098×0.1321) and distress period (0.0094×0.0817), respectively. Finally, the interaction variable in specification (vi) provides marginal evidence that shadow insurance has a more profound impact on systemic risk in the long run.

To sum up, the regressions of $\Delta CoVaR$ and $SRISK$ via LS provide evidence that the shadow indicator increases systemic risk in the distress period and the long run. For $\Delta CoVaR$, the effect is greater during financial distress, whereas $SRISK$ suggests a more pronounced long-run impact. The main results are further supported using GMM estimation. Overall, our analyses provide non-trivial evidence that the practice of shadow insurance affects systemic risk and confirm the central hypothesis of the paper.

1.4 Conclusions

In this paper, we evaluated the contribution of shadow insurance to systemic risk of the global financial sector over 2004–2017. We collected 215 international insurance entities from *Datastream* that made up our main sample. To identify shadow insurance activities, we scrutinised every reinsurance agreement from the NAIC Schedule S filings, available to us through *Market Intelligence*. We identified 29 key shadow insurers, and we found that shadow insurance had become an increasingly common practice to reduce regulatory capital with the ultimate goal to increase risk exposure. We documented about 2.8 cents every dollar ceded were shadow in 2004 with the figure growing significantly to 21 cents every dollar in 2017. We found shadow entities to be generally riskier, larger, more interconnected with the financial system and more systemic relevant than their non-shadow counterparts. Our panel analyses provided statistical evidence that the practice of shadow insurance affected financial stability, with $\Delta CoVaR$ suggested a stronger impact during distress period and $SRISK$ indicated a more profound long-run effect.

Table 1.8 Regression results: GMM estimation

	$\Delta CoVaR_{it}$ Full (i)	$\Delta CoVaR_{it}$ Distress (ii)	$\Delta CoVaR_{it}$ Full (iii)	$SRISK\%_{it}$ Full (iv)	$SRISK\%_{it}$ Distress (v)	$SRISK\%_{it}$ Full (vi)
$Shadow_{it-1}$	-0.2686*** (0.0913)	-0.6361*** (0.2269)	-0.0015 (0.0982)	0.1321*** (0.0508)	0.0817*** (0.0298)	0.1613*** (0.0387)
$Size_{it-1}$	-0.2755*** (0.0455)	-0.4230*** (0.1395)	-0.2517*** (0.0375)	0.0483*** (0.0143)	0.0336*** (0.0120)	0.0552*** (0.0111)
$Interconnectedness_{it-1}$	-0.0248*** (0.0054)	-0.0374*** (0.0115)	-0.0243*** (0.0049)	0.0021*** (0.0008)	0.0022*** (0.0006)	0.0025*** (0.0008)
VaR_{it-1}	0.3080*** (0.0354)	0.3067*** (0.0517)	0.2974*** (0.0303)			
$Leverage_{it-1}$				0.0007*** (0.0002)	0.0013*** (0.0002)	0.0006*** (0.0002)
$Debt\ maturity_{it-1}$	-0.0416** (0.0168)	-0.0678* (0.0355)	-0.0471*** (0.0159)	-0.0084** (0.0037)	-0.0131*** (0.0041)	-0.0077** (0.0036)
$Loss\ ratio_{it-1}$	-0.0000 (0.0000)	0.0006 (0.0008)	-0.0000* (0.0000)	0.0000 (0.0000)	-0.0000* (0.0000)	0.0000 (0.0000)
$Market\ to\ book_{it-1}$	0.0421*** (0.0140)	0.0234* (0.0141)	0.0385*** (0.0121)	-0.0033* (0.0017)	0.0033 (0.0028)	-0.0024* (0.0014)
$Operating\ expenses_{it-1}$	-0.0201*** (0.0070)	0.0646 (0.1216)	-0.0193*** (0.0065)	0.0432 (0.0327)	0.0325 (0.0332)	0.0446 (0.0298)
$Other\ income_{it-1}$	-0.4504 (1.0267)	0.4478 (1.5413)	-0.1678 (0.9506)	-1.1212 (0.8913)	-0.0356 (0.0317)	-1.3696 (0.9212)
RoA_{it-1}	-0.0467*** (0.0158)	-0.0415* (0.0238)	-0.0433*** (0.0135)	-0.0006* (0.0003)	-0.0014 (0.0015)	-0.0004* (0.0002)
$Shadow_{it-1}$ $\times \mathbb{1}(Distress)$			-0.7877*** (0.2854)			-0.1240* (0.0721)
# Observations	8,889	3,524	8,889	8,790	3,480	8,790
# Entities	215	215	215	215	215	215
# Instruments	151	75	154	152	74	154
AR(2) test	0.245	0.443	0.247	0.570	0.537	0.337
Hansen test	0.422	0.400	0.352	0.753	0.378	0.632
Diff-in-Hansen test	0.995	0.947	0.997	0.991	0.858	0.909

NOTES: The table reports the estimates of panel model regressions of quarterly $\Delta CoVaR$ and $SRISK\%$ systemic risk measures for a sample of international insurance entities on shadow indicator and various control variables using GMM. The model is given by:

$$SystemicRisk_{it} = \beta_0 + \beta_1 Shadow_{it-1} + \beta_2 Size_{it-1} + \beta_3 Interconnectedness_{it-1} + \Omega Controls'_{it-1} + \alpha_i + \eta_t + \epsilon_{it},$$

where i represents each entity and t represents each time period; $SystemicRisk_{it}$ is one of the two systemic risk measures ($\Delta CoVaR_{it}$ and $SRISK\%_{it}$) that quantify the contribution of entity i to systemic risk at time t ; $Shadow_{it-1}$, $Size_{it-1}$, $Interconnectedness_{it-1}$, and $Controls_{it-1}$ are, respectively, shadow indicator, size, interconnectedness, and the vector of control variables for entity i at time $t-1$; α_i are entity dummies; η_t are time dummies; and ϵ_{it} is the error term. The full sample period runs from 2004Q1 to 2017Q4, whereas the distress period runs from 2006Q1 to 2011Q2. $\mathbb{1}(Distress)$ is a dummy variable that takes the value of one during the distress period. Standard errors (reported in parentheses) are clustered by country and time. ***, ** and * represents the significance level at 1%, 5% and 10%, respectively. Data source: *Datastream* and *Market Intelligence*.

Appendix 1.A

1.A.1 Full sample

The composition of our full sample is listed in Table 1.A.1.

Table 1.A.1 Main sample

<i>Datastream Mnemonic</i>	Entity Name	Name Code	Country
A:IAGX	INSURANCE AUS.GROUP	INS	Australia
A:AMPX	AMP	AMP	Australia
A:QBEX	QBE INSURANCE GROUP	QBE	Australia
A:CGFX	CHALLENGER	CHA	Australia
O:UNIQ	UNIQA INSU GR AG	UNI_2	Austria
O:WNST	VIENNA INSURANCE GROUP A	VIE	Austria
B:AGS	AGEAS (EX-FORTIS)	AGE	Belgium
U:XL	XL GROUP	XL	Bermuda
@ACGL	ARCH CAP.GP.	ARC	Bermuda
U:RE	EVEREST RE GP.	EVE	Bermuda
HSX	HISCOX (DI)	HIS	Bermuda
U:RNR	RENAISSANCERE HDG.	REN	Bermuda
@AGII	ARGO GP.INTL.HOLDINGS	ARG	Bermuda
U:WTM	WHITE MOUNTAINS IN.GP.	WHI	Bermuda
K:ASIF	ASIA FINANCIAL HDG.	ASI	Bermuda
BR:SB3	SEG AL BAHIA ON	SEG	Brazil
C:MFC	MANULIFE FINANCIAL	MAN	Canada
C:GWO	GREAT WEST LIFECO	GRE	Canada
C:SLF	SUN LIFE FINL.	SUN	Canada
C:POWF	POWER FINL.	POW	Canada
C:FFH	FAIRFAX FINL.HDG.	FAI	Canada
C:POW	POWER CORPCANADA	POW_1	Canada
C:IAG	INDL.ALL.IN.& FINL.SVS.	IND	Canada
C:ELF	E-L FINANCIAL	E-L	Canada
C:KFS	KINGSWAY FINL.SVS.	KIN_1	Canada
C:WED	WESTAIM	WES	Canada
CL:CGR	CONSOGRAL	CON	Chile
CL:PVS	PREVISION	PRE	Chile
CP:ATL	ATLANTIC INSURANCES	ATL_1	Cyprus
CP:LLR	LIBERTY LIFE INSURANCE	LIB_1	Cyprus
DK:TOP	TOPDANMARK	TOP	Denmark
DK:ABF	ALM BRAND	ALM	Denmark
EG:DTI	DELTA INSURANCE	DEL	Egypt
M:SAMA	SAMPO 'A'	SAM	Finland
F:MIDI	AXA	AXA	France
F:CNP	CNP ASSURANCES	CNP	France
F:SCO	SCOR SE	SCO	France
F:EULE	EULER HERMES GROUP	EUL	France
F:APR	APRIL	APR	France
D:ALV	ALLIANZ	ALL	Germany
D:ALVX	ALLIANZ (XET)	ALL_1	Germany
D:MUV2	MUENCHENER RUCK.	MUE	Germany
D:MUV2X	MUENCHENER RUCK. (XET)	MUE_1	Germany
D:HNR1	HANNOVER RUCK.	HAN	Germany
D:HNR1X	HANNOVER RUCK. (XET)	HAN_1	Germany

D:NBG6	NUERNBERGER BETS.	NUE	Germany
D:NBG6X	NUERNBERGER BETS. (XET)	NUE_1	Germany
D:SGS	CASH LIFE	CAS	Germany
G:EUPC	EUROPEAN REL.GEN.INS.CR	EUR	Greece
K:CINS	CHINA TAIPING INSURANCE HLDGS	CHI	Hong Kong
K:MIXN	MIN XIN HOLDINGS	MIN	Hong Kong
IN:MAX	MAX FINANCIAL SVS.	MAX	India
IN:RC	RELIANCE CAPITAL	REL	India
IN:TUB	TI FINANCIAL HOLDINGS	TI	India
EG7	FBD HOLDINGS	FBD	Ireland
IS:CLN	CLAL INSURANCE	CLA	Israel
IS:DII	DIRECT INSURANCE	DIR	Israel
IS:HAL	HAREL IN.INVS.& FNSR.	HAR_1	Israel
IS:MNO	MENORA MIV HOLDING	MEN	Israel
IS:MIF	MIGDAL INSURANCE	MIG	Israel
IS:AYL	AYALON	AYA	Israel
IS:ZUR	ZUR	ZUR_1	Israel
IS:PHN	PHOENIX INSURANCE 1	PHO	Israel
I:G	ASSICURAZIONI GENERALI	ASS	Italy
I:BMED	BANCA MEDIOLANUM	BAN	Italy
I:US	UNIPOLSAI	UNI	Italy
I:UNI	UNIPOL GRUPPO FINANZIARI	UNI_1	Italy
I:CASS	CATTOLICA ASSICURAZIONI	CAT_1	Italy
I:VAS	VITTORIA ASSICURAZIONI	VIT	Italy
J:MSAD	MS&AD INSURANCE GPHDG.	MS&	Japan
J:MIHO	TOKIO MARINE HOLDINGS	TOK	Japan
KN:JUB	JUBILEE HOLDINGS	JUB_1	Kenya
KO:AFM	SAMSUNG FIRE & MAR.IN.	SAM_1	Korea
KO:KAF	DB INSURANCE	DB	Korea
KO:HMR	HYUNDAI MARINE & FIRE IN.	HYU	Korea
KO:SDF	HANWHA GENERAL INSURANCE	HAN_3	Korea
KO:KOR	KOREAN REINSURANCE	KOR	Korea
KO:YOF	HEUNGKUK F&M.IN.	HEU	Korea
KO:DHF	LOTTE NON-LIFE IN.	LOT	Korea
L:LPAC	LPI CAPITAL	LPI	Malaysia
L:SYKT	SYARIKAT TAKAFUL MAL.	SYA	Malaysia
L:MAAS	MAA GROUP	MAA	Malaysia
L:BAIS	MANULIFE HOLDINGS	MAN_1	Malaysia
L:MNRE	MNRB HOLDINGS	MNR	Malaysia
L:PAOZ	PACIFIC & ORIENT	PAC	Malaysia
MT:MMS	MAPFRE MIDDLESEA	MAP_1	Malta
MX:GSB	GENERAL SEGUROS	GEN	Mexico
MX:GNP	GRUPO NACIONAL PROVINCIAL	GRU_1	Mexico
MC:WAA	WAFI ASSURANCE	WAF	Morocco
MC:AGM	AGMA LAHLOU TAZI INTERMEDIAIRE D ASSCE.	AGM	Morocco
H:INGA	ING GROEP	ING	Netherlands
H:AGN	AEGON	AEG	Netherlands
Z:TWRZ	TOWER	TOW	New Zealand
N:STB	STOREBRAND	STO	Norway
PK:CUA	JUBILEE LIFE INSURANCE	JUB	Pakistan
PK:ADI	ADAMJEE INSURANCE	ADA	Pakistan
PK:CNI	CENTURY INSURANCE CO.	CEN_1	Pakistan
PK:CYA	CYAN LIMITED	CYA	Pakistan
PK:EFL	EFU LIFE ASSURANCE	EFU	Pakistan
PK:ILI	IGI LIFE INSURANCE	IGI	Pakistan

PK:IGI	INTL.GENERAL INSURANCE	INT	Pakistan
PK:JIN	JUBILLE INSURANCE	JUB_2	Pakistan
T:GELA	GREAT EASTERN HDG.	GRE_1	Singapore
T:HBMP	MEMORIES GROUP	MEM	Singapore
T:REIN	SINGAPORE REIN.	SIN	Singapore
T:UOSI	UNITED OVERSEAS IN.	UNI_8	Singapore
R:SLMJ	SANLAM	SAN	South Africa
R:DSYJ	DISCOVERY	DIS	South Africa
R:LBHJ	LIBERTY HOLDINGS	LIB	South Africa
R:MMIJ	MMI HOLDINGS	MMI	South Africa
R:SNTJ	SANTAM	SAN_1	South Africa
E:MAP	MAPFRE	MAP	Spain
E:GCO	GRUPO CATALANA OCCIDENTE	GRU	Spain
SL:CEI	AVIVA NDB INSURANCE	AVI_1	Sri Lanka
SL:CIS	CEYLINCO INSURANCE	CEY	Sri Lanka
SL:USR	UNION ASSURANCE	UNI_6	Sri Lanka
U:CB	CHUBB	CHU	Switzerland
S:ZURN	ZURICH INSURANCE GROUP	ZUR	Switzerland
S:SREN	SWISS RE	SWI	Switzerland
S:SLHN	SWISS LIFE HOLDING	SWI_1	Switzerland
S:BALN	BALOISE-HOLDING AG	BAL	Switzerland
S:HEPN	HELVETIA HOLDING N	HEL	Switzerland
S:VAH	VAUDOISE 'B'	VAU	Switzerland
TW:CFC	CATHAY FINL.HLDG.	CAT	Taiwan
TW:FUB	FUBON FINL.HLDG.	FUB	Taiwan
TW:CNI	CHINA LIFE INSURANCE	CHI_1	Taiwan
TW:SHK	SHIN KONG FINL.HLDG.	SHI	Taiwan
TW:CRC	CENTRAL REIN.	CEN	Taiwan
TW:TFI	FIRST INSURANCE	FIR_1	Taiwan
TW:SIZ	SHINKONG INSURANCE	SHI_1	Taiwan
TW:TFM	TAIWAN FIRE & MARINE IN.	TAI	Taiwan
TW:UIN	UNION INSURANCE	UNI_7	Taiwan
Q:BKIT	BANGKOK INSURANCE	BAN_1	Thailand
Q:CHAR	CHARAN INSURANCE	CHA_1	Thailand
Q:DHIP	DHIPAYA INSURANCE	DHI	Thailand
Q:INTE	INDARA INSURANCE	IND_2	Thailand
Q:NAMS	NAM SENG INSURANCE	NAM	Thailand
Q:NKIT	NAVAKIJ INSURANCE	NAV_1	Thailand
Q:AYIT	SRI AYUDHYA CAPITAL	SRI	Thailand
Q:TICT	THAI INSURANCE	THA	Thailand
TK:AND	ANADOLU ANONIM TURK SIGORTA SIRKETI LTD.	ANA	Turkey
TK:HAY	ANADOLU HAYAT EMEKLILIK	ANA_1	Turkey
TK:AGA	AKSIGORTA	AKS	Turkey
TK:GSA	GUNES SIGORTA	GUN	Turkey
TK:RAY	RAY SIGORTA	RAY	Turkey
PRU	PRUDENTIAL	PRU	United Kingdom
U:AON	AON CLASS A	AON	United Kingdom
AV	AVIVA	AVI	United Kingdom
LGEN	LEGAL & GENERAL	LEG	United Kingdom
OML	OLD MUTUAL	OLD	United Kingdom
RSA	RSA INSURANCE GROUP	RSA	United Kingdom
STJ	ST.JAMES'S PLACE	ST.	United Kingdom
JLT	JARDINE LLOYD THOMPSON	JAR	United Kingdom
PGH	PERSONAL GROUP HDG.	PER	United Kingdom
U:BRK.A	BERKSHIRE HATHAWAY 'A'	BER	United States
U:AIG	AMERICAN INTL.GP.	AME	United States
U:MET	METLIFE	MET	United States
U:MMC	MARSH & MCLENNAN	MAR	United States

U:TRV	TRAVELERS COS.	TRA	United States
U:PGR	PROGRESSIVE OHIO	PRO	United States
U:AFL	AFLAC	AFL	United States
U:ALL	ALLSTATE	ALL_2	United States
U:HIG	HARTFORD FINL.SVS.GP.	HAR	United States
U:L	LOEWS	LOE	United States
U:CNA	CNA FINANCIAL	CNA	United States
U:LNC	LINCOLN NATIONAL	LIN	United States
U:MKL	MARKEL	MAR_1	United States
U:AJG	ARTHUR J GALLAGHER	ART	United States
@CINF	CINCINNATI FINL.	CIN	United States
U:Y	ALLEGHANY	ALL_3	United States
U:AFG	AMERICAN FINL.GPOHIO	AME_1	United States
U:RGA	REINSURANCE GROUP OF AM.	REI	United States
U:TMK	TORCHMARK	TOR	United States
U:UNM	UNUM GROUP	UNU	United States
U:WRB	W R BERKLEY	W R	United States
U:BRO	BROWN & BROWN	BRO	United States
@ERIE	ERIE INDEMNITY 'A'	ERI	United States
U:THG	HANOVER INSURANCE GROUP	HAN_2	United States
U:ORI	OLD REPUBLIC INTL.	OLD_1	United States
@SIGI	SELECTIVE IN.GP.	SEL	United States
@ANAT	AMER.NAT.IN.	AME_2	United States
U:KMPR	KEMPER	KEM	United States
U:MCY	MERCURY GENERAL	MER	United States
U:PRA	PROASSURANCE	PRO_1	United States
U:RLI	RLI	RLI	United States
@EMCI	EMC INSURANCE GROUP	EMC	United States
U:FFG	FBL FINL.GROUP	FBL	United States
U:HMN	HORACE MANN EDUCATORS	HOR	United States
U:IHC	INDEPENDENCE HOLDING	IND_1	United States
U:MBI	MBIA	MBI	United States
@NWLI	NATIONAL WSTN.LEGP'A'	NAT	United States
@NAVG	NAVIGATORS GROUP	NAV	United States
@STFC	STATE AUTO FINL.	STA	United States
@UFCS	UNITED FIRE GROUP	UNI_3	United States
U:UVE	UNIVERSAL INSURANCE HDG.	UNI_4	United States
@AAME	ATLANTIC AMERICAN	ATL	United States
@BWINA	BALDWIN & LYONS	BAL_1	United States
U:CIA	CITIZENS 'A'	CIT	United States
@FNHC	FEDERATED NATIONAL HDG.	FED	United States
@FACO	FIRST ACCEP.	FIR	United States
@GANS	GAINSCO	GAI	United States
@HALL	HALLMARK FINL.SERVICES	HAL	United States
@KCLI	KANSAS CITY LIFE IN.	KAN	United States
@KINS	KINGSTONE COMPANIES	KIN	United States
@NSEC	NATIONAL SECURITY GROUP	NAT_1	United States
@PRZM	PRISM TECHNOLOGIES GP.	PRI	United States
@UNAM	UNICO AMERICAN	UNI_5	United States
@UTGN	UTG	UTG	United States
U:BRK.B	BERKSHIRE HATHAWAY 'B'	BER_1	United States
@BWINB	BALDWIN & LYON 'B'	BAL_2	United States
@DGICB	DONEGAL GP.'B'	DON	United States
U:CI	CIGNA	CIG	United States
U:CNC	CENTENE	CEN_2	United States
U:PRU	PRUDENTIAL FINL.	PRU_1	United States
@SNFCA	SCTY.NAT.FINL.'A'	SCT	United States

NOTES: List of insurers included in the sample. The table reports the name of all 215 insurers included in the sample, and their mnemonic code on *Datastream*. Sample period: 2004Q1–2017Q4. Data source: *Datastream*

1.A.2 Robustness checks

This section presents the results of other robustness checks that are not reported in the paper. The first robustness check involves using an alternative *FTSE World Financials Index* to estimate both the systemic risk measures $\Delta CoVaR$ and $SRISK$. The main regression results are reported in Table 1.A.2. Specification (i) reports the analysis results using $\Delta CoVaR_{it}$ measure for the full sample period. Similar to the original results, we find statistically significant evidence showing an entity that is highly interconnected with the financial system contributes more to systemic risk. Besides, size shows the expected negative coefficient and is significant at 5% level, implying a larger entity tends to be more systemic relevant. We observe that the shadow indicator is negative and statistically significant at the 5% level, confirming the main hypothesis of the paper. Specification (ii) reports the analysis results using $\Delta CoVaR_{it}$ for the period of financial distress. Size and interconnectedness continue to play a crucial role in driving systemic risk, although the former is only marginally significant. The shadow indicator shows the expected negative coefficient and is significant at the 5% level. The shadow-distress interaction variable in Specification (iii) is negative and significant, suggesting that shadow insurance has a greater impact during financial distress. Next, we refer to Specifications (iv) and (v) in Table 1.A.2 that report the analysis results using $SRISK\%_{it}$ as the dependent variable for the full sample and the distress period, respectively. For both estimation windows, size is positive and statistically significant, suggesting that a larger entity contributes more to systemic risk. Interconnectedness shows the expected positive sign, although it is only marginally significant for the full estimation window. The shadow indicator shows the expected positive and statistically significant coefficient for the analysis of both the full sample and the distress period. Finally, the distress-shadow interaction in Specification (vi) shows a negative and statistically significant coefficient, suggesting that shadow insurance has a more profound long-run effect on systemic risk. In summary, the regulatory metrics size and interconnectedness continue to highlight their pivotal role in the spreading of systemic risk, although with a weaker significance level in certain cases. Instead, the coefficient of shadow is always significant at the 5% level, with $\Delta CoVaR_{it}$ showing a stronger impact during financial distress and $SRISK\%_{it}$ suggesting a greater long-run effect.

The second robustness check involves using total assets as the scaling variable for the shadow indicator. The main regression results are reported in Table 1.A.3. In terms of statistical evidence, there is virtually no difference between the results from Table 1.A.3 and those reported in the main paper. In summary, the systemic risk metrics size and interconnectedness highlight their pivotal roles in driving systemic risk. Moreover, the practice of shadow insurance continues to pose a systemic threat to the financial system, with $\Delta CoVaR_{it}$ showing a stronger impact during distress period and $SRISK\%_{it}$ suggesting a greater long-run effect.

The third robustness check involves replacing total market equity with total assets for the computation of the variable *size*. The main regression results are reported in Table 1.A.4. Specification (i) reports the analysis results using $\Delta CoVaR_{it}$ measure for the full sample period. Similar to the

original results, we find statistically significant evidence that interconnectedness and size drive systemic risk. Besides, we observe that the shadow indicator is negative and statistically significant at the 5% level. Specification (ii) reports the analysis results using $\Delta CoVaR_{it}$ for the period of financial distress. Interconnectedness continues to play a crucial role in driving systemic risk. Size, however, does not significantly affect systemic risk despite showing the expected sign. The shadow indicator shows the expected negative coefficient and is significant at the 5% level. Specification (iii) suggests that the shadow variable has a greater economic impact during financial distress. Next, we refer to Specifications (iv) and (v) in Table 1.A.4 that report the analysis results using $SRISK\%_{it}$ as the dependent variable for the full sample and the distress period, respectively. For the full sample and the distress period, size is positive and statistically significant. Interconnectedness shows the expected positive sign and is significant at the 5% level. Besides, the shadow indicator shows the expected positive and statistically significant coefficient for the analysis of both the full sample as well as the distress period. Finally, the negative and significant distress-shadow interaction variable in Specification (vi) suggests that shadow insurance has a relatively stronger long-term effect on systemic risk. To sum up, except for the regression of $\Delta CoVaR_{it}$ during the financial distress in which the coefficient of size is insignificant, there is virtually no difference between the results from Table 1.A.3 and those reported in the main paper.

The fourth robustness check involves replacing *return of assets* with *return of equity*. The main regression results are reported in Table 1.A.5. Specification (i) reports the analysis results using $\Delta CoVaR_{it}$ measure for the full sample period. Similar to the original results, we find statistically significant evidence showing interconnectedness increases systemic risk. Besides, size shows the expected negative coefficient and is significant at 5% level. We observe that the shadow indicator is negative and statistically significant at the 5% level. Specification (ii) reports the analysis results using $\Delta CoVaR_{it}$ for the period of financial distress. Size and interconnectedness continue to play a crucial role in driving systemic risk, though the former is weakly significant at the 10% level. The shadow indicator shows the expected negative coefficient and is significant at the 1% level. We observe a negative and significant distress-shadow interaction variable in Specification (iii), suggesting that shadow insurance has a relatively stronger impact during financial distress. Next, we refer to Specification (iv) and (v) in Table 1.A.5 that report the analysis results using $SRISK\%_{it}$ as the dependent variable for the full sample and the distress period, respectively. For both estimation windows, size is positive and statistically significant. Interconnectedness shows the expected positive sign, although it is only marginally significant for the period of financial distress. Besides, the shadow indicator shows the expected positive and statistically significant coefficient for the analysis of both the full sample and the distress period. Finally, the distress-shadow interaction variable in Specification (vi) suggests that shadow insurance has a more profound long-run effect on systemic risk.

Summing up all of the robustness analyses, we find that the systemic metric size and interconnectedness play a pivotal role in the spreading of systemic risk, though in a few cases, the evidence is marginal. On the other hand, the coefficient of shadow is always significant at the 5% level, with

$\Delta CoVaR$ showing a stronger economic impact during financial distress and $SRISK$ suggesting a greater long-run effect. These analyses show the persistence of shadow insurance in driving systemic risk, and thus, confirm the central hypothesis of the paper.

Table 1.A.2 Regression results: Robustness 1

	$\Delta CoVaR_{it}$ Full (i)	$\Delta CoVaR_{it}$ Distress (ii)	$\Delta CoVaR_{it}$ Full (iii)	$SRISK\%_{it}$ Full (iv)	$SRISK\%_{it}$ Distress (v)	$SRISK\%_{it}$ Full (vi)
$Shadow_{it-1}$	-0.0888** (0.0450)	-0.1986** (0.0846)	0.1052 (0.0820)	0.1979*** (0.0198)	0.1317*** (0.0206)	0.2262*** (0.0200)
$Size_{it-1}$	-0.0931** (0.0434)	-0.1423* (0.0820)	-0.0887** (0.0433)	0.0865*** (0.0105)	0.1134*** (0.0251)	0.0871*** (0.0106)
$Interconnectedness_{it-1}$	-0.0067*** (0.0017)	-0.0112*** (0.0033)	-0.0067*** (0.0017)	0.0002* (0.0001)	0.0003** (0.0002)	0.0002** (0.0001)
VaR_{it-1}	0.3380*** (0.0103)	0.3552*** (0.0143)	0.3376*** (0.0104)			
$Leverage_{it-1}$				0.0005*** (0.0000)	0.0004*** (0.0001)	0.0005*** (0.0000)
$Debt\ maturity_{it-1}$	0.0050** (0.0021)	0.0129*** (0.0049)	0.0050** (0.0021)	-0.0065*** (0.0010)	-0.0060*** (0.0014)	-0.0065*** (0.0010)
$Loss\ ratio_{it-1}$	0.0000 (0.0000)	0.0000** (0.0000)	0.0000 (0.0000)	0.0000*** (0.0000)	0.0000 (0.0000)	0.0000*** (0.0000)
$Market\ to\ book_{it-1}$	0.0020** (0.0008)	0.0028 (0.0019)	0.0019** (0.0008)	-0.0006*** (0.0001)	-0.0009*** (0.0002)	-0.0006*** (0.0001)
$Operating\ expenses_{it-1}$	0.0003 (0.0002)	-0.0553*** (0.0172)	0.0003 (0.0002)	-0.0000 (0.0000)	-0.0013 (0.0010)	-0.0000 (0.0000)
$Other\ income_{it-1}$	0.0126 (0.0141)	0.0768* (0.0465)	0.0127 (0.0141)	0.0016 (0.0011)	-0.0004 (0.0024)	0.0016 (0.0011)
RoA_{it-1}	-0.0002 (0.0002)	-0.0001 (0.0002)	-0.0002 (0.0002)	-0.0001*** (0.0000)	-0.0001*** (0.0000)	-0.0001*** (0.0000)
$Shadow_{it-1}$ $\times \mathbb{1}(Distress)$			-0.4719** (0.1869)			-0.0688*** (0.0127)
# Observations	9,319	3,642	9,319	9,319	3,642	9,319
# Entities	215	215	215	215	215	215
Adjusted R^2	0.8260	0.8297	0.8265	0.8039	0.8762	0.8042

NOTES: The table reports the estimates of panel model regressions of quarterly $\Delta CoVaR$ and $SRISK\%$ systemic risk measures for a sample of international insurance entities on shadow indicator and various control variables using LS. The model is given by:

$$SystemicRisk_{it} = \beta_0 + \beta_1 Shadow_{it-1} + \beta_2 Size_{it-1} + \beta_3 Interconnectedness_{it-1} + \Omega Controls'_{it-1} + \alpha_i + \eta_t + \epsilon_{it},$$

where i represents each entity and t represents each time period; $SystemicRisk_{it}$ is one of the two systemic risk measures ($\Delta CoVaR_{it}$ and $SRISK\%_{it}$) that quantify the contribution of entity i to systemic risk at time t ; $Shadow_{it-1}$, $Size_{it-1}$, $Interconnectedness_{it-1}$, and $Controls_{it-1}$ are, respectively, shadow indicator, size, interconnectedness, and the vector of control variables for entity i at time $t-1$; α_i are entity dummies; η_t are time dummies; and ϵ_{it} is the error term. The full sample period runs from 2004Q1 to 2017Q4, whereas the distress period runs from 2006Q1 to 2011Q2. $\mathbb{1}(Distress)$ is a dummy variable that takes the value of one during the distress period. Standard errors (reported in parentheses) are clustered by country and time. ***, ** and * represents the significance level at 1%, 5% and 10%, respectively. Data source: *Datastream* and *Market Intelligence*.

Table 1.A.3 Regression results: Robustness 2

	$\Delta CoVaR_{it}$ Full (i)	$\Delta CoVaR_{it}$ Distress (ii)	$\Delta CoVaR_{it}$ Full (iii)	$SRISK\%_{it}$ Full (iv)	$SRISK\%_{it}$ Distress (v)	$SRISK\%_{it}$ Full (vi)
<i>Shadow</i> _{<i>i</i><i>t</i>-1}	-0.4148** (0.1929)	-0.9612*** (0.3529)	0.0392 (0.1449)	0.3845*** (0.0440)	0.2630*** (0.0558)	0.4224*** (0.0452)
<i>Size</i> _{<i>i</i><i>t</i>-1}	-0.0964** (0.0451)	-0.1760** (0.0856)	-0.0914** (0.0450)	0.0864*** (0.0105)	0.1125*** (0.0249)	0.0868*** (0.0105)
<i>Interconnectedness</i> _{<i>i</i><i>t</i>-1}	-0.0063*** (0.0017)	-0.0106*** (0.0035)	-0.0062*** (0.0017)	0.0002** (0.0001)	0.0003** (0.0002)	0.0002** (0.0001)
<i>VaR</i> _{<i>i</i><i>t</i>-1}	0.3526*** (0.0106)	0.3734*** (0.0151)	0.3521*** (0.0107)			
<i>Leverage</i> _{<i>i</i><i>t</i>-1}				0.0005*** (0.0000)	0.0003*** (0.0001)	0.0005*** (0.0000)
<i>Debt maturity</i> _{<i>i</i><i>t</i>-1}	0.0047** (0.0021)	0.0133*** (0.0050)	0.0047** (0.0021)	-0.0065*** (0.0010)	-0.0060*** (0.0014)	-0.0065*** (0.0010)
<i>Loss ratio</i> _{<i>i</i><i>t</i>-1}	0.0000 (0.0000)	0.0000** (0.0000)	0.0000 (0.0000)	0.0000*** (0.0000)	0.0000 (0.0000)	0.0000*** (0.0000)
<i>Market to book</i> _{<i>i</i><i>t</i>-1}	0.0020** (0.0008)	0.0034* (0.0019)	0.0019** (0.0008)	-0.0006*** (0.0001)	-0.0009*** (0.0002)	-0.0006*** (0.0001)
<i>Operating expenses</i> _{<i>i</i><i>t</i>-1}	0.0003 (0.0003)	-0.0527*** (0.0175)	0.0003 (0.0003)	-0.0000 (0.0000)	-0.0013 (0.0010)	-0.0000 (0.0000)
<i>Other income</i> _{<i>i</i><i>t</i>-1}	0.0132 (0.0146)	0.0753 (0.0469)	0.0132 (0.0145)	0.0016 (0.0011)	-0.0002 (0.0024)	0.0016 (0.0011)
<i>RoA</i> _{<i>i</i><i>t</i>-1}	-0.0002 (0.0002)	-0.0001 (0.0002)	-0.0002 (0.0002)	-0.0001*** (0.0000)	-0.0001*** (0.0000)	-0.0001*** (0.0000)
<i>Shadow</i> _{<i>i</i><i>t</i>-1} × $\mathbb{1}(Distress)$			-1.0972*** (0.4101)			-0.0916*** (0.0187)
# Observations	9,319	3,642	9,319	9,319	3,642	9,319
# Entities	215	215	215	215	215	215
Adjusted <i>R</i> ²	0.8264	0.8301	0.8272	0.8029	0.8761	0.8031

NOTES: The table reports the estimates of panel model regressions of quarterly $\Delta CoVaR$ and $SRISK\%$ systemic risk measures for a sample of international insurance entities on shadow indicator and various control variables using LS. The model is given by:

$$SystemicRisk_{it} = \beta_0 + \beta_1 Shadow_{it-1} + \beta_2 Size_{it-1} + \beta_3 Interconnectedness_{it-1} + \Omega Controls'_{it-1} + \alpha_i + \eta_t + \epsilon_{it},$$

where *i* represents each entity and *t* represents each time period; *SystemicRisk*_{*i**t*} is one of the two systemic risk measures ($\Delta CoVaR_{it}$ and $SRISK\%_{it}$) that quantify the contribution of entity *i* to systemic risk at time *t*; *Shadow*_{*i**t*-1}, *Size*_{*i**t*-1}, *Interconnectedness*_{*i**t*-1}, and *Controls*_{*i**t*-1} are, respectively, shadow indicator, size, interconnectedness, and the vector of control variables for entity *i* at time *t* - 1; α_i are entity dummies; η_t are time dummies; and ϵ_{it} is the error term. The full sample period runs from 2004Q1 to 2017Q4, whereas the distress period runs from 2006Q1 to 2011Q2. $\mathbb{1}(Distress)$ is a dummy variable that takes the value of one during the distress period. Standard errors (reported in parentheses) are clustered by country and time. ***, ** and * represents the significance level at 1%, 5% and 10%, respectively. Data source: *Datastream* and *Market Intelligence*.

Table 1.A.4 Regression results: Robustness 3

	$\Delta CoVaR_{it}$ Full (i)	$\Delta CoVaR_{it}$ Distress (ii)	$\Delta CoVaR_{it}$ Full (iii)	$SRISK\%_{it}$ Full (iv)	$SRISK\%_{it}$ Distress (v)	$SRISK\%_{it}$ Full (vi)
<i>Shadow</i> _{<i>it</i>-1}	-0.1034** (0.0457)	-0.2290** (0.0901)	0.1121 (0.0834)	0.1937*** (0.0194)	0.1266*** (0.0199)	0.2217*** (0.0195)
<i>Size</i> _{<i>it</i>-1}	-0.1133*** (0.0366)	-0.0481 (0.1077)	-0.1110*** (0.0364)	0.1245*** (0.0139)	0.2426*** (0.0442)	0.1249*** (0.0139)
<i>Interconnectedness</i> _{<i>it</i>-1}	-0.0062*** (0.0017)	-0.0103*** (0.0034)	-0.0062*** (0.0017)	0.0002** (0.0001)	0.0004** (0.0002)	0.0002** (0.0001)
<i>Var</i> _{<i>it</i>-1}	0.3511*** (0.0107)	0.3712*** (0.0150)	0.3507*** (0.0108)			
<i>Leverage</i> _{<i>it</i>-1}				0.0003*** (0.0000)	0.0002*** (0.0000)	0.0003*** (0.0000)
<i>Debt maturity</i> _{<i>it</i>-1}	0.0047** (0.0021)	0.0135*** (0.0049)	0.0047** (0.0021)	-0.0065*** (0.0010)	-0.0050*** (0.0013)	-0.0065*** (0.0010)
<i>Loss ratio</i> _{<i>it</i>-1}	0.0000* (0.0000)	0.0000** (0.0000)	0.0000* (0.0000)	0.0000** (0.0000)	0.0000 (0.0000)	0.0000** (0.0000)
<i>Market to book</i> _{<i>it</i>-1}	0.0010 (0.0008)	0.0015 (0.0018)	0.0010 (0.0008)	0.0002 (0.0001)	0.0002 (0.0002)	0.0002 (0.0001)
<i>Operating expenses</i> _{<i>it</i>-1}	0.0002 (0.0003)	-0.0499*** (0.0175)	0.0002 (0.0003)	0.0000* (0.0000)	0.0015 (0.0011)	0.0000* (0.0000)
<i>Other income</i> _{<i>it</i>-1}	0.0137 (0.0147)	0.0770 (0.0482)	0.0138 (0.0146)	0.0014 (0.0017)	-0.0087** (0.0039)	0.0014 (0.0017)
<i>RoA</i> _{<i>it</i>-1}	-0.0003 (0.0002)	-0.0002 (0.0002)	-0.0003 (0.0002)	-0.0000** (0.0000)	-0.0001*** (0.0000)	-0.0000** (0.0000)
<i>Shadow</i> _{<i>it</i>-1} × $\mathbb{1}(Distress)$			-0.5255*** (0.2006)			-0.0684*** (0.0124)
# Observations	9,319	3,642	9,319	9,319	3,642	9,319
# Entities	215	215	215	215	215	215
Adjusted <i>R</i> ²	0.8262	0.8296	0.8268	0.8065	0.8825	0.8068

NOTES: The table reports the estimates of panel model regressions of quarterly $\Delta CoVaR$ and $SRISK\%$ systemic risk measures for a sample of international insurance entities on shadow indicator and various control variables using LS. The model is given by:

$$SystemicRisk_{it} = \beta_0 + \beta_1 Shadow_{it-1} + \beta_2 Size_{it-1} + \beta_3 Interconnectedness_{it-1} + \Omega Controls'_{it-1} + \alpha_i + \eta_t + \epsilon_{it},$$

where i represents each entity and t represents each time period; $SystemicRisk_{it}$ is one of the two systemic risk measures ($\Delta CoVaR_{it}$ and $SRISK\%_{it}$) that quantify the contribution of entity i to systemic risk at time t ; $Shadow_{it-1}$, $Size_{it-1}$, $Interconnectedness_{it-1}$, and $Controls_{it-1}$ are, respectively, shadow indicator, size, interconnectedness, and the vector of control variables for entity i at time $t-1$; α_i are entity dummies; η_t are time dummies; and ϵ_{it} is the error term. The full sample period runs from 2004Q1 to 2017Q4, whereas the distress period runs from 2006Q1 to 2011Q2. $\mathbb{1}(Distress)$ is a dummy variable that takes the value of one during the distress period. Standard errors (reported in parentheses) are clustered by country and time. ***, ** and * represents the significance level at 1%, 5% and 10%, respectively. Data source: *Datastream* and *Market Intelligence*.

Table 1.A.5 Regression results: Robustness 4

	$\Delta CoVaR_{it}$ Full (i)	$\Delta CoVaR_{it}$ Distress (ii)	$\Delta CoVaR_{it}$ Full (iii)	$SRISK\%_{it}$ Full (iv)	$SRISK\%_{it}$ Distress (v)	$SRISK\%_{it}$ Full (vi)
<i>Shadow</i> _{<i>i</i><i>t</i>-1}	-0.1132** (0.0466)	-0.2386*** (0.0905)	0.1014 (0.0856)	0.1982*** (0.0199)	0.1321*** (0.0208)	0.2268*** (0.0199)
<i>Size</i> _{<i>i</i><i>t</i>-1}	-0.0954** (0.0478)	-0.1515* (0.0785)	-0.0903* (0.0480)	0.0828*** (0.0101)	0.1008*** (0.0235)	0.0834*** (0.0101)
<i>Interconnectedness</i> _{<i>i</i><i>t</i>-1}	-0.0063*** (0.0017)	-0.0105*** (0.0034)	-0.0062*** (0.0017)	0.0002** (0.0001)	0.0003* (0.0002)	0.0002** (0.0001)
<i>VaR</i> _{<i>i</i><i>t</i>-1}	0.3524*** (0.0105)	0.3737*** (0.0148)	0.3519*** (0.0106)			
<i>Leverage</i> _{<i>i</i><i>t</i>-1}				0.0005*** (0.0000)	0.0004*** (0.0001)	0.0005*** (0.0000)
<i>Debt maturity</i> _{<i>i</i><i>t</i>-1}	0.0046** (0.0021)	0.0133*** (0.0050)	0.0046** (0.0021)	-0.0065*** (0.0010)	-0.0062*** (0.0014)	-0.0065*** (0.0010)
<i>Loss ratio</i> _{<i>i</i><i>t</i>-1}	0.0000 (0.0000)	0.0000** (0.0000)	0.0000 (0.0000)	0.0000*** (0.0000)	0.0000 (0.0000)	0.0000*** (0.0000)
<i>Market to book</i> _{<i>i</i><i>t</i>-1}	0.0020** (0.0008)	0.0032* (0.0019)	0.0020** (0.0008)	-0.0005*** (0.0001)	-0.0008*** (0.0002)	-0.0005*** (0.0001)
<i>Operating expenses</i> _{<i>i</i><i>t</i>-1}	0.0003 (0.0003)	-0.0529*** (0.0175)	0.0003 (0.0003)	0.0000 (0.0000)	-0.0012 (0.0010)	0.0000 (0.0000)
<i>Other income</i> _{<i>i</i><i>t</i>-1}	0.0133 (0.0147)	0.0736 (0.0459)	0.0134 (0.0146)	0.0018 (0.0011)	0.0001 (0.0024)	0.0018 (0.0011)
<i>RoA</i> _{<i>i</i><i>t</i>-1}	-0.0000 (0.0001)	-0.0001 (0.0001)	-0.0000 (0.0001)	0.0000** (0.0000)	0.0000 (0.0000)	0.0000* (0.0000)
<i>Shadow</i> _{<i>i</i><i>t</i>-1} × $\mathbb{1}(Distress)$			-0.5220*** (0.2014)			-0.0697*** (0.0125)
# Observations	9,319	3,642	9,319	9,319	3,642	9,319
# Entities	215	215	215	215	215	215
Adjusted <i>R</i> ²	0.8265	0.8300	0.8271	0.8033	0.8766	0.8036

NOTES: The table reports the estimates of panel model regressions of quarterly $\Delta CoVaR$ and $SRISK\%$ systemic risk measures for a sample of international insurance entities on shadow indicator and various control variables using LS. The model is given by:

$$SystemicRisk_{it} = \beta_0 + \beta_1 Shadow_{it-1} + \beta_2 Size_{it-1} + \beta_3 Interconnectedness_{it-1} + \Omega Controls'_{it-1} + \alpha_i + \eta_t + \epsilon_{it},$$

where *i* represents each entity and *t* represents each time period; *SystemicRisk*_{*i**t*} is one of the two systemic risk measures ($\Delta CoVaR_{it}$ and $SRISK\%_{it}$) that quantify the contribution of entity *i* to systemic risk at time *t*; *Shadow*_{*i**t*-1}, *Size*_{*i**t*-1}, *Interconnectedness*_{*i**t*-1}, and *Controls*_{*i**t*-1} are, respectively, shadow indicator, size, interconnectedness, and the vector of control variables for entity *i* at time *t* - 1; α_i are entity dummies; η_t are time dummies; and ϵ_{it} is the error term. The full sample period runs from 2004Q1 to 2017Q4, whereas the distress period runs from 2006Q1 to 2011Q2. $\mathbb{1}(Distress)$ is a dummy variable that takes the value of one during the distress period. Standard errors (reported in parentheses) are clustered by country and time. ***, ** and * represents the significance level at 1%, 5% and 10%, respectively. Data source: *Datastream* and *Market Intelligence*.

A MULTIVARIATE NONPARAMETRIC TEST FOR VOLATILITY SPILLOVER[†]

2.1 Introduction

Volatility is undoubtedly one of the most informative indicators in finance as it is fundamentally related to, among others, market liquidity risk (Garbade and Silber, 1979), the interaction between informed and strategic traders (Admati and Pfleiderer, 1988), the rate of information flow to the market (Ross, 1989), revealed private information (Stoll and Whaley, 1990), and the degree of international markets links following attempts by participants to infer information from other markets (King and Wadhvani, 1990). At the regional level, empirical evidence suggests there is strong volatility comovement within and across asset classes (Bollerslev et al., 2018). Consequently, a statistical tool that detects volatility spillover between markets or asset classes could provide valuable information in hedging variance risk (Bakshi and Kapadia, 2003) as well as pricing the volatility index (VIX) derivatives (Bardgett et al., 2019).

The academics and practitioners in macroeconomics and finance regularly concern with testing volatility spillover between markets characterized by multiple indices in which a univariate test is inadequate because it does not take into account covariances. The latter can play a nontrivial role in driving spillover as shown in our Monte Carlo study. In this paper, we propose a new econometric strategy for testing volatility spillover between two potentially multivariate financial markets.¹ We begin by generalizing the univariate hypothesis of Hong (2001) to the multivariate setup. We follow the author to define volatility spillover using the notion of Granger (1969, 1980) causality in variance, in that there is volatility spillover from Y_2 to Y_1 if any of the past variances of

[†]A research manuscript (joint with G. Urga) based on the results in this chapter entitled “A Multivariate Nonparametric Test for Volatility Spillover” is under revision at *Econometric Theory*.

¹Other risk measures are proposed in, for instance, Acharya et al. (2017); Bouhaddioui and Roy (2006); Brownlees and Engle (2017); Candelon and Tokpavi (2016); Casarin et al. (2018); Corradi et al. (2019); Diebold and Yilmaz (2012); Forbes and Rigobon (2002); Fry et al. (2010); Hong et al. (2009); Weller (2019).

Y_2 has predictive power over the current variance of Y_1 . Therefore, the terms *variance causality* and *volatility spillover* may be used interchangeably. We derive testable statistics for our hypotheses using normalized cross-spectra and we develop the asymptotic theory. Our test statistics possess several appealing features. First, the computation of our test statistics is relatively simple since it requires only the estimation of standardized residuals which are the main event variables. Unlike most existing parameter restriction tests which estimate all series in a global model, our procedures allow the event variables of Y_1 and Y_2 to be estimated separately. Second, our tests check a large number of lag orders M as the sample size T increases. In fact, we allow (but we do not require) M to grow with T at a proper rate to ensure power against a broad class of alternatives such as delayed spillover effect. Third, our frequency domain kernel-based procedure allows flexible weighting of the cross-spectrum at each lag order. We show that the conventional Granger-type regression procedure can be viewed as a special case of our approach when the Truncated kernel is used. Both tests assign equal weight to each lag. Instead, we propose to use downward weighting kernels to enhance the power of our tests because empirical stylized facts suggest that market participants discount past information and thus spillover effect is expected to decay over time. Indeed, simulation evidence shows that our downward weighting tests can check a large number of lags without losing significant power when compared with an equally weighted test.

The paper further proposes an optimal multivariate volatility model to facilitate estimating the spillover test statistics in the higher dimension. The proposed structure resembles the constant conditional correlation (CCC) specification in Bollerslev (1990). Compare with the CCC model, we specify the elements in the diagonal matrix as general infinite order autoregressive conditional heteroskedasticity [ARCH(∞)] processes to minimize the risk of misspecification because a misspecified model may yield autocorrelated squared standardized residuals (see, e.g., Li and Mak, 1994). This will in turn contaminate the resulting test statistics by invalidating its asymptotic property. Indeed, our supplementary empirical study shows that serial correlation induced by an inadequate ARCH may give misleading inferential result.² In this aspect, the proposed long ARCH(∞) process — which is sometimes referred to as a “nonparametric” approach — is more appealing than conditional variance models with a prespecified order. Regarding model estimation, we show that least-squares (LS) is feasible and we thus propose its consistent estimators. Our method requires only about 5% of the computing time of quasi maximum likelihood estimation (QMLE). For notational simplicity, we call our approach the NCCC-LS model, where the acronym stands for Nonparametric-CCC-Least-Squares.

Our econometric strategy proceeds in two stages. First, we estimate the event variables by fitting the newly proposed NCCC-LS model to the observed data. Second, we compute our kernel-based test statistics to draw inference about volatility spillover. Throughout our econometric strategy, we need not perform numerical integration nor optimization. An extensive Monte Carlo study shows that our inferential strategy provides reliable finite sample inference even in the higher

²See Appendix 2.H.

dimension up to the case of 10 series while the simulation evidence in most other papers is limited to 2–3 series. We further provide a consistent bootstrap test whose finite sample size is found to converge at a faster rate. We apply our inferential strategy in a timely multivariate study in which we investigate the distortion in volatility spillover relations between the North America (NA) market and the UK market before and after the Brexit referendum. For a broader study, we also examine the spillover effect on the European Union (EU) market. Our main findings indicate that after the Brexit referendum, the UK market has lost its previous influence in that volatility spillover from UK to NA diminishes. This finding suggests that after Brexit, market participants in the NA region have a reduced interest to follow the UK market because of the concern that it might lose its access to the European Single Market, which is an important trading region for the NA. On the other hand, we find that the spillover effect from EU to NA is relatively delayed before Brexit but the nexus becomes more immediate after Brexit. This is because market participants in the NA that previously focus on the UK market have naturally switched their attention to the European market directly. Consequently, volatility in EU can propagate more immediately to NA, as captured by our testing strategy.

We emphasize that the application of our inferential strategy is not limited to the macro level financial markets. At the firm level, our statistical tool can assist policymakers to identify volatility transmitters and recipients in the financial system and thus to shape targeted policy to protect vulnerable volatility recipient as individual or group whenever necessary. The remainder of this paper is organized as follows. In Section 2.2, we derive kernel-based test statistics for the hypotheses of interest and we provide their asymptotic properties. Section 2.3 presents the NCCC-LS volatility model and its asymptotic validity. The finite sample performance of our econometric strategy is reported in Section 2.4 using a Monte Carlo study. In Section 2.5, we apply the proposed inferential strategy to empirically examine volatility spillover between the North American and European equity markets. Section 2.6 concludes. Most mathematical derivations and proofs along with additional simulation and empirical results are relegated to the Appendices of the paper. Throughout the paper, \xrightarrow{d} and \xrightarrow{p} denote convergences in distribution and probability, respectively. Unless otherwise indicated, all limits are taken as the sample size $T \rightarrow \infty$.

2.2 Multivariate Granger causality in variance

In this section, we introduce the formal hypotheses for volatility spillover using Granger causality in variance. We then construct kernel-based test statistics for the hypotheses using the quadratic distance between two spectral densities. Finally, we provide the asymptotic properties of the proposed tests.

2.2.1 From univariate to multivariate Granger causality in variance

For two stationary time series Y_{1t} and Y_{2t} , let I_{1t} and I_{2t} denote the respective information set available at time t . Further let $I_t \equiv (I_{1t}, I_{2t})$ denote the combined information set. Following the definition of Granger (1980), Y_{2t} Granger causes Y_{1t} with respect to I_{t-1} if

$$\mathbb{E}(Y_{1t}|I_{1t-1}) \neq \mathbb{E}(Y_{1t}|I_{t-1}). \quad (2.1)$$

Granger (1969) introduces a regression-based test for (2.1), which can be viewed as the *causality in mean* hypothesis. We note that there are other definitions of Granger causality such as those based on projections on Hilbert spaces (see, e.g., Boudjellaba et al., 1992; Comte and Lieberman, 2000). This is not pursued.

Next, Granger et al. (1986) propose the notion of *causality in variance*, which is sometimes referred to as second-order causality (see, e.g., Comte and Lieberman, 2000). Let $\mu_{it} \equiv \mathbb{E}(Y_{it}|I_{t-1})$, $i = 1, 2$, the causality in variance hypotheses are given by

$$\mathbb{H}_0 : \mathbb{E}[(Y_{1t} - \mu_{1t})^2 | I_{1t-1}] = \mathbb{E}[(Y_{1t} - \mu_{1t})^2 | I_{t-1}], \quad (2.2)$$

$$\mathbb{H}_A : \mathbb{E}[(Y_{1t} - \mu_{1t})^2 | I_{1t-1}] \neq \mathbb{E}[(Y_{1t} - \mu_{1t})^2 | I_{t-1}]. \quad (2.3)$$

Under the null hypothesis, the variance of Y_{1t} is not affected by I_{2t-1} , we say that Y_{2t} does not Granger cause Y_{1t} in variance. By construction, causality in mean has been filtered out because the hypotheses are not affected by causal relation in the mean equation. Therefore, any remaining causal effect is driven purely by volatility that is unaffected by mean and we follow Hong (2001) to use this information to test for *volatility spillover* from Y_{2t} to Y_{1t} in the higher dimension.

Let us now consider two stationary vectors of time series $(\mathbf{Y}_{1t}, \mathbf{Y}_{2t})$, where for $i = 1, 2$, $\mathbf{Y}_{it} = [Y_{it}(1), \dots, Y_{it}(d_i)]'$, $d_i \in \mathbb{Z}^+ < \infty$. Let \mathbf{I}_{1t} and \mathbf{I}_{2t} denote the information set available at time t of \mathbf{Y}_{1t} and \mathbf{Y}_{2t} , respectively. The combined information set is denoted by $\mathbf{I}_t \equiv (\mathbf{I}_{1t}, \mathbf{I}_{2t})$. Further let $\boldsymbol{\epsilon}_{it} \equiv \mathbf{Y}_{it} - \mathbb{E}(\mathbf{Y}_{it} | \mathbf{I}_{t-1})$. We suppose that the demeaned series exhibit conditional heteroskedasticity

$$\boldsymbol{\epsilon}_{it} = (\mathbf{H}_{it}^0)^{1/2} \boldsymbol{\Xi}_{it}, \quad (2.4)$$

where \mathbf{H}_{it}^0 is a $(d_i \times d_i)$ positive definite conditional variance-covariance matrix of $\boldsymbol{\epsilon}_{it}$, measurable with respect to \mathbf{I}_{it-1} . The innovation process $\boldsymbol{\Xi}_{it}$ is such that

$$\mathbb{E}(\boldsymbol{\Xi}_{it} | \mathbf{I}_{it-1}) = \mathbf{0} \text{ a.s.}, \quad \mathbb{E}(\boldsymbol{\Xi}_{it} \boldsymbol{\Xi}_{it}' | \mathbf{I}_{it-1}) = \mathbf{I}_{d_i} \text{ a.s.} \quad (2.5)$$

Using the notion of Granger et al. (1986), \mathbf{Y}_{2t} Granger causes \mathbf{Y}_{1t} in variance with respect to \mathbf{I}_{t-1} if $\mathbb{E}(\boldsymbol{\Xi}_{1t} \boldsymbol{\Xi}_{1t}' | \mathbf{I}_{1t-1}) \neq \mathbb{E}(\boldsymbol{\Xi}_{1t} \boldsymbol{\Xi}_{1t}' | \mathbf{I}_{t-1})$. However, this concept is too general to be empirically testable

considering the broad information set. Therefore, we specify the following feasible hypotheses

$$\mathbb{H}_0^1 : \Xi_{1t}\Xi'_{1t} \perp\!\!\!\perp \Xi_{2s}\Xi'_{2s}, \text{ for all } s < t, \quad (2.6)$$

$$\mathbb{H}_A^1 : \Xi_{1t}\Xi'_{1t} \not\perp\!\!\!\perp \Xi_{2s}\Xi'_{2s}, \text{ for at least one } s < t. \quad (2.7)$$

The null hypothesis implies $\mathbb{E}(\Xi_{1t}\Xi'_{1t}|\Xi_{2s}\Xi'_{2s}) = \mathbb{E}(\Xi_{1t}\Xi'_{1t})$ for all $s < t$, that is, the inclusion of $\Xi_{2s}\Xi'_{2s}$ does not improve the forecast of $\Xi_{1t}\Xi'_{1t}$. See [Cheung and Ng \(1996\)](#) and [Hong \(2001\)](#) for a similar consideration in the univariate framework. Although the history of the squared innovation $\{\Xi_{2s}\Xi'_{2s}, s < t\}$ is only a subset of \mathbf{I}_{2t-1} , one could certainly use other information in \mathbf{I}_{2t-1} to examine Granger causality. For instance, when extreme market events are used, our approach is related to testing systemic risk spillover (e.g., [Acharya et al., 2017](#); [Brownlees and Engle, 2017](#)). If the level of the innovation are used, our test can be viewed as the dependence test of [Bouhaddioui and Roy \(2006\)](#) with the extension to allow for series that exhibit conditional heteroskedasticity. When tail events are considered, our approach is related to testing for tail risk spillover (e.g., [Hong et al., 2009](#); [Weller, 2019](#)). The use of the squared innovations $\{\Xi_{2s}\Xi'_{2s}, s < t\}$ is particularly appropriate when one is interested in the volatility comovements between two markets. We note that [Corradi et al. \(2012\)](#) also consider the transmission of volatility across markets but their method requires the estimation of daily quadratic variation using high-frequency data which may be costly in practice.

On the other hand, the squared innovations $\Xi_{it}\Xi'_{it}$ can be consistently estimated using the squared standardized residuals based on the more readily available daily data. Let θ_i^0 denote the true unknown finite-dimensional parameters of \mathbf{H}_{it}^0 . Given $\{\epsilon_t\}_{t=1}^T$, where $\epsilon_t = (\epsilon_{1t}, \epsilon_{2t})'$, let $\hat{\theta}_i$ denote any \sqrt{T} -consistent estimator of θ_i^0 , such that $\hat{\mathbf{H}}_{it} = \mathbf{H}_{it}(\hat{\theta}_i)$, where \mathbf{H}_{it} is the pseudo version of \mathbf{H}_{it}^0 with initial value that is chosen arbitrarily. For notational simplicity, we further let $\hat{\mathbf{Z}}_{it} \equiv \text{vech}[(\hat{\mathbf{H}}_{it})^{-1/2} \epsilon_{it} \epsilon'_{it} (\hat{\mathbf{H}}_{it})^{-1/2}]$, a column vector with d_i^* components, where $d_i^* = d_i(d_i + 1)/2$. The vector $\hat{\mathbf{Z}}_{it}$ collects the squared standardized residuals and cross products of standardized residuals at time t . The event variables of interest are the centered version of $\hat{\mathbf{Z}}_{it}$. We denote

$$\hat{\mathbf{u}}_t \equiv \mathbf{u}_t(\hat{\theta}_1) = \hat{\mathbf{Z}}_{1t} - \text{vech}(\mathbf{I}_{d_1}), \quad \hat{\mathbf{v}}_t \equiv \mathbf{v}_t(\hat{\theta}_2) = \hat{\mathbf{Z}}_{2t} - \text{vech}(\mathbf{I}_{d_2}), \quad (2.8)$$

where \mathbf{I}_d is an identity matrix of dimension d . When $d_1 = d_2 = 1$, $\hat{\mathbf{u}}_t$ and $\hat{\mathbf{v}}_t$ reduce to [Hong's \(2001\)](#) univariate event variables. Similarly, we denote by \mathbf{u}_t^0 and \mathbf{v}_t^0 the pseudo version of the event variables based on the true volatility processes \mathbf{H}_{1t}^0 and \mathbf{H}_{2t}^0 , respectively. Note that we do not require the two event variables to have the same dimension. Essentially, our spillover test allows the number of indices to vary for the two markets of interest.

2.2.2 Test statistic and asymptotic properties

We now derive a test statistic for \mathbb{H}_0^1 based on the notion of cross-spectrum which is coherent within the concept of [Granger \(1969\)](#) causality. To see the implication of \mathbb{H}_0^1 on the cross-spectrum

between the event variables \mathbf{u}_t^0 and \mathbf{v}_t^0 , we first note that the multivariate normalized cross-spectral density of $(\mathbf{u}_t^0, \mathbf{v}_t^0)$ is given by

$$\mathbf{f}(\lambda) = \frac{1}{2\pi} \sum_{j=-\infty}^{\infty} \boldsymbol{\rho}(j) e^{-ij\lambda}, \quad \lambda \in [-\pi, \pi], \quad i = \sqrt{-1}, \quad (2.9)$$

where $\boldsymbol{\rho}(j) \equiv \text{corr}(\mathbf{u}_t^0, \mathbf{v}_{t-j}^0)$. Note that $\boldsymbol{\rho}(j)$ and $\mathbf{f}(\lambda)$ contain the same information about the cross-correlation between \mathbf{u}_t^0 and \mathbf{v}_{t-j}^0 since they are Fourier transforms of each other. We choose to use the frequency domain $\mathbf{f}(\lambda)$ for some desirable properties below. Under \mathbb{H}_0^1 , we have $\boldsymbol{\rho}(j) = 0, \forall j > 0$. As a result, $\mathbf{f}(\lambda)$ reduces to

$$\mathbf{f}^0(\lambda) = \frac{1}{2\pi} \sum_{j=-\infty}^0 \boldsymbol{\rho}(j) e^{-ij\lambda}. \quad (2.10)$$

Therefore, we can test \mathbb{H}_0^1 by quantifying the difference between the observed density $\mathbf{f}(\lambda)$ and the null density $\mathbf{f}^0(\lambda)$ using a proper divergence measure such as the quadratic norm. Any nontrivial deviation between $\mathbf{f}(\lambda)$ and $\mathbf{f}^0(\lambda)$ is evidence against the null hypothesis.

The true cross-spectra $\mathbf{f}(\lambda)$ and $\mathbf{f}^0(\lambda)$ are not known but they can be estimated consistently using nonparametric methods. Empirically, return series exhibit the volatility clustering characteristic as a volatile period tends to be followed by another volatile period. This is because financial markets are generally more influenced by recent information than remote information. Consequently, the magnitude of any economic movement, including volatility spillover, is expected to decay over time. We thus consider the kernel estimator that allows for flexible weighting at each lag order

$$\hat{\mathbf{f}}(\lambda) = \frac{1}{2\pi} \sum_{j=-T+1}^{T-1} k(j/M) \hat{\boldsymbol{\rho}}(j) e^{-ij\lambda}, \quad (2.11)$$

$$\hat{\mathbf{f}}^0(\lambda) = \frac{1}{2\pi} \sum_{j=-T+1}^0 k(j/M) \hat{\boldsymbol{\rho}}(j) e^{-ij\lambda}, \quad (2.12)$$

where $k(\cdot)$ is a kernel function and M is a truncation point when the kernel is bounded, or a smoothing parameter when the kernel has unbounded supports. The sample cross-correlation matrix $\hat{\boldsymbol{\rho}}(j)$ is given by

$$\hat{\boldsymbol{\rho}}(j) = \text{Diag}(\hat{\mathbf{C}}_{uu})^{-1/2} \hat{\mathbf{C}}_{uv}(j) \text{Diag}(\hat{\mathbf{C}}_{vv})^{-1/2}, \quad (2.13)$$

where $\hat{\mathbf{C}}_{uv}(j)$ is the sample cross-covariance matrix that is given by

$$\hat{\mathbf{C}}_{uv}(j) = \begin{cases} \frac{1}{T} \sum_{t=j+1}^T \hat{\mathbf{u}}_t \hat{\mathbf{v}}'_{t-j}, & j \geq 0, \\ \frac{1}{T} \sum_{t=-j+1}^T \hat{\mathbf{u}}_{t+j} \hat{\mathbf{v}}'_t, & j < 0, \end{cases} \quad (2.14)$$

and \hat{C}_{uu} and \hat{C}_{vv} are the sample covariance matrices of $\hat{\mathbf{u}}_t$ and $\hat{\mathbf{v}}_t$, respectively. The function $\text{Diag}(\cdot)$ returns a diagonal matrix consisting of the diagonal elements of the original matrix. Note that $\hat{\boldsymbol{\rho}}(j)$ is a matrix of dimension $(d_1^* \times d_2^*)$.

Recently, [Robbins and Fisher \(2015\)](#) propose a distance measure based on the Toeplitz matrix, though, positive definiteness of the measure cannot be guaranteed and some forms of correction are needed. Instead, we follow [Duchesne and Roy \(2004\)](#) to construct our test statistic based on the quadratic distance between $\hat{\mathbf{f}}(\lambda)$ and $\hat{\mathbf{f}}^0(\lambda)$ for tractability. The distance measure $\hat{L}^2[\hat{\mathbf{f}}(\lambda), \hat{\mathbf{f}}^0(\lambda)]$ is such that $\hat{L}^2[\hat{\mathbf{f}}(\lambda), \hat{\mathbf{f}}^0(\lambda)] \geq 0$, and $\hat{L}^2[\hat{\mathbf{f}}(\lambda), \hat{\mathbf{f}}^0(\lambda)] = 0$ if and only if $\hat{\mathbf{f}}(\lambda) = \hat{\mathbf{f}}^0(\lambda)$. Let $\hat{\Gamma}_u$ and $\hat{\Gamma}_v$ denote the sample correlation matrices of $\hat{\mathbf{u}}_t$ and $\hat{\mathbf{v}}_t$, respectively. We use the quadratic form

$$\begin{aligned} \hat{L}^2[\hat{\mathbf{f}}(\lambda), \hat{\mathbf{f}}^0(\lambda)] &\equiv 2\pi \int_{2\pi} \text{vec}[\overline{\hat{\mathbf{f}}(\lambda)} - \overline{\hat{\mathbf{f}}^0(\lambda)}]' (\hat{\Gamma}_v^{-1} \otimes \hat{\Gamma}_u^{-1}) \text{vec}[\hat{\mathbf{f}}(\lambda) - \hat{\mathbf{f}}^0(\lambda)] d\lambda \\ &= \sum_{j=1}^{T-1} k^2(j/M) \text{vec}[\hat{\boldsymbol{\rho}}(j)]' (\hat{\Gamma}_v^{-1} \otimes \hat{\Gamma}_u^{-1}) \text{vec}[\hat{\boldsymbol{\rho}}(j)], \end{aligned} \quad (2.15)$$

where $\overline{\mathbf{f}(\cdot)}$ denotes the complex conjugate of $\mathbf{f}(\cdot)$. The equality follows from Paserval's theorem. As a result, numerical integration over λ is not required in terms of the computation of $\hat{L}^2[\hat{\mathbf{f}}(\lambda), \hat{\mathbf{f}}^0(\lambda)]$. The derivation of (2.15) is provided in Appendix 2.A. Compared with [Duchesne and Roy \(2004\)](#), we do not integrate over the angular frequency. We allow for the case where $d_1 \neq d_2$. Besides, the authors work with the unstandardized version of spectral density. As a result, their test is based on covariances rather than correlations. We show in the analysis of Proposition 2.2.2 in Appendix 2.B that there is a cross-covariance representation of (2.15)

$$\hat{L}^2[\hat{\mathbf{f}}(\lambda), \hat{\mathbf{f}}^0(\lambda)] = \sum_{j=1}^{T-1} k^2(j/M) \text{vec}[\hat{C}_{uv}(j)]' (\hat{C}_{vv}^{-1} \otimes \hat{C}_{uu}^{-1}) \text{vec}[\hat{C}_{uv}(j)]. \quad (2.16)$$

Despite the equivalence, we choose to construct our test statistics using the standardized spectral density so that our measure naturally reduces to that of [Hong's \(2001\)](#) when $d_1 = d_2 = 1$. The proposed test statistic, Q_1 , is essentially the centered and scaled version of (2.15)

$$Q_1 = \frac{T \sum_{j=1}^{T-1} k^2(j/M) \text{vec}[\hat{\boldsymbol{\rho}}(j)]' (\hat{\Gamma}_v^{-1} \otimes \hat{\Gamma}_u^{-1}) \text{vec}[\hat{\boldsymbol{\rho}}(j)] - d_1^* d_2^* C_{1T}(k)}{[d_1^* d_2^* D_{1T}(k)]^{1/2}}, \quad (2.17)$$

where $C_{1T}(k)$ and $D_{1T}(k)$ are approximately the centering and scaling factors

$$C_{1T}(k) = \sum_{j=1}^{T-1} (1 - j/T) k^2(j/M), \quad (2.18)$$

$$D_{1T}(k) = 2 \sum_{j=1}^{T-1} (1 - j/T) [1 - (j+1)/T] k^4(j/M). \quad (2.19)$$

The constants $C_{1T}(k)$ and $D_{1T}(k)$ are readily computable given $k(\cdot)$ and M . Under some conditions on $k(\cdot)$ and by letting M goes to infinity properly with T , we have $M^{-1} C_{1T}(k) \rightarrow \int_0^\infty k^2(z) dz$ and

$M^{-1}D_{1T}(k) \rightarrow 2 \int_0^\infty k^4(z)dz$. As a result, $C_{1T}(k)$ and $D_{1T}(k)$ can be replaced, respectively, by $M \int_0^\infty k^2(z)dz$ and $2M \int_0^\infty k^4(z)dz$ without affecting the asymptotic properties of Q_1 .

We now establish the asymptotic properties of Q_1 . Let \tilde{H}_{it} denote the pseudo version of H_{it} with the true unobserved initial value. Note that $\tilde{H}_{it}(\theta_i^0) = H_{it}^0$, but $H_{it}(\theta_i^0) \neq H_{it}^0$ due to the initial value. As a result, $\tilde{u}_t(\theta_1^0) = u_t^0$ and $\tilde{v}_t(\theta_2^0) = v_t^0$, but $u_t(\theta_1^0) \neq u_t^0$ and $v_t(\theta_2^0) \neq v_t^0$. This discrepancy is properly addressed in the following. To begin with, we present some regularity conditions under the model described by (2.4)–(2.5).

Assumption 2.2.1. For $i = 1, 2$, $\{\Xi_{it}\}$ is multivariate independent and identically distributed sequence with $\mathbb{E}(\Xi_{it}) = \mathbf{0}$, $\mathbb{E}(\Xi_{it}\Xi_{it}') = I_{di}$ and finite eighth-order moment.

Assumption 2.2.2. For $i = 1, 2$, $\sqrt{T}(\hat{\theta}_i - \theta_i^0) = O_p(1)$, $\theta_i^0 \in \Theta_i$.

Assumption 2.2.3. For each $\theta_i \in \Theta_i$, $i = 1, 2$, $\sup_{\theta_1 \in \Theta_1} T \sum_{t=1}^T \mathbb{E} \|u_t(\theta_1) - \tilde{u}_t(\theta_1)\|^2 = O(1)$, $\sup_{\theta_2 \in \Theta_2} T \sum_{t=1}^T \mathbb{E} \|v_t(\theta_2) - \tilde{v}_t(\theta_2)\|^2 = O(1)$.

Assumption 2.2.4. Let ∇_{θ_i} and $\nabla_{\theta_i}^2$ denote, respectively, the gradient and Hessian operators w.r.t. θ_i . Then, $\sup_{\theta_1 \in \Theta_1} T^{-1} \sum_{t=1}^T \mathbb{E} \|\nabla_{\theta_1} \tilde{u}_t(\theta_1)\|^2 = O(1)$, $\sup_{\theta_2 \in \Theta_2} T^{-1} \sum_{t=1}^T \mathbb{E} \|\nabla_{\theta_2} \tilde{v}_t(\theta_2)\|^2 = O(1)$, $\sup_{\theta_1 \in \Theta_1} T^{-1} \sum_{t=1}^T \mathbb{E} \|\nabla_{\theta_1}^2 \tilde{u}_t(\theta_1)\|^2 = O(1)$, $\sup_{\theta_2 \in \Theta_2} T^{-1} \sum_{t=1}^T \mathbb{E} \|\nabla_{\theta_2}^2 \tilde{v}_t(\theta_2)\|^2 = O(1)$.

Assumption 2.2.5. The kernel $k: \mathbb{R} \rightarrow [-1, 1]$ is symmetric about 0, and is continuous at 0 and at all points except for a finite number of points, with $k(0) = 1$ and $\int_0^\infty k^2(z)dz < \infty$.

Assumption 2.2.6. $M/T \rightarrow 0$ as $T \rightarrow \infty$.

In Assumption 2.2.1, we do not assume any specific distribution for the innovation process Ξ_{1t} and Ξ_{2t} beyond the regularity moment condition. The i.i.d. condition on Ξ_{it} corresponds to the “strong ARCH” process defined in Hafner (2008) which is frequently used for estimation and inference in practice. Under this condition, Chan et al. (2007) derive the limiting distribution of the value-at-risk estimate in a ARCH process while Gao and Song (2008) extend the relevant works to cover the expected shortfall estimate. In this paper, the i.i.d. assumption ensures condition (2.5) that $\mathbb{E}(\Xi_{it}|I_{it-1}) = \mathbf{0}$ a.s. and $\mathbb{E}(\Xi_{it}\Xi_{it}'|I_{it-1}) = I_{di}$ a.s., and it also reduces the complexity of the asymptotic analysis. It appears the condition could be weakened so that Ξ_{it} is a martingale difference sequence at the cost of a more tedious proof but we do not pursue this possibility here. In Assumption 2.2.2, we do not impose any estimation restriction. Specifically, we allow for any \sqrt{T} -consistent estimator $\hat{\theta}_i$. Assumption 2.2.3 requires that the initial condition of the variance-covariance process is asymptotically negligible. In particular, we require that the difference between $u_t(\theta_1)$ and $\tilde{u}_t(\theta_1)$ goes to zero in probability at proper speed. Note that Assumption 2.2.3 becomes redundant under our nonparametric volatility specification discussed in Section 2.3. Assumption 2.2.4 requires that the event variables are twice continuously differentiable, with bounded derivatives. Assumption 2.2.5 is a standard regularity condition on the kernel function $k(\cdot)$. Most kernels used in spectral analysis satisfy this condition (see, e.g., Andrews, 1991; Priestley,

1981). Assumption 2.2.6 is rather weak. It allows M to be fixed, or to grow with the T but at a slower speed. Finally, we have thus far assume that the demeaned series $\boldsymbol{\epsilon}_{it}$ is observable for ease of exposition, but it can be replaced by any \sqrt{T} -consistent estimate without affecting the asymptotic properties of Q_1 given Assumptions 2.2.1–2.2.6.

We now state the asymptotic normality of Q_1 under \mathbb{H}_0^1 .

Theorem 2.2.1. Suppose Assumptions 2.2.1–2.2.6 hold under the model described by (2.4)–(2.5). Then, $Q_1 \xrightarrow{d} N(0, 1)$ under \mathbb{H}_0^1 .

Proof of Theorem 2.2.1. We let $\hat{S} \equiv T\hat{L}^2[\hat{\boldsymbol{f}}(\lambda), \hat{\boldsymbol{f}}^0(\lambda)]$, $\mathbf{C}_{uu}^0 \equiv E[\mathbf{u}_t^0(\mathbf{u}_t^0)']$ and $\mathbf{C}_{vv}^0 \equiv E[\mathbf{v}_t^0(\mathbf{v}_t^0)']$, the proof begins by defining the following pseudo statistic

$$S^* = T \sum_{j=1}^{T-1} k^2(j/M) \text{vec}[\hat{\boldsymbol{\rho}}^*(j)]' (\boldsymbol{\Gamma}_v^{-1} \otimes \boldsymbol{\Gamma}_u^{-1}) \text{vec}[\hat{\boldsymbol{\rho}}^*(j)], \quad (2.20)$$

where $\hat{\boldsymbol{\rho}}^*(j) = \text{Diag}(\mathbf{C}_{uu}^0)^{-1/2} \hat{\mathbf{C}}_{uv}(j) \text{Diag}(\mathbf{C}_{vv}^0)^{-1/2}$; and $\boldsymbol{\Gamma}_u = \text{Diag}(\mathbf{C}_{uu}^0)^{-1/2} \mathbf{C}_{uu}^0 \text{Diag}(\mathbf{C}_{uu}^0)^{-1/2}$ and $\boldsymbol{\Gamma}_v = \text{Diag}(\mathbf{C}_{vv}^0)^{-1/2} \mathbf{C}_{vv}^0 \text{Diag}(\mathbf{C}_{vv}^0)^{-1/2}$ are the true correlation matrices of true \mathbf{u}_t^0 and \mathbf{v}_t^0 , respectively. We can decompose Q_1 as

$$Q_1 = \frac{S^* - d_1^* d_2^* C_{1T}(k)}{[d_1^* d_2^* D_{1T}(k)]^{1/2}} + \frac{\hat{S} - S^*}{[d_1^* d_2^* D_{1T}(k)]^{1/2}}. \quad (2.21)$$

Then, the result of Theorem 2.2.1 follows from Propositions 2.2.1–2.2.2. ■

Proposition 2.2.1. Suppose the conditions of Theorem 2.2.1 hold, we have that

$$\frac{S^* - d_1^* d_2^* C_{1T}(k)}{[d_1^* d_2^* D_{1T}(k)]^{1/2}} \xrightarrow{d} N(0, 1).$$

Proposition 2.2.2. Suppose the conditions of Theorem 2.2.1 hold, we have that

$$\frac{\hat{S} - S^*}{[d_1^* d_2^* D_{1T}(k)]^{1/2}} \xrightarrow{p} 0.$$

Proof of Proposition 2.2.1. Let $\hat{\mathbf{C}}_{uv}^0$ denotes the sample cross-covariance matrix in (2.14) with true \mathbf{u}_t^0 and \mathbf{v}_{t-j}^0 . The proof of Proposition 2.2.1 begins by defining the another pseudo statistic

$$S = T \sum_{j=1}^{T-1} k^2(j/M) \text{vec}[\hat{\boldsymbol{\rho}}^0(j)]' (\boldsymbol{\Gamma}_v^{-1} \otimes \boldsymbol{\Gamma}_u^{-1}) \text{vec}[\hat{\boldsymbol{\rho}}^0(j)], \quad (2.22)$$

where $\hat{\boldsymbol{\rho}}^0(j) = \text{Diag}(\mathbf{C}_{uu}^0)^{-1/2} \hat{\mathbf{C}}_{uv}^0(j) \text{Diag}(\mathbf{C}_{vv}^0)^{-1/2}$. We consider a similar decomposition

$$\frac{S^* - d_1^* d_2^* C_{1T}(k)}{[d_1^* d_2^* D_{1T}(k)]^{1/2}} = \frac{S - d_1^* d_2^* C_{1T}(k)}{[d_1^* d_2^* D_{1T}(k)]^{1/2}} + \frac{S^* - S}{[d_1^* d_2^* D_{1T}(k)]^{1/2}}. \quad (2.23)$$

The result of Proposition 2.2.1 is given by Lemmas 2.2.1 and 2.2.2. ■

Lemma 2.2.1. Suppose the conditions of Theorem 2.2.1 hold, we have that

$$\frac{S - d_1^* d_2^* C_{1T}(k)}{[d_1^* d_2^* D_{1T}(k)]^{1/2}} \xrightarrow{d} N(0, 1).$$

Lemma 2.2.2. Suppose the conditions of Theorem 2.2.1 hold, we have that

$$S^* - S = o_p(M^{1/2}).$$

We shall defer the lengthy proofs of Lemmas 2.2.1–2.2.2 and Proposition 2.2.2 to Appendix 2.B. When the Truncated kernel is used to compute Q_1 , our test can be viewed as the Granger (1969)-type procedure. To see the intuition, we first note that the Truncated kernel is given by $k(z) = \mathbb{1}(|z| \leq 1)$, where $\mathbb{1}(\cdot)$ is the indicator function. For the purpose of illustration, suppose $d_1 = 1$ and $d_2 = 2$, we have the following test statistic³

$$Q_{1\text{TR}} = \left\{ T \sum_{j=1}^M \text{vec}[\hat{\boldsymbol{\rho}}(j)]' (\hat{\boldsymbol{\Gamma}}_u^{-1}) \text{vec}[\hat{\boldsymbol{\rho}}(j)] - 3M \right\} / (6M)^{1/2}, \quad (2.24)$$

where $\hat{\boldsymbol{\rho}}(j)$ is a (1×3) vector and $\hat{\boldsymbol{\Gamma}}_u^{-1}$ is a (3×3) matrix. On the other hand, the Granger-type procedure is based on the following regression

$$\hat{u}_t = \phi_0 + \sum_{j=1}^M \boldsymbol{\phi}_j \hat{\boldsymbol{v}}_{t-j} + w_t, \quad (2.25)$$

which checks whether the (1×3) parameter vector $\{\boldsymbol{\phi}_j\}_{j=1}^M$ are jointly zero. We do not have to include in the auxiliary regression (2.25) the lagged variables of \hat{u}_t given Assumption 2.2.1. There is evidence that $\hat{\boldsymbol{v}}_t$ Granger causes \hat{u}_t with respect to \boldsymbol{I}_{t-1} if at least one coefficient in $\{\boldsymbol{\phi}_j\}_{j=1}^M$ is significantly different from zero. A typical test statistic GR for this hypothesis obtained from, for instance, the Wald's procedure is asymptotically $\chi^2(3M)$ under \mathbb{H}_0^1 (see, e.g., Bauer and Maynard, 2012, Theorem 1). Now, for $Q_{1\text{TR}}$ in (2.24), we know that under \mathbb{H}_0^1 , $\sqrt{T} \text{vec}[\hat{\boldsymbol{\rho}}(j)]$ generally converges to a three dimensional zero mean normal distribution at each lag j . Then, $\sum_{j=1}^M T \text{vec}[\hat{\boldsymbol{\rho}}(j)]' (\hat{\boldsymbol{\Gamma}}_u^{-1}) \text{vec}[\hat{\boldsymbol{\rho}}(j)]$ being the M sum of the properly standardized independent $\chi^2(3)$ quantity is also asymptotically $\chi^2(3M)$ under \mathbb{H}_0^1 . To ensure power of the Granger regression-based test against a large class of alternatives, we allow M to grow with the sample size T properly. Using the well-known approximation of $\chi^2(3M)$ when M is large, we obtain the asymptotic normality of GR and $\sum_{j=1}^M T \text{vec}[\hat{\boldsymbol{\rho}}(j)]' (\hat{\boldsymbol{\Gamma}}_u^{-1}) \text{vec}[\hat{\boldsymbol{\rho}}(j)]$. With proper transformations, we have under \mathbb{H}_0^1 , $Q_{1\text{REG}} \equiv$

³Given the Truncated kernel function, we have $C_{1T}(k) = M[1 - (1 + M)/(2T)]$ and $D_{1T}(k) = 2M[1 - (2 + M)/T + (M + 1)(M + 2)/(3T^2)]$. Using a more stringent condition on M such that $M^{3/2}/T = o(1)$, we can conveniently approximate $C_{1T}(k)$ and $D_{1T}(k)$ by M and $2M$, respectively.

$(GR-3M)/(6M)^{1/2} \xrightarrow{d} N(0, 1)$ as well as $Q_{1TR} = \{T \sum_{j=1}^M \text{vec}[\hat{\boldsymbol{\rho}}(j)'(\hat{\boldsymbol{\Gamma}}_u^{-1})\text{vec}[\hat{\boldsymbol{\rho}}(j)] - 3M\}/(6M)^{1/2} \xrightarrow{d} N(0, 1)$.

When M is large, both Q_{1REG} and Q_{1TR} may not yield a good power against the alternatives of practical importance. Given that economic agents tend to discount past information, the effect of volatility spillover will fade as lag order j increases. Therefore, we propose to use downward weighting kernels such as the Bartlett, Daniell and Quadratic-Spectral kernels to increase the power performance of our Q_1 test. See Section 2.4 for more discussion and the Monte Carlo study.

To investigate the asymptotic behavior of Q_1 under the alternative hypothesis, we impose a condition on the cross-correlation $\boldsymbol{\rho}(j)$ and a fourth order cumulant condition.

Assumption 2.2.7. The two event variables \mathbf{u}_t^0 and \mathbf{v}_t^0 are jointly fourth order stationary and their cross-correlation structure is such that $\boldsymbol{\rho}(j) \neq 0$ for at least one $j > 0$ and

$$\sum_{j=1}^{\infty} \|\boldsymbol{\rho}(j)\|^2 < \infty, \quad \sum_{i=1}^{\infty} \sum_{j=1}^{\infty} \sum_{l=1}^{\infty} |\kappa_{rsrs}(i, j, l)| < \infty,$$

where $\kappa_{rsrs}(i, j, l)$ is the fourth order cumulant of the distribution of $u_{r,t}^0, v_{s,t-i}^0, u_{r,t-j}^0, v_{s,t-l}^0$, with $r \in \{1, \dots, d_1^*\}$ and $s \in \{1, \dots, d_2^*\}$.

The condition $\sum_{j=1}^{\infty} \|\boldsymbol{\rho}(j)\|^2 < \infty$ implies that the dependence of \mathbf{u}_t^0 on \mathbf{v}_{t-j}^0 decays to zero at a proper speed. However, it still permits a pair of highly cross-dependent processes whose cross-correlation decays to zero at a gradual hyperbolic rate. The cumulant condition is trivially satisfied if the joint process $\{\mathbf{u}_t^0, \mathbf{v}_t^0\}$ is Gaussian which implies zero fourth-order cumulants. Fourth-order stationary linear processes with absolutely summable coefficients and with innovations whose fourth-order moment exists, also satisfy the cumulant condition (Hannan, 1970, p.211).

The following theorem states the consistency of Q_1 under fixed alternatives.

Theorem 2.2.2. Suppose Assumptions 2.2.1–2.2.7 hold under the model described by (2.4)–(2.5). Then

$$\frac{M^{1/2}}{T} Q_1 \xrightarrow{p} \left[2 \int_0^{\infty} k^4(z) dz \right]^{-1/2} \sum_{j=1}^{\infty} \text{vec}[\boldsymbol{\rho}(j)]' (\boldsymbol{\Gamma}_v^{-1} \otimes \boldsymbol{\Gamma}_u^{-1}) \text{vec}[\boldsymbol{\rho}(j)].$$

Proof of Theorem 2.2.2. Recall that $C_{1T}(k) = O(M)$ and $D_{1T}(k) = 2M \int_0^{\infty} k^4(z) dz [1 + o(1)]$ as $M \rightarrow \infty$ and $M/T \rightarrow 0$, we have

$$\begin{aligned} \frac{M^{1/2}}{T} Q_1 &= \frac{\sum_{j=1}^{T-1} k^2(j/M) \text{vec}[\hat{\boldsymbol{\rho}}(j)]' (\hat{\boldsymbol{\Gamma}}_v^{-1} \otimes \hat{\boldsymbol{\Gamma}}_u^{-1}) \text{vec}[\hat{\boldsymbol{\rho}}(j)]}{\left[2 \int_0^{\infty} k^4(z) dz \right]^{1/2}} [1 + o(1)] + o(1) \\ &= T^{-1} \hat{S} \left[2 \int_0^{\infty} k^4(z) dz \right]^{-1/2} [1 + o(1)] + o(1). \end{aligned}$$

Therefore, the proof of Theorem 2.2.2 is given by Lemmas 2.2.3–2.2.5. ■

Lemma 2.2.3. Suppose the conditions of Theorem 2.2.2 hold, then $T^{-1}(S - S^*) = o_p(1)$.

Lemma 2.2.4. Suppose the conditions of Theorem 2.2.2 hold, then $T^{-1}(\hat{S} - S^*) = o_p(1)$.

Lemma 2.2.5. Suppose the conditions of Theorem 2.2.2 hold, then

$$\begin{aligned} \frac{1}{T}S &= \sum_{j=1}^{T-1} k^2(j/M) \text{vec}[\hat{\boldsymbol{\rho}}^0(j)]' (\boldsymbol{\Gamma}_v^{-1} \otimes \boldsymbol{\Gamma}_u^{-1}) \text{vec}[\hat{\boldsymbol{\rho}}^0(j)] \\ &\xrightarrow{p} \sum_{j=1}^{\infty} \text{vec}[\boldsymbol{\rho}(j)]' (\boldsymbol{\Gamma}_v^{-1} \otimes \boldsymbol{\Gamma}_u^{-1}) \text{vec}[\boldsymbol{\rho}(j)]. \end{aligned}$$

We shall defer the lengthy proofs of Lemmas 2.2.3–2.2.5 to Appendix 2.C. Theorem 2.2.2 implies that Q_1 goes to infinity at rate $T/M^{1/2}$ provided $\|\boldsymbol{\rho}(j)\| \neq 0$ for any $j > 0$. In the limit, negative values of Q_1 can only occur under \mathbb{H}_0^1 . Therefore, Q_1 is a one-sided test; upper-tailed $N(0,1)$ critical values should be used. Besides, the faster T grows, the quicker Q_1 will approach infinity and the test will become more powerful. In other words, Q_1 has asymptotic unit power against any linear pairwise volatility spillover. However, it should be noted that Q_1 has no power against the alternatives with zero cross-correlation for all values of $j > 0$, that is, $\|\boldsymbol{\rho}(j)\| = 0, \forall j > 0$, though we expect such highly nonlinear alternatives to be empirically rare in economics and finance.

2.2.3 Bidirectional Granger causality in variance

The proposed Q_1 test is readily extendable for testing bilateral variance causality. This extension is convenient when the direction of volatility spillover is not known *a priori*. We consider the multivariate version of Hong's (2001) bidirectional hypothesis that neither \mathbf{Y}_{2t} causes \mathbf{Y}_{1t} in variance with respect to $(\mathbf{I}_{1t}, \mathbf{I}_{2t-1})$ nor \mathbf{Y}_{1t} causes \mathbf{Y}_{2t} in variance with respect to $(\mathbf{I}_{1t-1}, \mathbf{I}_{2t})$. Essentially, we examine the following bidirectional hypotheses

$$\mathbb{H}_0^2 : \Xi_{1t} \Xi_{1t}' \perp\!\!\!\perp \Xi_{2s} \Xi_{2s}', \text{ for all } s, \quad (2.26)$$

$$\mathbb{H}_A^2 : \Xi_{1t} \Xi_{1t}' \not\perp\!\!\!\perp \Xi_{2s} \Xi_{2s}', \text{ for at least one } s. \quad (2.27)$$

Under \mathbb{H}_0^2 , we have $\boldsymbol{\rho}(j) = 0, \forall j$. As a result, the cross-spectrum $\mathbf{f}(\lambda)$ reduces to zero. The normalized quadratic distance between the kernel-based spectral density estimator and the null spectral density is given by

$$\hat{L}_2^2[\hat{\mathbf{f}}(\lambda), \hat{\mathbf{f}}^0(\lambda)] = \sum_{j=-T+1}^{T-1} k^2(j/M) \text{vec}[\hat{\boldsymbol{\rho}}(j)]' (\hat{\boldsymbol{\Gamma}}_v^{-1} \otimes \hat{\boldsymbol{\Gamma}}_u^{-1}) \text{vec}[\hat{\boldsymbol{\rho}}(j)]. \quad (2.28)$$

The proposed bidirectional test statistic Q_2 is a centered and scaled version of $\hat{L}_2^2[\hat{\mathbf{f}}(\lambda), \hat{\mathbf{f}}^0(\lambda)]$

$$Q_2 = \frac{T \sum_{j=-T+1}^{T-1} k^2(j/M) \text{vec}[\hat{\boldsymbol{\rho}}(j)]' (\hat{\boldsymbol{\Gamma}}_v^{-1} \otimes \hat{\boldsymbol{\Gamma}}_u^{-1}) \text{vec}[\hat{\boldsymbol{\rho}}(j)] - d_1^* d_2^* C_{2T}(k)}{[d_1^* d_2^* D_{2T}(k)]^{1/2}}, \quad (2.29)$$

where $C_{2T}(k)$ and $D_{2T}(k)$ are the bidirectional centering and scaling factors with

$$C_{2T}(k) = \sum_{j=-T+1}^{T-1} (1 - |j|/T) k^2(j/M), \quad (2.30)$$

$$D_{2T}(k) = 2 \sum_{j=-T+1}^{T-1} (1 - |j|/T) [1 - (|j| + 1)/T] k^4(j/M). \quad (2.31)$$

Similar to Q_1 , the bidirectional test statistic Q_2 converges in distribution to $N(0,1)$ under the bilateral null hypothesis and it has asymptotic unit power whenever $\|\boldsymbol{\rho}(j)\| \neq 0$ for at least one j . Likewise, upper-tailed $N(0,1)$ critical values should be used for Q_2 . The mathematical proof involved is similar to that of Theorems 2.2.1 and 2.2.2 by considering both positive and negative lag order j 's, and we shall refrain from repeating the details here. In summary, when prior knowledge about the direction of volatility spillover is not available, one may first test the bidirectional hypothesis that neither \mathbf{Y}_{2t} Granger causes \mathbf{Y}_{1t} in variance.

2.3 Estimation

The asymptotic analysis of Q_1 and Q_2 multivariate tests does not add complication relative to the univariate ones in that it explores the multivariate counterparts of algebra, calculus and mathematical inequalities such as the Kronecker product, matrix differentiation and Cauchy-Schwarz inequality. However, the proposed tests rely on \mathbf{H}_{it}^0 which can be a complex process to specify. The ideal specification should possess the following features. First, the structure of the specification should facilitate its estimation considering that it may house higher dimensional variance-covariance matrix. Second, conditions ensuring that the estimated \mathbf{H}_{it}^0 is nonnegative definite should be straightforward to impose. Third, model estimation should achieve convergence or preferably bypass any numerical optimization routine. Finally, along with these properties, the specified processes in the structure should minimize ARCH inadequacy. We now put forward a structure which intersects these features in an optimal manner. We suppose that \mathbf{H}_{it}^0 can be decomposed as follows

$$\mathbf{H}_{it}^0 = (\mathbf{D}_{it}^0)^{1/2} \mathbf{R}_i^0 (\mathbf{D}_{it}^0)^{1/2}, \text{ for } i = 1, 2, \quad (2.32)$$

where $\mathbf{D}_{it}^0 = \text{diag}(h_{i,1t}^0, \dots, h_{i,d_{it}}^0)$ is a diagonal matrix with univariate conditional variances and $\mathbf{R}_i^0 = \mathbb{E}[(\mathbf{D}_{it}^0)^{-1/2} \boldsymbol{\epsilon}_{it} \boldsymbol{\epsilon}_{it}' (\mathbf{D}_{it}^0)^{-1/2}]$ is the covariance matrix of the vector of element-wise standardized residuals by construction. Under this structure, \mathbf{H}_{it}^0 is positive semidefinite provided that the elements in \mathbf{D}_{it}^0 are nonnegative and that \mathbf{R}_i^0 is positive semidefinite.

We specify \mathbf{D}_{it}^0 as an infinite order ARCH process. For $n = 1, \dots, d_i$, we denote the n -th elements in \mathbf{D}_{it}^0 and $\boldsymbol{\epsilon}_{it}$ by $h_{i,n,t}^0$ and $\epsilon_{i,n,t}$, respectively. The ARCH(∞) representation takes the form

$$h_{i,n,t}^0 = \omega_{i,n}^0 + \sum_{j=1}^{\infty} a_{i,n,j}^0 \epsilon_{i,n,t-j}^2. \quad (2.33)$$

This general process includes Engle's (1982) ARCH(q), Bollerslev's (1986) generalized autoregressive conditional heteroskedasticity [GARCH(p, q)], and Engle and Bollerslev's (1986) integrated GARCH and fractionally differenced GARCH models. We can rewrite (2.33) as an infinite order autoregressive [AR(∞)] process

$$\epsilon_{i,n,t}^2 = \omega_{i,n}^0 + \sum_{j=1}^{\infty} a_{i,n,j}^0 \epsilon_{i,n,t-j}^2 + e_{i,n,t}, \quad (2.34)$$

where $e_{i,n,t} \equiv \epsilon_{i,n,t}^2 - h_{i,n,t}^0$ is such that $\mathbb{E}(e_{i,n,t} | I_{i,n,t-1}) = 0$. Because the assumption of an infinite autoregressive process is rather mild, this is sometimes referred to as a "nonparametric" approach (see, e.g., Lewis and Reinsel, 1985). Given realization $\{\epsilon_{i,n,t}^2\}_{t=1}^T$, we can approximate (2.34) by a finite order AR(p) process, where p is a function of T

$$\epsilon_{i,n,t}^2 = \omega_{i,n}^{(p)} + \sum_{j=1}^p a_{i,n,j}^{(p)} \epsilon_{i,n,t-j}^2 + e_{i,n,t}^{(p)}. \quad (2.35)$$

We propose to estimate (2.35) using least-squares. Although least-squares estimation may give larger standard errors than likelihood-based estimation, it is free from the complications of numerical optimization and likelihood misspecification (see, e.g., Newey and Steigerwald, 1997). Besides, it is computationally less demanding. As we show in a computational study provided in the supplementary document, our method requires only about 5% of the computing time of QMLE.⁴

For $i = 1, 2$, we let $\hat{\boldsymbol{\theta}}_i^{(p)} \equiv [(\hat{\omega}_{i,1}^{(p)}, \dots, \hat{\omega}_{i,d_i}^{(p)}), (\hat{a}_{i,1,1}^{(p)}, \dots, \hat{a}_{i,d_i,1}^{(p)}), \dots, (\hat{a}_{i,1,p}^{(p)}, \dots, \hat{a}_{i,d_i,p}^{(p)})]'$ collects the least-squares estimator of the vector of parameters $\boldsymbol{\theta}_i \equiv [(\omega_{i,1}, \dots, \omega_{i,d_i}), (a_{i,1,1}, \dots, a_{i,d_i,1}), \dots, (a_{i,1,p}, \dots, a_{i,d_i,p})]'$ with true value $\boldsymbol{\theta}_i^0 \equiv [(\omega_{i,1}^0, \dots, \omega_{i,d_i}^0), (a_{i,1,1}^0, \dots, a_{i,d_i,1}^0), \dots, (a_{i,1,p}^0, \dots, a_{i,d_i,p}^0)]'$. We now provide regularity conditions under which $\hat{\boldsymbol{\theta}}_i^{(p)}$ is a consistent estimator of $\boldsymbol{\theta}_i^0$.

Assumption 2.3.1. For $i = 1, 2$, $n = 1, \dots, d_i$, (a) $\{\epsilon_{i,n,t}^2\}$ and $\{e_{i,n,t}\}$ are strictly stationary and ergodic; (b) $\{e_{i,n,t}\}$ is strong mixing with $\mathbb{E}(e_{i,n,t}^2) = \Sigma_{e,i,n}$ and has finite fourth-order moment.

Assumption 2.3.2. The lag order p is chosen such that $p = o(T^{1/2}/M^{1/4})$ and $p/\log(T) \rightarrow \infty$.

As stated in Assumption 2.3.1(a), we do not consider nonstationary system in the present paper. Assumption 2.3.1(b) requires the process $\{e_{i,n,t}\}$ is strong mixing and has finite fourth-order moment. The former requirement is less restrictive than the martingale difference property of $\{e_{i,n,t}\}$ whereas the latter is of equal order to the moment condition in Assumption 2.2.1. Assumption 2.3.2

⁴See Appendix 2.H.

is a standard condition on p in the long AR literature. The condition $p = o(T^{1/2}/M^{1/4})$ requires that p not to grow too fast, whereas the condition $p/\log(T) \rightarrow \infty$ imposes a lower bound on the growth rate of p . The following proposition states the consistency of $\hat{\theta}_i^{(p)}$.

Proposition 2.3.1. Let the conditional variance process of model (2.4)–(2.5) be defined by (2.32)–(2.35). Suppose Assumptions 2.3.1 and 2.3.2 hold, then

$$\|\hat{\theta}_i^{(p)} - \theta_i^0\| = O_p(p^{1/2}T^{-1/2}), \text{ for } i = 1, 2.$$

The proof of Proposition 2.3.1 is provided in Appendix 2.D. We have shown the consistency of $\hat{\theta}_i^{(p)}$ but it does not converge at the required rate of \sqrt{T} . With the current speed, we can provide further conditions such that the spillover test is consistent but the asymptotic normality may not hold under the null hypothesis. We therefore invoke Theorem 5.52 in [van der Vaart \(1998\)](#) to provide conditions for the least-squares criterion function $\mathbf{m}(\theta_i, \epsilon_{i,n,t}^2) \equiv (\epsilon_{i,n,t}^2 - \omega_{i,n} - \sum_{j=1}^{\infty} a_{i,n,j} \epsilon_{i,n,t-j}^2)^2$ such that $\hat{\theta}_i^{(p)}$ achieves the required rate of convergence.

Assumption 2.3.3. For $i = 1, 2$, $n = 1, \dots, d_i$, let $\mathbf{m}(\theta_i, \epsilon_{i,n,t}^2)$ be any measurable function parameterized by θ_i such that for fixed constants Δ and $\alpha > \beta$, and for every sufficiently small $\zeta > 0$,

- (a) $\sup_{\|\theta_i - \theta_i^0\| < \zeta} \mathbb{E}[\mathbf{m}(\theta_i, \epsilon_{i,n,t}^2) - \mathbf{m}(\theta_i^0, \epsilon_{i,n,t}^2)] \leq -\Delta\zeta^\alpha$;
 - (b) $\mathbb{E}\{\sup_{\|\theta_i - \theta_i^0\| < \zeta} |\mathbb{G}_T[\mathbf{m}(\theta_i, \epsilon_{i,n,t}^2) - \mathbf{m}(\theta_i^0, \epsilon_{i,n,t}^2)]|\} \leq \Delta\zeta^\beta$;
 - (c) $T^{-1} \sum_{t=1}^T \mathbf{m}(\hat{\theta}_i^{(p)}, \epsilon_{i,n,t}^2) \geq T^{-1} \sum_{t=1}^T \mathbf{m}(\theta_i^0, \epsilon_{i,n,t}^2) - O_p(T^{\alpha/(2\beta-2\alpha)})$,
- where $\mathbb{G}_T[\mathbf{m}(\theta_i, \epsilon_{i,n,t}^2)] = \sqrt{T}\{T^{-1} \sum_{t=1}^T \mathbf{m}(\theta_i, \epsilon_{i,n,t}^2) - \mathbb{E}[\mathbf{m}(\theta_i, \epsilon_{i,n,t}^2)]\}$.

In general, $\mathbf{m}(\theta_i, \epsilon_{i,n,t}^2)$ can be the criterion function of any other M-estimators. See, for instance, [Antoine and Renault \(2012\)](#) for a comprehensive analysis in the context of generalized method of moments (GMM) estimation. The intuition of Assumption 2.3.3 is as follows: provided that (a) the deterministic map $\mathbb{E}[\mathbf{m}(\theta_i, \epsilon_{i,n,t}^2)]$ reacts rapid enough as θ_i moves away from θ_i^0 ; (b) the random fluctuation between $T^{-1} \sum_{t=1}^T \mathbf{m}(\theta_i, \epsilon_{i,n,t}^2)$ and $\mathbb{E}[\mathbf{m}(\theta_i, \epsilon_{i,n,t}^2)]$ is sufficiently small, then $\hat{\theta}_i^{(p)}$ has a high rate of convergence if its distance with θ_i^0 is properly bounded according to (c). By setting $\alpha = 1.5$ and $\beta = 0.5$, condition (c) is satisfied using the fact that the squared residuals are bounded by $O_p(p/T) = O_p(T^{-3/4})$, where the equality follows from Assumption 2.3.2. The desired convergence rate of $\hat{\theta}_i^{(p)}$ then follows. The following proposition states the formal result.

Proposition 2.3.2. Let the conditional variance process of model (2.4)–(2.5) be defined by (2.32)–(2.35). Suppose Assumptions 2.3.1–2.3.3 hold with $\alpha = 1.5$ and $\beta = 0.5$, then

$$\|\hat{\theta}_i^{(p)} - \theta_i^0\| = O_p(T^{-1/2}), \text{ for } i = 1, 2.$$

The proof of Proposition 2.3.2 is provided in Appendix 2.E. With this speed, our test remains valid in the limit, although negative volatilities are not precluded by $\hat{\theta}_i^{(p)}$. To adjust for this, in the following we provide the adjusted least-squares estimator $\hat{\theta}_i^{(p)a}$ that ensures positive-

semidefiniteness of D_{it}^0 . We show that the adjusted estimator can be computed based on an ex post estimate of $\hat{\theta}_i^{(p)}$. We require the following additional conditions to hold.

Assumption 2.3.4. For $i = 1, 2$, the true parameter vector θ_i^0 lies in the parameter space $[\mathcal{R}_i^{\min}, \mathcal{R}_i^{\max}]$ such that D_{it}^0 is positive-semidefinite.

Assumption 2.3.5. For $i = 1, 2$, there exists a vector δ_i with nonnegative entries such that $\hat{\theta}_i^{(p)} + \delta_i \in [\mathcal{R}_i^{\min}, \mathcal{R}_i^{\max}]$ and $(\hat{\theta}_i^{(p)} + \delta_i) \mathbb{1}(\delta_i > \mathbf{0}) = \mathcal{R}_i^{\min} \mathbb{1}(\delta_i > \mathbf{0})$.

Assumption 2.3.4 is a standard condition that restricts the true parameter such that D_{it}^0 is positive-semidefinite. The sufficient condition is that each element in θ_i^0 is nonnegative (i.e. $\mathcal{R}_i^{\min} = \mathbf{0}$, $\mathcal{R}_i^{\max} = \infty$). Assumption 2.3.5 requires the existence of a lower bound vector δ_i with nonnegative entries such that $\hat{\theta}_i^{(p)} + \delta_i$ yields a positive-semidefinite D_{it}^0 . In practice, we can replace the negative entries in $\hat{\theta}_i^{(p)}$ by zeros such that they corresponds to \mathcal{R}_i^{\min} , that is, $\delta_i = -\hat{\theta}_i^{(p)} \mathbb{1}(\hat{\theta}_i^{(p)} < 0)$. Note that δ_i is simply a vector of zeros if the unadjusted estimator lies in the desired parameter space.

Given δ_i , the adjusted least-squares estimators can be computed, on an ex post basis, by $\hat{\theta}_i^{(p)a} = \hat{\theta}_i^{(p)} + \delta_i$. The following proposition states the consistency of $\hat{\theta}_i^{(p)a}$.

Proposition 2.3.3. Let the conditional variance process of model (2.4)–(2.5) be defined by (2.32)–(2.35). Suppose Assumptions 2.3.1–2.3.5 hold, then

$$\|\hat{\theta}_i^{(p)a} - \theta_i^0\| = O_p(T^{-1/2}), \text{ for } i = 1, 2.$$

The proof of Proposition 2.3.3 is provided in Appendix 2.F. The proof uses the fact that the ex post adjustment does not affect the asymptotic properties of $\hat{\theta}_i^{(p)}$ because it is only applied to the entries that are outside of the true neighborhood of θ_i^0 .

To establish the asymptotic validity of (2.32)–(2.35) for our Q_1 and Q_2 tests, a final condition is required for the proper convergence of R_i^0 .

Assumption 2.3.6. For $i = 1, 2$, $(D_{it}^0)^{-1/2} \epsilon_{it}$ maintains the same stochastic properties as Ξ_{it} with covariance $\mathbb{E}[(D_{it}^0)^{-1/2} \epsilon_{it} \epsilon_{it}' (D_{it}^0)^{-1/2}] = R_i^0$.

It is evident that $(D_{it}^0)^{-1/2} \epsilon_{it}$ belongs to a special case of $\Xi_{it} = (H_{it}^0)^{-1/2} \epsilon_{it}$ with diagonal H_{it}^0 ; it is therefore natural for the former to inherit the stochastic properties of the latter but with covariance R_i^0 instead of identity covariance. Then, the estimation of (2.32) proceeds in two steps. First, we estimate (2.35) for each of the diagonal elements in D_{it}^0 using the adjusted least-squares estimator $\hat{\theta}_i^{(p)a}$. The estimated positive-semidefinite process is denoted by \hat{D}_{it} . In the second step, R_i^0 is estimated using the sample covariance of $\hat{D}_{it}^{-1/2} \epsilon_{it}$, which we denote by \hat{R}_i . Because \hat{R}_i is always positive-semidefinite, this ensures that the estimated time-varying covariance matrix is always positive-semidefinite.

The following proposition states the validity of Theorems 2.2.1 and 2.2.2 under the proposed volatility model.

Proposition 2.3.4. Let the conditional variance process of model (2.4)–(2.5) be defined by (2.32)–(2.35). Suppose Assumptions 2.2.1–2.2.2, 2.2.4–2.2.6, 2.3.1–2.3.6 hold, then the results of Theorem 2.2.1 remain valid. Additionally, suppose Assumption 2.2.7 holds, then the results of Theorem 2.2.2 remain valid.

The proof of Proposition 2.3.4 is provided in Appendix 2.G. The key is to show that the second step estimator $\hat{\mathbf{R}}_i$ is \sqrt{T} -consistent for \mathbf{R}_i^0 . Given this result and by collecting $\hat{\mathbf{R}}_i$ in the estimator vector, the results of Theorems 2.2.1 and 2.2.2 continue to hold under their respective conditions. Note that Assumption 2.2.3 is not needed here since we do not have to specify an initial value for our model. Besides, when the true data generating process has finite autoregressive order, we have \sqrt{T} -consistent estimators regardless of Assumption 2.3.3. We provide Assumption 2.3.3 as a formal condition to maintain the generality of our approach where we allow p to grow with T .

In summary, a multivariate volatility model is proposed to facilitate the estimation of Q_1 and Q_2 . The proposed specification enjoys estimation simplicity and computational efficiency. The approach is somewhat “nonparametric” in that it imposes minimal assumption on the structure of \mathbf{D}_{it}^0 . We also do not impose any parametric assumption on \mathbf{R}_i^0 . A similar structure of (2.32) was previously studied by Bollerslev (1990), which is often referred to as the CCC model. We differ from the author by specifying elements in \mathbf{D}_{it}^0 using a more general volatility process and we propose to estimate \mathbf{D}_{it}^0 by least-squares. We also demonstrate the consistency of our two-steps estimators. To highlight the dissimilarity and for notational simplicity, we shall denote our approach in short as the NCCC-LS approach, where the acronym stands for Nonparametric-CCC-Least-Squares.

2.4 Monte Carlo simulations

In this section, we investigate the finite sample performance of the proposed econometric strategy using Monte Carlo simulations. We first consider a bivariate setup (i.e., $d_1 = d_2 = 2$), where we conduct experiments to study the effect of covariance intensity on the finite sample size and power of our testing strategy. Then, we study the behavior of our method with increasing dimension. To save space, we focus here on the unidirectional test statistic Q_1 , and we report and discuss in Appendix 2.H the full results based on the bidirectional statistic Q_2 .

2.4.1 The bivariate case

We work with the following bivariate data generating process with persistent conditional means and variances

$$\begin{aligned} \mathbf{Y}_{it} &= \begin{pmatrix} Y_{i,1t} \\ Y_{i,2t} \end{pmatrix} = \begin{pmatrix} 1 + m_{i,1t} \\ 1 + m_{i,2t} \end{pmatrix} + \begin{pmatrix} \epsilon_{i,1t} \\ \epsilon_{i,2t} \end{pmatrix}, \quad i = 1, 2, \quad t = 1, \dots, T, \\ \begin{pmatrix} \epsilon_{i,1t} \\ \epsilon_{i,2t} \end{pmatrix} &\stackrel{\text{iid}}{\sim} \text{N} \left[\begin{pmatrix} 0 \\ 0 \end{pmatrix}, \begin{pmatrix} h_{i,1t}^0 & r_i(h_{i,1t}^0)^{1/2}(h_{i,2t}^0)^{1/2} \\ r_i(h_{i,2t}^0)^{1/2}(h_{i,1t}^0)^{1/2} & h_{i,2t}^0 \end{pmatrix} \right], \\ m_{i,1t} &= 0.8m_{i,1t-1} + e_{i,1t}, \quad m_{i,2t} = 0.8m_{i,2t-1} + e_{i,2t}, \quad e_{i,1t}, e_{i,2t} \stackrel{\text{iid}}{\sim} \text{N}(0, 4), \\ h_{i,1t}^0 &= 0.1 + 0.8h_{i,1t-1}^0 + 0.05\epsilon_{i,1t-1}^2, \quad h_{i,2t}^0 = 0.1 + 0.8h_{i,2t-1}^0 + 0.05\epsilon_{i,2t-1}^2. \end{aligned} \quad (2.36)$$

We consider the following correlation structures

$$\begin{aligned} \text{NullA: } &r_1 = r_2 = 0.2, \quad \text{NullB: } r_1 = r_2 = 0.5, \\ \text{NullC: } &r_1 = r_2 = r_t = 0.2 + 0.1 \times 0.2 \cos[2\pi t / (T/4)]. \end{aligned}$$

Under NullA, we have a relatively moderate correlation between the conditional variances in both \mathbf{Y}_{1t} and \mathbf{Y}_{2t} . Combination NullB increases the correlation magnitude. Under NullC, we have a stable time-varying correlation structure that is generated by a cosine function with four periods over sample size T . For more complex structures, the NCCC framework can always be extended by letting \mathbf{R}_i^0 evolve over time based on a parametric structure which relies on likelihood estimation (see, e.g., Aielli, 2013; Engle, 2002). To study the power of our testing strategy, we simulate the effect of volatility spillover by generating correlated squared innovation $\tilde{\epsilon}_{1,jt}^2$ and $\tilde{\epsilon}_{2,jt}^2$ using Cholesky transformation, where for $j = 1, 2$, $\tilde{\epsilon}_{1,jt}^2 = s_2\epsilon_{2,jt-1}^2 + (1 - s_2^2)^{1/2}\epsilon_{1,jt-1}^2$, $\tilde{\epsilon}_{2,jt}^2 = \epsilon_{2,jt}^2$. The parameter $s_2 \in [0, 1]$ controls the intensity of volatility spillover from \mathbf{Y}_{2t} to \mathbf{Y}_{1t} with respect to \mathbf{I}_{t-1} . We consider the following parameter combinations

$$\text{AlterA: } r_1 = r_2 = 0.2, s_2 = 0.35, \quad \text{AlterB: } r_1 = 0.2, r_2 = 0.5, s_2 = 0.35.$$

Both AlterA and AlterB generate equal spillover intensity ($s_2 = 0.35$) from \mathbf{Y}_{2t} to \mathbf{Y}_{1t} with respect to \mathbf{I}_{t-1} . This allows examining the power of our test. We increase the covariance of the risk transmitter \mathbf{Y}_{2t} under AlterB to study the role it plays in driving volatility spillover.

For each data generating process, we conduct 10000 Monte Carlo simulations with sample size $T = 1000$ and 1500, which correspond to approximately four and six years of daily financial data, respectively. For each T , we generate $T + 1000$ observations and then we discard the first 1000 observations to reduce possible effects from the chosen starting values $(h_{i,10}^0, h_{i,20}^0, m_{i,10}, m_{i,20}) = [0.1/(1 - 0.05 - 0.8), 0.1/(1 - 0.05 - 0.8), 0, 0]$. We consider the following three downward weighting kernel functions $k(\cdot)$.

The Bartlett (BAR) kernel,

$$k(z) = \begin{cases} 1 - |z|, & \text{if } |z| \leq 1, \\ 0, & \text{otherwise.} \end{cases}$$

The Daniell (DAN) kernel,

$$k(z) = \frac{\sin(\pi z)}{\pi z}, \quad z \in \mathbb{R}.$$

The Quadratic-Spectral (QS) kernel,

$$k(z) = \frac{25}{12\pi^2 z^2} \left[\frac{\sin(6\pi z/5)}{6\pi z/5} - \cos(6\pi z/5) \right], \quad z \in \mathbb{R}.$$

For comparison with an equally weighted test, we also include the Truncated (TR) kernel. Note that the selected kernels satisfy the requirements in Assumption 2.2.5. To assess the sensitivity of our approach to the kernel parameter M , we consider $M = 10, 20$ and 30 . All spillover tests are carried out at the 5% significance level.

For each simulation, the estimation and testing procedure proceeds in steps. First, we filter the conditional mean of \mathbf{Y}_{it} using least-squares which yields \sqrt{T} -consistent residuals (White, 2001, Theorem 5.11). Then, based on the procedures described in Section 2.3 we fit the NCCC-LS model. We select for the order of every diagonal ARCH process in the NCCC-LS structure using the Bayesian information criteria up to the 25th order. Finally, we test for spillover by computing Q_1 and Q_2 . It is worth highlighting that our econometric strategy is computationally simple in that numerical integration and optimization are not involved throughout model estimation and spillover testing.

In addition to asymptotic critical values, we also consider a nonparametric naive bootstrap in which we randomly re-sample the estimated residuals with replacement. As is well known, the bootstrap procedure can often yield a more accurate finite sample size (see, e.g., Chen and Hong, 2012a,b, 2016). We denote the bootstrap statistic using asterisk by Q_1^* . Step (i), retain fitted series and residuals $\hat{\mathbf{Y}}_{1t}, \hat{\mathbf{Y}}_{2t}, \hat{\boldsymbol{\epsilon}}_{1t}$ and $\hat{\boldsymbol{\epsilon}}_{2t}$. Step (ii), compute Q_1 . Step (iii), obtain naive bootstrap residuals $\hat{\boldsymbol{\epsilon}}_{1t}^*$ and $\hat{\boldsymbol{\epsilon}}_{2t}^*$ and construct bootstrap sample $\mathbf{Y}_{1t}^* = \hat{\mathbf{Y}}_{1t} + \hat{\boldsymbol{\epsilon}}_{1t}^*$ and $\mathbf{Y}_{2t}^* = \hat{\mathbf{Y}}_{2t} + \hat{\boldsymbol{\epsilon}}_{2t}^*$. Step (iv), compute the b -th statistic Q_1^{*b} in the same way as we compute Q_1 but with $\{\mathbf{Y}_{1t}^*, \mathbf{Y}_{2t}^*\}_{t=1}^T$ replacing the original sample $(\mathcal{Y}_1, \mathcal{Y}_2) \equiv \{\mathbf{Y}_{1t}, \mathbf{Y}_{2t}\}_{t=1}^T$. Step (v), repeat steps (iii) to (iv) B times to obtain B bootstrap test statistics $\{Q_1^{*b}\}_{b=1}^B$. Step (vi), compute bootstrap p -value by $B^{-1} \sum_{b=1}^B \mathbb{1}(Q_1^{*b} > Q_1)$. We set $B = 499$ and we maintain 10000 simulations. In the following we give the consistency of our bootstrap test. First, we state the following proposition.

Proposition 2.4.1. Suppose the conditions of Theorem 2.2.1 hold. Then, conditional on $(\mathcal{Y}_1, \mathcal{Y}_2)$, $Q_1^* \xrightarrow{d} N(0, 1)$.

Proof of Proposition 2.4.1. By design, the bootstrap approach ensures that the null hypothesis always holds in the bootstrap world since the two series $(\mathcal{Y}_1, \mathcal{Y}_2)$ are re-sampled independently. Taken together with the regularity conditions of Theorem 2.2.1, the asymptotic normality of Q_1^* follows. ■

The consistency of our bootstrap approach is given by combining the following two results. First, under the null hypothesis, the bootstrap approach gives asymptotically correct size since Q_1^* converges in distribution to $N(0, 1)$ given Proposition 2.4.1. Second, when the null hypothesis is false, our bootstrap approach has asymptotic unit power. This follows from the fact that while Q_1^* remains converging in distribution to $N(0, 1)$, Q_1 converges to positive infinity in probability given Theorem 2.2.2 and thus giving consistent bootstrap p -value.

Table 2.1 reports the empirical sizes of our volatility spillover tests under NullA, NullB and NullC based on the NCCC-LS modeling. In general, we find that Q_1 tends to over reject the null a little but not excessively. The size improves gradually as T increases. We find the rejection rates of Q_1 to be stable across the three parameter combinations. This implies that the size of our inferential strategy is not affected by increasing portfolio correlation and the time-varying cosine case. As expected, our bootstrap test Q_1^* yields a more accurate finite sample size than Q_1 , and it too is robust to changing correlations. Overall, we find the proposed econometric strategy to be reasonably sized. This result appears to hold across the kernel functions and the value of their smoothing parameter M .

We report the empirical powers of our testing approach in Table 2.2. For Q_1 , we use empirical critical values that are computed from the 10000 simulations under NullA. This gives size-adjusted powers. In general, we find that our inferential strategy becomes more powerful as T increases. We also find that both Q_1 and Q_1^* give rather similar power. The rejection rates of Q_1 and Q_1^* decrease in M . This is because under AlterA and AlterB, we have one-period lagged volatility spillover. Therefore, we expect a test that focuses on recent events to give better power. Besides, we find that the downward weighting kernels often yield better power than the TR kernel, and they are less affected by a large M . These results confirm our expectation that, compared with an equally weighted test, downward weighting tests alleviate the impact of choosing a relatively large M because they discount higher order lags. Interestingly, we find that the rejection rates of Q_1 and Q_1^* are higher under parameter combination AlterB. This implies that, other things being equal, an increase in the correlation within the risk transmitter \mathbf{Y}_{2t} can drive the overall effect of volatility spillover. This result highlights the nontrivial role covariance can play in driving spillover.

2.4.2 Higher dimensions

The finite sample performance of existing multivariate dependence tests is often demonstrated up to the case of three series. For instance, the bivariate case is examined in [Duchesne and Roy \(2004\)](#), whereas [Robbins and Fisher \(2015\)](#) study the relations between bivariate and trivariate processes, that is $d_1 = 3$, $d_2 = 2$. By contrast, we now demonstrate the finite sample performance of our

Table 2.1 Empirical sizes

T	M	NullA			NullB			NullC		
		10	20	30	10	20	30	10	20	30
<i>Rejection rates based on asymptotic critical values</i>										
1000	$Q_{1\text{BAR}}$	7.1	6.8	6.9	7.0	6.9	6.8	7.2	6.7	6.7
	$Q_{1\text{DAN}}$	7.1	6.8	6.9	7.0	6.7	7.1	7.0	6.7	6.8
	$Q_{1\text{QS}}$	7.1	6.9	6.8	7.1	6.8	7.1	6.8	6.7	6.9
	$Q_{1\text{TR}}$	7.1	6.9	7.0	7.0	7.3	7.1	6.6	6.6	6.7
1500	$Q_{1\text{BAR}}$	6.7	6.5	6.4	6.7	6.4	6.3	6.8	6.7	6.5
	$Q_{1\text{DAN}}$	6.8	6.6	6.4	6.7	6.3	6.5	6.7	6.6	6.2
	$Q_{1\text{QS}}$	6.8	6.5	6.3	6.6	6.4	6.5	6.8	6.5	6.3
	$Q_{1\text{TR}}$	6.5	6.4	6.4	6.1	6.3	6.3	6.3	6.4	6.4
<i>Rejection rates based on bootstrap critical values</i>										
1000	$Q_{1\text{BAR}}^*$	5.3	5.6	5.4	5.3	5.5	5.1	5.3	5.5	5.5
	$Q_{1\text{DAN}}^*$	5.4	5.3	5.2	5.3	5.3	5.1	5.4	5.3	5.2
	$Q_{1\text{QS}}^*$	5.5	5.4	5.0	5.5	5.2	5.2	5.5	5.4	5.1
	$Q_{1\text{TR}}^*$	5.0	5.0	5.2	5.0	4.9	5.1	5.1	5.1	5.1
1500	$Q_{1\text{BAR}}^*$	5.2	5.3	5.4	5.3	5.3	5.3	5.3	5.2	5.4
	$Q_{1\text{DAN}}^*$	5.3	5.1	5.3	5.2	5.2	5.3	5.3	5.2	5.3
	$Q_{1\text{QS}}^*$	5.2	5.2	5.3	5.3	5.3	5.2	5.3	5.2	5.3
	$Q_{1\text{TR}}^*$	4.9	5.3	5.3	4.9	5.5	5.2	4.8	5.3	5.3

NOTES: The table reports empirical sizes (in %) of Q_1 under NullA, NullB and NullC at the 5% significance level based on NCCC-LS modeling. Number of simulations = 10000. $Q_{1\text{BAR}}$, $Q_{1\text{DAN}}$, $Q_{1\text{QS}}$, $Q_{1\text{TR}}$ and $Q_{1\text{BAR}}^*$, $Q_{1\text{DAN}}^*$, $Q_{1\text{QS}}^*$, $Q_{1\text{TR}}^*$ denote the rejection rates of Q_1 using asymptotic and bootstrap critical values, respectively; the subscripts BAR, DAN, QS and TR denote, respectively, the Barlett kernel, the Daniell kernel, the Quadratic-Spectral kernel and the Truncated kernel. Number of bootstraps = 499. T and M denote the sample size and kernel smoothing parameter, respectively.

multivariate approach in higher dimensions, which is made feasible thanks to the proposed NCCC-LS modeling. We focus on the case where we analyze spillover effects on a relatively large market covering multiple countries such as the European Union. In particular, we study $d_1 = 3, 4, \dots, 10$ and $d_2 = 2$. We expect our approach to perform similarly given the opposite relation or any combinations of d_i with similar combination complexity.

We study the size of our inferential strategy under combination NullD, where with increasing d_1 , we retain the correlation intensity r_i of NullA because our bivariate simulations show stability across combinations NullA–NullC. In spite of that, we perform a sensitivity check to find that the performance of our approach in the higher dimensions is robust to the time-varying cosine correlation of NullC. For power study, we maintain the covariance structure in AlterA but we reduce the spillover intensity s_2 to 0.15 to highlight the power effects as d_1 increases. Given $d_1 > d_2$, we generate spillover to each series in Y_{1t} by repeating the influence of Y_{2t} . This ensures that every risk recipients in Y_{1t} is equally affected by the spillover effect. For instance, when $d_1 = 4$, $d_2 = 2$, $Y_{1,3t}$ and $Y_{1,4t}$ will be influenced by $Y_{2,1t}$ and $Y_{2,2t}$, respectively. We denote this parameter combination

Table 2.2 Empirical powers

T	M	AlterA			AlterB		
		10	20	30	10	20	30
<i>Rejection rates based on empirical critical values</i>							
1000	$Q_{1\text{BAR}}$	78.2	69.0	61.9	95.0	90.1	85.1
	$Q_{1\text{DAN}}$	74.5	62.1	53.4	93.3	85.1	78.2
	$Q_{1\text{QS}}$	73.1	59.8	51.7	92.7	83.8	76.6
	$Q_{1\text{TR}}$	51.5	38.4	32.0	76.8	61.1	51.7
1500	$Q_{1\text{BAR}}$	92.1	85.4	80.0	99.4	98.0	96.7
	$Q_{1\text{DAN}}$	89.8	79.6	72.3	99.0	96.6	93.7
	$Q_{1\text{QS}}$	88.9	78.2	70.9	98.8	96.2	92.8
	$Q_{1\text{TR}}$	71.1	55.1	46.4	92.9	83.3	73.2
<i>Rejection rates based on bootstrap critical values</i>							
1000	$Q_{1\text{BAR}}^*$	76.1	66.0	59.1	94.2	88.4	83.1
	$Q_{1\text{DAN}}^*$	71.7	58.8	49.7	92.4	82.9	75.1
	$Q_{1\text{QS}}^*$	70.3	57.0	48.2	91.6	81.4	73.7
	$Q_{1\text{TR}}^*$	47.9	34.8	29.0	73.6	58.3	49.3
1500	$Q_{1\text{BAR}}^*$	91.2	83.9	78.0	99.4	98.0	96.2
	$Q_{1\text{DAN}}^*$	88.4	77.9	69.1	99.0	96.2	92.8
	$Q_{1\text{QS}}^*$	87.2	76.3	67.6	98.7	95.6	91.9
	$Q_{1\text{TR}}^*$	67.6	52.0	42.8	92.0	80.9	72.0

NOTES: The table reports empirical powers (in %) of Q_1 under AlterA and AlterB at the 5% significance level based on NCCC-LS modeling. Number of simulations = 10000. $Q_{1\text{BAR}}$, $Q_{1\text{DAN}}$, $Q_{1\text{QS}}$, $Q_{1\text{TR}}$ and $Q_{1\text{BAR}}^*$, $Q_{1\text{DAN}}^*$, $Q_{1\text{QS}}^*$, $Q_{1\text{TR}}^*$ denote the rejection rates of Q_1 using empirical and bootstrap critical values, respectively; the subscripts BAR, DAN, QS and TR denote, respectively, the Barlett kernel, the Daniell kernel, the Quadratic-Spectral kernel and the Truncated kernel. Number of bootstraps = 499. T and M denote the sample size and kernel smoothing parameter, respectively.

by AlterC. Because the overall performance of our test is stable across M , we only report here the case where $M = 20$ to save space. The full set of results are reported in Appendix 2.H.

Table 2.3 reports the empirical sizes of our inferential approach. We find that the size of Q_1 increases in dimension, but not overly excessive nor rapid. The size of Q_1 generally improves and stabilizes as T increases. The rejection rates of our bootstrap approach Q_1^* also tend to increase in dimension when $T = 1000$, but they become very stable as T approaches 1500. Table 2.4 reports the power study. As with the bivariate study, we use empirical critical values for Q_1 . In general, our approach has power despite a rather low spillover intensity $s_2 = 0.15$. Both Q_1 and Q_1^* give similar rejection rates, and they become more powerful as T increases. We find that the power of our tests grows with d_1 . Because the number of risk recipients in Y_{1t} increases as d_1 increases, this yields a stronger evidence of spillover and thus increase the rejection rates Q_1 and Q_1^* .

Table 2.3 Empirical sizes

T	d_1	NullD							
		3	4	5	6	7	8	9	10
<i>Rejection rates based on asymptotic critical values</i>									
1000	$Q_{1\text{BAR}}$	7.1	7.1	7.1	7.2	7.4	7.9	7.9	7.6
	$Q_{1\text{DAN}}$	7.3	6.9	7.1	7.3	7.3	7.9	8.2	7.9
	$Q_{1\text{QS}}$	7.1	7.0	7.3	7.2	7.4	7.8	8.3	7.9
	$Q_{1\text{TR}}$	7.2	7.3	7.4	7.4	7.5	8.1	8.8	8.9
1500	$Q_{1\text{BAR}}$	6.7	7.0	6.6	6.8	6.3	7.2	7.1	6.8
	$Q_{1\text{DAN}}$	6.6	6.9	6.6	6.7	6.4	7.2	7.2	7.0
	$Q_{1\text{QS}}$	6.7	6.9	6.6	6.7	6.4	7.2	7.1	7.1
	$Q_{1\text{TR}}$	6.7	6.9	7.1	7.0	7.0	6.8	7.0	7.3
<i>Rejection rates based on bootstrap critical values</i>									
1000	$Q_{1\text{BAR}}^*$	4.8	5.5	5.5	5.2	5.5	5.2	5.3	5.8
	$Q_{1\text{DAN}}^*$	4.9	5.6	5.3	5.5	5.4	5.3	5.4	5.7
	$Q_{1\text{QS}}^*$	5.1	5.5	5.5	5.5	5.5	5.5	5.3	5.8
	$Q_{1\text{TR}}^*$	5.1	5.8	5.7	5.3	5.7	5.7	5.7	5.6
1500	$Q_{1\text{BAR}}^*$	5.1	5.2	4.8	5.0	5.4	5.5	5.4	5.1
	$Q_{1\text{DAN}}^*$	5.1	5.3	4.8	5.2	5.3	5.5	5.4	5.1
	$Q_{1\text{QS}}^*$	5.2	5.2	4.8	5.2	5.4	5.5	5.4	5.1
	$Q_{1\text{TR}}^*$	5.3	5.4	5.2	5.3	5.5	5.6	5.3	5.5

NOTES: The table reports empirical sizes (in %) of Q_1 under NullD at the 5% significance level based on NCCC-LS modeling. Number of simulations = 10000. $Q_{1\text{BAR}}$, $Q_{1\text{DAN}}$, $Q_{1\text{QS}}$, $Q_{1\text{TR}}$ and $Q_{1\text{BAR}}^*$, $Q_{1\text{DAN}}^*$, $Q_{1\text{QS}}^*$, $Q_{1\text{TR}}^*$ denote the rejection rates of Q_1 using asymptotic and bootstrap critical values, respectively; the subscripts BAR, DAN, QS and TR denote, respectively, the Barlett kernel, the Daniell kernel, the Quadratic-Spectral kernel and the Truncated kernel. Number of bootstraps = 499. T and d_1 denote the sample size and dimension of portfolio 1, respectively.

2.5 Empirical application

The North America (NA) has historically maintained a strong economic partnership with the UK but [Cumming and Zahra \(2016\)](#) suggest that this relation is to be challenged after the UK voted to leave the European Union on 23rd June 2016. In this section, we use the new inferential strategy to study, before and after the Brexit referendum, the spillover relations between the North American and the UK equity markets. We use the American S&P-500 and the Canadian S&P-TSX stock indices for the NA market, and we use the FTSE-All index for the UK market. To examine possible Brexit effect on the broader European market, we also study its spillover relations with the NA market. Regarding the former, we use the European Union (EU) portfolio previously constructed by [Baele \(2005\)](#): Austria, Belgium, France, Germany, Ireland, Italy, the Netherlands and Spain, where the market indices are taken as ATX, Bel-20, FrCAC-40, DAX-30, ISEQ-All, FTSE-MIB, AEX and IBEX-35, respectively. It is worth highlighting that this is the first study to provide insights into the distortion

Table 2.4 Empirical powers

T	d_1	AlterC							
		3	4	5	6	7	8	9	10
<i>Rejection rates based on empirical critical values</i>									
1000	$Q_{1\text{BAR}}$	27.6	40.8	55.2	65.5	73.9	77.1	80.9	83.0
	$Q_{1\text{DAN}}$	23.0	33.4	44.8	54.9	62.5	65.9	70.3	71.4
	$Q_{1\text{QS}}$	22.1	31.6	43.2	52.9	60.1	64.1	67.4	69.0
	$Q_{1\text{TR}}$	14.3	18.8	23.7	30.0	34.2	35.5	37.1	37.8
1500	$Q_{1\text{BAR}}$	42.6	63.0	84.2	91.4	96.0	97.7	98.6	99.1
	$Q_{1\text{DAN}}$	34.1	51.9	73.2	82.4	90.7	93.6	95.0	96.8
	$Q_{1\text{QS}}$	33.1	49.5	70.7	80.3	88.9	92.2	93.8	95.8
	$Q_{1\text{TR}}$	18.8	28.1	39.2	47.8	57.2	61.9	66.3	67.8
<i>Rejection rates based on bootstrap critical values</i>									
1000	$Q_{1\text{BAR}}^*$	23.8	36.6	52.0	62.2	70.1	74.9	78.6	80.9
	$Q_{1\text{DAN}}^*$	19.6	29.6	42.1	50.9	58.1	63.3	67.2	69.8
	$Q_{1\text{QS}}^*$	19.0	28.2	40.3	48.4	55.6	60.4	64.6	67.1
	$Q_{1\text{TR}}^*$	12.4	15.6	21.7	26.4	30.4	32.9	35.9	37.0
1500	$Q_{1\text{BAR}}^*$	38.7	62.3	81.3	89.9	94.8	97.3	98.4	98.9
	$Q_{1\text{DAN}}^*$	31.2	50.9	70.2	80.3	87.9	92.2	94.4	95.9
	$Q_{1\text{QS}}^*$	29.6	48.4	67.4	77.8	86.1	90.5	93.0	94.8
	$Q_{1\text{TR}}^*$	16.9	26.0	36.4	44.5	52.0	58.3	61.8	65.9

NOTES: The table reports empirical powers (in %) of Q_1 under AlterC at the 5% significance level based on NCCC-LS modeling. Number of simulations = 10000. $Q_{1\text{BAR}}$, $Q_{1\text{DAN}}$, $Q_{1\text{QS}}$, $Q_{1\text{TR}}$ and $Q_{1\text{BAR}}^*$, $Q_{1\text{DAN}}^*$, $Q_{1\text{QS}}^*$, $Q_{1\text{TR}}^*$ denote the rejection rates of Q_1 using empirical and bootstrap critical values, respectively; the subscripts BAR, DAN, QS and TR denote, respectively, the Barlett kernel, the Daniell kernel, the Quadratic-Spectral kernel and the Truncated kernel. Number of bootstraps = 499. T and d_1 denote the sample size and dimension of portfolio 1, respectively.

of spillover relation between the North American and the European equity markets in the aftermath of the Brexit referendum.

We sample our data centering the referendum event from 2nd January 2012 to 31st December 2019 at the daily frequency from *Datastream*. This gives 2087 observations. Then, we divide the sample into two subperiods: the pre-Brexit sample (2nd January 2012 – 23rd June 2016) and the post-Brexit sample (24th June 2016 – 31st December 2019). We collect all data in US dollar to minimize potential bias due to currency risk. Return series are calculated by taking the first difference of the price indices in natural logarithm.

We begin with the NA-UK study. First, we estimate our NCCC-LS conditional variance model for both subsamples. To filter out possible mean causality, each return variable is regressed on the remaining lagged series. With the residuals that are free from mean causality, we estimate the NCCC-LS model. The best fitting model lag orders are selected on the basis of Bayesian information criteria and diagnostic examinations. Regarding the pre-Brexit period, we obtain orders 9, 3 and 11 for the conditional variances of the UK, US and Canada markets, respectively. As for the post-Brexit

sample, we obtain orders 4, 16 and 12 for the conditional variances of the UK, US and Canada series, respectively. We carry out for the NA portfolio the [Engle and Sheppard's \(2001\)](#) diagnosis to find that we cannot reject the null of stable correlation structure at the usual significance level, with p -values of 0.8969 and 0.1325 for the pre-Brexit and post-Brexit samples, respectively. The optimal orders of the correlation stability test are automatically selected based on Bayesian information criteria. This, together with a series of conventional Ljung-Box examinations reported in [Table 2.5](#), suggests the adequacy of our NCCC-LS modeling.

Next, we compute our bootstrap Q_1^* tests using the Barlett kernel since simulations suggest similar performance across the downward weighting kernels. We report the p -values in [Table 2.6](#). In the pre-Brexit sample, we find that the spillover effect from the NA market to the UK market is statistically significant at the 5% level for all M 's. This finding implies that the NA market has a significant influence on the UK market in both the short term and the long run. In the other direction, we find evidence of spillover effect from the UK market to the NA market at the 10% level for all M 's. Our findings imply feedback spillovers in the NA-UK nexus. This interdependent relation, however, diminishes in the post-Brexit period.

Before Brexit, the feedback spillover in the NA-UK nexus can be explained by the closely interconnected economic activities in the two regions. Since the two markets rely on each other, the market participants in the two regions tend to follow each other closely. Therefore, an increase in uncertainty or volatility of one market would inevitably affect the other. Interestingly, the spillover effects between NA and UK disappear after Brexit. In other words, the NA (UK) market is no longer significantly affected by the volatility in the UK (NA) market. After the Brexit referendum, market participants in the UK may be discouraged to infer information from the NA market because they are less confident about the UK's bargaining position in the international market especially among major players such as NA. Consequently, uncertainty in NA does not spill to UK. In the other direction, market participants in the NA region tend to divert their focus away from the UK because of the fear that it will lose its access to the European Single Market, which is an important trading region for the NA. As a result, the NA is less driven by the UK and thus uncertainty from the latter does not propagate to the former.

We now examine the NA-EU spillover relation. In the pre-Brexit sample, we obtain orders 16, 14, 12, 11, 7, 18, 9, 15, 3 and 15 for the conditional variances of the Austria, Belgium, France, Germany, Ireland, Italy, the Netherlands, Spain, US and Canada markets, respectively. As for the post-Brexit period, we obtain orders 11, 16, 10, 12, 9, 10, 11, 8, 9 and 10 for the conditional variances of the Austria, Belgium, France, Germany, Ireland, Italy, the Netherlands, Spain, US and Canada series, respectively. As with the NA-UK study, we perform the [Engle and Sheppard's \(2001\)](#) diagnosis to find that we cannot reject the null of stable correlation structure at the usual significance level for both subsamples and for both portfolios. Regarding the EU portfolio, we obtain p -values of 0.5472 and 0.1183 for the pre-Brexit and post-Brexit samples, respectively. As for the NA portfolio, we obtain p -values of 0.6592 and 0.5472 for the pre-Brexit and post-Brexit

Table 2.5 Diagnostic tests (UK–NA)

	LB(10)	LB(20)	LB(30)	LB ² (10)	LB ² (20)	LB ² (30)
<i>Pre–Brexit (2nd January 2012 – 23rd June 2016)</i>						
UK	7.155 [0.711]	22.093 [0.335]	36.494 [0.192]	6.177 [0.800]	18.319 [0.566]	25.026 [0.724]
US	13.169 [0.214]	20.312 [0.439]	32.243 [0.356]	12.124 [0.277]	20.539 [0.425]	30.504 [0.440]
Canada	4.224 [0.937]	20.656 [0.418]	34.183 [0.274]	2.911 [0.983]	23.436 [0.268]	38.206 [0.145]
<i>Post–Brexit (24th June 2016 – 31st December 2019)</i>						
UK	11.071 [0.352]	19.740 [0.474]	27.036 [0.621]	10.468 [0.400]	14.336 [0.813]	16.783 [0.975]
US	15.436 [0.117]	18.869 [0.530]	23.736 [0.784]	10.546 [0.394]	13.020 [0.877]	17.188 [0.970]
Canada	6.779 [0.746]	18.437 [0.559]	22.004 [0.854]	4.432 [0.926]	18.823 [0.533]	21.513 [0.871]

NOTES: The table reports diagnostic analyses for all fitted series. $LB(M)$ and $LB^2(M)$ are the Ljung-Box tests for the null of no serial correlation (up to lag order M) on the standardized and squared standardized residuals, respectively. The values in the squared parentheses are the p -values of the tests.

samples, respectively. These examinations, along with a series of Ljung-Box diagnoses reported in Tables 2.7 and 2.8, confirm the adequacy of our NCCC-LS model parameterizations.

Table 2.9 reports the volatility spillover test results. In the pre–Brexit period, we find that the spillover effect from the NA market to the EU market is statistically significant at the 10% level for $M = 10, 30$. This finding suggests that the NA market has nontrivial influences on the broader EU market in the short and long terms. In the opposite direction, the spillover effect from the EU market is significant at the 10% level for $M = 30$. In the post–Brexit sample, the spillover effect between the NA market and the EU market persists, with the impact from the latter occurs at a lower M .

Before Brexit, the feedback spillover in the NA–EU nexus can be largely attributed to the interlinked economic activities in the two regions. Therefore, uncertainty in one market would naturally spill to the other. Interestingly, the spillover effect from the EU is somehow delayed as the effect is not felt immediately by the NA market. One possible explanation for this finding is that, before Brexit, market participants in the NA can access the Single market seamlessly through the UK. Thus, they may tend to focus primarily on the UK, which results in their delayed response to the volatility in the EU market. However, we find that the NA–EU spillover nexus becomes more immediate after Brexit. This is because market participants that previously focus on the UK have naturally switched their attention to the European Single Market directly. As a result, the NA reacts more rapidly to the uncertainty in the EU market.

Table 2.6 Spillover results (UK–NA)

M	<i>Pre–Brexit</i>			<i>Post–Brexit</i>		
	10	20	30	10	20	30
$Q_{1\text{BAR}}^*$	0.028	0.036	0.038	0.168	0.154	0.186
$Q_{-1\text{BAR}}^*$	0.088	0.058	0.054	0.729	0.677	0.774

NOTES: The table reports bootstrap p -values of the proposed spillover tests. Number of bootstraps = 499. $Q_{1\text{BAR}}^*$ denotes the one-way test for the null hypothesis of no volatility spillover from the NA market to the UK market. $Q_{-1\text{BAR}}^*$ denotes the one-way test for the null hypothesis of no volatility spillover from the UK market to the NA market. The subscript BAR denotes the Barlett kernel. M denotes the kernel smoothing parameter.

In summary, our findings suggest that, before the Brexit referendum, participants in the NA market pay a relatively closer attention to the UK than the EU market. Consequently, the NA is driven more immediately by the volatility in the UK. After Brexit, the NA tends not to focus on the UK, and it prefers to follow the EU more closely. As a result, uncertainty in the UK does not significantly affect the NA while that in the EU has a more immediate effect on the NA.

Table 2.7 Diagnostic tests (EU–NA)

	LB(10)	LB(20)	LB(30)	LB ² (10)	LB ² (20)	LB ² (30)
<i>Pre–Brexit (2nd January 2012 – 23rd June 2016)</i>						
Austria	8.839 [0.547]	11.259 [0.939]	29.522 [0.490]	1.821 [0.998]	2.540 [1.000]	15.942 [0.983]
Belgium	7.327 [0.694]	17.561 [0.616]	39.203 [0.121]	2.063 [0.996]	14.773 [0.789]	31.616 [0.386]
France	7.405 [0.687]	18.745 [0.538]	38.255 [0.143]	5.597 [0.848]	16.625 [0.677]	27.864 [0.578]
Germany	4.424 [0.926]	20.098 [0.452]	37.650 [0.159]	1.810 [0.998]	16.234 [0.702]	26.026 [0.674]
Ireland	7.429 [0.684]	21.941 [0.344]	37.667 [0.158]	4.151 [0.940]	21.944 [0.344]	40.053 [0.104]
Italy	5.208 [0.877]	24.126 [0.237]	39.677 [0.111]	4.861 [0.900]	18.723 [0.540]	29.314 [0.501]
Netherlands	7.255 [0.701]	19.837 [0.468]	37.514 [0.163]	2.467 [0.991]	14.265 [0.817]	21.344 [0.877]
Spain	11.198 [0.342]	22.854 [0.296]	39.655 [0.112]	8.825 [0.549]	18.703 [0.541]	37.979 [0.150]
US	13.084 [0.219]	21.296 [0.380]	36.398 [0.195]	15.271 [0.122]	22.915 [0.293]	34.113 [0.276]
Canada	3.926 [0.951]	17.647 [0.611]	30.166 [0.457]	3.113 [0.979]	20.511 [0.426]	33.009 [0.322]

NOTES: The table reports diagnostic analyses for all fitted series. LB(M) and LB²(M) are the Ljung-Box tests for the null of no serial correlation (up to lag order M) on the standardized and squared standardized residuals, respectively. The values in the squared parentheses are the p -values of the tests.

Table 2.8 Diagnostic tests (EU–NA)

	LB(10)	LB(20)	LB(30)	LB ² (10)	LB ² (20)	LB ² (30)
<i>Post–Brexit (24th June 2016 – 31st December 2019)</i>						
Austria	3.371 [0.971]	15.052 [0.773]	19.516 [0.929]	2.601 [0.989]	13.909 [0.835]	17.353 [0.968]
Belgium	7.672 [0.661]	18.799 [0.535]	24.333 [0.757]	1.892 [0.997]	5.901 [0.999]	7.232 [1.000]
France	10.970 [0.360]	16.590 [0.679]	27.751 [0.584]	5.436 [0.860]	9.278 [0.979]	14.264 [0.993]
Germany	2.087 [0.996]	15.826 [0.727]	24.130 [0.766]	1.233 [1.000]	10.628 [0.955]	14.429 [0.993]
Ireland	4.952 [0.894]	15.662 [0.737]	29.053 [0.515]	0.465 [1.000]	15.670 [0.737]	22.324 [0.842]
Italy	5.015 [0.890]	21.839 [0.349]	26.462 [0.651]	2.595 [0.989]	11.920 [0.919]	18.647 [0.947]
Netherlands	4.078 [0.944]	7.539 [0.995]	17.054 [0.972]	1.409 [0.999]	8.056 [0.991]	12.786 [0.997]
Spain	6.255 [0.793]	21.479 [0.369]	23.440 [0.797]	2.728 [0.987]	15.164 [0.767]	25.255 [0.713]
US	7.289 [0.698]	21.190 [0.386]	30.560 [0.437]	15.012 [0.132]	23.508 [0.265]	25.919 [0.679]
Canada	5.511 [0.855]	27.150 [0.131]	33.990 [0.281]	3.446 [0.969]	26.552 [0.148]	30.657 [0.432]

NOTES: The table reports diagnostic analyses for all fitted series. LB(M) and LB²(M) are the Ljung-Box tests for the null of no serial correlation (up to lag order M) on the standardized and squared standardized residuals, respectively. The values in the squared parentheses are the p -values of the tests.

Table 2.9 Spillover results (EU–NA)

M	<i>Pre–Brexit</i>			<i>Post–Brexit</i>		
	10	20	30	10	20	30
$Q_{1\text{BAR}}^*$	0.046	0.124	0.070	0.078	0.128	0.182
$Q_{-1\text{BAR}}^*$	0.210	0.144	0.072	0.132	0.080	0.078

NOTES: The table reports bootstrap p -values of the proposed spillover tests. Number of bootstraps = 499. $Q_{1\text{BAR}}^*$ denotes the one-way test for the null hypothesis of no volatility spillover from the NA market to the EU market. $Q_{-1\text{BAR}}^*$ denotes the one-way test for the null hypothesis of no volatility spillover from the EU market to the NA market. The subscript BAR denotes the Barlett kernel. M denotes the kernel smoothing parameter.

2.6 Conclusions

In this paper, we proposed a class of asymptotic $N(0, 1)$ multivariate econometric strategy for testing volatility spillover. The test statistics were constructed based on the quadratic distance between a kernel-based spectral density estimator and the null spectral density. The proposed test statistics are convenient to compute and they check a growing number of lags as the sample size increases. The Granger regression-type method can be viewed as a special case of the proposed procedure under the uniformly weighted Truncated kernel, but downward weighting kernels were proposed to be in line with financial markets stylized facts and thus to improve the power performance of the tests. To facilitate the estimation of the our test statistics, we proposed a new NCCC-LS volatility structure that can be estimated element by element. Consistent least-squares estimators that are computationally efficient were provided. Numerical optimization and integration are not required throughout the proposed econometric strategy. The optimality of the multivariate testing strategy was highlighted using Monte Carlo experiments. First, it can check a large number of lags without losing significant power thanks to the use of downward weighting kernel functions. Second, the testing strategy performed reasonably well in the higher dimension up to 10 series. Furthermore, the paper provided a bootstrap version of the spillover tests whose size was found to converge at a faster speed. Finally, the paper included a timely empirical study in which the volatility spillover relations between the North America (NA) market and the greater European market (both UK and EU) before and after the Brexit referendum were examined. Before the Brexit referendum, it was found that the NA was driven more immediately by UK volatility than EU volatility. After Brexit, it was found that volatility in the UK did not spill to NA while that in the EU had a more immediate spillover effect on NA. This finding can be interpreted as that most NA participants switched their attention from the UK to the EU market because of the fear that UK might lose its access to the European Single Market.

Although our simulation study is supportive of the asymptotic theory, there are however circumstances in which we would not recommend to use the proposed testing strategy. First, the Hessian condition implies that the squared innovation can be twice differentiable with respect to the parameter vector. For any variable to be differentiable, it should be continuous. Thus, if an estimated innovation series appears to be discontinuous with jumps, we would not recommend to use the proposed testing strategy. Second, another assumption of the theory is the existence of the finite eighth moment of the innovation. Random vectors following the multivariate normal distribution, t-distribution and generalised error distribution satisfy this assumption. Therefore, if the empirical distribution of an estimated innovation sequence appears not to be “well-behaved” — such as a distribution with unreasonably many extreme occurrences — we would not recommend to use the proposed testing strategy. However, dataset with the discussed features might contain valuable information about market jumps. Therefore, we propose to develop econometric tool for market jumps and extreme events spillover in future research.

Appendix 2.A

Derivation of (2.15). Recall that the normalized quadratic distance is given as

$$\begin{aligned}
\hat{L}^2[\hat{\mathbf{f}}(\lambda), \hat{\mathbf{f}}^0(\lambda)] &= 2\pi \int_{2\pi} \text{vec}[\overline{\hat{\mathbf{f}}(\lambda) - \hat{\mathbf{f}}^0(\lambda)}]' (\hat{\mathbf{\Gamma}}_v^{-1} \otimes \hat{\mathbf{\Gamma}}_u^{-1}) \text{vec}[\hat{\mathbf{f}}(\lambda) - \hat{\mathbf{f}}^0(\lambda)] d\lambda \\
&= 2\pi \int_{2\pi} \text{vec}[\overline{\hat{\mathbf{f}}(\lambda) - \hat{\mathbf{f}}^0(\lambda)}]' (\hat{\mathbf{\Gamma}}_v^{-1} \otimes \hat{\mathbf{\Gamma}}_u^{-1}) \text{vec}[\hat{\mathbf{f}}(\lambda) - \hat{\mathbf{f}}^0(\lambda)] d\lambda \\
&= 2\pi \int_{2\pi} \text{tr}\left\{ \left[\overline{\hat{\mathbf{f}}(\lambda) - \hat{\mathbf{f}}^0(\lambda)} \right]' \hat{\mathbf{\Gamma}}_u^{-1} [\hat{\mathbf{f}}(\lambda) - \hat{\mathbf{f}}^0(\lambda)] \hat{\mathbf{\Gamma}}_v^{-1} \right\} d\lambda \\
&= 2\pi \int_{2\pi} \text{tr}\left\{ \left[\overline{\hat{\mathbf{f}}(\lambda) - \hat{\mathbf{f}}^0(\lambda)} \right]' \hat{\mathbf{\Gamma}}_u^{-1} [\hat{\mathbf{f}}(\lambda) - \hat{\mathbf{f}}^0(\lambda)] \hat{\mathbf{\Gamma}}_v^{-1} \right\} d\lambda \\
&= 2\pi \int_{2\pi} \text{tr}\left\{ \left[\overline{\hat{\mathbf{f}}(\lambda) - \hat{\mathbf{f}}^0(\lambda)} \right]' \hat{\mathbf{\Gamma}}_u^{-1} [\hat{\mathbf{f}}(\lambda) - \hat{\mathbf{f}}^0(\lambda)] \hat{\mathbf{\Gamma}}_v^{-1} \right\} d\lambda, \tag{2.A.1}
\end{aligned}$$

where $\overline{\mathbf{f}}$ denotes the complex conjugate of \mathbf{f} . The second equality follows from the fact that complex conjugate of a sum of individuals is the sum of the complex conjugate of the individuals. The third equality follows from the matrix relation $\text{tr}(\mathbf{A}'\mathbf{B}\mathbf{C}\mathbf{D}') = [\text{vec}(\mathbf{A})]'(\mathbf{D}\otimes\mathbf{B})[\text{vec}(\mathbf{C})]$, (see, e.g., [Harville, 1997](#), Theorem 16.2.2). The fourth equality follows from the interchangeability of complex conjugation and transposition. The fifth equality follows from the fact that the complex conjugate of real matrix is the real matrix itself. Let $\mathbf{C}(\lambda) \equiv [\hat{\mathbf{f}}(\lambda) - \hat{\mathbf{f}}^0(\lambda)]' \hat{\mathbf{\Gamma}}_u^{-1}$, $\mathbf{D}(\lambda) \equiv [\hat{\mathbf{f}}(\lambda) - \hat{\mathbf{f}}^0(\lambda)] \hat{\mathbf{\Gamma}}_v^{-1}$, and put $\mathbf{A}_j \equiv (2\pi)^{-1} k(j/M) \hat{\boldsymbol{\rho}}(j)' \hat{\mathbf{\Gamma}}_u^{-1}$, $\mathbf{B}_j \equiv (2\pi)^{-1} k(j/M) \hat{\boldsymbol{\rho}}(j) \hat{\mathbf{\Gamma}}_v^{-1}$. We have $\mathbf{C}(\lambda) = \sum_{j=1}^{T-1} \mathbf{A}_j e^{-ij\lambda}$ and $\mathbf{D}(\lambda) = \sum_{j=1}^{T-1} \mathbf{B}_j e^{-ij\lambda}$, for $\lambda \in [-\pi, \pi]$ and $i = \sqrt{-1}$. We can rewrite (2.A.1) as

$$\begin{aligned}
\hat{L}^2[\hat{\mathbf{f}}(\lambda), \hat{\mathbf{f}}^0(\lambda)] &= 2\pi \int_{2\pi} \text{tr}[\overline{\mathbf{C}(\lambda)} \mathbf{D}(\lambda)] d\lambda \\
&= 2\pi \text{tr} \left[\int_{2\pi} \overline{\mathbf{C}(\lambda)} \mathbf{D}(\lambda) d\lambda \right] \\
&= 2\pi \text{tr} \left(2\pi \sum_{j=1}^{T-1} \overline{\mathbf{A}_j} \mathbf{B}_j \right) \\
&= (2\pi)^2 \text{tr} \left(\sum_{j=1}^{T-1} \overline{\mathbf{A}_j} \mathbf{B}_j \right),
\end{aligned}$$

where the second equality follows from the interchangeability of trace and integral and the third equality follows from Parseval's identity (see, e.g., [Wiener and Masani, 1957](#), Theorem 3.9). Substi-

tuting the relevant terms back into the normalized quadratic equation, we have

$$\begin{aligned}
\hat{L}^2[\hat{\mathbf{f}}(\lambda), \hat{\mathbf{f}}^0(\lambda)] &= (2\pi)^2 \text{tr} \left[\sum_{j=1}^{T-1} \frac{1}{2\pi} k(j/M) \hat{\boldsymbol{\rho}}(j)' \hat{\boldsymbol{\Gamma}}_u^{-1} \frac{1}{2\pi} k(j/M) \hat{\boldsymbol{\rho}}(j) \hat{\boldsymbol{\Gamma}}_v^{-1} \right] \\
&= \text{tr} \left[\sum_{j=1}^{T-1} k^2(j/M) \hat{\boldsymbol{\rho}}(j)' \hat{\boldsymbol{\Gamma}}_u^{-1} \hat{\boldsymbol{\rho}}(j) \hat{\boldsymbol{\Gamma}}_v^{-1} \right] \\
&= \sum_{j=1}^{T-1} k^2(j/M) \text{tr} \{ \hat{\boldsymbol{\rho}}(j)' \hat{\boldsymbol{\Gamma}}_u^{-1} \hat{\boldsymbol{\rho}}(j) \hat{\boldsymbol{\Gamma}}_v^{-1} \} \\
&= \sum_{j=1}^{T-1} k^2(j/M) \text{vec}[\hat{\boldsymbol{\rho}}(j)]' (\hat{\boldsymbol{\Gamma}}_v^{-1} \otimes \hat{\boldsymbol{\Gamma}}_u^{-1}) \text{vec}[\hat{\boldsymbol{\rho}}(j)],
\end{aligned}$$

where the fourth equality follows from the interchangeability of trace and summation. This completes the derivation. ■

Appendix 2.B

Throughout Appendices 2.B–2.G, the following notations are adopted. The Euclidean norm of vector \mathbf{x} is denoted by $\|\mathbf{x}\|$. The inner product between vector \mathbf{x}_1 and vector \mathbf{x}_2 is denoted by $\langle \mathbf{x}_1, \mathbf{x}_2 \rangle$. The Frobenius norm of matrix \mathbf{X} is denoted by $\|\mathbf{X}\|_F$. The notations O_p and o_p are the usual order in probability notations. The scalar Δ represents a positive finite generic constant that may differ at every occurrence.

Proof of Lemma 2.2.1. We begin by showing the covariance representation of S . Then, the asymptotic normality follows from Lemma 2.2 in [Candelon and Tokpavi \(2016\)](#) and Lemma 1 in [Bouhaddioui and Roy \(2006\)](#). Using the properties $\text{vec}(\mathbf{A}\mathbf{X}\mathbf{B}) = (\mathbf{B}' \otimes \mathbf{A})\text{vec}(\mathbf{X})$; $(\mathbf{A} \otimes \mathbf{B})' = \mathbf{A}' \otimes \mathbf{B}'$; $(\mathbf{A}')^{-1} = (\mathbf{A}^{-1})'$; $(\mathbf{A} \otimes \mathbf{B})(\mathbf{C} \otimes \mathbf{D}) = (\mathbf{A}\mathbf{C}) \otimes (\mathbf{B}\mathbf{D})$; $(\mathbf{A}\mathbf{B}\mathbf{C})^{-1} = \mathbf{C}^{-1}\mathbf{B}^{-1}\mathbf{A}^{-1}$; $(\mathbf{A} \otimes \mathbf{B})^{-1} = \mathbf{A}^{-1} \otimes \mathbf{B}^{-1}$, we write for the correlation components of S

$$\begin{aligned}
& \text{vec}[\hat{\boldsymbol{\rho}}^0(j)]'(\boldsymbol{\Gamma}_v^{-1} \otimes \boldsymbol{\Gamma}_u^{-1})\text{vec}[\hat{\boldsymbol{\rho}}^0(j)] \\
&= \text{vec}[\hat{\mathbf{C}}_{uv}^0(j)]'[\text{Diag}(\mathbf{C}_{vv}^0)^{-1/2} \otimes \text{Diag}(\mathbf{C}_{uu}^0)^{-1/2}](\boldsymbol{\Gamma}_v^{-1} \otimes \boldsymbol{\Gamma}_u^{-1})\text{vec}[\hat{\boldsymbol{\rho}}^0(j)] \\
&= \text{vec}[\hat{\mathbf{C}}_{uv}^0(j)]'[\text{Diag}(\mathbf{C}_{vv}^0)^{-1/2}\boldsymbol{\Gamma}_v^{-1}] \otimes [\text{Diag}(\mathbf{C}_{uu}^0)^{-1/2}\boldsymbol{\Gamma}_u^{-1}]\text{vec}[\hat{\boldsymbol{\rho}}^0(j)] \\
&= \text{vec}[\hat{\mathbf{C}}_{uv}^0(j)]' \{(\mathbf{C}_{vv}^0)^{-1}[\text{Diag}(\mathbf{C}_{vv}^0)^{-1/2}]^{-1}\} \otimes \{(\mathbf{C}_{uu}^0)^{-1}[\text{Diag}(\mathbf{C}_{uu}^0)^{-1/2}]^{-1}\} \text{vec}[\hat{\boldsymbol{\rho}}^0(j)] \\
&= \text{vec}[\hat{\mathbf{C}}_{uv}^0(j)]'[(\mathbf{C}_{vv}^0)^{-1} \otimes (\mathbf{C}_{uu}^0)^{-1}] \{[\text{Diag}(\mathbf{C}_{vv}^0)^{-1/2}]^{-1} \otimes [\text{Diag}(\mathbf{C}_{uu}^0)^{-1/2}]^{-1}\} \text{vec}[\hat{\boldsymbol{\rho}}^0(j)] \\
&= \text{vec}[\hat{\mathbf{C}}_{uv}^0(j)]'[(\mathbf{C}_{vv}^0)^{-1} \otimes (\mathbf{C}_{uu}^0)^{-1}] \{[\text{Diag}(\mathbf{C}_{vv}^0)^{-1/2}] \otimes [\text{Diag}(\mathbf{C}_{uu}^0)^{-1/2}]\}^{-1} \text{vec}[\hat{\boldsymbol{\rho}}^0(j)] \\
&= \text{vec}[\hat{\mathbf{C}}_{uv}^0(j)]'[(\mathbf{C}_{vv}^0)^{-1} \otimes (\mathbf{C}_{uu}^0)^{-1}] \{[\text{Diag}(\mathbf{C}_{vv}^0)^{-1/2}] \otimes [\text{Diag}(\mathbf{C}_{uu}^0)^{-1/2}]\}^{-1} \\
&\quad \times [\text{Diag}(\mathbf{C}_{vv}^0)^{-1/2} \otimes \text{Diag}(\mathbf{C}_{uu}^0)^{-1/2}]\text{vec}[\hat{\mathbf{C}}_{uv}^0(j)] \\
&= \text{vec}[\hat{\mathbf{C}}_{uv}^0(j)]'[(\mathbf{C}_{vv}^0)^{-1} \otimes (\mathbf{C}_{uu}^0)^{-1}]\text{vec}[\hat{\mathbf{C}}_{uv}^0(j)]. \tag{2.B.1}
\end{aligned}$$

We have

$$\begin{aligned}
S &= T \sum_{j=1}^{T-1} k^2(j/M) \text{vec}[\hat{\boldsymbol{\rho}}^0(j)]'(\boldsymbol{\Gamma}_v^{-1} \otimes \boldsymbol{\Gamma}_u^{-1})\text{vec}[\hat{\boldsymbol{\rho}}^0(j)] \\
&= T \sum_{j=1}^{T-1} k^2(j/M) \text{vec}[\hat{\mathbf{C}}_{uv}^0(j)]'[(\mathbf{C}_{vv}^0)^{-1} \otimes (\mathbf{C}_{uu}^0)^{-1}]\text{vec}[\hat{\mathbf{C}}_{uv}^0(j)]. \tag{2.B.2}
\end{aligned}$$

With this representation, the result of Lemma 2.2.1 follows from Lemma 2.2 in [Candelon and Tokpavi \(2016\)](#), which is based on Lemma 1 in [Bouhaddioui and Roy \(2006\)](#). In both papers, the asymptotic normality result is obtained under the following conditions: (i) The event variables \mathbf{u}_t^0 and \mathbf{v}_t^0 are multivariate i.i.d. sequences with finite fourth-order moment. (ii) Mutual independence between \mathbf{u}_t^0 and \mathbf{v}_{t-j}^0 for $j > 0$. In our framework, condition (i) is satisfied given Assumption 2.2.1, and condition (ii) is satisfied under the null hypothesis, this completes the proof. \blacksquare

Proof of Lemma 2.2.2. We begin by defining the following notations. Let $\mathbf{b}_{1t} \equiv (\mathbf{C}_{uu}^0)^{-1/2} \mathbf{u}_t^0$ and $\mathbf{b}_{2t} \equiv (\mathbf{C}_{vv}^0)^{-1/2} \mathbf{v}_t^0$. Similarly, we let $\hat{\mathbf{b}}_{1t} \equiv (\mathbf{C}_{uu}^0)^{-1/2} \hat{\mathbf{u}}_t$ and $\hat{\mathbf{b}}_{2t} \equiv (\mathbf{C}_{vv}^0)^{-1/2} \hat{\mathbf{v}}_t$, denote the analogues of \mathbf{b}_{1t} and \mathbf{b}_{2t} based on estimated event variables $\hat{\mathbf{u}}_t$ and $\hat{\mathbf{v}}_t$. Then, we obtain $\mathbf{C}_{\hat{\mathbf{b}}}(j) \equiv (\mathbf{C}_{uu}^0)^{-1/2} \hat{\mathbf{C}}_{uv}(j) (\mathbf{C}_{vv}^0)^{-1/2}$, the sample cross-covariance matrix between $\hat{\mathbf{b}}_{1t}$ and $\hat{\mathbf{b}}_{2t}$ at lag order j . Similarly, we have $\mathbf{C}_{\mathbf{b}}(j) \equiv (\mathbf{C}_{uu}^0)^{-1/2} \hat{\mathbf{C}}_{uv}^0(j) (\mathbf{C}_{vv}^0)^{-1/2}$, the sample cross-covariance matrix between \mathbf{b}_{1t} and \mathbf{b}_{2t} at lag order j . By reasonings similar to the derivation of (2.B.1) in Lemma 2.2.1, we write S^* in terms of covariances

$$\begin{aligned} S^* &= T \sum_{j=1}^{T-1} k^2(j/M) \text{vec}[\hat{\boldsymbol{\rho}}^*(j)]' (\boldsymbol{\Gamma}_v^{-1} \otimes \boldsymbol{\Gamma}_u^{-1}) \text{vec}[\hat{\boldsymbol{\rho}}^*(j)] \\ &= T \sum_{j=1}^{T-1} k^2(j/M) \text{vec}[\hat{\mathbf{C}}_{uv}(j)]' [(\mathbf{C}_{vv}^0)^{-1} \otimes (\mathbf{C}_{uu}^0)^{-1}] \text{vec}[\hat{\mathbf{C}}_{uv}(j)]. \end{aligned} \quad (2.B.3)$$

With these results and based on the proof of Candelon and Tokpavi (2016, Lemma 2.1) and Bouhadjioui and Roy (2006, Lemma 2), $S - S^*$ can be written as

$$\begin{aligned} S - S^* &= T \sum_{j=1}^{T-1} k^2(j/M) \|\text{vec}[\mathbf{C}_{\hat{\mathbf{b}}}(j)] - \text{vec}[\mathbf{C}_{\mathbf{b}}(j)]\|^2 \\ &\quad + 2T \sum_{j=1}^{T-1} k^2(j/M) \langle \text{vec}[\mathbf{C}_{\mathbf{b}}(j)], \text{vec}[\mathbf{C}_{\hat{\mathbf{b}}}(j)] - \text{vec}[\mathbf{C}_{\mathbf{b}}(j)] \rangle \\ &= \mathcal{A}_{1T} + 2\mathcal{A}_{2T}, \text{ say.} \end{aligned} \quad (2.B.4)$$

We shall show that both \mathcal{A}_{1T} and \mathcal{A}_{2T} are $o_p(M^{1/2})$. The first term \mathcal{A}_{1T} can be written as

$$\begin{aligned} \mathcal{A}_{1T} &= T \sum_{j=1}^{T-1} k^2(j/M) \\ &\quad \times \left\| (\mathbf{C}_{vv}^0)^{-1/2} \otimes (\mathbf{C}_{uu}^0)^{-1/2} \text{vec}[\hat{\mathbf{C}}_{uv}(j)] - (\mathbf{C}_{vv}^0)^{-1/2} \otimes (\mathbf{C}_{uu}^0)^{-1/2} \text{vec}[\hat{\mathbf{C}}_{uv}^0(j)] \right\|^2 \\ &= T \sum_{j=1}^{T-1} k^2(j/M) \left\| [(\mathbf{C}_{vv}^0)^{-1/2} \otimes (\mathbf{C}_{uu}^0)^{-1/2}] \{ \text{vec}[\hat{\mathbf{C}}_{uv}(j)] - \text{vec}[\hat{\mathbf{C}}_{uv}^0(j)] \} \right\|^2 \\ &\leq T \sum_{j=1}^{T-1} k^2(j/M) \left\| (\mathbf{C}_{vv}^0)^{-1/2} \otimes (\mathbf{C}_{uu}^0)^{-1/2} \right\|_F^2 \left\| \text{vec}[\hat{\mathbf{C}}_{uv}(j)] - \text{vec}[\hat{\mathbf{C}}_{uv}^0(j)] \right\|^2, \end{aligned} \quad (2.B.5)$$

which we make use the property $\text{vec}(\mathbf{AXB}) = (\mathbf{B}' \otimes \mathbf{A}) \text{vec}(\mathbf{X})$ and Cauchy-Schwarz inequality. Because $\|(\mathbf{C}_{vv}^0)^{-1/2} \otimes (\mathbf{C}_{uu}^0)^{-1/2}\|_F^2 = O_p(1)$ by Assumption 2.2.1, it suffices to show that $\mathcal{A}_{11T} =$

$o_p(M^{1/2})$, with

$$\begin{aligned} \mathcal{A}_{11T} &= T \sum_{j=1}^{T-1} k^2(j/M) \left\| \text{vec}[\hat{\mathbf{C}}_{uv}(j)] - \text{vec}[\hat{\mathbf{C}}_{uv}^0(j)] \right\|^2 \\ &= T \sum_{m=1}^{d_1^*} \sum_{n=1}^{d_2^*} \sum_{j=1}^{T-1} k^2(j/M) [\hat{C}_{uv}^{m,n}(j) - \hat{C}_{uv}^{0,m,n}(j)]^2, \end{aligned} \quad (2.B.6)$$

where $\hat{C}_{uv}^{m,n}(j)$ and $\hat{C}_{uv}^{0,m,n}(j)$ are the (m, n) -th elements of matrices $\hat{\mathbf{C}}_{uv}(j)$ and $\hat{\mathbf{C}}_{uv}^0(j)$, respectively. It suffices to show that $\sum_{j=1}^{T-1} k^2(j/M) [\hat{C}_{uv}^{m,n}(j) - \hat{C}_{uv}^{0,m,n}(j)]^2 = o_p(M^{1/2}/T)$. Let $u_{m,t}^0$ and $\hat{u}_{m,t}$ denote the m -th element of \mathbf{u}_t^0 and $\hat{\mathbf{u}}_t$, respectively. Similarly, let $v_{n,t}^0$ and $\hat{v}_{n,t}$ denote the n -th element of \mathbf{v}_t^0 and $\hat{\mathbf{v}}_t$, respectively. We have

$$\begin{aligned} \hat{C}_{uv}^{m,n}(j) - \hat{C}_{uv}^{0,m,n}(j) &= \frac{1}{T} \sum_{t=j+1}^T \hat{u}_{m,t} \hat{v}_{n,t-j} - u_{m,t}^0 v_{n,t-j}^0 \\ &= \frac{1}{T} \sum_{t=j+1}^T (\hat{u}_{m,t} - u_{m,t}^0) v_{n,t-j}^0 + \frac{1}{T} \sum_{t=j+1}^T u_{m,t}^0 (\hat{v}_{n,t-j} - v_{n,t-j}^0) \\ &\quad + \frac{1}{T} \sum_{t=j+1}^T (\hat{u}_{m,t} - u_{m,t}^0) (\hat{v}_{n,t-j} - v_{n,t-j}^0) \\ &= \mathcal{B}_{1T}(j) + \mathcal{B}_{2T}(j) + \mathcal{B}_{3T}(j), \text{ say.} \end{aligned} \quad (2.B.7)$$

It follows that

$$\sum_{j=1}^{T-1} k^2(j/M) [\hat{C}_{uv}^{m,n}(j) - \hat{C}_{uv}^{0,m,n}(j)]^2 \leq \Delta \sum_{j=1}^{T-1} k^2(j/M) [\mathcal{B}_{1T}^2(j) + \mathcal{B}_{2T}^2(j) + \mathcal{B}_{3T}^2(j)]. \quad (2.B.8)$$

Applying Cauchy-Schwarz inequality to the last term $\mathcal{B}_{3T}^2(j)$, we have

$$\sup_{1 \leq j \leq T-1} \mathcal{B}_{3T}^2(j) \leq \left[\frac{1}{T} \sum_{t=1}^T (\hat{u}_{m,t} - u_{m,t}^0)^2 \right] \left[\frac{1}{T} \sum_{t=1}^T (\hat{v}_{n,t} - v_{n,t}^0)^2 \right].$$

We shall show that $T^{-1} \sum_{t=1}^T (\hat{u}_{m,t} - u_{m,t}^0)^2 = O_p(T^{-1})$. The proof for $T^{-1} \sum_{t=1}^T (\hat{v}_{n,t} - v_{n,t}^0)^2$ is the same. Using Cauchy-Schwarz inequality and noting that $\hat{u}_{m,t} - u_{m,t}^0 = u_{m,t}(\hat{\boldsymbol{\theta}}_1) - u_{m,t}^0 = [u_{m,t}(\hat{\boldsymbol{\theta}}_1) - \tilde{u}_{m,t}(\hat{\boldsymbol{\theta}}_1)] + [\tilde{u}_{m,t}(\hat{\boldsymbol{\theta}}_1) - u_{m,t}^0]$, we have

$$\begin{aligned} \frac{1}{T} \sum_{t=1}^T [u_{m,t}(\hat{\boldsymbol{\theta}}_1) - u_{m,t}^0]^2 &\leq 2 \frac{1}{T} \sum_{t=1}^T [u_{m,t}(\hat{\boldsymbol{\theta}}_1) - \tilde{u}_{m,t}(\hat{\boldsymbol{\theta}}_1)]^2 \\ &\quad + 2 \frac{1}{T} \sum_{t=1}^T [\tilde{u}_{m,t}(\hat{\boldsymbol{\theta}}_1) - u_{m,t}^0]^2 \\ &= 2\mathcal{B}_{31T}(j) + 2\mathcal{B}_{32T}(j), \text{ say.} \end{aligned} \quad (2.B.9)$$

We have $\mathcal{B}_{31T}(j) = O_p(T^{-2})$ by Assumption 2.2.3, it remains to show that $\mathcal{B}_{32T}(j) = O_p(T^{-1})$. By the mean value theorem and Cauchy-Schwarz inequality, we have

$$\mathcal{B}_{32T}(j) \leq \|\hat{\boldsymbol{\theta}}_1 - \boldsymbol{\theta}_1^0\|^2 \left(\frac{1}{T} \sum_{t=1}^T \|\nabla_{\boldsymbol{\theta}_1} \tilde{u}_{m,t}(\bar{\boldsymbol{\theta}}_1)\|^2 \right), \quad (2.B.10)$$

where $\nabla_{\boldsymbol{\theta}_1}$ is the gradient operator with respect to $\boldsymbol{\theta}_1$ and $\bar{\boldsymbol{\theta}}_1$ lies in the segment between $\hat{\boldsymbol{\theta}}_1$ and $\boldsymbol{\theta}_1^0$. Given Assumption 2.2.2, we have $\|\hat{\boldsymbol{\theta}}_1 - \boldsymbol{\theta}_1^0\|^2 = O_p(T^{-1})$. Given Assumption 2.2.4, we have $T^{-1} \sum_{t=1}^T \|\nabla_{\boldsymbol{\theta}_1} \tilde{u}_{m,t}(\bar{\boldsymbol{\theta}}_1)\|^2 = O_p(1)$ by Markov's inequality. Therefore, we have $\mathcal{B}_{32T}(j) = O_p(T^{-1})$. Subsequently,

$$\begin{aligned} \sum_{j=1}^{T-1} k^2(j/M) \mathcal{B}_{3T}^2(j) &\leq M \sup_{1 \leq j \leq T-1} \mathcal{B}_{3T}^2(j) \left[\frac{1}{M} \sum_{j=1}^{T-1} k^2(j/M) \right] \\ &= O_p(M/T^2), \end{aligned} \quad (2.B.11)$$

where $M^{-1} \sum_{j=1}^{T-1} k^2(j/M) \rightarrow \int_0^\infty k^2(z) dz < \infty$ follows by Assumptions 2.2.5-2.2.6.

Next, we rewrite $\mathcal{B}_{1T}(j)$ as

$$\begin{aligned} \mathcal{B}_{1T}(j) &= \frac{1}{T} \sum_{t=j+1}^T [u_{m,t}(\hat{\boldsymbol{\theta}}_1) - \tilde{u}_{m,t}(\hat{\boldsymbol{\theta}}_1)] v_{n,t-j}^0 + \frac{1}{T} \sum_{t=j+1}^T [\tilde{u}_{m,t}(\hat{\boldsymbol{\theta}}_1) - u_{m,t}^0] v_{n,t-j}^0 \\ &= \mathcal{B}_{11T}(j) + \mathcal{B}_{12T}(j), \text{ say.} \end{aligned} \quad (2.B.12)$$

Applying Cauchy-Schwarz inequality to the first term $\mathcal{B}_{11T}(j)$, we have

$$\begin{aligned} &\sum_{j=1}^{T-1} k^2(j/M) \mathcal{B}_{11T}^2(j) \\ &\leq \frac{1}{T^2} \sum_{j=1}^{T-1} k^2(j/M) \left\{ \sum_{t=j+1}^T [u_{m,t}(\hat{\boldsymbol{\theta}}_1) - \tilde{u}_{m,t}(\hat{\boldsymbol{\theta}}_1)]^2 \right\} \left[\sum_{t=j+1}^T (v_{n,t-j}^0)^2 \right] \\ &\leq \frac{1}{T} \sum_{j=1}^{T-1} k^2(j/M) \left\{ \sum_{t=1}^T [u_{m,t}(\hat{\boldsymbol{\theta}}_1) - \tilde{u}_{m,t}(\hat{\boldsymbol{\theta}}_1)]^2 \right\} \left[\frac{1}{T} \sum_{t=1}^T (v_{n,t}^0)^2 \right] \\ &= O_p(M/T^2), \end{aligned} \quad (2.B.13)$$

given Assumption 2.2.3, and $T^{-1} \sum_{t=1}^T (v_{n,t}^0)^2 = O_p(1)$ by Markov's inequality. Applying two-term Taylor expansion to the second term $\mathcal{B}_{12T}(j)$, we have

$$\begin{aligned} \mathcal{B}_{12T}(j) &= (\hat{\boldsymbol{\theta}}_1 - \boldsymbol{\theta}_1^0)' \frac{1}{T} \sum_{t=j+1}^T \nabla_{\boldsymbol{\theta}_1} \tilde{u}_{m,t}(\boldsymbol{\theta}_1^0) v_{n,t-j}^0 \\ &\quad + \frac{1}{2} (\hat{\boldsymbol{\theta}}_1 - \boldsymbol{\theta}_1^0)' \left[\frac{1}{T} \sum_{t=j+1}^T \nabla_{\boldsymbol{\theta}_1}^2 \tilde{u}_{m,t}(\bar{\boldsymbol{\theta}}_1) v_{n,t-j}^0 \right] (\hat{\boldsymbol{\theta}}_1 - \boldsymbol{\theta}_1^0) \\ &= \mathcal{B}_{121T}(j) + \mathcal{B}_{122T}(j), \text{ say,} \end{aligned} \quad (2.B.14)$$

where $\nabla_{\boldsymbol{\theta}_1}^2$ is the Hessian operator with respect to $\boldsymbol{\theta}_1$ and $\bar{\boldsymbol{\theta}}_1$ lies in the segment between $\hat{\boldsymbol{\theta}}_1$ and $\boldsymbol{\theta}_1^0$. By Cauchy-Schwarz inequality, we obtain for the first term

$$\begin{aligned} & \sum_{j=1}^{T-1} k^2(j/M) \mathcal{B}_{121T}^2(j) \\ & \leq \|\hat{\boldsymbol{\theta}}_1 - \boldsymbol{\theta}_1^0\|^2 \left\{ \sum_{j=1}^{T-1} k^2(j/M) \frac{1}{T^2} \left[\sum_{t=j+1}^T \|\nabla_{\boldsymbol{\theta}_1} \tilde{u}_{m,t}(\boldsymbol{\theta}_1^0)\| v_{n,t-j}^0 \right]^2 \right\} \\ & = O_p(M/T^2), \end{aligned}$$

given Assumption 2.2.2 and $\sum_{j=1}^{T-1} k^2(j/M) T^{-2} \left[\sum_{t=j+1}^T \|\nabla_{\boldsymbol{\theta}_1} \tilde{u}_{m,t}(\boldsymbol{\theta}_1^0)\| v_{n,t-j}^0 \right]^2 = O_p(M/T)$, which follows from Markov's inequality, Assumption 2.2.4 and

$$\begin{aligned} \mathbb{E} \left\{ \frac{1}{T^2} \left[\sum_{t=j+1}^T \|\nabla_{\boldsymbol{\theta}_1} \tilde{u}_{m,t}(\boldsymbol{\theta}_1^0)\| v_{n,t-j}^0 \right]^2 \right\} &= \frac{1}{T^2} \sum_{t=j+1}^T \mathbb{E} \left\{ \left[\|\nabla_{\boldsymbol{\theta}_1} \tilde{u}_{m,t}(\boldsymbol{\theta}_1^0)\| v_{n,t-j}^0 \right]^2 \right\} \\ &= \frac{1}{T^2} \sum_{t=j+1}^T \mathbb{E} \left[\|\nabla_{\boldsymbol{\theta}_1} \tilde{u}_{m,t}(\boldsymbol{\theta}_1^0)\|^2 \right] \mathbb{E} \left[(v_{n,t-j}^0)^2 \right] \\ &= O(T^{-1}), \end{aligned}$$

where the first equality follows from Assumption 2.2.1 and the second equality follows from the independence between $\Xi_{1t} \Xi_{1t}'$ and $\Xi_{2t-j} \Xi_{2t-j}'$ under the null hypothesis. By Cauchy-Schwarz inequality, we can write the second term $\mathcal{B}_{122T}(j)$ as

$$\begin{aligned} & \sum_{j=1}^{T-1} k^2(j/M) \mathcal{B}_{122T}^2(j) \\ & \leq \frac{1}{T^2} \|\hat{\boldsymbol{\theta}}_1 - \boldsymbol{\theta}_1^0\|^4 \sum_{j=1}^{T-1} k^2(j/M) \left[\sum_{t=j+1}^T \|\nabla_{\boldsymbol{\theta}_1}^2 \tilde{u}_{m,t}(\bar{\boldsymbol{\theta}}_1)\|_F v_{n,t-j}^0 \right]^2 \\ & \leq \frac{1}{T^2} \|\hat{\boldsymbol{\theta}}_1 - \boldsymbol{\theta}_1^0\|^4 \sum_{j=1}^{T-1} k^2(j/M) \left[\sum_{t=j+1}^T \|\nabla_{\boldsymbol{\theta}_1}^2 \tilde{u}_{m,t}(\bar{\boldsymbol{\theta}}_1)\|_F^2 \right] \left[\sum_{t=j+1}^T (v_{n,t-j}^0)^2 \right] \\ & = \|\hat{\boldsymbol{\theta}}_1 - \boldsymbol{\theta}_1^0\|^4 \sum_{j=1}^{T-1} k^2(j/M) \left[\frac{1}{T} \sum_{t=j+1}^T \|\nabla_{\boldsymbol{\theta}_1}^2 \tilde{u}_{m,t}(\bar{\boldsymbol{\theta}}_1)\|_F^2 \right] \left[\frac{1}{T} \sum_{t=j+1}^T (v_{n,t-j}^0)^2 \right] \\ & = O_p(M/T^2), \end{aligned}$$

having used Assumptions 2.2.2 and 2.2.4 with Markov's inequality. Therefore,

$$\sum_{j=1}^{T-1} k^2(j/M) \mathcal{B}_{1T}^2(j) = O_p(M/T^2) = o_p(M^{1/2}/T). \quad (2.B.15)$$

By the same reasonings, we also have

$$\sum_{j=1}^{T-1} k^2(j/M) \mathcal{B}_{2T}^2(j) = O_p(M/T^2) = o_p(M^{1/2}/T). \quad (2.B.16)$$

Collecting (2.B.6), (2.B.7), (2.B.11), (2.B.15) and (2.B.16), we have $\mathcal{A}_{1T} = o_p(M^{1/2})$.

For the second term \mathcal{A}_{2T} in (2.B.4), we have

$$\begin{aligned} \mathcal{A}_{2T} &= T \sum_{j=1}^{T-1} k^2(j/M) \text{vec}[\mathbf{C}_b(j)]' (\text{vec}[\mathbf{C}_{\hat{b}}(j)] - \text{vec}[\mathbf{C}_b(j)]) \\ &= T \sum_{j=1}^{T-1} k^2(j/M) \left\{ (\mathbf{C}_{vv}^0)^{-1/2} \otimes (\mathbf{C}_{uu}^0)^{-1/2} \text{vec}[\hat{\mathbf{C}}_{uv}^0(j)] \right\}' \left[(\mathbf{C}_{vv}^0)^{-1/2} \otimes (\mathbf{C}_{uu}^0)^{-1/2} \right] \\ &\quad \times \{ \text{vec}[\hat{\mathbf{C}}_{uv}(j)] - \text{vec}[\hat{\mathbf{C}}_{uv}^0(j)] \} \\ &= T \sum_{j=1}^{T-1} k^2(j/M) \text{vec}[\hat{\mathbf{C}}_{uv}^0(j)]' \left[(\mathbf{C}_{vv}^0)^{-1} \otimes (\mathbf{C}_{uu}^0)^{-1} \right] \{ \text{vec}[\hat{\mathbf{C}}_{uv}(j)] - \text{vec}[\hat{\mathbf{C}}_{uv}^0(j)] \}, \end{aligned}$$

having used again the properties $\text{vec}(\mathbf{ABC}) = (\mathbf{C}' \otimes \mathbf{A})\text{vec}(\mathbf{B})$ and $(\mathbf{A} \otimes \mathbf{B})(\mathbf{C} \otimes \mathbf{D}) = (\mathbf{AC}) \otimes (\mathbf{BD})$. For $p = 1, \dots, d_1^* d_2^*$, let $\hat{C}_{uv}^p(j)$ and $\hat{C}_{uv}^{0,p}(j)$ denote the p -th element of $\text{vec}[\hat{\mathbf{C}}_{uv}(j)]$ and $\text{vec}[\hat{\mathbf{C}}_{uv}^0(j)]$, respectively. Similarly, we denote by $\hat{C}_{uv}^q(j)$ and $\hat{C}_{uv}^{0,q}(j)$ the q -th element of $\text{vec}[\hat{\mathbf{C}}_{uv}(j)]$ and $\text{vec}[\hat{\mathbf{C}}_{uv}^0(j)]$, respectively. Further let $G^{p,q}$ denotes the (p, q) -th element of \mathbf{G} , where $\mathbf{G} \equiv (\mathbf{C}_{vv}^0)^{-1} \otimes (\mathbf{C}_{uu}^0)^{-1}$. Then,

$$\begin{aligned} \mathcal{A}_{2T} &= T \sum_{j=1}^{T-1} k^2(j/M) \left\{ \sum_{p=1}^{d_1^* d_2^*} \sum_{q=1}^{d_1^* d_2^*} \hat{C}_{uv}^{0,p}(j) [\hat{C}_{uv}^q(j) - \hat{C}_{uv}^{0,q}(j)] G^{p,q} \right\} \\ &= T \sum_{p=1}^{d_1^* d_2^*} \sum_{q=1}^{d_1^* d_2^*} G^{p,q} \sum_{j=1}^{T-1} k^2(j/M) \hat{C}_{uv}^{0,p}(j) [\hat{C}_{uv}^q(j) - \hat{C}_{uv}^{0,q}(j)]. \end{aligned} \quad (2.B.17)$$

Because $G^{p,q} = O_p(1)$ by Assumption 2.2.1, it suffices to show that $\sum_{j=1}^{T-1} k^2(j/M) \hat{C}_{uv}^p(j) [\hat{C}_{uv}^q(j) - \hat{C}_{uv}^{0,q}(j)] = O_p(M/T^{3/2})$. By Cauchy-Schwarz inequality, we can write

$$\begin{aligned} &\left| \sum_{j=1}^{T-1} k^2(j/M) \hat{C}_{uv}^{0,p}(j) [\hat{C}_{uv}^q(j) - \hat{C}_{uv}^{0,q}(j)] \right| \\ &\leq \left[\sum_{j=1}^{T-1} k^2(j/M) \hat{C}_{uv}^{0,p}(j)^2 \right]^{1/2} \left\{ \sum_{j=1}^{T-1} k^2(j/M) [\hat{C}_{uv}^q(j) - \hat{C}_{uv}^{0,q}(j)]^2 \right\}^{1/2}. \end{aligned}$$

We have $\sum_{j=1}^{T-1} k^2(j/M) [\hat{C}_{uv}^q(j) - \hat{C}_{uv}^{0,q}(j)]^2 = O_p(M/T^2)$ from the proof of (2.B.8) and we have $\sum_{j=1}^{T-1} k^2(j/M) \hat{C}_{uv}^{0,p}(j)^2 = O_p(M/T)$ by Markov's inequality and

$$\begin{aligned} \sum_{j=1}^{T-1} k^2(j/M) \mathbb{E}[\hat{C}_{uv}^{0,p}(j)^2] &= \frac{M}{T} C_{uu}^{0,p} C_{vv}^{0,p} \left(\frac{1}{M} \sum_{j=1}^{T-1} (1-j/T) k^2(j/M) \right) \\ &= O(M/T), \end{aligned} \tag{2.B.18}$$

where $C_{uu}^{0,p}$ and $C_{vv}^{0,p}$ denote the p -th entries of $\text{vec}(\mathbf{C}_{uu}^0)$ and $\text{vec}(\mathbf{C}_{vv}^0)$, respectively. This gives $\mathcal{A}_{2T} = O_p(M/T^{1/2}) = o_p(M^{1/2})$ and completes the proof. ■

Proof of Proposition 2.2.2. Recall Proposition 2.2.2 is stated as

Proposition 2.2.2. Suppose the conditions of Theorem 2.2.1 hold, we have that

$$\frac{\hat{S} - S^*}{[d_1^* d_2^* D_{1T}(k)]^{1/2}} \xrightarrow{p} 0.$$

Given Assumption 2.2.5 and since $M \rightarrow \infty$ as $T \rightarrow \infty$, it follows that

$$D_{1T}(k) = M \int_0^\infty k^4(z) dz [1 + o(1)].$$

Therefore, the result of Proposition 2.2.2 can be obtained by showing that $\hat{S} - S^* = O_p(M/T^{1/2})$. By reasonings similar to the derivations of (2.B.1) and (2.B.3), we write for \hat{S}

$$\begin{aligned} \hat{S} &= T \sum_{j=1}^{T-1} k^2(j/M) \text{vec}[\hat{\boldsymbol{\rho}}(j)]' (\hat{\boldsymbol{\Gamma}}_v^{-1} \otimes \hat{\boldsymbol{\Gamma}}_u^{-1}) \text{vec}[\hat{\boldsymbol{\rho}}(j)] \\ &= T \sum_{j=1}^{T-1} k^2(j/M) \text{vec}[\hat{\mathbf{C}}_{uv}(j)]' (\hat{\mathbf{C}}_{vv}^{-1} \otimes \hat{\mathbf{C}}_{uu}^{-1}) \text{vec}[\hat{\mathbf{C}}_{uv}(j)]. \end{aligned} \quad (2.B.19)$$

Then, $\hat{S} - S^*$ is equal to

$$\begin{aligned} \hat{S} - S^* &= T \sum_{j=1}^{T-1} k^2(j/M) \text{vec}[\hat{\mathbf{C}}_{uv}(j)]' [\hat{\mathbf{C}}_{vv}^{-1} \otimes \hat{\mathbf{C}}_{uu}^{-1} - (\mathbf{C}_{vv}^0)^{-1} \otimes (\mathbf{C}_{uu}^0)^{-1}] \text{vec}[\hat{\mathbf{C}}_{uv}(j)] \\ &= T \sum_{j=1}^{T-1} k^2(j/M) \text{vec}[\hat{\mathbf{C}}_{uv}(j)]' [(\hat{\mathbf{C}}_{vv} \otimes \hat{\mathbf{C}}_{uu})^{-1} - (\mathbf{C}_{vv}^0 \otimes \mathbf{C}_{uu}^0)^{-1}] \text{vec}[\hat{\mathbf{C}}_{uv}(j)]. \end{aligned}$$

We proceed by showing that $\hat{\mathbf{C}}_{vv} \otimes \hat{\mathbf{C}}_{uu} - \mathbf{C}_{vv}^0 \otimes \mathbf{C}_{uu}^0 = O_p(T^{-1/2})$. Its inverse counterpart has the same stochastic order by the Delta method. For $m = 1, \dots, d_1^*$, we let $\hat{C}_{uu}^{m,m}$ and $C_{uu}^{0,m,m}$ denote the (m, m) -th elements of matrices $\hat{\mathbf{C}}_{uu}$ and \mathbf{C}_{uu}^0 , respectively. Similarly, for $n = 1, \dots, d_2^*$, we let $\hat{C}_{vv}^{n,n}$ and $C_{vv}^{0,n,n}$ denote the (n, n) -th entries of matrices $\hat{\mathbf{C}}_{vv}$ and \mathbf{C}_{vv}^0 , respectively. Then, we have the $[d_1^*(n-1) + m, d_1^*(n-1) + m]$ -th entry in $\hat{\mathbf{C}}_{vv} \otimes \hat{\mathbf{C}}_{uu}$ and $\mathbf{C}_{vv}^0 \otimes \mathbf{C}_{uu}^0$ be given, respectively, by $\hat{C}_{vv}^{n,n} \hat{C}_{uu}^{m,m}$ and $C_{vv}^{0,n,n} C_{uu}^{0,m,m}$. It suffices to show that $\hat{C}_{vv}^{n,n} \hat{C}_{uu}^{m,m} - C_{vv}^{0,n,n} C_{uu}^{0,m,m} = O_p(T^{-1/2})$. Since $\hat{C}_{vv}^{n,n} \hat{C}_{uu}^{m,m} - C_{vv}^{0,n,n} C_{uu}^{0,m,m} = (\hat{C}_{vv}^{n,n} - C_{vv}^{0,n,n}) C_{uu}^{0,m,m} + C_{vv}^{0,n,n} (\hat{C}_{uu}^{m,m} - C_{uu}^{0,m,m}) + (\hat{C}_{vv}^{n,n} - C_{vv}^{0,n,n}) (\hat{C}_{uu}^{m,m} - C_{uu}^{0,m,m})$ and given $C_{vv}^{0,n,n} = O_p(1)$ and $C_{uu}^{0,m,m} = O_p(1)$ by Assumption 2.2.1, we know that the controlling terms in $\hat{C}_{vv}^{n,n} \hat{C}_{uu}^{m,m} - C_{vv}^{0,n,n} C_{uu}^{0,m,m}$ are $\hat{C}_{uu}^{m,m} - C_{uu}^{0,m,m}$ and $\hat{C}_{vv}^{n,n} - C_{vv}^{0,n,n}$. It therefore suffices to show that $\hat{C}_{uu}^{m,m} - C_{uu}^{0,m,m} = O_p(T^{-1/2})$, the proof for $\hat{C}_{vv}^{n,n} - C_{vv}^{0,n,n}$ is similar. It follows from the triangle inequality that

$$|\hat{C}_{uu}^{m,m} - C_{uu}^{0,m,m}| \leq |\hat{C}_{uu}^{m,m} - \hat{C}_{uu}^{0,m,m}| + |\hat{C}_{uu}^{0,m,m} - C_{uu}^{0,m,m}|,$$

where we have $\hat{C}_{uu}^{0,m,m} - C_{uu}^{0,m,m} = O_p(T^{-1/2})$ by Chebyshev's inequality and Assumption 2.2.1. Applying Cauchy-Schwarz inequality to the first term, we have

$$\begin{aligned}\hat{C}_{uu}^{m,m} - \hat{C}_{uu}^{0,m,m} &= \frac{1}{T} \sum_{t=j+1}^T \hat{u}_{m,t} \hat{u}_{m,t} - u_{m,t}^0 u_{m,t}^0 \\ &= 2 \frac{1}{T} \sum_{t=j+1}^T (\hat{u}_{m,t} - u_{m,t}^0) u_{m,t}^0 + \frac{1}{T} \sum_{t=j+1}^T (\hat{u}_{m,t} - u_{m,t}^0)^2 \\ &\leq 2 \left[\frac{1}{T} \sum_{t=j+1}^T (u_{m,t}^0)^2 \right]^{1/2} \left\{ \frac{1}{T} \sum_{t=j+1}^T (\hat{u}_{m,t} - u_{m,t}^0)^2 \right\}^{1/2} \\ &\quad + \frac{1}{T} \sum_{t=j+1}^T (\hat{u}_{m,t} - u_{m,t}^0)^2.\end{aligned}$$

We have $T^{-1} \sum_{t=j+1}^T (\hat{u}_{m,t} - u_{m,t}^0)^2 = O_p(T^{-1})$ from the proof of (2.B.9) and $T^{-1} \sum_{t=j+1}^T (u_{m,t}^0)^2 = O_p(1)$ by Markov's inequality and Assumption 2.2.1. It follows that $\hat{C}_{uu}^{m,m} - \hat{C}_{uu}^{0,m,m} = O_p(T^{-1/2})$. Therefore,

$$\begin{aligned}\hat{S} - S^* &= T \sum_{j=1}^{T-1} k^2(j/M) \text{vec}[\hat{C}_{uv}(j)]' [O_p(T^{-1/2})] \text{vec}[\hat{C}_{uv}(j)] \\ &= O_p(T^{1/2}) \sum_{j=1}^{T-1} k^2(j/M) \text{vec}[\hat{C}_{uv}(j)]' \text{vec}[\hat{C}_{uv}(j)].\end{aligned}\tag{2.B.20}$$

For the rest of the proof, it suffices to show that $\mathcal{F}_T = O_p(M/T)$, where

$$\begin{aligned}\mathcal{F}_T &= \sum_{j=1}^{T-1} k^2(j/M) \text{vec}[\hat{C}_{uv}(j)]' \text{vec}[\hat{C}_{uv}(j)] \\ &= \sum_{j=1}^{T-1} k^2(j/M) \text{vec}[\hat{C}_{uv}(j)]' \text{vec}[\hat{C}_{uv}(j)] - \text{vec}[\hat{C}_{uv}^0(j)]' \text{vec}[\hat{C}_{uv}^0(j)] \\ &\quad + \sum_{j=1}^{T-1} k^2(j/M) \text{vec}[\hat{C}_{uv}^0(j)]' \text{vec}[\hat{C}_{uv}^0(j)] \\ &= \mathcal{F}_{1T} + \mathcal{F}_{2T}, \text{ say.}\end{aligned}\tag{2.B.21}$$

We write for the first term \mathcal{F}_{1T}

$$\begin{aligned}\mathcal{F}_{1T} &= \sum_{j=1}^{T-1} k^2(j/M) \sum_{m=1}^{d_1^*} \sum_{n=1}^{d_2^*} \left[\hat{C}_{uv}^{m,n}(j)^2 - \hat{C}_{uv}^{0,m,n}(j)^2 \right] \\ &= \sum_{m=1}^{d_1^*} \sum_{n=1}^{d_2^*} \sum_{j=1}^{T-1} k^2(j/M) \left[\hat{C}_{uv}^{m,n}(j)^2 - \hat{C}_{uv}^{0,m,n}(j)^2 \right],\end{aligned}\tag{2.B.22}$$

where $\hat{C}_{uv}^{m,n}(j)$ and $\hat{C}_{uv}^{0,m,n}(j)$ are the (m, n) -th elements of matrices $\hat{\mathbf{C}}_{uv}(j)$ and $\hat{\mathbf{C}}_{uv}^0(j)$, respectively. It suffices to show that $\sum_{j=1}^{T-1} k^2(j/M) [\hat{C}_{uv}^{m,n}(j)^2 - \hat{C}_{uv}^{0,m,n}(j)^2] = O_p(M/T)$. We write

$$\begin{aligned} \sum_{j=1}^{T-1} k^2(j/M) [\hat{C}_{uv}^{m,n}(j)^2 - \hat{C}_{uv}^{0,m,n}(j)^2] &= \sum_{j=1}^{T-1} k^2(j/M) [\hat{C}_{uv}^{m,n}(j) - \hat{C}_{uv}^{0,m,n}(j)]^2 \\ &\quad + 2 \sum_{j=1}^{T-1} k^2(j/M) \hat{C}_{uv}^{0,m,n}(j) [\hat{C}_{uv}^{m,n}(j) - \hat{C}_{uv}^{0,m,n}(j)] \\ &= \mathcal{F}_{11T} + 2\mathcal{F}_{12T}, \text{ say.} \end{aligned}$$

We have $\mathcal{F}_{11T} = O_p(M/T^2)$ from the proof of (2.B.8) and we have $\mathcal{F}_{12T} = O_p(M/T^{3/2})$ from the proof of (2.B.17). Thus, $\mathcal{F}_{1T} = O_p(M/T)$.

Next, we rewrite the second term \mathcal{F}_{2T} as

$$\mathcal{F}_{2T} = \sum_{j=1}^{T-1} k^2(j/M) \left[\sum_{p=1}^{d_1^* d_2^*} \hat{C}_{uv}^{0,p}(j)^2 \right] = \sum_{p=1}^{d_1^* d_2^*} \sum_{j=1}^{T-1} k^2(j/M) \hat{C}_{uv}^{0,p}(j)^2, \quad (2.B.23)$$

where $\hat{C}_{uv}^{0,p}(j)$ is the p -th element in $\text{vec}[\hat{\mathbf{C}}_{uv}^0(j)]$, $p = 1, \dots, d_1^* d_2^*$. By Markov's inequality and (2.B.18), we have $\mathcal{F}_{2T} = O_p(M/T)$. This completes the proof. \blacksquare

Appendix 2.C

Proof of Lemma 2.2.3. The proof of Lemma 2.2.3 follows largely from the proof of Lemma 2.2.2 with some modifications as we are now under the alternative hypothesis. We have $T^{-1}(S - S^*) = T^{-1}(\mathcal{A}_{1T} + 2\mathcal{A}_{2T})$ as in (2.B.4). We shall show that $T^{-1}\mathcal{A}_{1T} = o_p(1)$ and $T^{-1}\mathcal{A}_{2T} = o_p(1)$. We begin with \mathcal{A}_{1T} , we have from (2.B.5) that

$$T^{-1}\mathcal{A}_{1T} \leq \sum_{j=1}^{T-1} k^2(j/M) \left\| (\mathbf{C}_{uv}^0)^{-1/2} \otimes (\mathbf{C}_{uu}^0)^{-1/2} \right\|_F^2 \left\| \text{vec}[\hat{\mathbf{C}}_{uv}(j)] - \text{vec}[\hat{\mathbf{C}}_{uv}^0(j)] \right\|^2. \quad (2.C.1)$$

It suffices to show that $T^{-1}\mathcal{A}_{11T} = o_p(1)$, where

$$\begin{aligned} T^{-1}\mathcal{A}_{11T} &= \sum_{j=1}^{T-1} k^2(j/M) \left\| \text{vec}[\hat{\mathbf{C}}_{uv}(j)] - \text{vec}[\hat{\mathbf{C}}_{uv}^0(j)] \right\|^2 \\ &= \sum_{m=1}^{d_1^*} \sum_{n=1}^{d_2^*} \sum_{j=1}^{T-1} k^2(j/M) [\hat{C}_{uv}^{m,n}(j) - \hat{C}_{uv}^{0,m,n}(j)]^2. \end{aligned} \quad (2.C.2)$$

As in (2.B.8), we have

$$\sum_{j=1}^{T-1} k^2(j/M) [\hat{C}_{uv}^{m,n}(j) - \hat{C}_{uv}^{0,m,n}(j)]^2 \leq \Delta \sum_{j=1}^{T-1} k^2(j/M) [\mathcal{B}_{1T}^2(j) + \mathcal{B}_{2T}^2(j) + \mathcal{B}_{3T}^2(j)]. \quad (2.C.3)$$

It suffices to show that $\sum_{j=1}^{T-1} k^2(j/M) [\mathcal{B}_{iT}^2(j)] = o_p(1)$, for $i = 1, 2, 3$. As shown in (2.B.11), we have $\sum_{j=1}^{T-1} k^2(j/M) \mathcal{B}_{3T}^2(j) = O_p(M/T^2) = o_p(1)$ under Assumptions 2.2.1-2.2.6. Next, from (2.B.12), we have $\mathcal{B}_{1T}(j) = \mathcal{B}_{11T}(j) + \mathcal{B}_{12T}(j)$. We know from (2.B.13) that $\sum_{j=1}^{T-1} k^2(j/M) \mathcal{B}_{11T}^2(j) = O_p(M/T^2) = o_p(1)$ under Assumptions 2.2.1-2.2.6. Applying Cauchy-Schwarz inequality to the second term $\mathcal{B}_{12T}(j)$, we have

$$\begin{aligned} & \sum_{j=1}^{T-1} k^2(j/M) \mathcal{B}_{12T}^2(j) \\ & \leq \frac{1}{T^2} \sum_{j=1}^{T-1} k^2(j/M) \left\{ \sum_{t=j+1}^T [\tilde{u}_{m,t}(\hat{\boldsymbol{\theta}}_1) - u_{m,t}^0]^2 \right\} \left[\sum_{t=j+1}^T (v_{n,t-j}^0)^2 \right] \\ & \leq \sum_{j=1}^{T-1} k^2(j/M) \left\{ \frac{1}{T} \sum_{t=j+1}^T [\tilde{u}_{m,t}(\hat{\boldsymbol{\theta}}_1) - u_{m,t}^0]^2 \right\} \left[\frac{1}{T} \sum_{t=1}^T (v_{n,t}^0)^2 \right] \\ & = O_p(M/T), \end{aligned} \tag{2.C.4}$$

given $\sum_{j=1}^{T-1} k^2(j/M) = O(M)$, $T^{-1} \sum_{t=j+1}^T [\tilde{u}_{m,t}(\hat{\boldsymbol{\theta}}_1) - u_{m,t}^0]^2 = O_p(T^{-1})$ from (2.B.10) and $T^{-1} \sum_{t=1}^T (v_{n,t}^0)^2 = O_p(1)$ by Markov's inequality. It follows that $\sum_{j=1}^{T-1} k^2(j/M) \mathcal{B}_{1T}^2(j) = O_p(M/T) = o_p(1)$. By the same reasonings, we also have $\sum_{j=1}^{T-1} k^2(j/M) \mathcal{B}_{2T}^2(j) = o_p(1)$. Therefore, $T^{-1} \mathcal{A}_{1T} = o_p(1)$.

Next, we shall show that $T^{-1} \mathcal{A}_{2T} = o_p(1)$. From (2.B.17), we have

$$T^{-1} \mathcal{A}_{2T} = \sum_{p=1}^{d_1^*} \sum_{q=1}^{d_2^*} G^{p,q} \sum_{j=1}^{T-1} k^2(j/M) \hat{C}_{uv}^{0,p}(j) [\hat{C}_{uv}^q(j) - \hat{C}_{uv}^{0,q}(j)]. \tag{2.C.5}$$

It suffices to show that $\sum_{j=1}^{T-1} k^2(j/M) \hat{C}_{uv}^{0,p}(j) [\hat{C}_{uv}^q(j) - \hat{C}_{uv}^{0,q}(j)] = o_p(1)$. By Cauchy-Schwarz inequality, we have

$$\begin{aligned} & \left| \sum_{j=1}^{T-1} k^2(j/M) \hat{C}_{uv}^{0,p}(j) [\hat{C}_{uv}^q(j) - \hat{C}_{uv}^{0,q}(j)] \right| \\ & \leq \left[\sum_{j=1}^{T-1} k^2(j/M) \hat{C}_{uv}^{0,p}(j)^2 \right]^{1/2} \left\{ \sum_{j=1}^{T-1} k^2(j/M) [\hat{C}_{uv}^q(j) - \hat{C}_{uv}^{0,q}(j)]^2 \right\}^{1/2}. \end{aligned}$$

We have $\sum_{j=1}^{T-1} k^2(j/M) [\hat{C}_{uv}^q(j) - \hat{C}_{uv}^{0,q}(j)]^2 = o_p(1)$ from (2.C.2) and $\sum_{j=1}^{T-1} k^2(j/M) \hat{C}_{uv}^{0,p}(j)^2 = O_p(1)$ by Lemma 2.2.5 and $\sum_{j=1}^{\infty} \|\boldsymbol{\rho}(j)\|^2 < \infty$. This completes the proof. \blacksquare

Proof of Lemma 2.2.4. The proof of Lemma 2.2.4 can be readily deduced from the proofs of Proposition 2.2.2 and Lemma 2.2.3. Based on Assumptions 2.2.1-2.2.6, we have shown that $T^{-1}(\hat{S} - S^*) = T^{-1} O_p(T^{1/2}) \mathcal{F}_T = O_p(T^{-1/2}) \mathcal{F}_T$ in (2.B.20) and (2.B.21). It suffices to show that $\mathcal{F}_T = \mathcal{F}_{1T} + \mathcal{F}_{2T} = O_p(1)$. Using the results in (2.C.2) and (2.C.5), we have $\mathcal{F}_{1T} = O_p(1)$ under the alternative hypothesis. Finally, $\mathcal{F}_{2T} = O_p(1)$ by Lemma 2.2.5 and $\sum_{j=1}^{\infty} \|\boldsymbol{\rho}(j)\|^2 < \infty$. This completes the proof. \blacksquare

Proof of Lemma 2.2.5. First, we write

$$\begin{aligned}
\frac{1}{T}S &= \sum_{j=1}^{T-1} k^2(j/M) \text{vec}[\boldsymbol{\rho}(j)]' (\boldsymbol{\Gamma}_v^{-1} \otimes \boldsymbol{\Gamma}_u^{-1}) \text{vec}[\boldsymbol{\rho}(j)] \\
&\quad + \left\{ \sum_{j=1}^{T-1} k^2(j/M) \text{vec}[\hat{\boldsymbol{\rho}}^0(j)]' (\boldsymbol{\Gamma}_v^{-1} \otimes \boldsymbol{\Gamma}_u^{-1}) \text{vec}[\hat{\boldsymbol{\rho}}^0(j)] \right. \\
&\quad \quad \left. - \sum_{j=1}^{T-1} k^2(j/M) \text{vec}[\boldsymbol{\rho}(j)]' (\boldsymbol{\Gamma}_v^{-1} \otimes \boldsymbol{\Gamma}_u^{-1}) \text{vec}[\boldsymbol{\rho}(j)] \right\} \\
&= \mathcal{G}_{1T} + \mathcal{G}_{2T}, \text{ say.} \tag{2.C.6}
\end{aligned}$$

For the first term \mathcal{G}_{1T} in (2.C.6), we have

$$\begin{aligned}
\mathcal{G}_{1T} &= \sum_{j=1}^{\infty} \text{vec}[\boldsymbol{\rho}(j)]' (\boldsymbol{\Gamma}_v^{-1} \otimes \boldsymbol{\Gamma}_u^{-1}) \text{vec}[\boldsymbol{\rho}(j)] \\
&\quad + \sum_{j=1}^{T-1} (k^2(j/M) - 1) \text{vec}[\boldsymbol{\rho}(j)]' (\boldsymbol{\Gamma}_v^{-1} \otimes \boldsymbol{\Gamma}_u^{-1}) \text{vec}[\boldsymbol{\rho}(j)] \\
&\quad - \sum_{j=T}^{\infty} \text{vec}[\boldsymbol{\rho}(j)]' (\boldsymbol{\Gamma}_v^{-1} \otimes \boldsymbol{\Gamma}_u^{-1}) \text{vec}[\boldsymbol{\rho}(j)] \\
&\xrightarrow{p} \sum_{j=1}^{\infty} \text{vec}[\boldsymbol{\rho}(j)]' (\boldsymbol{\Gamma}_v^{-1} \otimes \boldsymbol{\Gamma}_u^{-1}) \text{vec}[\boldsymbol{\rho}(j)]. \tag{2.C.7}
\end{aligned}$$

The convergence follows because the first term $\sum_{j=T}^{\infty} \text{vec}[\boldsymbol{\rho}(j)]' (\boldsymbol{\Gamma}_v^{-1} \otimes \boldsymbol{\Gamma}_u^{-1}) \text{vec}[\boldsymbol{\rho}(j)]$ goes to zero as a consequence of the absolute summable condition $\sum_{j=1}^{\infty} \|\boldsymbol{\rho}(j)\|^2 < \infty$; and the second term $\sum_{j=1}^{T-1} [k^2(j/M) - 1] \text{vec}[\boldsymbol{\rho}(j)]' (\boldsymbol{\Gamma}_v^{-1} \otimes \boldsymbol{\Gamma}_u^{-1}) \text{vec}[\boldsymbol{\rho}(j)] \rightarrow 0$, which follows from the dominated convergence theorem, $\lim_{M \rightarrow \infty} [k^2(j/M) - 1] \rightarrow 0$ and $\sum_{j=1}^{\infty} \|\boldsymbol{\rho}(j)\|^2 < \infty$.

We now consider the second term \mathcal{G}_{2T} in (2.C.6). Let $\mathbf{C}_{uv}^0(j) \equiv \mathbb{E}[\mathbf{u}_t^0 (\mathbf{v}_{t-j}^0)']$, we have $\mathbf{C}_b^0(j) \equiv (\mathbf{C}_{uu}^0)^{-1/2} \mathbf{C}_{uv}^0(j) (\mathbf{C}_{vv}^0)^{-1/2}$ the true cross-covariance between \mathbf{b}_{1t} and \mathbf{b}_{2t} at lag order j . As in (2.B.4), we write \mathcal{G}_{2T} as

$$\begin{aligned}
\mathcal{G}_{2T} &= \sum_{j=1}^{T-1} k^2(j/M) \|\text{vec}[\mathbf{C}_b(j)] - \text{vec}[\mathbf{C}_b^0(j)]\|^2 \\
&\quad + 2 \sum_{j=1}^{T-1} k^2(j/M) \langle \text{vec}[\mathbf{C}_b^0(j)], \text{vec}[\mathbf{C}_b(j)] - \text{vec}[\mathbf{C}_b^0(j)] \rangle \\
&= \mathcal{G}_{21T} + 2\mathcal{G}_{22T}, \text{ say.} \tag{2.C.8}
\end{aligned}$$

For the rest of the proof, it suffices to show that the first term \mathcal{G}_{21T} goes to zero in probability because \mathcal{G}_{22T} can be bounded by the product of the first term and a finite constant using Cauchy-

Schwarz inequality. Following a similar decomposition as in (2.B.5), we have

$$\mathcal{G}_{21T} \leq \sum_{j=1}^{T-1} k^2(j/M) \left\| (\mathbf{C}_{vv}^0)^{-1/2} \otimes (\mathbf{C}_{uu}^0)^{-1/2} \right\|_F^2 \left\| \text{vec}[\hat{\mathbf{C}}_{uv}^0(j)] - \text{vec}[\mathbf{C}_{uv}^0(j)] \right\|^2. \quad (2.C.9)$$

It suffices to show that $\mathcal{G}_{211T} = o_p(1)$, with

$$\begin{aligned} \mathcal{G}_{211T} &= \sum_{j=1}^{T-1} k^2(j/M) \left\| \text{vec}[\hat{\mathbf{C}}_{uv}^0(j)] - \text{vec}[\mathbf{C}_{uv}^0(j)] \right\|^2 \\ &= \sum_{m=1}^{d_1^*} \sum_{n=1}^{d_2^*} \sum_{j=1}^{T-1} k^2(j/M) [\hat{C}_{uv}^{0,m,n}(j) - C_{uv}^{0,m,n}(j)]^2, \end{aligned} \quad (2.C.10)$$

where $\hat{C}_{uv}^{0,m,n}(j)$ and $C_{uv}^{0,m,n}(j)$ are the (m, n) -th elements of matrices $\hat{\mathbf{C}}_{uv}^0(j)$ and $\mathbf{C}_{uv}^0(j)$, respectively. We have $\sup_{1 \leq j \leq T-1} \text{Var}[\hat{C}_{uv}^{0,m,n}(j)] \leq \Delta T^{-1}$ given Assumption 2.2.7 (see, e.g., Hannan, 1970, p.209). Therefore, $\mathcal{G}_{21T} = O_p(M/T) = o_p(1)$, where we make use of Markov's inequality and $\sum_{j=1}^{T-1} k^2(j/M) = O(M)$. This completes the proof. ■

Appendix 2.D

Proof of Proposition 2.3.1. The desired result follows from a simple modification of the proof of Theorem 4.1 in Dufour and Pelletier (2020). The consistency result in Dufour and Pelletier (2020) is obtained under the following conditions: (i) The sequence $\{\epsilon_{i,n,t}^2\}$ and $\{e_{i,n,t}\}$ are strictly stationary and ergodic. (ii) The error term $\{e_{i,n,t}\}$ is strong mixing with finite fourth-order moment and regular variance. (iii) The lag order p is such that $p/\log(T) \rightarrow \infty$ and $p^2/T \rightarrow 0$. (iv) The process of interest has an infinite vector autoregressive representation with zero mean. Given conditions (i)–(iv), it follows from Dufour and Pelletier (2020) that $\|\hat{\boldsymbol{\theta}}_i^{(p)} - \boldsymbol{\theta}_i^0\| = O_p(p^{1/2}T^{-1/2})$. In our framework, conditions (i) and (ii) are satisfied under Assumption 2.3.1, whereas condition (iii) is implied by Assumption 2.3.2. For condition (iv), we show in (2.34) that the process of interest has an AR(∞) representation. Besides, it is straightforward to show that the proof in Dufour and Pelletier (2020) holds with the addition of an intercept term by putting $\mathbf{Y}_{t-1}^{(p)} \equiv [1, \epsilon_{i,n,t-1}^2, \dots, \epsilon_{i,n,t-p}^2]$ and $\hat{\Pi}^{(p)} \equiv [\hat{\omega}_{i,n}^{(p)}, \hat{a}_{i,n,1}^{(p)}, \dots, \hat{a}_{i,n,p}^{(p)}]'$. This completes the proof. ■

Appendix 2.E

Proof of Proposition 2.3.2. Given Assumption 2.3.3 with $\alpha = 1.5$ and $\beta = 0.5$, we have for $i = 1, 2$, $\|\hat{\boldsymbol{\theta}}_i^{(p)} - \boldsymbol{\theta}_i^0\| = O_p(T^{-1/(2\alpha-2\beta)}) = O_p(T^{-1/2})$, which follows from Theorem 5.52 in van der Vaart (1998). This completes the proof. ■

Appendix 2.F

Proof of Proposition 2.3.3. Given $\hat{\theta}_i^{(p)a} = \hat{\theta}_i^{(p)} + \delta_i$, we have $\|\hat{\theta}_i^{(p)a} - \theta_i^0\| = \|\hat{\theta}_i^{(p)} + \delta_i - \theta_i^0\| \leq \|\hat{\theta}_i^{(p)} - \theta_i^0\| = O_p(T^{-1/2})$. The inequality follows from Assumptions 2.3.4 and 2.3.5 that the positive elements of δ_i , when added by $\hat{\theta}_i^{(p)}$, is always less than or equal to the corresponding entries of the true θ_i^0 . This completes the proof. ■

Appendix 2.G

Proof of Proposition 2.3.4. For $i = 1, 2$, recall $R_i^0 = \mathbb{E}[(D_{it}^0)^{-1/2} \epsilon_{it} \epsilon'_{it} (D_{it}^0)^{-1/2}]$ and $\hat{R}_i = T^{-1} \sum_{t=1}^T \hat{D}_{it}^{-1/2} \epsilon_{it} \epsilon'_{it} \hat{D}_{it}^{-1/2}$. We shall show that $\hat{R}_i - R_i^0 = O_p(T^{-1/2})$, $i = 1, 2$. Let $\hat{R}_i^0 \equiv T^{-1} \sum_{t=1}^T (D_{it}^0)^{-1/2} \epsilon_{it} \epsilon'_{it} (D_{it}^0)^{-1/2}$ denote the analogue of \hat{R}_i based on true variance. We consider the following decomposition

$$\hat{R}_i - R_i^0 = (\hat{R}_i - \hat{R}_i^0) + (\hat{R}_i^0 - R_i^0).$$

By Chebyshev's inequality and Assumption 2.3.6, we have for the second term $\hat{R}_i^0 - R_i^0 = O_p(T^{-1/2})$. It remains to show that the first term $\hat{R}_i - \hat{R}_i^0 = O_p(T^{-1/2})$. We write

$$\begin{aligned} \hat{R}_i - \hat{R}_i^0 &= \frac{1}{T} \sum_{t=1}^T \hat{D}_{it}^{-1/2} \epsilon_{it} \epsilon'_{it} \hat{D}_{it}^{-1/2} - (D_{it}^0)^{-1/2} \epsilon_{it} \epsilon'_{it} (D_{it}^0)^{-1/2} \\ &= \frac{1}{T} \sum_{t=1}^T \Psi_{it}(\hat{\theta}_i^{(p)a}) - \Psi_{it}(\theta_i^0), \text{ say.} \end{aligned}$$

Let $\Psi_{it}^{m,n}(\hat{\theta}_i^{(p)a})$ and $\Psi_{it}^{m,n}(\theta_i^0)$ denote the (m, n) -th entries of $\Psi_{it}(\hat{\theta}_i^{(p)a})$ and $\Psi_{it}(\theta_i^0)$, respectively. It suffices to show that $T^{-1} \sum_{t=1}^T \Psi_{it}^{m,n}(\hat{\theta}_i^{(p)a}) - \Psi_{it}^{m,n}(\theta_i^0) = O_p(T^{-1/2})$. By the mean value theorem and Cauchy-Schwarz inequality, we have

$$\begin{aligned} \frac{1}{T} \sum_{t=1}^T \Psi_{it}^{m,n}(\hat{\theta}_i^{(p)a}) - \Psi_{it}^{m,n}(\theta_i^0) &= \frac{1}{T} \sum_{t=1}^T [\nabla_{\theta_i} \Psi_{it}^{m,n}(\bar{\theta}_i)]' [\hat{\theta}_i^{(p)a} - \theta_i^0] \\ &\leq \|\hat{\theta}_i^{(p)a} - \theta_i^0\| \frac{1}{T} \sum_{t=1}^T \|\nabla_{\theta_i} \Psi_{it}^{m,n}(\bar{\theta}_i)\|, \end{aligned}$$

where $\bar{\theta}_i$ lies between $\hat{\theta}_i^{(p)a}$ and θ_i^0 . Given Assumption 2.2.4, we have $T^{-1} \sum_{t=1}^T \|\nabla_{\theta_i} \Psi_{it}^{m,n}(\bar{\theta}_i)\| = O_p(1)$ by Markov's inequality. Next, we have $\|\hat{\theta}_i^{(p)a} - \theta_i^0\| = O_p(T^{-1/2})$ from Proposition 2.3.3. This gives $\hat{R}_i - \hat{R}_i^0 = O_p(T^{-1/2})$ and completes the proof. ■

Appendix 2.H

2.H.1 Simulation results of Tables 2.3 and 2.4 for all M

We collect in this section the full set of simulation results for the dimensional study in Section 2.4.2 of the main paper where only the results for $M = 20$ are reported to save space. It is useful to recall that the size study under NullID and the power study under AlterC are reported, respectively, in Tables 2.3 and 2.4 of the paper.

Now, we report for $M = 10, 20, 30$, the size study under NullID in Table 2.H.1, and the power study under AlterC in Table 2.H.2. Consistent with the paper, we report here both the results based on asymptotic critical values (Q_1) and bootstrap critical values (Q_1^*). In general, we find that the size of both the Q_1 and Q_1^* to be reasonably stable across M for each of the dimension considered. This result is consistent with the bivariate case reported in Table 2.1 of the paper. As for the power study, we find that the rejection rates of Q_1 and Q_1^* decrease in M . This is because we have one-period lag in volatility spillover under AlterC. Thus, a test that focuses on recent events is expected give better power. This finding is consistent with the bivariate case reported in Table 2.2 of the paper. We also observe that the rejection rates of both Q_1 and Q_1^* increase in T and d_1 , consistent with the higher dimensional results reported in Table 2.4 of the paper. This finding appears to hold regardless of the choice M .

Table 2.H.1 Empirical sizes

		NullID																																																																																																									
d_1	M	3						4						5						6						7						8						9						10																																																															
		10	20	30	10	20	30	10	20	30	10	20	30	10	20	30	10	20	30	10	20	30	10	20	30	10	20	30	10	20	30	10	20	30	10	20	30																																																																						
<i>Rejection rates based on asymptotic critical values</i>																																																																																																											
1000	Q ₁ BAR	7.0	7.1	7.2	7.0	7.1	7.0	7.2	7.1	7.4	7.4	7.2	7.3	7.5	7.4	7.5	7.4	7.5	7.9	7.9	8.0	7.9	8.4	7.5	7.6	8.0	Q ₁ DAN	6.9	7.3	7.2	7.1	6.9	6.9	7.2	7.1	7.5	7.6	7.3	7.5	7.3	7.3	7.7	7.9	7.9	8.2	8.1	8.2	8.1	8.2	8.7	7.5	7.9	8.6	Q ₁ QS	6.9	7.1	7.2	7.1	7.0	7.0	7.2	7.3	7.4	7.4	7.2	7.4	7.4	7.4	7.5	7.5	7.8	7.8	8.1	8.1	8.1	8.3	8.3	7.5	7.9	8.7	Q ₁ TR	7.1	7.2	7.4	6.5	7.3	7.5	6.9	7.4	8.0	7.5	7.4	8.0	7.3	7.5	8.4	7.6	8.1	8.9	8.0	8.8	8.0	8.8	9.0	7.8	8.9	9.9
1500	Q ₁ BAR	7.0	6.7	6.8	6.7	7.0	7.1	6.9	6.6	6.7	6.8	6.7	6.5	6.3	6.6	6.9	7.2	7.1	6.9	7.1	6.9	7.1	7.2	7.2	6.8	7.1	Q ₁ DAN	7.0	6.6	6.7	6.8	6.9	7.1	6.7	6.6	6.8	6.8	6.7	6.7	6.5	6.4	6.5	7.0	7.2	7.1	6.9	7.2	7.2	7.4	7.0	7.0	7.2	Q ₁ QS	6.9	6.7	6.7	6.8	6.9	7.0	6.6	6.6	6.9	6.9	6.7	6.7	6.3	6.4	6.6	7.2	7.2	7.2	7.2	6.9	7.1	7.4	6.8	7.1	7.1	Q ₁ TR	6.3	6.7	6.5	7.0	6.9	7.0	7.0	7.1	7.4	6.8	7.0	7.2	6.4	7.0	7.6	7.1	6.8	7.4	7.1	7.0	8.1	7.0	7.0	7.3	7.9			
<i>Rejection rates based on bootstrap critical values</i>																																																																																																											
1000	Q ₁ BAR	4.8	4.8	5.0	5.3	5.5	5.0	5.5	5.4	5.1	5.2	5.5	5.5	5.5	5.6	5.0	5.2	5.5	5.3	5.3	5.3	5.3	5.4	5.8	5.8	Q ₁ DAN	5.0	4.9	5.1	5.3	5.6	5.7	5.1	5.3	5.6	5.2	5.7	5.4	5.7	5.4	5.7	5.1	5.3	5.5	5.4	5.4	5.6	5.8	5.7	5.7	Q ₁ QS	5.0	5.1	5.2	5.3	5.5	5.7	5.1	5.5	5.5	5.4	5.6	5.5	5.6	5.5	5.7	5.1	5.5	5.6	5.3	5.3	5.6	5.8	5.8	5.7	Q ₁ TR	5.1	5.1	5.5	5.5	5.8	5.9	5.2	5.7	5.3	5.3	5.6	5.7	5.7	5.9	5.5	5.7	5.6	5.5	5.7	5.7	5.7	5.7	5.8	5.6	5.7						
1500	Q ₁ BAR	4.9	5.1	5.3	5.4	5.2	5.3	5.0	4.8	4.9	5.1	5.0	5.2	5.0	5.4	5.5	5.4	5.5	5.4	5.5	5.4	5.5	5.4	5.2	5.1	5.3	Q ₁ DAN	5.1	5.1	5.1	5.2	5.3	5.1	5.0	4.8	5.0	5.0	5.2	5.3	5.1	5.3	5.5	5.4	5.5	5.4	5.2	5.4	5.6	5.1	5.1	5.4	Q ₁ QS	5.1	5.2	5.2	5.1	5.2	4.9	4.8	4.9	5.1	5.2	5.3	5.3	5.4	5.5	5.3	5.5	5.5	5.5	5.1	5.4	5.5	5.1	5.1	5.5	Q ₁ TR	5.3	5.3	5.4	5.5	5.4	5.2	4.6	5.2	5.1	5.0	5.3	5.3	5.2	5.5	5.2	5.5	5.5	5.6	5.2	5.2	5.3	5.6	5.5	5.3						

NOTES: The table reports empirical sizes (in %) of Q_1 under NullID at the 5% significance level based on NCCC-LS modeling. Number of simulations = 10000. Q₁BAR, Q₁DAN, Q₁QS, Q₁TR and Q₁BAR, Q₁DAN, Q₁QS, Q₁TR denote the rejection rates of Q_1 using asymptotic and bootstrap critical values, respectively; the subscripts BAR, DAN, QS and TR denote, respectively, the Bartlett kernel, the Daniell kernel, the Quadratic-Spectral kernel and the Truncated kernel. Number of bootstraps = 499. M denotes the kernel smoothing parameter. T and d_1 denote the sample size and dimension of portfolio 1, respectively.

Table 2.H.2 Empirical powers

d_1		AlterC																													
		3			4			5			6			7			8			9			10								
T	M	10	20	30	10	20	30	10	20	30	10	20	30	10	20	30	10	20	30	10	20	30	10	20	30	10	20	30	10	20	30
<i>Rejection rates based on empirical critical values</i>																															
1000	Q_{IBAR}	38.4	27.6	23.1	55.3	40.8	33.2	72.9	55.2	45.6	82.7	65.5	55.0	89.3	73.9	62.6	91.5	77.1	66.8	93.7	80.9	70.4	95.3	83.0	71.4	93.7	80.9	70.4	95.3	83.0	71.4
	Q_{IDAN}	33.0	23.0	19.2	48.2	33.4	27.1	66.3	44.8	35.6	75.9	54.9	43.9	83.2	62.5	50.7	86.3	65.9	53.9	89.3	70.3	57.5	91.3	71.4	58.2	89.3	70.3	57.5	91.3	71.4	58.2
	Q_{IQS}	31.9	22.1	18.7	46.0	31.6	25.9	64.0	43.2	33.5	73.4	52.9	41.9	80.9	60.1	48.2	84.3	64.1	51.9	87.4	67.4	54.9	89.4	69.0	55.5	87.4	67.4	54.9	89.4	69.0	55.5
	Q_{ITR}	18.2	14.3	12.7	26.4	18.8	15.7	34.4	23.7	19.5	41.7	30.0	23.3	50.5	34.2	26.9	52.9	35.5	28.7	55.1	37.1	29.5	57.7	37.8	28.8	55.1	37.1	29.5	57.7	37.8	28.8
1500	Q_{IBAR}	57.2	42.6	34.7	82.2	63.0	52.0	95.5	84.2	72.8	98.6	91.4	82.6	99.6	96.0	90.6	99.8	97.7	93.6	100.0	98.6	94.9	99.9	99.1	96.6	99.6	98.6	94.9	99.9	99.1	96.6
	Q_{IDAN}	50.3	34.1	27.1	74.8	51.9	41.3	91.8	73.2	59.5	96.5	82.4	70.6	98.8	90.7	80.3	99.5	93.6	84.2	99.8	95.0	87.4	99.8	96.8	89.6	99.8	95.0	87.4	99.8	96.8	89.6
	Q_{IQS}	48.1	33.1	26.0	72.1	49.5	39.6	90.4	70.7	56.5	95.7	80.3	68.5	98.3	88.9	77.8	99.2	92.2	81.8	99.6	93.8	85.1	99.7	95.8	88.1	99.6	93.8	85.1	99.7	95.8	88.1
	Q_{ITR}	27.9	18.8	16.7	39.7	28.1	23.3	57.2	39.2	30.5	68.5	47.8	37.2	79.2	57.2	45.6	84.0	61.9	49.5	85.7	66.3	51.2	89.0	67.8	54.0	85.7	66.3	51.2	89.0	67.8	54.0
<i>Rejection rates based on bootstrap critical values</i>																															
1000	Q_{IBAR}^*	33.1	23.8	20.0	50.8	36.6	29.4	70.4	52.0	42.2	79.8	62.2	51.1	86.7	70.1	58.2	90.7	74.9	63.0	93.2	78.6	67.2	94.0	80.9	69.4	93.2	78.6	67.2	94.0	80.9	69.4
	Q_{IDAN}^*	28.4	19.6	16.7	43.5	29.6	23.4	62.2	42.1	33.4	72.6	50.9	40.1	80.3	58.1	46.3	84.6	63.3	50.4	88.0	67.2	53.7	89.2	69.8	56.6	88.0	67.2	53.7	89.2	69.8	56.6
	Q_{IQS}^*	27.2	19.0	16.0	41.8	28.2	22.3	59.5	40.3	31.8	70.1	48.4	38.2	77.9	55.6	44.4	82.4	60.4	48.1	85.8	64.6	51.8	87.5	67.1	54.1	85.8	64.6	51.8	87.5	67.1	54.1
	Q_{ITR}^*	15.7	12.4	10.9	22.1	15.6	13.7	31.8	21.7	18.0	38.2	26.4	21.4	43.7	30.4	24.4	48.3	32.9	26.6	52.2	35.9	28.4	54.9	37.0	29.4	52.2	35.9	28.4	54.9	37.0	29.4
1500	Q_{IBAR}^*	54.3	38.7	31.1	80.7	62.3	50.9	94.7	81.3	70.3	98.1	89.9	80.3	99.4	94.8	88.3	99.8	97.3	92.1	99.9	98.4	94.4	100.0	98.9	95.9	99.9	98.4	94.4	100.0	98.9	95.9
	Q_{IDAN}^*	47.0	31.2	24.4	73.3	50.9	39.9	90.0	70.2	56.5	95.7	80.3	67.1	98.3	87.9	76.2	99.3	92.2	81.9	99.6	94.4	85.8	99.9	95.9	88.1	99.6	94.4	85.8	99.9	95.9	88.1
	Q_{IQS}^*	44.9	29.6	23.7	70.7	48.4	38.0	88.3	67.4	54.1	94.7	77.8	64.4	97.7	86.1	73.5	99.0	90.5	79.5	99.5	93.0	83.7	99.8	94.8	86.0	99.5	93.0	83.7	99.8	94.8	86.0
	Q_{ITR}^*	23.5	16.9	14.1	37.6	26.0	20.9	54.1	36.4	28.3	64.8	44.5	35.0	75.0	52.0	41.0	80.8	58.3	46.4	83.8	61.8	49.2	86.8	65.9	52.2	83.8	61.8	49.2	86.8	65.9	52.2

NOTES: The table reports empirical powers (in %) of Q_1 under AlterC at the 5% significance level based on NCCC-LS modeling. Number of simulations = 10000. Q_{IBAR} , Q_{IDAN} , Q_{IQS} , Q_{ITR} and Q_{IBAR}^* , Q_{IDAN}^* , Q_{IQS}^* , Q_{ITR}^* denote the rejection rates of Q_1 using empirical and bootstrap critical values, respectively, the subscripts BAR, DAN, QS and TR denote, respectively, the Barlett kernel, the Daniell kernel, the Quadratic-Spectral kernel and the Truncated kernel. Number of bootstraps = 499. M denotes the kernel smoothing parameter. T and d_1 denote the sample size and dimension of portfolio 1, respectively.

2.H.2 Monte Carlo study of the bidirectional test

We report and discuss in this section the full set of simulation results for our bidirectional spillover test based on the proposed NCCC-LS modeling. To ensure consistency and comparability, we maintain the same experimental design and parameter combinations as those described in Section 2.4 of the paper. As per the unidirectional study, we conduct simulations based on both the asymptotic critical values (Q_2) and bootstrap critical values (Q_2^*). Overall, the finite sample performance of Q_2 and Q_2^* is very similar to that of Q_1 and Q_1^* , as will be discussed in the following.

To keep the presentation consistent, we tabulate and present the simulation results of the bidirectional tests in the same ordering as their unidirectional counterparts. First, we report the bivariate simulation results in Tables 2.H.3 and 2.H.4, which represents the bidirectional counterparts of Tables 2.1 and 2.2 in the paper. Next, we report the dimensional study (for the case of $M = 20$) in Tables 2.H.5 and 2.H.6, which correspond to Tables 2.3 and 2.4 in the paper. Finally, we also report the full set of dimensional study (i.e., for $M = 10, 20, 30$) in Tables 2.H.7 and 2.H.8, which represent the bidirectional counterparts of Tables 2.H.1 and 2.H.2 in this appendix.

We begin with the bivariate study. Table 2.H.3 reports the size performance of our bidirectional testing strategy. We find that the size pattern of Q_2 and Q_2^* is very similar to that of Q_1 and Q_1^* reported in Table 2.1 of the paper. In general, the size of our bidirectional approach is reasonable and it improves as T increases. The size is also stable across the different parameter combinations considered; the four kernel functions studied and their smoothing parameters M . Table 2.H.4 reports the power performance of our bidirectional testing approach. We can see that the power of Q_2 and Q_2^* is slightly lower than that of Q_1 and Q_1^* reported in Table 2.2 of the paper. This minor loss in power is expected because the bidirectional tests check both positive and negative lag order j 's for evidence of spillover, whereas the unidirectional tests check only the positive ones. Other than this, the overall power pattern of Q_2 and Q_2^* is very similar to that of Q_1 and Q_1^* .

We now turn to the simulation results of the higher dimensional study of Q_2 and Q_2^* reported in Tables 2.H.5, 2.H.6, 2.H.7 and 2.H.8. Because the results in Tables 2.H.5 and 2.H.6 are embedded, respectively, in Tables 2.H.7 and 2.H.8, we shall focus on discussing the latter. Table 2.H.7 reports the size study of Q_2 and Q_2^* as the portfolio dimension increases. First, we find that the size of Q_2 and Q_2^* increases in d_1 , but not overly excessive nor rapid. The size generally improves and stabilizes as T increases. The observed trend is similar to that of the unidirectional tests reported in Table 2.3 of the paper. We also find the size of Q_2 and Q_2^* to be stable across M for each of the dimension studied, consistent with their unidirectional counterparts reported in Table 2.H.1.

Table 2.H.8 reports the power study of our bidirectional inferential approach as d_1 increases. We find that Q_2 and Q_2^* have power despite a rather low spillover intensity. We also find that the power increases in d_1 as the spillover evidence becomes stronger due to the increased number of risk recipients. This power trend is consistent with that of the unidirectional tests reported in Table 2.4 of the paper. We also find that the rejection rates of Q_2 and Q_2^* decrease in M due to the one-period lag spillover, in line with the pattern given by Q_1 and Q_1^* in Table 2.H.2. Similar to the

Table 2.H.3 Empirical sizes

T	M	NullA			NullB			NullC		
		10	20	30	10	20	30	10	20	30
<i>Rejection rates based on asymptotic critical values</i>										
1000	$Q_{2\text{BAR}}$	7.0	6.9	6.8	7.0	6.9	6.7	7.0	7.0	6.8
	$Q_{2\text{DAN}}$	6.9	6.9	6.8	6.8	6.9	6.8	6.8	6.9	6.9
	$Q_{2\text{QS}}$	7.0	6.9	6.9	6.9	6.9	6.8	7.0	6.9	6.9
	$Q_{2\text{TR}}$	7.0	6.8	6.4	7.1	6.8	6.6	6.9	6.8	6.4
1500	$Q_{2\text{BAR}}$	6.7	6.7	6.5	6.7	6.7	6.6	6.7	6.7	6.4
	$Q_{2\text{DAN}}$	6.7	6.6	6.3	6.7	6.8	6.5	6.8	6.5	6.3
	$Q_{2\text{QS}}$	6.7	6.5	6.3	6.8	6.8	6.3	6.8	6.6	6.4
	$Q_{2\text{TR}}$	6.7	6.1	6.4	6.8	6.2	6.5	6.7	6.1	6.4
<i>Rejection rates based on bootstrap critical values</i>										
1000	$Q_{2\text{BAR}}^*$	5.4	5.4	5.4	5.3	5.4	5.4	5.3	5.3	5.4
	$Q_{2\text{DAN}}^*$	5.5	5.4	5.2	5.4	5.5	5.4	5.5	5.5	5.2
	$Q_{2\text{QS}}^*$	5.3	5.3	5.3	5.3	5.5	5.2	5.4	5.5	5.3
	$Q_{2\text{TR}}^*$	5.5	5.1	5.3	5.5	5.3	5.4	5.5	5.3	5.3
1500	$Q_{2\text{BAR}}^*$	4.5	4.7	5.0	4.5	4.6	5.1	4.6	4.7	5.1
	$Q_{2\text{DAN}}^*$	4.6	4.8	5.2	4.5	4.8	5.2	4.7	4.9	5.3
	$Q_{2\text{QS}}^*$	4.6	4.8	5.2	4.6	5.0	5.1	4.6	4.8	5.2
	$Q_{2\text{TR}}^*$	4.9	5.2	5.3	4.8	5.1	5.1	4.9	5.2	5.3

NOTES: The table reports empirical sizes (in %) of Q_2 under NullA, NullB and NullC at the 5% significance level based on NCCC-LS modeling. Number of simulations = 10000. $Q_{2\text{BAR}}$, $Q_{2\text{DAN}}$, $Q_{2\text{QS}}$, $Q_{2\text{TR}}$ and $Q_{2\text{BAR}}^*$, $Q_{2\text{DAN}}^*$, $Q_{2\text{QS}}^*$, $Q_{2\text{TR}}^*$ denote the rejection rates of Q_2 using asymptotic and bootstrap critical values, respectively; the subscripts BAR, DAN, QS and TR denote, respectively, the Barlett kernel, the Daniell kernel, the Quadratic-Spectral kernel and the Truncated kernel. Number of bootstraps = 499. T and M denote the sample size and kernel smoothing parameter, respectively.

bivariate study reported in Table 2.H.4, we observe here some minor loss in power of Q_2 and Q_2^* compared with Q_1 and Q_1^* . This is again due to the fact that Q_2 and Q_2^* examine both positive and negative directions for spillover evidence while Q_1 and Q_1^* check only the positive direction. Apart from this, the overall power pattern of Q_2 and Q_2^* is very similar to that of Q_1 and Q_1^* , and the power generally improves as T increases.

Table 2.H.4 Empirical powers

T	M	AlterA			AlterB		
		10	20	30	10	20	30
<i>Rejection rates based on empirical critical values</i>							
1000	$Q_{2\text{BAR}}$	61.2	52.4	45.7	84.5	76.7	69.9
	$Q_{2\text{DAN}}$	58.7	46.0	38.5	82.5	70.4	61.5
	$Q_{2\text{QS}}$	57.6	44.4	37.3	81.5	68.4	59.9
	$Q_{2\text{TR}}$	37.3	27.5	23.0	60.2	45.7	37.3
1500	$Q_{2\text{BAR}}$	79.3	70.5	63.9	96.7	93.4	89.9
	$Q_{2\text{DAN}}$	76.6	64.0	55.1	95.8	89.9	82.8
	$Q_{2\text{QS}}$	75.4	61.9	53.2	95.3	88.6	81.3
	$Q_{2\text{TR}}$	53.2	40.8	33.6	81.9	67.5	57.1
<i>Rejection rates based on bootstrap critical values</i>							
1000	$Q_{2\text{BAR}}^*$	59.4	49.9	43.8	83.7	75.9	68.3
	$Q_{2\text{DAN}}^*$	56.4	43.4	36.6	81.6	68.5	59.2
	$Q_{2\text{QS}}^*$	54.9	42.2	35.0	80.4	66.6	57.4
	$Q_{2\text{TR}}^*$	35.1	25.0	20.8	57.5	42.4	35.1
1500	$Q_{2\text{BAR}}^*$	77.7	69.4	62.0	95.9	92.2	87.9
	$Q_{2\text{DAN}}^*$	75.5	62.1	52.9	95.0	88.3	81.5
	$Q_{2\text{QS}}^*$	74.1	60.3	51.2	94.6	86.9	80.0
	$Q_{2\text{TR}}^*$	51.7	36.9	30.2	80.3	64.6	53.8

NOTES: The table reports empirical powers (in %) of Q_2 under AlterA and AlterB at the 5% significance level based on NCCC-LS modeling. Number of simulations = 10000. $Q_{2\text{BAR}}$, $Q_{2\text{DAN}}$, $Q_{2\text{QS}}$, $Q_{2\text{TR}}$ and $Q_{2\text{BAR}}^*$, $Q_{2\text{DAN}}^*$, $Q_{2\text{QS}}^*$, $Q_{2\text{TR}}^*$ denote the rejection rates of Q_2 using empirical and bootstrap critical values, respectively; the subscripts BAR, DAN, QS and TR denote, respectively, the Barlett kernel, the Daniell kernel, the Quadratic-Spectral kernel and the Truncated kernel. Number of bootstraps = 499. T and M denote the sample size and kernel smoothing parameter, respectively.

Table 2.H.5 Empirical sizes

T	d_1	NullD							
		3	4	5	6	7	8	9	10
<i>Rejection rates based on asymptotic critical values</i>									
1000	$Q_{2\text{BAR}}$	7.1	7.0	7.6	7.9	7.3	7.6	7.9	8.3
	$Q_{2\text{DAN}}$	7.0	7.1	7.8	8.0	7.4	8.0	8.3	8.5
	$Q_{2\text{QS}}$	6.9	7.1	7.8	7.9	7.3	7.9	8.3	8.5
	$Q_{2\text{TR}}$	6.9	7.1	7.5	8.6	8.1	8.6	8.7	9.3
1500	$Q_{2\text{BAR}}$	6.3	6.4	6.6	6.8	6.9	7.5	7.4	7.3
	$Q_{2\text{DAN}}$	6.3	6.6	6.8	6.9	6.9	7.4	7.5	7.5
	$Q_{2\text{QS}}$	6.3	6.5	6.6	7.0	6.9	7.6	7.3	7.5
	$Q_{2\text{TR}}$	6.3	6.2	7.0	7.4	7.5	7.4	7.9	7.7
<i>Rejection rates based on bootstrap critical values</i>									
1000	$Q_{2\text{BAR}}^*$	5.3	5.7	5.2	5.4	6.1	6.2	6.0	6.2
	$Q_{2\text{DAN}}^*$	5.6	5.7	5.1	5.3	6.3	6.1	6.0	6.2
	$Q_{2\text{QS}}^*$	5.5	5.6	5.3	5.3	6.2	6.1	6.0	6.2
	$Q_{2\text{TR}}^*$	5.7	5.8	5.5	5.5	6.2	6.3	6.3	6.1
1500	$Q_{2\text{BAR}}^*$	4.6	5.2	4.8	4.6	5.6	5.0	5.7	5.4
	$Q_{2\text{DAN}}^*$	4.9	5.3	4.8	5.1	5.5	5.1	5.8	5.2
	$Q_{2\text{QS}}^*$	5.0	5.3	4.8	5.1	5.3	5.0	5.9	5.3
	$Q_{2\text{TR}}^*$	4.8	5.0	5.1	5.4	5.8	5.5	5.6	5.6

NOTES: The table reports empirical sizes (in %) of Q_2 under NullD at the 5% significance level based on NCCC-LS modeling. Number of simulations = 10000. $Q_{2\text{BAR}}$, $Q_{2\text{DAN}}$, $Q_{2\text{QS}}$, $Q_{2\text{TR}}$ and $Q_{2\text{BAR}}^*$, $Q_{2\text{DAN}}^*$, $Q_{2\text{QS}}^*$, $Q_{2\text{TR}}^*$ denote the rejection rates of Q_2 using asymptotic and bootstrap critical values, respectively; the subscripts BAR, DAN, QS and TR denote, respectively, the Barlett kernel, the Daniell kernel, the Quadratic-Spectral kernel and the Truncated kernel. Number of bootstraps = 499. T and d_1 denote the sample size and dimension of portfolio 1, respectively.

Table 2.H.6 Empirical powers

T	d_1	AlterC							
		3	4	5	6	7	8	9	10
<i>Rejection rates based on empirical critical values</i>									
1000	$Q_{2\text{BAR}}$	18.6	25.5	34.6	39.7	48.9	55.1	55.9	58.0
	$Q_{2\text{DAN}}$	16.8	21.9	28.4	32.6	41.2	45.8	46.7	48.2
	$Q_{2\text{QS}}$	16.5	21.2	27.3	31.3	39.6	43.9	44.3	45.3
	$Q_{2\text{TR}}$	11.6	14.0	17.2	18.9	22.4	24.5	24.7	25.1
1500	$Q_{2\text{BAR}}$	28.5	42.9	58.0	69.0	78.5	82.7	86.1	89.4
	$Q_{2\text{DAN}}$	23.7	36.0	48.2	59.0	68.0	73.0	77.4	80.5
	$Q_{2\text{QS}}$	23.4	34.8	45.8	56.8	65.4	70.9	75.1	78.3
	$Q_{2\text{TR}}$	14.3	20.3	25.0	31.4	35.9	40.1	42.9	45.4
<i>Rejection rates based on bootstrap critical values</i>									
1000	$Q_{2\text{BAR}}^*$	16.0	23.4	32.1	38.9	46.1	50.7	53.4	57.5
	$Q_{2\text{DAN}}^*$	14.0	20.1	26.3	32.7	37.9	41.6	44.6	47.6
	$Q_{2\text{QS}}^*$	13.8	19.0	25.1	31.2	36.1	39.7	42.5	45.3
	$Q_{2\text{TR}}^*$	10.1	12.0	16.0	18.0	20.8	22.0	23.8	25.1
1500	$Q_{2\text{BAR}}^*$	23.2	38.3	56.0	66.8	75.7	80.7	85.6	87.6
	$Q_{2\text{DAN}}^*$	19.7	31.7	46.7	56.4	65.6	70.7	76.7	79.1
	$Q_{2\text{QS}}^*$	19.3	30.5	44.8	54.0	62.7	68.0	74.0	76.6
	$Q_{2\text{TR}}^*$	13.3	17.2	24.2	29.5	34.0	38.2	41.3	43.9

NOTES: The table reports empirical powers (in %) of Q_2 under AlterC at the 5% significance level based on NCCC-LS modeling. Number of simulations = 10000. $Q_{2\text{BAR}}$, $Q_{2\text{DAN}}$, $Q_{2\text{QS}}$, $Q_{2\text{TR}}$ and $Q_{2\text{BAR}}^*$, $Q_{2\text{DAN}}^*$, $Q_{2\text{QS}}^*$, $Q_{2\text{TR}}^*$ denote the rejection rates of Q_2 using empirical and bootstrap critical values, respectively; the subscripts BAR, DAN, QS and TR denote, respectively, the Barlett kernel, the Daniell kernel, the Quadratic-Spectral kernel and the Truncated kernel. Number of bootstraps = 499. T and d_1 denote the sample size and dimension of portfolio 1, respectively.

Table 2.H.7 Empirical sizes

d_1		NullID																									
		3			4			5			6			7			8			9			10				
T	M	10	20	30	10	20	30	10	20	30	10	20	30	10	20	30	10	20	30	10	20	30	10	20	30		
<i>Rejection rates based on asymptotic critical values</i>																											
1000	Q ₂ BAR	7.4	7.1	7.0	6.8	7.0	7.0	7.1	7.6	7.7	7.4	7.9	8.2	7.1	7.3	7.7	7.1	7.6	7.9	7.6	8.0	7.9	8.6	7.7	8.3	8.7	
	Q ₂ DAN	7.2	7.0	6.9	7.0	7.1	7.1	7.3	7.8	7.7	7.6	8.0	8.4	7.1	7.4	7.7	7.1	8.0	8.3	7.6	8.5	8.3	8.8	7.8	8.5	9.0	
	Q ₂ QS	7.1	6.9	7.1	7.0	7.1	7.0	7.1	7.8	7.7	7.7	7.9	8.4	7.0	7.3	7.5	7.1	7.9	8.4	7.7	8.4	7.7	8.3	8.9	7.7	8.5	9.1
	Q ₂ TR	7.1	6.9	7.2	6.9	7.1	7.5	7.5	7.5	7.8	7.9	8.6	8.9	7.3	8.1	8.2	7.8	8.6	9.3	8.2	8.7	10.1	8.1	9.3	9.9		
1500	Q ₂ BAR	6.4	6.3	6.2	6.7	6.4	6.3	6.8	6.6	6.6	6.6	6.8	7.1	6.8	6.9	7.2	7.1	7.5	7.6	7.1	7.4	7.6	7.4	7.3	7.6		
	Q ₂ DAN	6.4	6.3	6.2	6.6	6.6	6.3	6.9	6.8	6.7	6.5	6.9	7.3	6.6	6.9	7.2	7.2	7.4	7.3	7.4	7.3	7.6	7.4	7.5	7.9		
	Q ₂ QS	6.4	6.3	6.2	6.7	6.5	6.2	6.8	6.6	6.8	6.4	7.0	7.1	6.6	6.9	7.1	7.1	7.6	7.4	7.4	7.4	7.3	7.6	7.4	7.5	7.8	
	Q ₂ TR	6.3	6.3	6.4	6.5	6.2	6.4	6.7	7.0	6.8	6.7	7.4	7.6	6.9	7.5	7.8	7.4	7.4	7.4	7.2	8.3	7.2	7.9	8.3	7.4	7.7	8.2
<i>Rejection rates based on bootstrap critical values</i>																											
1000	Q ₂ BAR	5.1	5.3	5.7	5.2	5.7	5.8	5.3	5.2	5.2	5.2	5.4	5.4	5.5	6.1	6.1	5.7	6.2	6.1	5.7	6.0	6.0	6.0	5.3	6.2	6.2	
	Q ₂ DAN	5.0	5.6	5.9	5.4	5.7	5.7	5.1	5.1	5.3	5.5	5.3	5.3	5.7	6.3	6.0	6.0	6.1	6.2	5.6	6.0	6.2	5.4	6.2	6.1	6.1	
	Q ₂ QS	5.1	5.5	5.7	5.5	5.6	5.8	5.3	5.3	5.5	5.3	5.3	5.3	5.8	6.2	6.2	6.0	6.1	6.2	5.4	6.0	6.1	5.8	6.2	6.0	6.0	
	Q ₂ TR	5.8	5.7	5.8	5.6	5.8	5.5	5.1	5.5	5.5	5.4	5.5	5.6	6.2	6.2	5.9	6.1	6.3	6.4	5.9	6.3	6.6	6.1	6.1	6.1	6.1	
1500	Q ₂ BAR	4.9	4.6	5.0	5.5	5.2	5.4	5.1	4.8	4.9	4.9	4.6	5.3	5.6	5.6	5.6	5.3	5.0	5.2	5.5	5.7	5.9	5.2	5.4	5.4		
	Q ₂ DAN	4.9	4.9	4.8	5.2	5.3	5.1	5.2	4.8	4.9	4.9	5.1	5.3	5.8	5.5	5.7	5.3	5.1	5.3	5.3	5.3	5.8	6.0	5.2	5.2	5.8	
	Q ₂ QS	4.7	5.0	4.8	5.3	5.3	5.2	5.3	4.8	4.9	4.8	5.1	5.4	5.7	5.3	5.8	5.3	5.0	5.1	5.5	5.9	6.1	5.2	5.3	5.5	5.5	
	Q ₂ TR	5.0	4.8	4.9	5.3	5.0	5.2	4.5	5.1	4.8	5.1	5.4	5.1	5.8	5.8	5.5	5.0	5.5	5.5	6.0	5.6	5.8	5.3	5.6	5.3	5.6	

NOTES: The table reports empirical sizes (in %) of Q_2 under NullID at the 5% significance level based on NCCC-LS modeling. Number of simulations = 10000. $Q_{2\text{BAR}}$, $Q_{2\text{DAN}}$, $Q_{2\text{QS}}$, $Q_{2\text{TR}}$ and $Q_{2\text{BAR}}^*$, $Q_{2\text{DAN}}^*$, $Q_{2\text{QS}}^*$, $Q_{2\text{TR}}^*$ denote the rejection rates of Q_2 using asymptotic and bootstrap critical values, respectively; the subscripts BAR, DAN, QS and TR denote, respectively, the Bartlett kernel, the Daniell kernel, the Quadratic-Spectral kernel and the Truncated kernel. Number of bootstraps = 499. M denotes the kernel smoothing parameter. T and d_1 denote the sample size and dimension of portfolio 1, respectively.

Table 2.H.8 Empirical powers

d_1		AlterC																																															
		3			4			5			6			7			8			9			10																										
T	M	10	20	30	10	20	30	10	20	30	10	20	30	10	20	30	10	20	30	10	20	30	10	20	30	10	20	30	10	20	30																		
<i>Rejection rates based on empirical critical values</i>																																																	
1000	Q_{2BAR}^*	22.2	18.6	16.5	32.2	25.5	21.9	44.8	34.6	28.7	53.0	39.7	33.3	61.9	48.9	40.9	69.4	55.1	44.8	70.6	55.9	45.9	72.8	58.0	47.1	20.9	16.8	15.0	30.0	21.9	18.4	42.1	28.4	23.3	48.8	32.6	26.6	58.0	41.2	33.2	64.8	45.8	35.1	66.3	46.7	36.2	69.1	48.2	37.4
	Q_{2DAN}^*	20.0	16.5	14.4	28.9	21.2	17.6	40.8	27.3	22.6	47.3	31.3	25.9	56.4	39.6	31.8	62.5	43.9	33.6	64.2	44.3	34.2	66.6	45.3	35.6	14.3	11.6	10.6	18.0	14.0	11.9	22.3	17.2	14.7	26.3	18.9	15.8	32.1	22.4	19.4	35.5	24.5	20.4	36.5	24.7	19.1	37.8	25.1	20.8
	Q_{2TR}^*	14.3	11.6	10.6	18.0	14.0	11.9	22.3	17.2	14.7	26.3	18.9	15.8	32.1	22.4	19.4	35.5	24.5	20.4	36.5	24.7	19.1	37.8	25.1	20.8	34.8	28.5	24.4	53.9	42.9	36.4	72.4	58.0	48.4	82.5	69.0	58.6	90.3	78.5	67.7	92.9	82.7	72.8	95.2	86.1	77.5	96.6	89.4	80.1
1500	Q_{2BAR}^*	34.8	28.5	24.4	53.9	42.9	36.4	72.4	58.0	48.2	82.5	69.0	58.6	90.3	78.5	67.7	92.9	82.7	72.8	95.2	86.1	77.5	96.6	89.4	80.1	33.0	23.7	20.6	49.5	36.0	29.4	67.8	48.2	38.4	79.9	59.0	47.5	87.1	68.0	56.0	90.0	73.0	61.0	92.9	77.4	64.8	94.7	80.5	67.7
	Q_{2DAN}^*	31.4	23.4	19.3	48.1	34.8	28.3	65.6	45.8	36.8	77.9	56.8	45.6	85.3	65.4	53.6	88.7	70.9	58.7	91.4	75.1	61.7	93.8	78.3	64.8	31.4	23.4	19.3	48.1	34.8	28.3	65.6	45.8	36.8	77.9	56.8	45.6	85.3	65.4	53.6	88.7	70.9	58.7	91.4	75.1	61.7	93.8	78.3	64.8
	Q_{2QS}^*	19.2	14.3	13.2	28.2	20.3	17.0	37.5	25.0	21.1	46.8	31.4	25.3	53.4	35.9	28.4	58.6	40.1	31.0	63.0	42.9	33.0	67.2	45.4	36.8	19.2	14.3	13.2	28.2	20.3	17.0	37.5	25.0	21.1	46.8	31.4	25.3	53.4	35.9	28.4	58.6	40.1	31.0	63.0	42.9	33.0	67.2	45.4	36.8
<i>Rejection rates based on bootstrap critical values</i>																																																	
1000	Q_{2BAR}^*	19.2	16.0	14.1	29.4	23.4	19.8	41.8	32.1	26.7	51.0	38.9	32.7	59.8	46.1	37.8	64.0	50.7	41.1	67.3	53.4	44.5	70.6	57.5	47.4	18.2	14.0	12.6	27.5	20.1	15.8	38.3	26.3	21.9	47.3	32.7	26.4	55.5	37.9	30.1	59.8	41.6	32.9	62.3	44.6	35.2	66.6	47.6	37.4
	Q_{2DAN}^*	17.6	13.8	12.7	26.6	19.0	15.3	37.4	25.1	21.1	45.4	31.2	24.9	53.4	36.1	29.3	57.6	39.7	31.5	60.5	42.5	34.2	64.5	45.3	36.0	17.6	13.8	12.7	26.6	19.0	15.3	37.4	25.1	21.1	45.4	31.2	24.9	53.4	36.1	29.3	57.6	39.7	31.5	60.5	42.5	34.2	64.5	45.3	36.0
	Q_{2QS}^*	12.2	10.1	9.3	15.6	12.0	10.9	21.1	16.0	13.2	25.0	18.0	15.3	29.6	20.8	17.8	31.0	22.0	18.1	34.8	23.8	19.1	35.5	25.1	19.7	12.2	10.1	9.3	15.6	12.0	10.9	21.1	16.0	13.2	25.0	18.0	15.3	29.6	20.8	17.8	31.0	22.0	18.1	34.8	23.8	19.1	35.5	25.1	19.7
1500	Q_{2BAR}^*	29.8	23.2	20.2	48.9	38.3	32.0	69.6	56.0	46.2	80.9	66.8	56.3	88.5	75.7	65.2	91.8	80.7	70.2	94.5	85.6	75.9	96.2	87.6	78.4	27.7	19.7	17.1	45.3	31.7	25.9	65.7	46.7	36.9	76.9	56.4	45.7	85.5	65.6	52.1	89.3	70.7	57.8	92.3	76.7	63.0	94.2	79.1	66.1
	Q_{2DAN}^*	26.6	19.3	16.7	43.6	30.5	24.8	63.5	44.8	35.2	74.8	54.0	43.5	83.6	62.7	49.7	87.4	68.0	55.2	90.9	74.0	60.6	92.7	76.6	63.2	26.6	19.3	16.7	43.6	30.5	24.8	63.5	44.8	35.2	74.8	54.0	43.5	83.6	62.7	49.7	87.4	68.0	55.2	90.9	74.0	60.6	92.7	76.6	63.2
	Q_{2QS}^*	16.3	13.3	12.0	23.4	17.2	14.2	35.6	24.2	18.6	43.5	29.5	23.6	50.9	34.0	26.9	55.4	38.2	29.3	61.4	41.3	32.3	65.1	43.9	34.6	16.3	13.3	12.0	23.4	17.2	14.2	35.6	24.2	18.6	43.5	29.5	23.6	50.9	34.0	26.9	55.4	38.2	29.3	61.4	41.3	32.3	65.1	43.9	34.6

NOTES: The table reports empirical powers (in %) of Q_2 under AlterC at the 5% significance level based on NCCC-LS modeling. Number of simulations = 10000. Q_{2BAR}^* , Q_{2DAN}^* , Q_{2QS}^* , Q_{2TR}^* and Q_{2BAR}^{**} , Q_{2DAN}^{**} , Q_{2QS}^{**} , Q_{2TR}^{**} denote the rejection rates of Q_2 using empirical and bootstrap critical values, respectively; the subscripts BAR, DAN, QS and TR denote, respectively, the Bartlett kernel, the Daniell kernel, the Quadratic-Spectral kernel and the Truncated kernel. Number of bootstraps = 499. M denotes the kernel smoothing parameter. T and d_1 denote the sample size and dimension of portfolio 1, respectively.

2.H.3 GARCH misspecification

Based on a correctly specified model, in the paper we find no evidence of volatility spillover between the UK market and the NA market after Brexit. In this section, we investigate the consequence of model misspecification on testing for volatility spillover. To this purpose, we repeat the examination of spillover between UK and NA in the post-Brexit sample with a deliberately misspecified model.

Recall that a well specified model requires order 4 for the conditional variance of the UK series. We first include a control study that is correctly specified. We specify a model with random order 6 for the conditional variance of the UK series. Diagnostic tests reported in Table 2.H.9 suggest that the model is well specified. Table 2.H.10 reports the volatility spillover test results. Consistent with the findings in the paper, we find no evidence of volatility spillover between the UK market and the NA market. Moreover, the p -values reported in Table 2.H.10 are very similar to those reported in the paper. This control study serves two purposes. First, it ensures that our conclusion is not affected by the sensitivity of a correctly specified model lag order. Second, it ensures that any changes in conclusion in the next study is likely to be driven by model misspecification.

To impose model misspecification, we now use order 1 for the variance of the UK market. Diagnostic results reported in Table 2.H.11 suggests model misspecification. Table 2.H.12 reports the volatility spillover test results. In contrast to the findings based on a correctly specified model, we find that the NA market has a significant spillover effect to the UK market at all M 's. Given the control study, this false-positive result is likely to be induced by serial correlations in the event variables as a result of model misspecification. In summary, the exercises in this section highlight the importance of a correctly specified model in testing volatility spillover.

Table 2.H.9 Diagnostic tests (UK–NA, Control)

	LB(10)	LB(20)	LB(30)	LB ² (10)	LB ² (20)	LB ² (30)
<i>Post-Brexit (24th June 2016 – 31st December 2019)</i>						
UK	8.342 [0.595]	17.378 [0.628]	24.770 [0.736]	7.035 [0.722]	12.227 [0.908]	15.502 [0.987]
US	15.436 [0.117]	18.869 [0.530]	23.736 [0.784]	10.546 [0.394]	13.020 [0.877]	17.188 [0.970]
Canada	6.779 [0.746]	18.437 [0.559]	22.004 [0.854]	4.432 [0.926]	18.823 [0.533]	21.513 [0.871]

NOTES: The table reports diagnostic analyses for all fitted series. $LB(M)$ and $LB^2(M)$ are the Ljung-Box tests for the null of no serial correlation (up to lag order M) on the standardized and squared standardized residuals, respectively. The values in the squared parentheses are the p -values of the tests.

Table 2.H.10 Spillover results (UK–NA, Control)

M	<i>Post–Brexit</i>		
	10	20	30
$Q_{1\text{BAR}}^*$	0.172	0.166	0.236
$Q_{-1\text{BAR}}^*$	0.643	0.599	0.673

NOTES: The table reports bootstrap p -values of the proposed spillover tests. Number of bootstraps = 499. Q_{BAR}^* denotes the one-way test for the null hypothesis of no volatility spillover from the NA market to the UK market. $Q_{-1\text{BAR}}^*$ denotes the one-way test for the null hypothesis of no volatility spillover from the UK market to the NA market. The subscript BAR denotes the Barlett kernel. M denotes the kernel smoothing parameter.

Table 2.H.11 Diagnostic tests (UK–NA, Misspecified)

	LB(10)	LB(20)	LB(30)	LB ² (10)	LB ² (20)	LB ² (30)
<i>Post–Brexit (24th June 2016 – 31st December 2019)</i>						
UK	33.666 [0.000]	49.171 [0.000]	55.323 [0.003]	22.971 [0.011]	38.451 [0.008]	41.231 [0.083]
US	15.436 [0.117]	18.869 [0.530]	23.736 [0.784]	10.546 [0.394]	13.020 [0.877]	17.188 [0.970]
Canada	6.779 [0.746]	18.437 [0.559]	22.004 [0.854]	4.432 [0.926]	18.823 [0.533]	21.513 [0.871]

NOTES: The table reports diagnostic analyses for all fitted series. $LB(M)$ and $LB^2(M)$ are the Ljung-Box tests for the null of no serial correlation (up to lag order M) on the standardized and squared standardized residuals, respectively. The values in the squared parentheses are the p -values of the tests.

Table 2.H.12 Spillover results (UK–NA, Misspecified)

M	<i>Post–Brexit</i>		
	10	20	30
$Q_{1\text{BAR}}^*$	0.078	0.048	0.060
$Q_{-1\text{BAR}}^*$	0.721	0.607	0.687

NOTES: The table reports bootstrap p -values of the proposed spillover tests. Number of bootstraps = 499. Q_{BAR}^* denotes the one-way test for the null hypothesis of no volatility spillover from the NA market to the UK market. $Q_{-1\text{BAR}}^*$ denotes the one-way test for the null hypothesis of no volatility spillover from the UK market to the NA market. The subscript BAR denotes the Barlett kernel. M denotes the kernel smoothing parameter.

2.H.4 Computational efficiency study

In this section, we conduct a computational efficiency experiment to highlight the speed advantage of our adjusted least-squares estimation over its likelihood counterparts. We simulate the following simple ARCH(1) process with the standard Gaussian error

$$\begin{aligned} \epsilon_t &= \sqrt{h_t} \xi_t, \quad \xi_t \stackrel{\text{iid}}{\sim} N(0, 1), \\ h_t &= 0.1 + 0.2\epsilon_{t-1}^2. \end{aligned}$$

Next, we fit the simulated ARCH process h_t using our adjusted least-squares estimation as well as QMLE. During estimation, we measure the machine elapsed time using the Matlab `tic` and `toc` functions. For improved accuracy, we repeat the procedure 10000 times and we compute the mean elapsed time. We find that the average machine time required by our estimation method is about 0.0012 (machine unit) per simulation, while that required by QMLE is about 0.0266 per simulation. In other words, our method requires only about 4.3% of the the computational time of QMLE.

GLOBAL CRUDE OIL AND THE CHINESE OIL-INTENSIVE SECTORS: A COMPREHENSIVE CAUSALITY STUDY[‡]

3.1 Introduction

Crude oil is often described as the *lifeblood* of modern economies because it fuels essential economic activities such as agricultural productions, chemical engineerings, construction operations, industrial manufacturings, power generations and transportations. Despite advancement in the renewable alternatives, crude oil remains the world's most important source of energy after the mid-1950s. China has been importing crude oil to facilitate its rapid economic growth ever since 1995. Now, China is the second largest economy in the world by gross domestic product (GDP), and its petroleum consumption has more than tripled between 1995 (160.65 million tons) and 2017 (587.45 million tons).¹ Armed with ambitious economic development plans, China's demand for international oil has been rising consistently over the past 15 years, as depicted in Figure 3.1. With more than eight million barrels of daily crude oil imports in 2017, China has since then surpassed the US to become the top crude oil importer. Therefore, it is evident that global crude oil and the Chinese economy are closely interdependent. In particular, the oil-intensive sectors in China directly influence the demand for, and the price of international oil, whereas a global reduction in the supply of oil affects the Chinese industries due to increase in operational costs.

In this paper, we study Granger causal relations between global crude oil and the sectoral stock market index returns in China. We focus on the industrial, construction, agricultural and

[‡]A research manuscript based on the results in this chapter entitled "Global crude oil and the Chinese oil-intensive sectors: A comprehensive causality study" is under revision at *Energy Economics*.

¹Data source: China Statistical Yearbook. Besides, petroleum is a general term consisting of crude oil and its processed products.

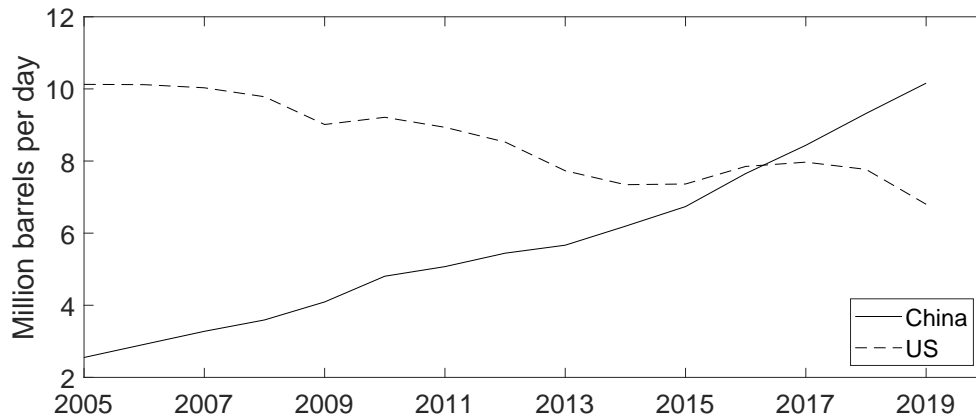


Figure 3.1 Crude oil imports. This figure plots the crude oil imports in China (solid line) and in the US (dashed line) over the 2005–2019 period, in million barrels per day. Data source: *Datastream* and *EIA*.

transportation (ICAT) sectors which collectively accounts for more than 80% of China's petroleum consumption in 2017.² We make use of daily observations over the 2005–2019 period, which allows studying the changes in causal linkages after key economic and political events such as the US subprime mortgage financial crisis in 2008 and the Chinese reformation of domestic refined oil pricing mechanism in 2013. We combine a set of Granger causality inferential procedures that is based on the cross-correlation function (CCF) approach to analyse the oil-ICAT nexus. Our bidirectional methodology uncovers causal relations in the mean, variance, risky quantiles and distribution between the markets of interest. To the best of our knowledge, this is the first study that unifies the extensive CCF-based causality tests proposed over the past two decades.

This paper offers several contributions to the literature. First, we investigate causal relations between global crude oil and the Chinese industries that are oil intensive. This is in stark contrast to most existing studies, which analyse the Chinese market at the broader sectoral or aggregate level. The ICAT sectors deserve particular attention as they consume most of the oil in China to fuel the country's modern and advanced economy. For instance, the agricultural industry depends on oil-driven machineries that are capable of accelerating food production such as automated harvesters and tractors to feed the population. The industrial sector relies on crude oil to power cities and to manufacture essential everyday products that includes electronic devices, textiles, and medicines. The construction of skyscrapers that shape major cities speeds up with the ability to mass produce high-strength materials such as steel, which is an oil-consuming process. Finally, most of the transportation modes connecting goods, people, places and services are powered by oil. Compared with papers that focus on the composite market index, we provide a more in-depth and focused examination by featuring the top oil-intensive sectors individually. Besides, we offer

²Data source: China Statistical Yearbook.

a set of conclusions that is, relatively speaking, more definite than studies using firm-level data since the reactions can vary for firms within the same sector.

Second, we consolidate the extensive literature on CCF-based inferential procedures and we show that various forms of causality can be examined. Under this unified framework, we provide a comprehensive analysis covering the mean, variance, risky quantiles (both positive and negative) and distribution, where each element reveals a unique economic relation. The causality-in-mean analysis investigates return predictability, whereas the presence of variance causality can be viewed as volatility spillover. The causality-in-risk test examines the existence of extreme risk spillovers and it covers both positive and negative relations. This is convenient given that crude oil and stock markets might be negatively correlated (see e.g., [Du and He, 2015](#); [Mollick and Assefa, 2013](#)). Finally, the long-term causal linkages are analysed using the causality-in-distribution test. Because all of our analyses are based on the CCF approach, we minimise potential inferential biases due to methodological disparities. Compared with a handful of papers that focus on crude oil's impact on the Chinese markets, we do not presume any dependence directions in the oil-ICAT nexus and our approach allows for potential feedback effects.

Third, we make use of our sample length to investigate possible changes in causal relations after the 2008 US financial crisis and the 2013 refined oil pricing mechanism reform in China. The former is well known for affecting the global economies including crude oil (see, e.g., [Broadstock et al., 2012](#); [Xu et al., 2019](#)), whereas the latter is a relatively new event that is of great significance to the Chinese economy. Although a few papers consider the effects of oil reform (see, e.g., [Bouri et al., 2017](#); [Peng et al., 2018](#); [Xiao et al., 2018](#)), neither of them focuses on the ICAT industries. Traditionally, the price of domestic oil in China is capped and strictly regulated by its central government. Consequently, the world oil price has a limited influence on the oil-intensive sectors in China. On 27 March 2013, the Chinese government launched a major reformation of its domestic refined oil pricing mechanism to greatly relax its control over local oil price. Generally regarded as the major milestone in the transformation to a market-oriented pricing of retail oil, this reform discourages the government from setting a ceiling price for domestic oil so long as international oil price stays under USD 130 per barrel. This has nontrivial impact to the Chinese markets, particularly the ICAT sectors as they become more exposed to global oil price movement.

In summary, we complement a growing literature on the oil-stock nexus by providing novel perspectives from the industries in China that are oil intensive. We combine a series of inferential tests to thoroughly examine the oil-ICAT nexus while taking into consideration the effects of China's oil reform. The remainder of this paper is organised as follows. Section 3.2 reviews the existing literature. We introduce the unified causality methodology in Section 3.3. Section 3.4 describes our dataset. Empirical findings are reported and discussed in Section 3.5. Section 3.6 concludes.

3.2 Literature review

In this section, we review and summarise existing studies on the relations between global crude oil and the Chinese markets. Note that we only provide a very brief overview of the literature's conclusions as the main purpose of this review is to highlight the breadth of the related literature. We emphasise that each study is highly detailed, adopting differing econometric strategies, with different datasets spanning over different time periods, among others. For a survey on other countries including the US, we refer the readers to see, e.g., [Broadstock et al. \(2016, Table 1\)](#).

Using structural vector autoregression (SVAR) model together with the Baba-Engle-Kraft-Kroner (BEKK) specification, [Broadstock and Filis \(2014\)](#) find that crude oil affects the two largest economies (China and US) in the world, though the Chinese market is more resilient to the impact than its US counterpart. Based on extreme value analysis, [Chen and Lv \(2015\)](#) document positive dependence between international oil and the Chinese stock market. [Ding et al. \(2016\)](#) study positive Granger causality between global crude oil and the major stock indices over 1996–2012 to find that the causal relations between the Shanghai composite index and the West Texas Intermediate (WTI) oil varies across quantiles. Based on a set of monthly data spanning from 1994 to 2014, [Zhu et al. \(2016\)](#) study if crude oil affects the broader industries in China using quantile regression. The authors find that the dependence on oil varies across sectors and quantiles. Based on asset pricing models, [Broadstock et al. \(2016\)](#) focus on firm-level data covering the 2005–2013 period to find that 89.2% of the Chinese listed entities respond to oil return.

Using daily data from 2005 to 2015, [Bouri et al. \(2017\)](#) find that the oil reform in 2013 strengthens the mean but weakens the variance relations between global oil and the broader Chinese markets. Based on the SVAR framework and monthly data from 2005 to 2015, [Ding et al. \(2017\)](#) document that international crude oil affects the investor sentiments in China. Using monthly data from 1996 to 2015, [Wei and Guo \(2017\)](#) find that the link between crude oil and the Chinese aggregate market changes after major events such as a financial crisis. Based on crude oil volatility index and the vector autoregression (VAR) methodology, [Luo and Qin \(2017\)](#) confirm that oil price uncertainty impacts the broader stock markets in China over 2007–2015. Using a similar set of data, [Xiao et al. \(2018\)](#) find that crude oil volatility has negative impacts on the wider Chinese stock markets under the quantile regression framework. [Kirkulak-Uludag and Safarzadeh \(2018\)](#) focus on the organization of the petroleum exporting countries (OPEC) oil data spanning from 2004 to 2014 and the generalized autoregressive conditional heteroskedasticity (GARCH) methodology to find evidence of volatility spillover between crude oil and the broader markets in China. By combining variational model decomposition method, copula functions and systemic risk measure, [Li and Wei \(2018\)](#) document positive risk spillover effects from global oil to the Shanghai composite market index over 2000–2017.

Using daily data from 2005 to 2017 and the CCF method, [Peng et al. \(2018\)](#) investigate the spillover effects from crude oil to 529 Chinese firms. The authors find that most of the firms react to extreme oil return with a stronger magnitude after the oil reform in 2013. Based on intraday

data from 2006 to 2015 and realised measures, [Luo and Ji \(2018\)](#) evidence volatility spillover from international oil to major agricultural products in China. [Zhang et al. \(2018\)](#) focus on the broader commodity markets to find that they, too, are affected by crude oil based on autoregressive jump intensity (ARJI) model and data from 2005 to 2016. Using daily data from 2007 to 2017 and the VAR-BEKK framework, [Yun and Yoon \(2019\)](#) evidence mean and variance spillover between international oil and the stock return of major airlines in Korea and China.

Based on nonlinear autoregressive distributed lags (NARDL) model and weekly data over 2001–2016, [Wen et al. \(2019\)](#) find that crude oil can affect the broader Chinese stock indices through nonlinear channel. Using frequency-based methodology and daily data from 2000 to 2018, [Wang and Wang \(2019\)](#) find that the impact of crude oil volatility on the markets in China varies across sectors and time periods. Based on quantile regression framework and daily data over 2011–2018, [Xiao et al. \(2019\)](#) find that the crude oil volatility index affects the implied volatility indicator of the aggregate Chinese market. Using intraday data from 2007 to 2016 and directional realised measures, [Xu et al. \(2019\)](#) evidence volatility spillover between crude oil and the composite stock index in China.

Much of the literature focuses on the links between crude oil and the Chinese composite stock index or the broader markets. Some papers study moment relations such as the mean and/or volatility, whereas some authors consider quantile linkages such as extreme returns. Conclusions have been drawn based on various methods including the CCF, copula, GARCH, quantile regression and VAR, among others. Certain studies implicitly assume one-way nexus that crude oil affects the Chinese markets while some papers restrict their analysis to positive correlations. Besides, dependence measures such as the copulas do not distinguish the direction of impact. In this paper, we focus on the Granger causality relations between global crude oil and the Chinese oil-intensive sectors. We study the industrial, construction, agricultural and transportation sectors, which are the major oil-consuming industries in China. We offer a comprehensive bidirectional study that covers seven perspectives in the oil-ICAT nexus: the mean, variance, distribution, downside risk, upside risk, down-to-up risk and up-to-down risk. All of our analyses and conclusions are based on a standard family of CCF-based causality tests, which minimise biases that may arise from differing frameworks.

3.3 Methodology

We combine the extensive Granger causality tests developed in [Hong \(2001\)](#), [Hong et al. \(2009\)](#), [Du and He \(2015\)](#) and [Candelon and Tokpavi \(2016\)](#), all of which are based on the CCF of a pair of event variables. This unified methodological framework allows testing for causal relations in the mean, variance, extreme risks (both positive and negative) and distribution between global crude oil and the oil-intensive sectoral returns in China. First, we suppose that the return series can be

described as follows

$$\begin{cases} Y_t = \mu_t + \varepsilon_t, \\ \varepsilon_t = \sqrt{h_t} \xi_t, \\ \{\xi_t\} \sim \text{i.i.d.}(0, 1) \text{ with CDF } F(\cdot) \end{cases} \quad (3.1)$$

where μ_t and h_t are, respectively, the conditional mean and variance of Y_t ; ε_t denotes the innovation term; and $\{\xi_t\}$ is the standardised innovation sequence that is independent and identically distributed with cumulative distribution function $F(\cdot)$.

We specify μ_t as an order p autoregressive process with day dummies to control for possible day-of-the-week effects, where the Monday, ..., Thursday day dummies are denoted, respectively, by d_1, \dots, d_4 . The resulting process is denoted by $\text{ARX}(p)$. We consider $\text{GARCH}(1, 1)$ for the conditional variance h_t because it is widely regarded as the workhorse model (Lee and Hansen, 1994). Although the $\text{GARCH}(1, 1)$ is able to outperform more sophisticated models in most occasions, Hansen and Lunde (2005) find that in certain cases it is inferior to a model that can accommodate leverage effect. Therefore, we further consider two asymmetric specifications as competing models: the Exponential $\text{GARCH}(1, 1)$ and the Glosten-Jagannathan-Runkle $\text{GARCH}(1, 1)$, which are denoted in short by $\text{EGARCH}(1, 1)$ and $\text{GJR-GARCH}(1, 1)$, respectively. Regarding the innovation distribution $F(\cdot)$, we consider both the generalised error distribution (GED) and the Hansen (1994) skewed- t distribution, which are known for capturing well the empirical features of returns series such as heavy tails (see. e.g., Bouri et al., 2016; Du and He, 2015). The best-fitting specification is selected on the basis of Schwartz-Bayesian Information Criteria (SBIC) and a range of diagnostic examinations.

Given a pair of realised returns $\{Y_{1,t}, Y_{2,t}\}_{t=1}^T$ of size T , we let $\{\hat{Z}_{1,t}, \hat{Z}_{2,t}\}$ collect the possibly n -variate estimated event variables derived from the realised returns. Depending on the hypothesis of interest, we derive different event variables from the realised samples. For each set of event variables, the CCF-based Granger causality testing procedure is based on their sample cross-covariance matrix that is given by

$$\hat{C}(j) = \begin{cases} T^{-1} \sum_{t=1+|j|}^T (\hat{Z}_{1,t} - \hat{\Pi}_1)(\hat{Z}_{2,t-j} - \hat{\Pi}_2)', & 0 \leq j \leq T-1, \\ T^{-1} \sum_{t=1-|j|}^T (\hat{Z}_{1,t+|j|} - \hat{\Pi}_1)(\hat{Z}_{2,t} - \hat{\Pi}_2)', & 1-T \leq j < 0, \end{cases} \quad (3.2)$$

where $\hat{\Pi}_i = T^{-1} \sum_{t=1}^T \hat{Z}_{i,t}$, $i = 1, 2$. Then, the sample CCF between $\{\hat{Z}_{1,t}\}$ and $\{\hat{Z}_{2,t}\}$ is given by

$$\hat{R}(j) = \text{diag}(\hat{\Sigma}_1)^{-1/2} \hat{C}(j) \text{diag}(\hat{\Sigma}_2)^{-1/2}, \quad (3.3)$$

where $\hat{\Sigma}_1$ and $\hat{\Sigma}_2$ are the sample covariance matrices of $\{\hat{Z}_{1,t}\}$ and $\{\hat{Z}_{2,t}\}$, respectively; and $\text{diag}(\mathbf{X})$ denotes the matrix containing the diagonal elements of \mathbf{X} . Intuitively speaking, the CCF in (3.3) captures the causal relation from $\{Y_{2,t}\}$ to $\{Y_{1,t}\}$ in the form of cross-correlation between their corresponding derived event variables $\{\hat{Z}_{2,t}\}$ and $\{\hat{Z}_{1,t}\}$. If $\{Y_{2,t}\}$ does not Granger cause $\{Y_{1,t}\}$, the cross-correlation between their derived quantities naturally reduces to zero since $\{Y_{2,t}\}$ has no

explanatory power for $\{Y_{1,t}\}$. The properly weighted and standardised test statistic for the generic Granger causality from $\{Y_{2,t}\}$ to $\{Y_{1,t}\}$ is given by

$$\hat{Q}(Y_{2,t} \rightarrow Y_{1,t}) = \frac{T \sum_{j=1}^{T-1} k^2(j/M) \text{vec}[\hat{\mathbf{R}}(j)]' (\hat{\mathbf{\Gamma}}_2^{-1} \otimes \hat{\mathbf{\Gamma}}_1^{-1}) \text{vec}[\hat{\mathbf{R}}(j)] - n^2 C_T(M)}{[n^2 D_T(M)]^{1/2}}, \quad (3.4)$$

where $k(\cdot)$ is a kernel function with smoothing parameter M ; $\hat{\mathbf{\Gamma}}_1$ and $\hat{\mathbf{\Gamma}}_2$ are the sample correlation matrices of $\{\hat{\mathbf{Z}}_{1,t}\}$ and $\{\hat{\mathbf{Z}}_{2,t}\}$, respectively; n is the dimension of the event variables; and $C_T(M)$ and $D_T(M)$ are given by

$$C_T(M) = \sum_{j=1}^{T-1} (1 - j/T) k^2(j/M), \quad (3.5)$$

$$D_T(M) = 2 \sum_{j=1}^{T-1} (1 - j/T)(1 - (j+1)/T) k^4(j/M). \quad (3.6)$$

Under standard regularity conditions, $\hat{Q}(Y_{2,t} \rightarrow Y_{1,t})$ converges in distribution to $N(0, 1)$ under the null hypothesis that $\{Y_{2,t}\}$ does not Granger cause $\{Y_{1,t}\}$. Because $\hat{Q}(Y_{2,t} \rightarrow Y_{1,t})$ diverges to positive infinity under the alternative hypothesis, upper-tailed critical values are used.

To test the null hypothesis that $\{Y_{2,t}\}$ does not Granger cause $\{Y_{1,t}\}$ in variance, we follow [Hong \(2001\)](#) to set the event variables $\hat{\mathbf{Z}}_{1,t}$ and $\hat{\mathbf{Z}}_{2,t}$ as the estimated univariate squared standardised residuals $\hat{\xi}_{1,t}^2$ and $\hat{\xi}_{2,t}^2$, respectively. For causality-in-mean analysis, the event variables are set to be the standardised residuals. Intuitively speaking, the cross-correlation between the properly normalised return series in the first (second) moment contain information about Granger causality in the mean (variance). The causality-in-risk test of [Hong et al. \(2009\)](#) begins by defining the value-at-risk (VaR) which is given by $\hat{V}_t(\alpha) = \hat{\mu}_t + \sqrt{\hat{h}_t} \hat{z}(\alpha)$, where $\hat{\mu}_t$ and \hat{h}_t are the estimated conditional mean and variance, respectively; and $\hat{z}(\alpha)$ is the support value at risk level α of the estimated distribution $\hat{F}(\cdot)$ that satisfies $\hat{F}[\hat{z}(\alpha)] = \alpha$. To test the null that $\{Y_{2,t}\}$ does not Granger cause $\{Y_{1,t}\}$ in downside risk, we set the event variables as $\hat{\mathbf{Z}}_{1,t} = \mathbb{1}[Y_{1,t} < \hat{V}_{1,t}(\alpha)]$ and $\hat{\mathbf{Z}}_{2,t} = \mathbb{1}[Y_{2,t} < \hat{V}_{2,t}(\alpha)]$. To test for up-to-up risk causality, we set $\hat{\mathbf{Z}}_{1,t} = \mathbb{1}[Y_{1,t} > \hat{V}_{1,t}(1 - \alpha)]$ and $\hat{\mathbf{Z}}_{2,t} = \mathbb{1}[Y_{2,t} > \hat{V}_{2,t}(1 - \alpha)]$. The intuition is that if $\{Y_{2,t}\}$ Granger cause $\{Y_{1,t}\}$ in the upside (downside) risk, the cross-correlation between their upside (downside) risky quantiles would be nontrivial. In a similar vein, we can study negative risk causality effects by using the inversed relations. For down-to-up risk causality, we follow [Du and He \(2015\)](#) to set $\hat{\mathbf{Z}}_{1,t} = \mathbb{1}[Y_{1,t} > \hat{V}_{1,t}(1 - \alpha)]$ and $\hat{\mathbf{Z}}_{2,t} = \mathbb{1}[Y_{2,t} < \hat{V}_{2,t}(\alpha)]$; for up-to-down risk causality, we set $\hat{\mathbf{Z}}_{1,t} = \mathbb{1}[Y_{1,t} < \hat{V}_{1,t}(\alpha)]$ and $\hat{\mathbf{Z}}_{2,t} = \mathbb{1}[Y_{2,t} > \hat{V}_{2,t}(1 - \alpha)]$. In our analyses, we consider risk level $\alpha = 1\%$ which equals to studying the 99%-VaR — the typical regulatory reporting requirement. Besides, the 99%-VaR is also widely used in empirical study. For instance, [Dias \(2013\)](#) focuses on the same level to study the role of market capitalisation in the estimation of financial risk. Finally, the causality-in-distribution test of [Candelon and Tokpavi \(2016\)](#) considers a set $\mathbf{A} = \{\alpha_1, \dots, \alpha_{n+1}\}$ of $n+1$ risk levels covering the distribution support of $\hat{F}(\cdot)$. For $i = 1, 2$, the event variable $\hat{\mathbf{Z}}_{i,t}$ is a n -dimensional column vector, where its s -th

element is given by $\hat{Z}_{i,t,s} = \mathbb{1}[\hat{V}_{i,t}(\alpha_s) \leq Y_{i,t} < \hat{V}_{i,t}(\alpha_{s+1})]$, $s = 1, \dots, n$. Given that distribution tails are studied by the causality-in-risk tests, we now cover the centre of the distribution by setting $A = \{20\%, 40\%, 60\%, 80\%\}$, which examines long-run causality according to [Candelon and Tokpavi \(2016\)](#). It is worth highlighting that the causality-in-distribution test also acts as a filter that captures any remaining causal links including nonlinear relations.

Because the Chinese stock market closes before the price of global crude oil is marked and off-market trading is not a common practice in China, instantaneous causal effects from the Chinese market to crude oil should be studied. More precisely, international data providers such as *Datastream* mark the daily Brent oil price at 4:30pm [Greenwich Mean Time (GMT) + 00:00] during the winter season and at 3:30pm (GMT + 01:00) during the summer season, whereas the equity markets in mainland China close at 3:00pm (GMT + 08:00) with strict restriction on off-market trading. Hence, it is natural to study instantaneous Granger causality from the oil-intensive sectors in China to global crude oil. This is achieved by considering lag 0 in the CCF in (3.4)

$$\hat{Q}(Y_{2,t} \Rightarrow Y_{1,t}) = \frac{T \sum_{j=0}^{T-2} k^2(j/M) \text{vec}[\hat{\mathbf{R}}(j)]' (\hat{\mathbf{\Gamma}}_2^{-1} \otimes \hat{\mathbf{\Gamma}}_1^{-1}) \text{vec}[\hat{\mathbf{R}}(j)] - n^2 C_T(M)}{[n^2 D_T(M)]^{1/2}}. \quad (3.7)$$

The instantaneous Granger causality test statistic $\hat{Q}(Y_{2,t} \Rightarrow Y_{1,t})$ has the same asymptotic properties as $\hat{Q}(Y_{2,t} \rightarrow Y_{1,t})$. Therefore, inferences for both causality directions can be drawn based on the same limiting critical value. Throughout our empirical analysis, we use the Daniell kernel $k(x) = \sin(\pi x)/\pi x$ because it enjoys optimal power under appropriate conditions as shown in [Hong \(1996\)](#); we set the truncation parameter $M = \lceil 1.5T^{0.3} \rceil$ following [Candelon and Tokpavi \(2016\)](#).

3.4 Data

We analyse Granger causality between global crude oil and the Chinese oil-intensive sectors using daily observations from January 2005 to December 2019. We focus on the agricultural, construction, industrial and transportation sectoral indices published by the Shenzhen stock exchange, which is the larger of the two equity markets in China (the other being the Shanghai stock exchange) by number of listed companies and by trading volume. Besides, the fact that the Shenzhen stock exchange publishes all the indices that are required by this study is not surprising because Shanghai is a financial hub whereas Shenzhen is well-known for its industrialised entrepreneurial companies. Indeed, the major composition of the Shanghai stock exchange is financial companies whereas that of the Shenzhen stock exchange is industrial manufacturing companies. Regarding crude oil, we use daily Brent spot price for its global representativeness since it is the benchmark for more than two-thirds of all international crude oil contracts. It is therefore not a surprise that Brent is often the first choice when studying international crude oil in the literature. For instance, it is used as the main proxy for global oil in [Bouri \(2015\)](#); [Bouri et al. \(2016\)](#); [Chen and Lv \(2015\)](#);

Peng et al. (2018). To account for the effect of inflation, we deflate the nominal crude oil price and equity indices by the monthly consumer price index (CPI) in the US and China, respectively. The American CPI is reported by the Bureau of Labor Statistics, whereas the Chinese CPI is provided by the Organisation for Economic Co-operation and Development. All data are obtained through *Datastream*. Return series are calculated by taking the first difference of the inflation adjusted price indices in natural logarithm. For notational simplicity, we denote by CO_t , AG_t , CON_t , IND_t and TRP_t the return series of crude oil, agricultural, construction, industrial and transportation indices, respectively.

Considering possible structural change in causal links and the fact that information spillover between international markets is not constant over time, we divide our sample by two key events: the US subprime financial crisis in 2008 and the Chinese oil reform in 2013. Particularly, we select 15 September 2008 and 27 March 2013, which correspond to, respectively, the day Lehman Brothers filed for Chapter 11 protection and the date China launched its major domestic refined oil pricing mechanism reformation. First, we truncate our full sample by one year before and after the two key dates to yield three subsamples. Then, we increase the length of each subsample with the guidance from unit root and stationarity examinations to minimise the loss of information.³ Our first subsample runs from 3 January 2005 to 10 October 2007, covering the pre-crisis period. The second subsample spans from 7 October 2008 to 17 May 2012, consisting of the post-crisis period. The third subsample runs from 28 March 2013 to 31 December 2019, which reflects the effects of China's domestic oil pricing reform. Overall, our setup allows the study of possible changes in the market linkages after each key event.

Table 3.1 summarises the daily return series of Brent crude oil and the ICAT sectors in China. Before the oil reform, all variables exhibit positive mean returns; in the post-reform period, CO_t , CON_t and IND_t yield negative mean return. On average, the Chinese ICAT industries and CO_t display larger unconditional variance after the financial crisis, and the volatility reduces after the oil reform. All series exhibit negative skewness and heavy tails except for CO_t which becomes positively skewed after the oil reform. Not surprisingly, the Jarque and Bera (1980) (JB) test statistics suggest that all return variables are not normally distributed. We reject the null hypothesis of a unit root for all series at every standard significance level using the Augmented Dickey and Fuller (1979) (ADF) and Phillips and Perron (1988) (PP) tests. Additionally, the Kwiatkowski et al. (1992) (KPSS) test suggests that all return variables are stationary for each subsample. The optimal number of lagged difference terms for the ADF test and the optimal autocovariance lag order for the PP and KPSS tests are independently selected based on SBIC up to order $\lceil T^{0.5} \rceil$.

3.5 Results

In this section, we report the model estimates and causality analysis results for each subperiods. All specifications are estimated using Kevin Sheppard's Matlab MFE Toolbox.

³We thank an anonymous referee for this suggestion.

Table 3.1 Descriptive statistics

	Mean	Std.	Skew.	Kur.	JB	ADF	PP	KPSS	<i>T</i>
<i>Pre-crisis (3 January 2005 – 10 October 2007)</i>									
CO_t	0.08	1.88	-0.07	3.37	4.73*	-27.91***	-27.95***	0.07	723
AG_t	0.15	2.04	-0.58	5.16	180.96***	-25.24***	-25.27***	0.11	723
CON_t	0.24	2.25	-0.62	5.50	234.81***	-24.78***	-24.81***	0.04	723
IND_t	0.18	1.87	-0.60	5.81	281.89***	-25.40***	-25.43***	0.06	723
TRP_t	0.15	1.87	-0.75	7.12	581.01***	-26.10***	-26.14***	0.06	723
<i>Post-crisis (7 October 2008 – 17 May 2012)</i>									
CO_t	0.02	2.49	0.00	10.41	2159.00***	-31.69***	-31.73***	0.12	943
AG_t	0.06	2.12	-0.33	3.99	55.70***	-28.64***	-28.67***	0.03	943
CON_t	0.11	2.15	-0.58	5.03	213.57***	-27.90***	-27.93***	0.04	943
IND_t	0.04	1.96	-0.39	4.84	156.87***	-28.62***	-28.65***	0.04	943
TRP_t	0.00	1.77	-0.79	5.57	357.97***	-30.75***	-30.79***	0.05	943
<i>Post-reform (28 March 2013 – 31 December 2019)</i>									
CO_t	-0.03	2.00	0.32	5.94	664.04***	-41.00***	-41.02***	0.07	1764
AG_t	0.04	1.86	-0.73	6.66	1140.93***	-39.12***	-39.14***	0.06	1764
CON_t	-0.02	1.78	-0.92	6.68	1246.37***	-38.18***	-38.20***	0.06	1764
IND_t	-0.00	1.72	-1.01	7.68	1910.78***	-38.61***	-38.63***	0.07	1764
TRP_t	0.01	1.90	-1.11	8.40	2508.84***	-38.21***	-38.23***	0.06	1764

NOTES: This table reports the descriptive statistics for all variables. CO_t represents global crude oil daily return. AG_t , CON_t , IND_t and TRP_t are, respectively, the daily agricultural, construction, industrial and transportation sectoral returns in China. Std., Skew., and Kur. are standard deviation, skewness and kurtosis, respectively. JB is the Jarque and Bera (1980) test statistic for normality under the null hypothesis. ADF and PP are, respectively, the Augmented Dickey and Fuller (1979) and Phillips and Perron (1988) test statistics; both assess the null hypothesis of a unit root. KPSS is the Kwiatkowski et al. (1992) test statistic for stationarity under the null hypothesis. The optimal number of lagged difference terms for the ADF test and the optimal number of autocovariance lags for the PP and KPSS tests are selected (up to $\lceil T^{0.5} \rceil$) based on SBIC. The significance levels of all statistical tests are abbreviated with asterisks: ***, **, and * indicate statistical significance at the 1%, 5%, and 10% level, respectively. *T* denotes the number of observations.

3.5.1 Model estimates

Table 3.2 reports the model estimations and diagnostic analyses for the pre-crisis sample. Regarding mean equations, the parsimonious ARX(1) is suggested for all return series. Except for AG_t and CON_t , the constant terms of all other return variables are significant. As expected, the estimated autoregressive coefficients for all equations are statistically significant and are smaller than one in absolute value. The latter outcome suggests that the mean stationarity condition is satisfied. We observe that most of the day dummies are significant, which highlight the importance to control for the day-of-the-week effects.

The suggested model for the variance equation of CO_t and AG_t is GJR-GARCH(1, 1), whereas that of CON_t , IND_t and TRP_t is GARCH(1, 1). All of the estimated parameters are significant at the 1% level and satisfy the requirement for a stationary variance process. Besides, the selected

models capture well the volatility clustering property of return series as suggested by a relatively large GARCH coefficient that ranges from 0.706 to 0.978. We observe a positive estimate for the asymmetric term in the variance equation for CO_t , implying that past negative news have higher impact on the current variance of Brent crude than positive ones. This is known as the leverage effect. Interestingly, the opposite relation is found for AG_t , though this phenomenon is not uncommon in the agricultural sector (see, e.g., [Silvennoinen and Thorp, 2016](#); [Zhang et al., 2018](#)). In terms of probability densities, the skewed-t distribution is suggested for all variables with reasonable parameter estimates. For instance, the degree of freedom coefficient η is larger than 4, which implies excess kurtosis. The estimated skewness parameter λ yields negative values, suggesting asymmetric distribution that has a longer left tail. These parameter estimates are consistent with the stylised fact that most financial returns are negatively skewed and exhibit heavy tails.

We report a range of diagnostic test statistics at the bottom panel in [Table 3.2](#) that plays a pivotal role to the reliability of our subsequent causality study. We compute the [Ljung and Box \(1978\)](#) test statistic on the standardised residuals (LB) and the squared standardised residuals (LB^2) to find that for both innovation series, we cannot reject the null hypothesis of no autocorrelation up to the 15th lag order, which is approximately the largest order of the causality tests. This diagnostic result suggests that our mean and variance equations successfully capture the serial dependence in the first and second moments of all return variables. The former outcome is important for the causality-in-mean study, whereas the latter result is essential for the variance causality analysis. We carry out the [Kupiec \(1995\)](#) (Ku) test to ensure that the fitted density functions adequately describe the empirical distribution of the return series. Under the null hypothesis, we have that the estimated probability of occurrence within a distribution range ($x\%$, $y\%$) is equal to the theoretical frequency. We find that we cannot reject the null at the lower (0%, 1%) and upper tails (99%, 100%), and at the centre (20%, 80%) of the estimated densities. The former result is essential for the extreme risk causality analysis, whereas the latter outcome is important for the causality-in-distribution study. To further demonstrate that our distributional modellings are appropriate and adequate, we perform the Pearson Chi-squared (χ^2) examination as an independent misspecification diagnosis.⁴ The Pearson Chi-squared test checks the null hypothesis of a correctly specified distribution, and the test accounts for the entire distributional support. We find that we cannot reject the test at the usual significance level for each series. This double validation provides further statistical justifications for our distributional modellings.

[Table 3.3](#) reports the model estimations and diagnostic tests for the post-crisis period. The ARX(1) process is selected for the mean equation of AG_t , CON_t and TRP_t , whereas CO_t and IND_t are adequately described by ARX(7) and ARX(4), respectively. For brevity and to save space, only the first order coefficient is reported. Consistent with the pre-crisis sample, we observe that most of the right hand side variables are statistically significant. Regarding variance equations, the

⁴We thank an anonymous referee for this comment.

EGARCH(1, 1) is suggested for CO_t while AG_t requires the higher order GJR-GARCH(3, 3). The GARCH(1, 1) is selected for all other variables. The estimated negative asymmetric term in the GJR-GARCH modelling of AG_t is consistent with the pre-crisis sample. Similarly, the leverage effect in CO_t is also consistent with the pre-crisis period, as implied by a negative asymmetric parameter estimate in the EGARCH model. The first order GARCH coefficient for AG_t has a low estimate because the dynamic is largely captured by the third order coefficient with an estimate of 0.632. For all return variables, the skewed-t distribution provides a better fit with parameter estimates that reflect heavy tails and negative skewness, consistent with the pre-crisis sample. Diagnostic test results confirm the adequacy of our model parametrisations.

Table 3.4 reports the model estimates and diagnoses for the post-reform sample. The ARX(1) mean equation is selected for CO_t and AG_t , whereas the ARX(8), ARX(4) and ARX(6) are suggested for, respectively, CON_t , IND_t and TRP_t . The EGARCH(1, 1) with GED is suggested for CO_t while the EGARCH(1, 1) with skewed-t distribution is selected for TRP_t . The GARCH(1, 1) with skewed-t distribution is fitted to all other return series. We observe leverage effect for TRP_t , where the effect also persists in CO_t . The estimated GED shape parameter γ of CO_t lies between one and two, suggesting excess kurtosis. This is consistent with all other subperiods. The stylised features of the remaining variables such as volatility clusters, heavy tails and negative skewness are also well captured by the suggested models. Diagnostic results further support the selected specifications.

To sum up, our model parametrisations capture many stylised features of the data in the mean, variance, extreme quantiles and the distribution. Most of the estimated parameters are reasonable and significant. A series of diagnostic analyses suggest that the selected models are adequately specified, which are essential to the reliability of our subsequent causality study.

3.5.2 Causality results

Given the model estimates, we conveniently compute the event variables for each Granger causality hypothesis. Then, we compute the corresponding test statistics using the closed-form expressions given by (3.4) and (3.7). Inferences are drawn based on the asymptotic upper-tailed critical values of $N(0, 1)$ distribution at the standard significance levels. We report the causality analysis results for all subperiods in Table 3.5. The test statistics are not reported because they do not add to our conclusions. Instead, we report the statistical significance of each causality analysis.

We begin with the pre-crisis sample that spans from 3 January 2005 to 10 October 2007. We observe that the Chinese ICAT sectors Granger cause global crude oil in the mean, and the results are statistically significant at the 1% level. We note that the variance causality test of Hong (2001) is based on analysis that is not affected by causal relation from the mean equation. Hence, for the testing of variance causality, we pre-filter any relations in mean by including the lagged causing term (instantaneous version for ICAT causing terms) when estimating the mean equation of the caused term. Our modellings are then re-examined using the LB and LB^2 tests to ensure adequacy. We observe significant bidirectional causality in variance between the ICAT sectors and crude oil.

Table 3.2 Model estimations and diagnostics

	CO_t	AG_t	CON_t	IND_t	TRP_t
	ARX	ARX	ARX	ARX	ARX
	GJR-GARCH	GJR-GARCH	GARCH	GARCH	GARCH
<i>Pre-crisis (3 January 2005 – 10 October 2007)</i>					
<i>Mean equation</i>					
Constant	0.335***	0.027	0.004	0.123***	0.059***
AR(1)	-0.039***	0.054***	0.071***	0.044***	0.020***
d_1	-0.570***	0.350***	0.658***	0.437***	0.411***
d_2	-0.282***	0.207***	0.199***	0.083**	0.118***
d_3	-0.421***	0.091*	0.348***	-0.054	0.045
d_4	0.007	-0.064	-0.098*	-0.208***	-0.116***
<i>Variance equation</i>					
Constant	0.032***	0.163***	0.736***	0.065***	0.089***
ARCH(1)	0.000***	0.162***	0.156***	0.069***	0.084***
Asymmetric term	0.022***	-0.111***			
GARCH(1)	0.978***	0.870***	0.706***	0.918***	0.897***
GED γ					
Skewed-t η	23.507	5.230***	5.503***	4.532***	4.261***
Skewed-t λ	-0.078***	-0.180***	-0.128***	-0.101***	-0.085***
<i>Diagnostics</i>					
LB(10)	5.18	4.36	3.19	6.10	11.19
LB(15)	8.06	8.36	4.42	11.37	18.85
LB ² (10)	7.93	6.27	6.86	5.21	3.51
LB ² (15)	18.21	15.31	10.02	9.81	4.94
Ku(0, 1%)	0.77	0.22	0.01	0.41	0.97
Ku(20%, 80%)	1.11	0.16	0.16	1.11	0.22
Ku(99%, 100%)	0.77	0.77	0.77	0.77	1.73
Pearson χ^2	2.25	1.75	1.54	3.33	3.13

NOTES: This table reports the model estimations and diagnostic analyses for all variables. CO_t represents global crude oil daily return. AG_t , CON_t , IND_t and TRP_t are, respectively, the daily agricultural, construction, industrial and transportation sectoral returns in China. d_i is the day dummy, $i = 1, 2, 3, 4$. γ is the shape parameter of the GED. η and λ are, respectively, the degree of freedom and skewness parameters of the skewed-t distribution. LB(M) and LB²(M) are the Ljung and Box (1978) test statistics for the null of no serial correlation (up to lag M) on the standardised and squared standardised residuals, respectively. Ku($x\%$, $y\%$) is the Kupiec (1995) test statistic for correct proportion of return occurrence within the distribution range ($x\%$, $y\%$) under the null hypothesis. The Pearson χ^2 test statistic checks the null hypothesis of a correctly specified distribution. The significance levels of all model estimates and diagnostic tests are abbreviated with asterisks: ***, **, and * indicate statistical significance at the 1%, 5%, and 10% level, respectively.

The downside risk of CON_t , IND_t and TRP_t causes the downside risk of CO_t , whereas the upside risk of TRP_t and CO_t affects each other. Interestingly, the downside risk of CON_t , IND_t and TRP_t also causes the upside risk of CO_t . There is no evidence of up-to-down risk spillover between the

Table 3.3 Model estimations and diagnostics

	CO_t	AG_t	CON_t	IND_t	TRP_t
	ARX	ARX	ARX	ARX	ARX
	EGARCH	GJR-GARCH	GARCH	GARCH	GARCH
<i>Post-crisis (7 October 2008 – 17 May 2012)</i>					
<i>Mean equation</i>					
Constant	0.198***	0.442***	0.200***	0.223***	0.186***
AR(1)	-0.025***	0.072***	0.092***	0.069***	0.001
d_1	-0.230***	-0.569***	-0.225***	-0.398***	-0.382***
d_2	0.018	-0.329***	-0.044	-0.063*	-0.065**
d_3	-0.086*	-0.535***	-0.197***	-0.319***	-0.276***
d_4	-0.439***	-0.484***	-0.051	-0.120***	-0.192***
<i>Variance equation</i>					
Constant	0.011***	0.551***	0.148***	0.117***	0.079***
ARCH(1)	0.085***	0.149***	0.088***	0.063***	0.060***
Asymmetric term	-0.024***	-0.034***			
GARCH(1)	0.993***	0.000***	0.878***	0.902***	0.913***
GED γ					
Skewed-t η	7.569***	17.991	9.542	7.890**	5.971***
Skewed-t λ	-0.046***	-0.141***	-0.179***	-0.148***	-0.247***
<i>Diagnostics</i>					
LB(10)	10.02	7.03	9.25	9.88	15.58
LB(15)	11.84	10.11	15.49	19.89	20.25
LB ² (10)	6.33	9.13	7.58	11.48	11.53
LB ² (15)	9.04	15.97	21.85	16.64	15.68
Ku(0, 1%)	0.21	0.27	1.28	0.04	0.27
Ku(20%, 80%)	0.06	0.24	0.00	0.01	0.00
Ku(99%, 100%)	0.66	0.04	1.40	0.66	0.66
Pearson χ^2	3.87	3.44	6.52	2.65	3.70

NOTES: This table reports the model estimations and diagnostic analyses for all variables. CO_t represents global crude oil daily return. AG_t , CON_t , IND_t and TRP_t are, respectively, the daily agricultural, construction, industrial and transportation sectoral returns in China. Higher order coefficients for the mean and variance equations are not shown for brevity. d_i is the day dummy, $i = 1, 2, 3, 4$. γ is the shape parameter of the GED. η and λ are, respectively, the degree of freedom and skewness parameters of the skewed-t distribution. LB(M) and LB²(M) are the [Ljung and Box \(1978\)](#) test statistics for the null of no serial correlation (up to lag M) on the standardised and squared standardised residuals, respectively. Ku($x\%$, $y\%$) is the [Kupiec \(1995\)](#) test statistic for correct proportion of return occurrence within the distribution range ($x\%$, $y\%$) under the null hypothesis. The Pearson χ^2 test statistic checks the null hypothesis of a correctly specified distribution. The significance levels of all model estimates and diagnostic tests are abbreviated with asterisks: ***, **, and * indicate statistical significance at the 1%, 5%, and 10% level, respectively.

ICAT industries and international oil. We observe feedback causality between the distribution of global crude oil and the ICAT sectors.

Table 3.4 Model estimations and diagnostics

	CO_t	AG_t	CON_t	IND_t	TRP_t
	ARX	ARX	ARX	ARX	ARX
	EGARCH	GARCH	GARCH	GARCH	EGARCH
<i>Post-reform (28 March 2013 – 31 December 2019)</i>					
<i>Mean equation</i>					
Constant	0.071***	-0.044***	0.055***	0.026***	0.092***
AR(1)	0.022***	0.068***	0.090***	0.082***	0.091***
d_1	0.052**	-0.141***	-0.307***	-0.260***	-0.265***
d_2	-0.119***	0.052***	-0.132***	-0.049***	-0.126***
d_3	-0.223***	0.206***	-0.024*	0.054***	-0.138***
d_4	-0.223***	0.284***	0.111***	0.116***	0.123***
<i>Variance equation</i>					
Constant	0.006***	0.029***	0.038***	0.026***	0.026***
ARCH(1)	0.064***	0.084***	0.069***	0.067***	0.170***
Asymmetric term	-0.054***				-0.003***
GARCH(1)	0.998***	0.916***	0.922***	0.926***	0.988***
GED γ	1.271***				
Skewed-t η		4.397***	4.493***	4.731***	4.341***
Skewed-t λ		-0.112***	-0.154***	-0.155***	-0.164***
<i>Diagnostics</i>					
LB(10)	10.84	6.08	4.82	10.47	15.19
LB(15)	17.32	12.61	6.28	15.34	19.77
LB ² (10)	3.40	9.81	7.66	9.38	9.10
LB ² (15)	6.29	14.16	9.53	11.59	12.28
Ku(0, 1%)	0.14	1.05	0.64	1.55	0.64
Ku(20%, 80%)	1.00	0.03	0.18	0.01	0.99
Ku(99%, 100%)	0.40	2.00	2.00	2.00	1.31
Pearson χ^2	0.53	0.15	0.38	4.02	1.29

NOTES: This table reports the model estimations and diagnostic analyses for all variables. CO_t represents global crude oil daily return. AG_t , CON_t , IND_t and TRP_t are, respectively, the daily agricultural, construction, industrial and transportation sectoral returns in China. Higher order coefficients for the mean and variance equations are not shown for brevity. d_i is the day dummy, $i = 1, 2, 3, 4$. γ is the shape parameter of the GED. η and λ are, respectively, the degree of freedom and skewness parameters of the skewed-t distribution. $LB(M)$ and $LB^2(M)$ are the [Ljung and Box \(1978\)](#) test statistics for the null of no serial correlation (up to lag M) on the standardised and squared standardised residuals, respectively. $Ku(x\%, y\%)$ is the [Kupiec \(1995\)](#) test statistic for correct proportion of return occurrence within the distribution range ($x\%$, $y\%$) under the null hypothesis. The Pearson χ^2 test statistic checks the null hypothesis of a correctly specified distribution. The significance levels of all model estimates and diagnostic tests are abbreviated with asterisks: ***, **, and * indicate statistical significance at the 1%, 5%, and 10% level, respectively.

During the 2005–2007 period, the Chinese economy was developing at a rapid rate with an average annual GDP growth of 12.8%.⁵ The strong economic growth drove the consumption of oil,

⁵Data Source: World Bank.

Table 3.5 Causality results

	Mean	Variance	Risk D-to-D	Risk U-to-U	Risk D-to-U	Risk U-to-D	Distribution
<i>Pre-crisis (3 January 2005 – 10 October 2007)</i>							
$\hat{Q}(CO_t \rightarrow AG_t)$		***					***
$\hat{Q}(CO_t \rightarrow CON_t)$		***					***
$\hat{Q}(CO_t \rightarrow IND_t)$		***					***
$\hat{Q}(CO_t \rightarrow TRP_t)$		***		***			***
$\hat{Q}(AG_t \Rightarrow CO_t)$	***	***					***
$\hat{Q}(CON_t \Rightarrow CO_t)$	***	***	***		***		***
$\hat{Q}(IND_t \Rightarrow CO_t)$	***	***	***		***		***
$\hat{Q}(TRP_t \Rightarrow CO_t)$	***	***	***	***	***		***
<i>Post-crisis (7 October 2008 – 17 May 2012)</i>							
$\hat{Q}(CO_t \rightarrow AG_t)$		***		***		*	***
$\hat{Q}(CO_t \rightarrow CON_t)$		***					***
$\hat{Q}(CO_t \rightarrow IND_t)$		***					***
$\hat{Q}(CO_t \rightarrow TRP_t)$	*	***					***
$\hat{Q}(AG_t \Rightarrow CO_t)$	***	***		***			***
$\hat{Q}(CON_t \Rightarrow CO_t)$	***	***					***
$\hat{Q}(IND_t \Rightarrow CO_t)$	***	***					***
$\hat{Q}(TRP_t \Rightarrow CO_t)$	***	***					***
<i>Post-reform (28 March 2013 – 31 December 2019)</i>							
$\hat{Q}(CO_t \rightarrow AG_t)$		***	*	**		**	***
$\hat{Q}(CO_t \rightarrow CON_t)$		***			***	*	***
$\hat{Q}(CO_t \rightarrow IND_t)$		***			**		***
$\hat{Q}(CO_t \rightarrow TRP_t)$	*	***			***	***	***
$\hat{Q}(AG_t \Rightarrow CO_t)$	*	***					***
$\hat{Q}(CON_t \Rightarrow CO_t)$		***					***
$\hat{Q}(IND_t \Rightarrow CO_t)$		***					***
$\hat{Q}(TRP_t \Rightarrow CO_t)$		***		*			***

NOTES: This table reports the causality analysis results. CO_t represents global crude oil daily return. AG_t , CON_t , IND_t and TRP_t are, respectively, the daily agricultural, construction, industrial and transportation sectoral returns in China. $\hat{Q}(Y_t \rightarrow X_t)$ is the Granger causality test that examines the null hypothesis that $\{X_t\}$ does not cause $\{Y_t\}$. $\hat{Q}(Y_t \Rightarrow X_t)$ is the instantaneous Granger causality test that examine the null hypothesis that $\{X_t\}$ does not cause $\{Y_t\}$ contemporaneously. D-to-D, U-to-U, D-to-U and U-to-D denote, respectively, down-to-down, up-to-up, down-to-up and up-to-down risk causality. The significance levels of all tests are abbreviated with asterisks: ***, **, and * indicate statistical significance at the 1%, 5%, and 10% level, respectively. For brevity, only the statistical significance of the test results are reported.

especially in the oil-intensive sectors. This explains the ICAT industries' influence in the mean of international crude oil. Our finding agrees with He et al. (2010), who find that major economic activity affects global oil. Next, we find evidence of bidirectional volatility spillover between crude oil and the ICAT sectors. Because the ICAT industries and international crude oil depend heavily

on each other, an increase in uncertainty of one market would inevitably affect the other. We find downside risk spillover from the majority of the oil-intensive sectors (construction, industrial and transportation) to crude oil. An extreme negative return in a particular industry could be a signal of low demand for the sector's finished products. This reduces energy consumption and oil import, which in turn drive down international oil price. Our finding agrees with [Du and He \(2015\)](#) based on aggregate US data. Interestingly, the downside risk of the construction, industrial and transportation sectors also Granger causes the upside risk of crude oil. This phenomenon is largely driven by government intervention. In 2007, China suffered from high inflation as a result of the overheated domestic economic growth and the price increase in imported food ([Giles, 2008](#)). This had adverse impact on the major sectors in the economy. To reduce inflation and prevent social instability, the central government reduced oil tariffs and even offered subsidy for oil consumption. [Lin and Jiang \(2011\)](#) estimate that in 2007 alone, the oil subsidy in China amounted to CNY 189.03 billions, which is approximately equivalent to USD 24.87 billions at the average exchange rate of 7.6 CNY/USD in that year. This intervention — which cost nearly 0.8% of the country's economy — had aided to reduce prices of domestic goods but inevitably drove up international oil price according to the analysis by [Balke et al. \(2015\)](#). In terms of upside risk spillover, the only causal linkage exists between crude oil and the transportation sector, where the relation is bidirectional. In other words, the positive outlook in the oil and transportation market benefited each other. This is due to the rapid growth in China that stimulated the movement of people and goods. Together with a strong GDP growth, in two years time from 2005 to 2007, China expanded its highway by 7.13% and its aviation route by 18.78%.⁶ This ambitious expansion drove oil consumption and pushed for more crude oil import, which in turn increased the outlook of international oil. In the opposite direction, one might expect a positive outlook in international crude oil to adversely affect the oil-consuming transportation sector. On the contrary, we observe that the positive outlook in crude oil to have positively influenced the transportation industry. This positive effect can be explained by the heavy government fuel subsidy during this period as documented by [Lin and Jiang \(2011\)](#). In other words, the transportation sector in China enjoyed low cost government subsidised oil to support its expansion despite the rise in international oil price. Finally, our causality-in-distribution test results suggest long-run links between global oil and the ICAT industries. This finding is consistent with China's growing long-term demand for international oil in [Figure 3.1](#). From the perspective of econometrics, the existence of causality in any order of moment or quantile implies the more general causality in distribution, which is also reflected in our findings.

We now consider the post-crisis sample over the 7 October 2008 – 17 May 2012 period. Similar to the pre-crisis results, the ICAT sectors in China Granger cause crude oil in the mean. Besides, the bidirectional volatility spillover and long-run causality in the oil-ICAT nexus persist. There is marginal evidence that CO_t influences TRP_t in the mean, and that the upside risk of CO_t causes

⁶Data Source: China Statistical Yearbook.

the downside risk of AG_t . Regarding up-to-up risk causality, we have bidirectional effect between CO_t and AG_t . No down-to-down and down-to-up risk causality is found.

Despite the subprime crisis that affected most of the western economies, the Chinese GDP continued to grow at an average of 9.81% annually from 2008 to 2011.⁷ The strong persistence of economic activities provides explanation as to why the ICAT industries in China continued to Granger cause global crude oil in mean. Besides, China's demand for international oil continued to rise while other major economies such as the United States reduced its oil imports during the same period. This explains the continuation of bidirectional volatility spillover effects between global crude oil and the ICAT sectors. We find that the upside risk of global crude oil plays a key role in pushing the agricultural index upwards. As crude oil becomes more expensive, there is increasing demand for alternative energy sources such as biofuel which is derived from agricultural commodity. [Kristoufek et al. \(2012\)](#) find that the connection between biofuel and the agricultural products becomes more profound after the 2008 global food insecurity. This coincides with our findings and provides explanation for the driving forces behind the agricultural sector in China. Indeed, we learn from the Chinese Statistical Yearbook that from 2008 to 2010, the farmland area allocated for corn — the primary ingredient for ethanol biofuel — had increased by 12.90%, whereas the area allocated for its main staple rice had only increased by 2.55%. In the opposite direction, we find upside risk spillover from the Chinese agricultural sector to the global crude oil. For two years in a row from 2009 to 2010, the Chinese agricultural sector was badly hit by severe drought and flood that affected more than 16 million hectares of its farm land.⁸ This inevitably increases food prices and the upside risk of the agricultural industry in China. Consequently, the Chinese government had to rely on food import to feed the country. This naturally drove international energy consumption and global oil price. Our finding is consistent with [Silvennoinen and Thorp \(2016\)](#), who find that the global food and energy markets were especially integrated between 2008 and 2010 where the price levels of food and oil were high. Finally, the long-term relation between global crude oil and the ICAT industries is confirmed by our causality-in-distribution analyses.

We now discuss causality results for the post-reform sample from 28 March 2013 to 31 December 2019. Unlike previous periods, the mean causality effect from the ICAT sectors in China to crude oil is virtually nonexistent. We find marginal evidence that CO_t causes TRP_t in the mean. The bidirectional volatility spillover and long-run causality in the oil-ICAT nexus persist. We observe with marginal evidence downside risk spillover from CO_t to AG_t and upside risk spillover from TRP_t to CO_t . The upside risk spillover from CO_t to AG_t persists. In terms of inverse risk spillover, the downside risk of CO_t significantly causes the upside risk of CON_t , IND_t and TRP_t , whereas the upside risk of CO_t causes the downside risk of AG_t , CON_t and TRP_t .

Between 2014 and 2019, China's economy grew by an annual average of 6.85%, which saw a significant slowdown compared with its peak GDP growth of 14.23% in 2007.⁹ As a result, the

⁷Data Source: World Bank.

⁸Data Source: China Statistical Yearbook.

⁹Data Source: World Bank.

ICAT industries were unable to maintain the previous positive outlook and productivity, causing their explanatory power for the mean return of crude oil to fade during this period. Compared with the period where the GDP growth peaked, the weakened evidence of upside risk spillover from the transportation sector to crude oil is another indication of the economic slowdown. Although the ICAT sectors were slowing down, their dependence on international oil is however not zero. Therefore, uncertainty in one market still had nontrivial effects on the other. This provides explanation for the persistence of bidirectional volatility spillover and long-term causality in the oil-ICAT nexus. It is worth highlighting that China's demand for international oil was still on the rise despite the economic slowdown, which can be attributed to its plan of establishing a strategic national oil reserve (Zhou and Yep, 2019). The upside risk spillover from international oil to the agricultural sector persist as China continued to invest in renewable energy such as the biofuel. Indeed, the farmland area allocated for corn in China has been growing consistently since 2010 according to the Chinese Statistical Yearbook. Because a growing portion of farmland has been allocated for corn to make biofuel, a sharp decrease in the price of international crude oil would incur losses on this renewable industry since the price of biofuel are no longer competitive. This is why we observe marginal evidence of negative risk spillover from international crude oil to the agricultural sector. Interestingly, the negative outlook in the global oil market had a positive impact on the construction, industrial and transportation sectors. On several occasions between 2014 and 2016, international crude oil suffers from oversupply due to geopolitical rivalries and the invention of hydraulic fracking technology. This decreased oil price but increased the profit of most oil-consuming industries as they benefited from cheaper oil. On the other hand, most ICAT sectors were negatively affected when the global oil price was high due to increase in operational costs. This explains why the positive outlook in crude oil adversely affected most of the ICAT industries.

3.5.3 Implications for investors and policymakers

There are several implications that we can draw from the findings in this study that can contribute to future policymaking and investment management. First, we observe that the extreme impact from international crude oil on the Chinese ICAT sectors became more apparent after the major domestic oil pricing reformation in 2013. As the market-oriented pricing mechanism with minimal government intervention was introduced, the ICAT industries became, to a greater extent, exposed to international crude oil movement and the price risk that accompanied. This also provides explanation for the marginal influence of global oil on the mean of TRP_t . By the same rationale, it is worth mentioning that China introduced a preliminary oil pricing reform in 2009 that is of smaller scale than the 2013 counterpart. This posed nontrivial impact to certain local oil-intensive sectors. For instance, we observe marginal evidence that, for the 7 October 2008 – 17 March 2012 sample, global oil affected the transportation industry in the mean, and the positive outlook in oil began to adversely affect the agricultural sector. These findings shall advise policymakers to be

cautious in the future when implementing similar reformations because they may distort statistical relations on an international level.

Second, our study in the 3 January 2005 – 10 October 2007 sample reveals heavy oil subsidy by the Chinese government to deal with its overheated economy. From the perspective of policymaking, this had aided to reduce the prices of domestic goods but that came at a cost of nearly 0.8% of the country's economy. Besides, the government subsidy may be miss-used by some companies to increase their own private profit, which does not necessary help to ease the overheated economy. Moreover, as shown in [Balke et al. \(2015\)](#), such heavy oil subsidy is detrimental to the rest of the world because it drives international oil price. Thus, oil subsidy should be implemented with care and should only be used in extreme situations. Indeed, knowing that such policy is only a short-term alleviation, the Chinese government subsequently reduced to a great extent its fuel subsidy after 2008, as depicted in [Lin and Ouyang \(2014, Figure 2\)](#). This is a crucial step because according to our analysis, there exists significant long-term linkages between the ICAT sectors and international crude oil. Thus, our findings agree with the decision implemented by the Chinese policymakers and shall advise them to continue investing in long-term visions and solutions.

Finally, our findings suggest strong evidence of volatility spillover between the ICAT sectors and international crude oil. This should be viewed a healthy economic relation between the ICAT and oil markets because it implies that the market participants have been following each other closely due to the interdependent relation. As a result, uncertainty in one market would naturally propagate to the other market. For participants in the ICAT and oil markets, our analysis emphasises the importance of using hedging instruments to minimise investment losses that could arise from uncertainty in the opposite markets. For instance, the managing directors of international oil drilling companies are advised to invest in crude oil futures contracts should they wish to hedge against uncertainty in fuel price which could be a result of the volatile demand from the oil-intensive ICAT sectors. By taking short positions in the crude oil futures contracts, the directors are entitled to sell the companies' oil at a predetermined price in the future to avoid severe losses should fuel demand becomes uncertain. By the same reasonings, the farmland owners in China are advised to short corn futures should they wish to hedge against uncertainty in corn price which could be a result of volatile fuel price.

3.6 Conclusions

The paper analysed Granger causality between global crude oil and the sectoral equity index returns in China from 2005 to 2019. We unified the extensive Granger causality tests proposed over the past two decades that are based on the cross-correlation function approach to study causal relations in the mean, variance, risky quantiles and distribution. The paper focused on the industrial, construction, agricultural and transportation (ICAT) sectors as they are the country's primary oil consumers. Various stylised features in the data were captured by our modellings which were properly examined to ensure adequacy.

Main findings can be summarised as follows. First, volatility spillover and long-term dependence in the oil-ICAT nexus were confirmed throughout the sample by the causality-in-variance analysis and causality-in-distribution analysis, respectively. As for mean causality, results showed that the oil-intensive sectors in China affected international crude oil before 2013 when the country's economy was growing at a rapid rate; the effects faded after the economic growth slowed down. In terms of downside risk causality, extreme losses in the construction, industrial and transportation sectors negatively influenced international oil in the pre-crisis sample. No relation was found after the financial crisis. As for upside risk spillover, crude oil and the transportation industry affect each other in the pre-crisis sample partly due to the ambitious aviation route expansion. After 2008, the upside risk causality between the agricultural sector and international oil strengthened, which could be attributed to the global food insecurity. Regarding negative risk causality, the downside risk of the construction, industrial and transportation sectors caused the upside risk of international oil before 2009, which could be attributed to heavy government oil subsidy. After the major Chinese domestic refined oil pricing mechanism reform in 2013, it was found that the downside risk of global oil benefited most of the oil-intensive sectors and that the upside risk of international oil negatively influenced most ICAT industries. Overall, our analyses disentangled the complex oil-ICAT nexus to find that it had been nontrivially related to various factors such as demand and supply of oil, economic growth rate, government subsidies and local oil pricing reformation.

Market participants especially investors and policymakers may find the results of this paper useful. In particular, policymakers are advised to be cautious when implementing similar oil reformations in the future as they may distort statistical relations on an international level. Besides, policymakers are advised to invest in long-term solutions when dealing with an overheated economy because of the documented long-term relation between global oil and the ICAT industries. Finally, due to the persistent volatility spillover in the oil-ICAT nexus, investors are advised to use financial instruments such as futures contracts to hedge against uncertainty from the opposite markets.

CONCLUSIVE REMARKS AND FUTURE WORKS

This dissertation centred on the modelling and testing of risk with the emphasis on gauging novel issues in finance. Chapter 1 modelled the stability of financial system using prominent systemic risk measures, and tested for various risk factors affecting financial stability including the risky practice of shadow insurance. In Chapter 2, I proposed a new multivariate econometric strategy for examining the spillover of volatility — the most fundamental risk measure — and I applied it to study the North American and European financial markets. Chapter 3 consolidated the comprehensive literature on Granger causality methods, and applied the unified methodology to examine different components of risk spillover between international crude oil and the Chinese equity markets that are fuel intensive. In what follows I highlight the contributions and implications that we can draw from the results in this dissertation — covering the aspects of econometric methodology, finance, and policymaking — and I provide some discussions regarding future developments.

Methodological implications

This dissertation has several methodological implications and contributions. Chapter 1 compared and contrasted existing systemic risk measures to find that the delta conditional value-at-risk ($\Delta CoVaR$) and systemic risk measure ($SRISK$) were the more suitable methods in terms of capturing financial system risk since the marginal expected shortfall (MES) method captured largely the systematic risk. Next, based on a representative data universe of 215 insurance entities, the chapter provided a close empirical examination on $\Delta CoVaR$ and $SRISK$ to find that the extent to which the two measures react to financial distress varies. For instance, $\Delta CoVaR$ was more reactive to the US subprime crisis whereas the response from $SRISK$ was less profound. I conjectured that the difference was due to the distinct ways the two measures were constructed. For instance, although they are classed as systemic risk measures, $\Delta CoVaR$ is a function of value-at-risk whereas $SRISK$ is based on expected shortfall. Hence, the results in this chapter call for cautious future

implementations of the methods and whenever possible, the chapter suggests that both measures should be used for a rigour empirical analysis.

The application of systemic risk measures is limited to cases where the transmission or spillover of risk is unidirectional, therefore I proposed in Chapter 2 a new (bi)directional econometric method to examine volatility spillover — the most fundamental risk measure — between two potentially multivariate time series, where volatility spillover was defined using the notion of Granger causality in variance. The chapter further proposed a new nonparametric specification to facilitate the estimation of volatility and hence the computation of the test statistic. In terms of estimation, I proposed consistent least-squares estimators which are computationally efficient and are free from convergence issue. I developed the asymptotic theory of the new approach. Throughout the proposed econometric strategy, numerical integration and optimisation are not involved. An extensive simulation study showed that the proposed method performed reasonably well even in the higher dimension. Overall, the chapter contributes to the financial econometrics literature by providing a new and convenient inferential methodology for volatility spillover.

While volatility is considered the most fundamental risk measure, the causality literature had proposed other methods to capture different components of risk spillover. Chapter 3 unified the extensive literature on causality methods and demonstrated how various forms of spillover can be examined. This unified methodology can examine spillovers in the mean, variance, risky quantiles (both positive and negative) and distribution, where each element reveals a unique relation. The causality-in-mean analysis uncovers return spillover, whereas the presence of variance causality can be viewed as volatility spillover. The causality-in-risk analysis detects the existence of extreme risk spillovers and it covers both positive and negative relations. The long-term spillover effects can be evaluated by the causality-in-distribution examination. This unified methodology minimises inferential biases because all of the analyses are based on causality methods within the same family. Besides, the finite sample performance of this univariate methodology based on asymptotic critical values is generally reliable as reported in the mainstream literature. In summary, the chapter provides academics, investors, market participants and policymakers with a unified methodology to examine various components of risk spillover.

Implications in finance and policymaking

This dissertation has profound implications in finance and policymaking. In Chapter 1, I extracted the lesser-known shadow insurance dataset from the data universe of about 200,000 reinsurance agreements to find that the practice of shadow insurance had grown nearly 17 times from \$15 billion in 2004 to over \$250 billion in 2017. Second, I documented that about 2.8 cents every dollar ceded was shadow in 2004 and this figure had grown to 21 cents every dollar in 2017. Third, the chapter tabulated the key entities practising shadow insurance — the shadow insurers — by the dollar amount of shadow insurance and by a shadow index quantifying the aggressiveness of the practice. Fourth, I documented that shadow insurers are typically larger, riskier, more interconnected with

other market participants and more likely to contribute to financial instability. Naturally, the chapter hypothesised that the practice of shadow insurance affects financial stability. Finally, I tested the hypothesis using panel analysis and found statistical significant evidence that the practice of shadow insurance had indeed contributed to the spreading of systemic risk. Overall, these results have direct implications in the shadow banking and financial stability literature and call for new policies to regulate the risky practice of shadow insurance.

In Chapter 2, I proposed an econometric testing strategy that has practical applications in finance. The chapter included a timely empirical study in which I applied the new inferential strategy to examine, before and after the Brexit referendum, the spillover relations between the North American (NA) and the UK financial markets. To examine possible Brexit effect on the European Union (EU) market, I also studied its spillover relations with the NA market. Before the Brexit referendum, it was found that the NA was driven more immediately by UK volatility than EU volatility. After Brexit, it was found that volatility in the UK did not spill to NA while that in the EU had a more immediate spillover effect on NA as most NA participants switched their attention from the UK to the EU market because of the fear that UK might lose its access to the European Single Market. These findings have direct implications in the financial market literature by providing statistical evidence suggesting that the participants in key international financial markets have a reduced interest to follow the UK market after Brexit. In terms of policymaking, the chapter encourages UK policymakers to develop new policies aiming to bolster the confidence of overseas investors in the UK market as the starting step to retain the market's global influence. I shall emphasise that the applications of the proposed inferential strategy is not limited to the macro level financial markets. At the firm level, the proposed statistical tool can assist policymakers to identify volatility transmitters and recipients in the financial system and thus to shape targeted policy to protect vulnerable volatility recipient as individual or group whenever necessary.

In Chapter 3, I unified a series of Granger causality methodology that has practical applications in finance. I applied the unified methodology to study risk spillovers between international crude oil and the oil-intensive equity markets in China. The Chinese market is worth studying for a few reasons. First, I documented that since 2017, China had surpassed the US to become the top crude oil importer in the world with more than eight million barrels of crude oil imports per day. Second, the Chinese market had experienced a major government intervention. On 27 March 2013, the Chinese government launched a major reformation of its domestic refined oil pricing mechanism to greatly relax its control over local oil price. Generally regarded as the major milestone in the transformation to a market-oriented pricing of retail oil, this reform discourages the government from setting a ceiling price for domestic oil so long as international oil price stays under \$130 per barrel. My analysis suggested that, before the oil reform, the Chinese industries were not significantly affected by extreme international oil price movement. This was because domestic oil price in China was capped and strictly regulated by its central government. Consequently, the global oil price had a limited influence on the Chinese sectors. After the oil reform, I found that extreme negative returns of global oil benefit most oil-intensive sectors while positive outlook in

Brent adversely affect most the industries. These findings were driven by the fact that the Chinese markets had naturally become more exposed to international oil after the reformation. Therefore, an extreme negative (positive) outlook in global oil directly reduced (increased) the operational costs of the Chinese sectors. Hence, the findings in this chapter encourage policymakers to be cautious when implementing similar reformations in the future because they may distort statistical relations on an international level.

Further developments

Based on the results in this dissertation, several future works can be suggested. First, the inferential strategy that I put forward in Chapter 2 can be readily applied to the shadow insurance data that I collected in Chapter 1. Compared with the analysis in Chapter 1 which focuses on the effect from the mean, using the statistical tool from Chapter 2 the new study can focus on the effect from the volatility. Using the collected data, I can first form a vector containing key shadow insurers which can represent the *shadow insurance sector*. Since I documented in Chapter 1 that most of the shadow insurers are public entities, I can conveniently download their daily stock prices which are the main input of the methodology in Chapter 2. Because a large portion of shadow insurance is funded through the banking system, I formulate the following hypothesis.

Hypothesis 1. There is volatility spillover from the shadow insurance sector to the banking or financial sector.

Besides, it is important to check the relation between the shadow and the non-shadow sectors.

Hypothesis 2. There is volatility spillover from the shadow insurance sector to the non-shadow insurance sector.

As documented in Figure 1.5, the risk of shadow insurance is time varying. Hence, I propose to examine the possible time-varying spillover effects using rolling window method so long as I keep a rolling window of about four years of daily data, which is suggested by the Monte Carlo study in Chapter 2. Given the evidence in Figure 1.5, I formulate a further hypothesis.

Hypothesis 3. The spillover effect from the shadow insurance sector is the most significant in the run-up to the subprime crisis.

Addressing these hypotheses can make up a small but interesting research paper in the shadow banking literature.

Second, I can apply the set of Granger causality methods that I unified in Chapter 3 to study another set of commodity data. Because the unified methodology is able to detect possible negative causal relations, I can propose a thorough study to examine the nexus between international gold market and the leading global financial markets since it is often hypothesised that gold and equity are negative related. For instance, [Basher and Sadorsky \(2016\)](#) find that gold could be effective in

terms of hedging stock prices in the emerging markets. This research idea can form a small but interesting research paper in the commodity and financial market literature. Along the same line, I would like to note that the autoregressive conditional heteroskedasticity in mean (ARCH-in-mean) model is often recommended for commodity data given its relevance to the theory of storage. For instance, [Bernard et al. \(2015\)](#) find that on several occasions, the ARCH-in-mean model gives better forecast performances with respect to several other workhorse models based on oil futures data. Therefore, the ARCH-in-mean model is very much worth exploring in future works especially when it comes to forecast-based analysis of commodity futures data.

Third, I can put forward a new measure for financial market jump spillover which complements the volatility spillover approach in Chapter 2. To study financial jumps, I shall assume that asset prices (in logarithms) follow the conventional continuous jump-diffusion process

$$\begin{pmatrix} dp_{A,s} \\ dp_{B,s} \end{pmatrix} = \begin{pmatrix} \mu_{A,s} \\ \mu_{B,s} \end{pmatrix} ds + \begin{pmatrix} \sigma_{AA,s} & \sigma_{AB,s} \\ \sigma_{BA,s} & \sigma_{BB,s} \end{pmatrix} \begin{pmatrix} dW_{A,s} \\ dW_{B,s} \end{pmatrix} + \begin{pmatrix} \kappa_{AA,s} & \kappa_{AB,s} \\ \kappa_{BA,s} & \kappa_{BB,s} \end{pmatrix} \begin{pmatrix} dJ_{A,s} \\ dJ_{B,s} \end{pmatrix},$$

where $(\mu_{A,s}, \mu_{B,s})$ are predictable drift processes; $(W_{A,s}, W_{B,s})$ are standard Brownian motions; $(\sigma_{AA,s}, \sigma_{AB,s}, \sigma_{BA,s}, \sigma_{BB,s})$ follow a multivariate *càdlàg* process; $(J_{A,s}, J_{B,s})$ are Poisson processes with possibly time-varying intensity; $(\kappa_{AA,s}, \kappa_{AB,s}, \kappa_{BA,s}, \kappa_{BB,s})$ describe the sizes of jumps at time s .

It is natural to decompose the quadratic variation process $\langle \cdot, \cdot \rangle_t$ of a given asset price, say p_A , over the time interval $(t-1, t)$ into the part due to the discontinuous jump component $p_A^{(d)}$ and the part due to the continuous diffusive component $p_A^{(c)}$. In particular, $\langle p_A, p_A \rangle_t \equiv A_t = V_{A,t} + D_{A,t}$, where $V_{A,t} = \langle p_A^{(c)}, p_A^{(c)} \rangle_t = \int_{t-1}^t \sigma_{A,s}^2 ds + \int_{t-1}^t \sigma_{AB,s}^2 ds$ is the integrated variance over the time interval $(t-1, t)$ and $D_{A,t} = \langle p_A^{(d)}, p_A^{(d)} \rangle_t = \sum_{s=J_{A,t-1}}^{J_{A,t}} \kappa_{AA,s}^2 + \sum_{s=J_{B,t-1}}^{J_{B,t}} \kappa_{AB,s}^2$ corresponds to the jump contribution to the quadratic variation. Similarly, we have $\langle p_B, p_B \rangle_t \equiv B_t = V_{B,t} + D_{B,t}$, where $V_{B,t} = \langle p_B^{(c)}, p_B^{(c)} \rangle_t = \int_{t-1}^t \sigma_{B,s}^2 ds + \int_{t-1}^t \sigma_{BA,s}^2 ds$ and $D_{B,t} = \langle p_B^{(d)}, p_B^{(d)} \rangle_t = \sum_{s=J_{A,t-1}}^{J_{A,t}} \kappa_{BA,s}^2 + \sum_{s=J_{B,t-1}}^{J_{B,t}} \kappa_{BB,s}^2$. It is easy to appreciate from the above setup that A_t is not affected by $D_{B,\tau}$ for any $\tau \leq t$, denoted by $B \xrightarrow{D} A$, if and only if

- (i) $\kappa_{AB,s} = \kappa_{BA,s} = 0$ almost surely;
- (ii) $\kappa_{AB,s}$ and $\kappa_{BA,s}$ are independent; and
- (iii) $J_{A,s}$ and $J_{B,s}$ are independent.

If any of the above conditions fail to hold, then A_t remains dependent upon $D_{B,\tau}$, even after conditioning on its own past values. We have jump spillover from asset B to asset A . To quantify the effect of jump spillover, I can propose to quantify the extent to which (i)-(iii) are violated using proper dependence measures. By studying the limiting distribution of the proposed measures, I can put forward inferential procedures for the null hypothesis that (i)-(iii) hold (i.e., no jump spillover). This can form a research paper with methodological contribution.

BIBLIOGRAPHY

- Abedifar, P., Giudici, P., Hashem, S.Q., 2017. Heterogeneous market structure and systemic risk: Evidence from dual banking systems. *Journal of Financial Stability* 33, 96–119.
- Acharya, V., Engle, R., Richardson, M., 2012. Capital shortfall: A new approach to ranking and regulating systemic risks. *American Economic Review* 102, 59–64.
- Acharya, V., Pedersen, L.H., Philippon, T., Richardson, M., 2017. Measuring systemic risk. *Review of Financial Studies* 30, 2–47.
- Admati, A.R., Pfleiderer, P., 1988. A theory of intraday patterns: Volume and price variability. *Review of Financial Studies* 1, 3–40.
- Adrian, T., Brunnermeier, M.K., 2016. CoVaR. *American Economic Review* 106, 1705–1741.
- Aielli, G.P., 2013. Dynamic conditional correlation: On properties and estimation. *Journal of Business & Economic Statistics* 31, 282–299.
- Andrews, D.W., 1991. Heteroskedasticity and autocorrelation consistent covariance matrix estimation. *Econometrica*, 817–858.
- Antoine, B., Renault, E., 2012. Efficient minimum distance estimation with multiple rates of convergence. *Journal of Econometrics* 170, 350–367.
- Arghyrou, M.G., Tsoukalas, J.D., 2011. The Greek debt crisis: Likely causes, mechanics and outcomes. *The World Economy* 34, 173–191.
- Baele, L., 2005. Volatility spillover effects in European equity markets. *Journal of Financial and Quantitative Analysis* 40, 373–401.
- Bakshi, G., Kapadia, N., 2003. Delta-hedged gains and the negative market volatility risk premium. *Review of Financial Studies* 16, 527–566.
- Balke, N.S., Plante, M., Yücel, M., 2015. Fuel subsidies, the oil market and the world economy. *Energy Journal* 36.
- Bardgett, C., Gourier, E., Leippold, M., 2019. Inferring volatility dynamics and risk premia from the S&P 500 and VIX markets. *Journal of Financial Economics* 131, 593–618.
- Basher, S.A., Sadorsky, P., 2016. Hedging emerging market stock prices with oil, gold, VIX, and bonds: A comparison between DCC, ADCC and GO-GARCH. *Energy Economics* 54, 235–247.

- Bauer, D., Maynard, A., 2012. Persistence-robust surplus-lag Granger causality testing. *Journal of Econometrics* 169, 293–300.
- Benoit, S., Colletaz, G., Hurlin, C., Pérignon, C., 2013. A theoretical and empirical comparison of systemic risk measures. HEC Paris Research Paper No. FIN-2014-1030 .
- Benoit, S., Colliard, J.E., Hurlin, C., Pérignon, C., 2017. Where the risks lie: A survey on systemic risk. *Review of Finance* 21, 109–152.
- Bernard, J.T., Khalaf, L., Kichian, M., McMahon, S., 2015. The convenience yield and the informational content of the oil futures price. *Energy Journal* 36, 29–46.
- Bierth, C., Irresberger, F., Weiß, G.N., 2015. Systemic risk of insurers around the globe. *Journal of Banking & Finance* 55, 232–245.
- Billio, M., Getmansky, M., Lo, A.W., Pelizzon, L., 2012. Econometric measures of systemic risk in the finance and insurance sector. *Journal of Financial Economics* 104, 535–559.
- Bollerslev, T., 1986. Generalized autoregressive conditional heteroskedasticity. *Journal of Econometrics* 31, 307–327.
- Bollerslev, T., 1990. Modelling the coherence in short-run nominal exchange rates: A multivariate generalized ARCH model. *Review of Economics and Statistics* 72, 498–505.
- Bollerslev, T., Hood, B., Huss, J., Pedersen, L.H., 2018. Risk everywhere: Modeling and managing volatility. *Review of Financial Studies* 31, 2729–2773.
- Boudjellaba, H., Dufour, J.M., Roy, R., 1992. Testing causality between two vectors in multivariate autoregressive moving average models. *Journal of the American Statistical Association* 87, 1082–1090.
- Bouhaddioui, C., Roy, R., 2006. A generalized portmanteau test for independence of two infinite-order vector autoregressive series. *Journal of Time Series Analysis* 27, 505–544.
- Bouri, E., 2015. Return and volatility linkages between oil prices and the lebanese stock market in crisis periods. *Energy* 89, 365–371.
- Bouri, E., Awartani, B., Maghyereh, A., 2016. Crude oil prices and sectoral stock returns in Jordan around the Arab uprisings of 2010. *Energy Economics* 56, 205–214.
- Bouri, E., Chen, Q., Lien, D., Lv, X., 2017. Causality between oil prices and the stock market in China: The relevance of the reformed oil product pricing mechanism. *International Review of Economics & Finance* 48, 34–48.
- Broadstock, D.C., Cao, H., Zhang, D., 2012. Oil shocks and their impact on energy related stocks in China. *Energy Economics* 34, 1888–1895.
- Broadstock, D.C., Fan, Y., Ji, Q., Zhang, D., 2016. Shocks and stocks: a bottom-up assessment of the relationship between oil prices, gasoline prices and the returns of Chinese firms. *Energy Journal* 37.
- Broadstock, D.C., Filis, G., 2014. Oil price shocks and stock market returns: New evidence from the United States and China. *Journal of International Financial Markets, Institutions and Money* 33, 417–433.
- Brownlees, C., Engle, R.F., 2017. SRISK: A conditional capital shortfall measure of systemic risk. *Review of Financial Studies* 30, 48–79.

- Cai, J., Eidam, F., Saunders, A., Steffen, S., 2018. Syndication, interconnectedness, and systemic risk. *Journal of Financial Stability* 34, 105–120.
- Candelon, B., Tokpavi, S., 2016. A nonparametric test for Granger causality in distribution with application to financial contagion. *Journal of Business & Economic Statistics* 34, 240–253.
- Casarin, R., Sartore, D., Tronzano, M., 2018. A Bayesian markov-switching correlation model for contagion analysis on exchange rate markets. *Journal of Business & Economic Statistics* 36, 101–114.
- Chan, N.H., Deng, S.J., Peng, L., Xia, Z., 2007. Interval estimation of value-at-risk based on GARCH models with heavy-tailed innovations. *Journal of Econometrics* 137, 556–576.
- Chen, B., Hong, Y., 2012a. Testing for smooth structural changes in time series models via nonparametric regression. *Econometrica* 80, 1157–1183.
- Chen, B., Hong, Y., 2012b. Testing for the Markov property in time series. *Econometric Theory* 28, 130–178.
- Chen, B., Hong, Y., 2016. Detecting for smooth structural changes in GARCH models. *Econometric Theory* 32, 740–791.
- Chen, Q., Lv, X., 2015. The extreme-value dependence between the crude oil price and Chinese stock markets. *International Review of Economics & Finance* 39, 121–132.
- Cheung, Y.W., Ng, L.K., 1996. A causality-in-variance test and its application to financial market prices. *Journal of Econometrics* 72, 33–48.
- Coleman, T.F., LaPlante, A., Rubtsov, A., 2018. Analysis of the SRISK measure and its application to the Canadian banking and insurance industries. *Annals of Finance* 14, 547–570.
- Comte, F., Lieberman, O., 2000. Second-order noncausality in multivariate GARCH processes. *Journal of Time Series Analysis* 21, 535–557.
- Corradi, V., Distaso, W., Fernandes, M., 2012. International market links and volatility transmission. *Journal of Econometrics* 170, 117–141.
- Corradi, V., Distaso, W., Fernandes, M., 2019. Testing for jump spillovers without testing for jumps. *Journal of the American Statistical Association* , 1–52.
- Cumming, D.J., Zahra, S.A., 2016. International business and entrepreneurship implications of Brexit. *British Journal of Management* 27, 687–692.
- Dias, A., 2013. Market capitalization and Value-at-Risk. *Journal of Banking & Finance* 37, 5248–5260.
- Dickey, D.A., Fuller, W.A., 1979. Distribution of the estimators for autoregressive time series with a unit root. *Journal of the American Statistical Association* 74, 427–431.
- Diebold, F.X., Yilmaz, K., 2012. Better to give than to receive: Predictive directional measurement of volatility spillovers. *International Journal of Forecasting* 28, 57–66.
- Ding, H., Kim, H.G., Park, S.Y., 2016. Crude oil and stock markets: Causal relationships in tails? *Energy Economics* 59, 58–69.
- Ding, Z., Liu, Z., Zhang, Y., Long, R., 2017. The contagion effect of international crude oil price fluctuations on Chinese stock market investor sentiment. *Applied Energy* 187, 27–36.

- Dou, Y., Liu, Y., Richardson, G., Vyas, D., 2014. The risk-relevance of securitizations during the recent financial crisis. *Review of Accounting Studies* 19, 839–876.
- Drehmann, M., Tarashev, N., 2013. Measuring the systemic importance of interconnected banks. *Journal of Financial Intermediation* 22, 586–607.
- Du, L., He, Y., 2015. Extreme risk spillovers between crude oil and stock markets. *Energy Economics* 51, 455–465.
- Duchesne, P., Roy, R., 2004. On consistent testing for serial correlation of unknown form in vector time series models. *Journal of Multivariate Analysis* 89, 148–180.
- Dufour, J.M., Pelletier, D., 2020. Practical methods for modelling weak VARMA processes: Identification, estimation and specification with a macroeconomic application. Unpublished manuscript .
- Engle, R., 2002. Dynamic conditional correlation: A simple class of multivariate generalized autoregressive conditional heteroskedasticity models. *Journal of Business & Economic Statistics* 20, 339–350.
- Engle, R.F., 1982. Autoregressive conditional heteroscedasticity with estimates of the variance of United Kingdom inflation. *Econometrica* 50, 987–1007.
- Engle, R.F., Bollerslev, T., 1986. Modelling the persistence of conditional variances. *Econometric Reviews* 5, 1–50.
- Engle, R.F., Sheppard, K., 2001. Theoretical and empirical properties of dynamic conditional correlation multivariate GARCH. Technical Report. National Bureau of Economic Research.
- Forbes, K.J., Rigobon, R., 2002. No contagion, only interdependence: Measuring stock market comovements. *Journal of Finance* 57, 2223–2261.
- Fry, R., Martin, V.L., Tang, C., 2010. A new class of tests of contagion with applications. *Journal of Business & Economic Statistics* 28, 423–437.
- Gao, F., Song, F., 2008. Estimation risk in GARCH VaR and ES estimates. *Econometric Theory* , 1404–1424.
- Garbade, K.D., Silber, W.L., 1979. Structural organization of secondary markets: Clearing frequency, dealer activity and liquidity risk. *Journal of Finance* 34, 577–593.
- Garriga, C., Hedlund, A., 2020. Mortgage debt, consumption, and illiquid housing markets in the great recession. *American Economic Review* 110, 1603–34.
- Giles, C., 2008. China: Inflation fear as Olympic host goes for growth. *Financial Times* URL: <https://www.ft.com/content/c5564f16-89ca-11dd-8371-0000779fd18c>.
- Granger, C.W.J., 1969. Investigating causal relations by econometric models and cross-spectral methods. *Econometrica* 37, 424–438.
- Granger, C.W.J., 1980. Testing for causality: A personal viewpoint. *Journal of Economic Dynamics and Control* 2, 329–352.
- Granger, C.W.J., Robins, R., Engle, R.F., 1986. Wholesale and retail prices: Bivariate time-series modeling with forecastable error variances, in: Belsley, D.A., Kuh, E. (Eds.), *Model Reliability*. MIT Press, Cambridge, MA. chapter 1, pp. 1–17.

- Hafner, C.M., 2008. Temporal aggregation of multivariate GARCH processes. *Journal of Econometrics* 142, 467–483.
- Hannan, E.J., 1970. *Multiple Time Series*. John Wiley and Sons. New York.
- Hansen, B.E., 1994. Autoregressive conditional density estimation. *International Economic Review* , 705–730.
- Hansen, P.R., Lunde, A., 2005. A forecast comparison of volatility models: Does anything beat a GARCH (1,1)? *Journal of Applied Econometrics* 20, 873–889.
- Harville, D.A., 1997. *Matrix Algebra From a Statistician's Perspective*. Springer. New York.
- He, Y., Wang, S., Lai, K.K., 2010. Global economic activity and crude oil prices: A cointegration analysis. *Energy Economics* 32, 868–876.
- Hong, Y., 1996. Testing for independence between two covariance stationary time series. *Biometrika* 83, 615–625.
- Hong, Y., 2001. A test for volatility spillover with application to exchange rates. *Journal of Econometrics* 103, 183–224.
- Hong, Y., Liu, Y., Wang, S., 2009. Granger causality in risk and detection of extreme risk spillover between financial markets. *Journal of Econometrics* 150, 271–287.
- Huang, X., Zhou, H., Zhu, H., 2012. Assessing the systemic risk of a heterogeneous portfolio of banks during the recent financial crisis. *Journal of Financial Stability* 8, 193–205.
- Jarque, C.M., Bera, A.K., 1980. Efficient tests for normality, homoscedasticity and serial independence of regression residuals. *Economics Letters* 6, 255–259.
- King, M.A., Wadhvani, S., 1990. Transmission of volatility between stock markets. *Review of Financial Studies* 3, 5–33.
- Kirkulak-Uludag, B., Safarzadeh, O., 2018. The interactions between OPEC oil price and sectoral stock returns: Evidence from China. *Physica A: Statistical Mechanics and its Applications* 508, 631–641.
- Koijen, R.S.J., Yogo, M., 2016. Shadow insurance. *Econometrica* 84, 1265–1287.
- Koijen, R.S.J., Yogo, M., 2017. Risk of life insurers: Recent trends and transmission mechanisms, in: Hufeld, F., Koijen, R.S.J., Thimann, C. (Eds.), *The Economics, Regulation, and Systemic Risk of Insurance Markets*. Oxford University Press, Oxford. chapter 4, pp. 79–99.
- Kristoufek, L., Janda, K., Zilberman, D., 2012. Correlations between biofuels and related commodities before and during the food crisis: A taxonomy perspective. *Energy Economics* 34, 1380–1391.
- Kupiec, P., 1995. Techniques for verifying the accuracy of risk measurement models. *Journal of Derivatives* 3.
- Kwiatkowski, D., Phillips, P.C., Schmidt, P., Shin, Y., 1992. Testing the null hypothesis of stationarity against the alternative of a unit root. *Journal of Econometrics* 54, 159–178.
- Laeven, L., Ratnovski, L., Tong, H., 2016. Bank size, capital, and systemic risk: Some international evidence. *Journal of Banking & Finance* 69, 25–34.

- Lawsky, B.M., 2013. Shining a light on shadow insurance: A little-known loophole that puts insurance policyholders and taxpayers at greater risk. Unpublished Manuscript, New York State Department of Financial Services .
- Lee, S.W., Hansen, B.E., 1994. Asymptotic theory for the GARCH (1,1) quasi-maximum likelihood estimator. *Econometric Theory* 10, 29–52.
- Lewis, R., Reinsel, G.C., 1985. Prediction of multivariate time series by autoregressive model fitting. *Journal of Multivariate Analysis* 16, 393–411.
- Li, W.K., Mak, T., 1994. On the squared residual autocorrelations in non-linear time series with conditional heteroskedasticity. *Journal of Time Series Analysis* 15, 627–636.
- Li, X., Wei, Y., 2018. The dependence and risk spillover between crude oil market and China stock market: New evidence from a variational mode decomposition-based copula method. *Energy Economics* 74, 565–581.
- Lin, B., Jiang, Z., 2011. Estimates of energy subsidies in China and impact of energy subsidy reform. *Energy Economics* 33, 273–283.
- Lin, B., Ouyang, X., 2014. A revisit of fossil-fuel subsidies in China: Challenges and opportunities for energy price reform. *Energy Conversion and Management* 82, 124–134.
- Ljung, G.M., Box, G.E., 1978. On a measure of lack of fit in time series models. *Biometrika* 65, 297–303.
- López-Espinosa, G., Moreno, A., Rubia, A., Valderrama, L., 2012. Short-term wholesale funding and systemic risk: A global CoVaR approach. *Journal of Banking & Finance* 36, 3150–3162.
- Luo, J., Ji, Q., 2018. High-frequency volatility connectedness between the US crude oil market and China's agricultural commodity markets. *Energy Economics* 76, 424–438.
- Luo, X., Qin, S., 2017. Oil price uncertainty and Chinese stock returns: New evidence from the oil volatility index. *Finance Research Letters* 20, 29–34.
- Mollick, A.V., Assefa, T.A., 2013. Us stock returns and oil prices: The tale from daily data and the 2008–2009 financial crisis. *Energy Economics* 36, 1–18.
- Newey, W.K., Steigerwald, D.G., 1997. Asymptotic bias for quasi-maximum-likelihood estimators in conditional heteroskedasticity models. *Econometrica* , 587–599.
- Peng, C., Zhu, H., Guo, Y., Chen, X., 2018. Risk spillover of international crude oil to China's firms: Evidence from Granger causality across quantile. *Energy Economics* 72, 188–199.
- Phillips, P.C., Perron, P., 1988. Testing for a unit root in time series regression. *Biometrika* 75, 335–346.
- Priestley, M.B., 1981. Spectral analysis and time series: probability and mathematical statistics. 04; QA280, P7.
- Robbins, M.W., Fisher, T.J., 2015. Cross-correlation matrices for tests of independence and causality between two multivariate time series. *Journal of Business & Economic Statistics* 33, 459–473.
- Roodman, D., 2009. A note on the theme of too many instruments. *Oxford Bulletin of Economics and Statistics* 71, 135–158.

- Ross, S.A., 1989. Information and volatility: The no-arbitrage martingale approach to timing and resolution irrelevancy. *Journal of Finance* 44, 1–17.
- Schwarcz, D., 2015. The risks of shadow insurance. *Georgia Law Review* 50, 163.
- Silvennoinen, A., Thorp, S., 2016. Crude oil and agricultural futures: An analysis of correlation dynamics. *Journal of Futures Markets* 36, 522–544.
- Stoll, H.R., Whaley, R.E., 1990. Stock market structure and volatility. *Review of Financial Studies* 3, 37–71.
- Ureche-Rangau, L., Burietz, A., 2013. One crisis, two crises... the subprime crisis and the European sovereign debt problems. *Economic Modelling* 35, 35–44.
- van der Vaart, A.W., 1998. *Asymptotic statistics*. Cambridge University Press.
- Wang, X., Wang, Y., 2019. Volatility spillovers between crude oil and Chinese sectoral equity markets: Evidence from a frequency dynamics perspective. *Energy Economics* 80, 995–1009.
- Wei, Y., Guo, X., 2017. Oil price shocks and China's stock market. *Energy* 140, 185–197.
- Weller, B.M., 2019. Measuring tail risks at high frequency. *Review of Financial Studies* 32, 3571–3616.
- Wen, F., Xiao, J., Xia, X., Chen, B., Xiao, Z., Li, J., 2019. Oil prices and chinese stock market: Nonlinear causality and volatility persistence. *Emerging Markets Finance and Trade* 55, 1247–1263.
- White, H., 2001. *Asymptotic theory for econometricians*. Academic press.
- Wiener, N., Masani, P., 1957. The prediction theory of multivariate stochastic processes. *Acta Mathematica* 98, 111–150.
- Xiao, J., Hu, C., Ouyang, G., Wen, F., 2019. Impacts of oil implied volatility shocks on stock implied volatility in China: Empirical evidence from a quantile regression approach. *Energy Economics* 80, 297–309.
- Xiao, J., Zhou, M., Wen, F., Wen, F., 2018. Asymmetric impacts of oil price uncertainty on Chinese stock returns under different market conditions: Evidence from oil volatility index. *Energy Economics* 74, 777–786.
- Xu, W., Ma, F., Chen, W., Zhang, B., 2019. Asymmetric volatility spillovers between oil and stock markets: Evidence from China and the United States. *Energy Economics* 80, 310–320.
- Yun, X., Yoon, S.M., 2019. Impact of oil price change on airline's stock price and volatility: Evidence from China and South Korea. *Energy Economics* 78, 668–679.
- Zhang, C., Liu, F., Yu, D., 2018. Dynamic jumps in global oil price and its impacts on China's bulk commodities. *Energy Economics* 70, 297–306.
- Zhang, Q., Vallascas, F., Keasey, K., Cai, C.X., 2015. Are market-based measures of global systemic importance of financial institutions useful to regulators and supervisors? *Journal of Money, Credit and Banking* 47, 1403–1442.
- Zhou, O., Yep, E., 2019. Analysis: China puts Iranian crude into strategic petroleum reserves in June. S&P Global URL: <https://www.spglobal.com/platts/en/market-insights/latest-news/oil/073019-analysis-china-puts-iranian-crude-into-strategic-petroleum-reserves-in-june>.
- Zhu, H., Guo, Y., You, W., Xu, Y., 2016. The heterogeneity dependence between crude oil price changes and industry stock market returns in China: Evidence from a quantile regression approach. *Energy Economics* 55, 30–41.

